NOTE TO USERS

This reproduction is the best copy available

UMI

THE IDENTIFICATION OF A NOVEL RENAL ORGANIC CATION

TRANSPORT PROCESS: IMPLICATIONS FOR DRUG

INTERACTIONS AND ALTERED RENAL DRUG ELIMINATION

BY

KERRY BRENNAN GORALSKI

A THESIS SUBMITTED TO THE FACULTY OF GRADUATE STUDIES IN

PARTIAL FULFILLMENT OF THE REQUIREMENTS FOR THE DEGREE OF

DOCTOR OF PHILOSOPHY

DEPARTMENT OF PHARMACOLOGY AND THERAPEUTICS

FACULTY OF MEDICINE

UNIVERSITY OF MANITOBA

WINNIPEG, MANITOBA, CANADA

© 23 AUGUST 1999

The author has granted a non-exclusive licence allowing the National Library of Canada to reproduce, loan, distribute or sell copies of this thesis in microform, paper or electronic formats.

L'auteur a accordé une licence non exclusive permettant à la Bibliothèque nationale du Canada de reproduire, prêter, distribuer ou vendre des copies de cette thèse sous la forme de microfiche/film, de reproduction sur papier ou sur format électronique.

The author retains ownership of the copyright in this thesis. Neither the thesis nor substantial extracts from it may be printed or otherwise reproduced without the author's permission.

L'auteur conserve la propriété du droit d'auteur qui protège cette thèse. Ni la thèse ni des extraits substantiels de celle-ci ne doivent être imprimés ou autrement reproduits sans son autorisation.

0-612-44997-1

Canada

THE UNIVERSITY OF MANITOBA

FACULTY OF GRADUATE STUDIES
*****
COPYRIGHT PERMISSION PAGE

The Identification of a Novel Renal Organic Cation Transport Process:

Implications for Drug Interactions and Altered Renal Drug Elimination

BY

Kerry Brennan Goralski

A Thesis/Practicum submitted to the Faculty of Graduate Studies of The University

of Manitoba in partial fulfillment of the requirements of the degree

of

Doctor of Philosophy

KERRY BRENNAN GORALSKI©1999

Table of Contents

ABSTRACT

The mechanisms that mediate and factors that modulate amantadine transport in isolated renal tubules have been previously characterized. However, amantadine may describe a different organic cation transport system compared to that described by the prototypical organic cation substrate tetraethylammonium (TEA). We performed amantadine and TEA uptake and efflux studies using isolated rat renal proximal and distal tubules. The kinetic data indicate the presence of two sites for amantadine and TEA uptake across the basolateral membrane. The major difference in mechanism was that amantadine uptake was bicarbonate-dependent whereas TEA uptake was not. Inhibition and efflux studies confirmed that amantadine and TEA identify disparate transporters. From these data we proposed that basolateral organic cation transporters be classified as amantadine-selective and TEA-selective. TEA does not interact and is not transported by the amantadine-selective transporters whereas amantadine can interact with the TEA-selective transporters but is not significantly transported by them. Furthermore inhibition studies using substrates or inhibitors of the cloned rat organic cation transporters rOCT1 and rOCT2 indicate that TEA transport into isolated rat renal tubules reflects transport by rOCT1 and rOCT2 whereas amantadine transport reflects neither rOCT1 nor rOCT2. These data suggest that rOCT1 and rOCT2 are insufficient in describing renal tubule organic cation transport in its entirety. The remaining experiments focused on further characterizing the bicarbonate-dependent amantadine transporter under potential pathological conditions and in vivo.

The effects of early-stage diabetes and uninephrectomy on renal tubule uptake of amantadine were investigated. It was determined that early-stage streptozotocin-induced diabetes and uninephrectomy induce changes in the kidney that result in a similar selective increase in bicarbonate-dependent amantadine uptake in the proximal tubule. The increase in proximal tubule transport capacity in the streptozotocin induced diabetic rats was reversed by insulin treatment. The findings suggest potential implications for altered organic cation drug elimination by the kidney in diabetes and in compensation to decreased renal mass.

It has generally been accepted that the administration of NH_4Cl enhances the renal elimination of several organic cations through a pH-dependent decrease in passive reabsorption of the organic cation. As an alternative explanation of this phenomenon, the present data provide in vitro evidence that NH_4^+ may modulate renal organic cation elimination by pH-independent effects on protein-mediated organic cation transport. We investigated the effects of NH_4^+ on the renal tubule energy-dependent uptake of the organic cation amantadine into isolated renal proximal and distal tubules from male and female rats. With some variation, NH_4^+ inhibited the energy-dependent uptake of amantadine into renal proximal and distal tubules of males and female rats. At low NH_4^+ concentrations, the NH_4^+ inhibition involved a competitive component, as detected by increases in apparent K_m, but unchanging V_{max} for proximal and distal tubule amantadine uptake. The effects of NH_4^+ on amantadine transport were not due to changes in intracellular or extracellular pH, as determined by fluorescence imaging with the pH

sensitive dye BCECF. These data indicate that NH_4^+ may have a role in modulating access of organic cation drugs to the renal tubular organic cation transport systems.

In vivo studies were carried out to address the effect of bicarbonate on the renal clearance and urinary excretion of amantadine. The major finding of this study was that an acute increase in plasma bicarbonate substantially decreased amantadine clearance. Coupled with the previous in vitro demonstration of bicarbonate-dependent organic cation transport, the present findings suggest that bicarbonate inhibition of renal tubule secretion may explain the observation that bicarbonate dosing decreases amantadine excretion by the kidney.

ACKNOWLEDGMENTS

Reflecting on the past four years, I honestly admit that there were many times that I felt overwhelmed by the long hours, and days, performing countless experiments and data analysis, reading infinite numbers of journal articles, and writing, oh all that writing, that was required for the completion of this thesis. It was a very daunting task, but it was made much more enjoyable, manageable and rewarding with the assistance, advice, guidance and moral support that I received from the faculty, support staff, and colleagues here in the Department. I would like to take this opportunity to thank some of these very special people that made this work possible for me.

LIST OF FIGURES

Figure 5-4   Plasma concentration versus time profiles for amantadine and   **190**

kynurenate in the anaesthetized rat.

LIST OF TABLES

ABBREVIATIONS

AM	Amantadine
ANOVA	Analysis of variance
$\alpha_{t\frac{1}{2}}$	Half-life of initial drug disposition
AUC	Area under the plasma concentration vs. time curve
BCECF	BCECF, 2' 7'-bis-(2-carboxyethyl)-5-(and-6)-carboxyfluorescein
BCECF-AM	BCECF- AM, 2' 7'-bis-(2-carboxyethyl)-5-(and-6)-carboxyfluorescein- acetoxymethyl ester
$\beta_{t\frac{1}{2}}$	Half-life of terminal drug disposition
Cl_p	Plasma drug clearance
Cl_r	Renal drug clearance
CPM	Counts per minute
CT	Cross-Taggart buffer
DPM	Disintegrations per minute
HEPES	N-[2-Hydroxyethyl]piperazine-N'-[2-ethanesulfonic acid]
IC_{50}	Concentration of inhibitor required to inhibit transport by 50 %
K_i	Enzyme-inhibitor dissociation constant
KHS	Krebs-Henseleit solution
K_m	Michaelis-Menten constant
NMN	N^1-Methylnicotinamide
OAT	Organic anion transporter

Oatp	Organic anion transporting polypeptide
OCT	Organic cation transporter
SE	Standard error of mean
STZ	Streptozotocin
TEA	Tetraethylammonium
t.l.c	Thin layer chromatography
Tukey's HSD	Tukey's Honestly Significant Difference test
UNX	Uninephrectomized
Vd_{ss}	Volume of distribution at steady-state
V_{max}	Maximal rate of membrane transport

GENERAL INTRODUCTION

Foreword

Renal tubule organic cation transport plays an important role in the excretion of many organic cationic drugs that are used for therapeutic purposes. Some representative classes of organic cations that are excreted to varying extents by the kidney include adrenoceptor-blocking drugs (nadolol, sotalol), muscarinic receptor antagonists (atropine), calcium channel antagonists (verapamil), diuretics (triamterene), anti-arrhythmic drugs (procainamide, flecanide), histamine H_2-receptor antagonists (cimetidine), aminoglycoside antibiotics (gentamicin), anti-viral agents (amantadine), sympathomimetic agents (pseudoephedrine, methamphetamine) and NMDA receptor antagonists (memantine). Many factors, including age, drug chirality, interactions with other cationic drugs and alterations in endogenous metabolite levels may contribute to the variability in renal excretion of organic cation drugs. The variability in renal excretion of organic cations may be due to modulation of function of the organic cation drug transport system but the exact mechanisms are not known. Such modulation of organic cation transport may present the potential for clinically important interactions such as increased drug accumulation and toxicity due to decreased renal drug excretion. The clinical significance of these interactions becomes even more apparent in persons with decreased renal function, or in people predisposed to taking many medications concurrently, such as the chronically ill or the elderly. Further investigations of renal organic cation transport are needed to provide the mechanistic and functional information necessary to better understand conditions that contribute to variability of renal organic cation drug transport and excretion. Ultimately, this information may be applied to improving clinical use of existing organic cationic drugs.

Part I. Membrane transport processes and kinetics of transport

All living cells are separated from their external environments by a plasma membrane. One of the major functions of the plasma membrane is to control the movement of substances into and out of the cell, and thus regulate the composition of the intracellular fluid (Sha'afi, 1981). Passive diffusion and protein-mediated transport are the two types of membrane transport processes that allow for movement of compounds through biological membranes. The study of membrane drug transport processes and the information gained from kinetic analysis forms an integral portion of this dissertation. These studies rely on appropriately designed kinetic experiments to characterize the transport proteins involved and to describe their mechanisms of action. The following section is dedicated to reviewing the fundamental properties and kinetics of membrane transport and inhibition kinetics.

I.1   *Passive diffusion*

Passive diffusion is an equilibrative process by which a substance moves by random motion from an area of high concentration to an area of low concentration. According to Fick's first law of diffusion the flux of a substance across a membrane can be expressed by the following equation:

$$v = K_d(S_1 - S_2) \qquad (1)$$

where v is the rate of diffusion, K_d is the diffusion constant and S_1 and S_2 represent the substrate concentration on either side of the membrane (Christensen, 1975). K_d decreases with increasing molecular size, with decreasing lipid solubility, decreased temperature,

increased membrane thickness and with a decreased surface area available for diffusion. Thus for any given membrane, small hydrophobic molecules will passively diffuse through the membrane at a higher rate than larger more hydrophilic molecules. It is also apparent from the equation, that for an uncharged molecule, the rate of diffusion will be directly proportional to the trans-membrane concentration difference of the diffusing substance. When the substrate concentration on each side of the membrane becomes equal, the net rate of diffusion becomes zero. Diffusion across the membrane will be initially linear when all solute (S) originates on one side of the membrane and the initial velocity becomes directly proportional to the starting solute concentration (**fig. I-1**).

$$V_{initial} = K_d(S_1) \qquad (2)$$

Due to the hydrophobic nature of the plasma membrane, a strong permeability barrier is formed to most water-soluble and charged molecules. Thus, through evolution, plasma membranes have adapted specialized protein-mediated transport systems to facilitate the rapid and efficient transmembrane movement of important compounds such as inorganic ions, organic ions, nutrients and metabolites that do not readily cross the membrane by passive diffusion.

I.2   *Protein mediated transport*

There are several characteristics that distinguish the more interesting protein-mediated transport from passive diffusion (Rosenberg and Wilbrandt, 1955; Christensen, 1975):

Its rate is faster than predicted by passive diffusion.

It is saturable because there are finite numbers of transport sites.

3
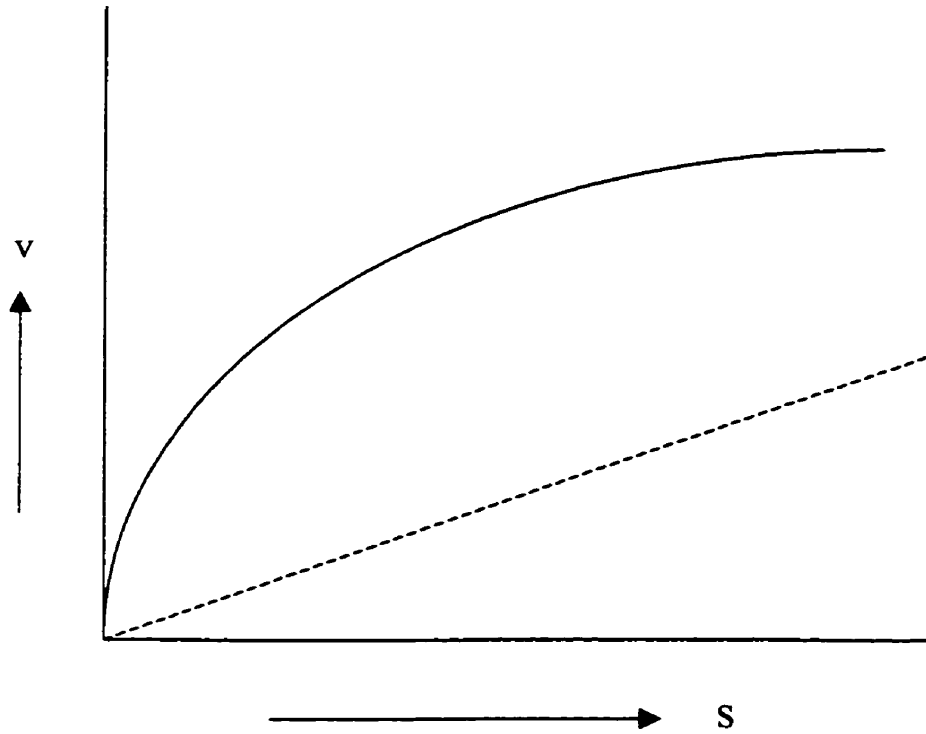
Figure I-1: Contrast between rate of transport (v) versus substrate concentration (S) for passive diffusion (dotted line) and protein mediate transport (solid line).

It displays chemical specificity for its substrates and,

It is susceptible to competitive inhibitors.

Protein-mediated transport can be categorized as either facilitative diffusion or active transport. Facilitative diffusion equilibrates a substance across a membrane but more rapidly than passive diffusion. It is not linked to metabolic energy and can't move ions against electrochemical gradients or uncharged molecules against chemical gradients. Active transport requires energy, and unlike facilitative diffusion, this process can move compounds against concentration or electrochemical gradients. In addition to the properties described above, active transport is susceptible to inhibition by metabolic inhibitors such as 2,4-dinitrophenol. Active transport may be primary, secondary or tertiary (**fig. I-2**). A primary active transport process is directly coupled to a high-energy releasing reaction (such as hydrolysis of ATP). An example (**fig. I-2**) is the Na^+/K^+ ATPase, which uses the energy from the hydrolysis of ATP to pump Na^+ and K^+ against their chemical gradients. Secondary and tertiary active transport generally use the energy stored in ionic gradients (originally linked to energy expenditure by the cell) as driving forces for transport of a compound against its electrochemical or chemical gradient. In this situation the movement of one chemical across the membrane, down its concentration gradient drives the transport of a second compound uphill against its concentration gradient. The direction of transport of the two substrates may be in the same direction (cotransporters) or opposite direction (antiporters). The Na^+/H^+ exchanger in the luminal membrane of proximal tubules (**fig. I-2**) is an example of a secondary active transport process. It uses the Na^+ gradient (inside low, outside high) which is

5

established by the Na^+/K^+ ATPase to drive the extrusion of H^+ from the cell. The organic cation/ H^+ exchanger in the luminal membrane of proximal tubules **(fig. I-2)** is an example of a tertiary active process that uses the energy stored in the form H^+ gradient (established by the secondary active Na^+/H^+ exchanger) to drive organic cation extrusion from the cell (Takano *et al.*, 1984; Wright and Wunz, 1988; Rafizadeh *et al.*, 1987).

I.3   *Kinetics of protein-mediated transport*

The relationship between S and v for initial rates of a protein-mediated transport reaction is described by a rectangular hyperbola **(fig. I-1)**. As opposed to linear passive diffusion, when concentration of the substrate is raised the rate of mediated-transport increases in a nonlinear fashion until it reaches a maximum value, at which further increases in substrate concentration does not increase the rate of transport. The hyperbolic shape of the curve implies, for protein-mediated transport, that the substrate is transiently bound to a mediating structure that is present in finite quantity and is similar to that relationship described by enzyme-mediated catalysis (Christensen, 1975).

A single substrate enzyme catalyzed reaction can be described by the following reaction:

$$E + S \underset{k_{-1}}{\overset{k_1}{\leftrightarrow}} ES \overset{k_2}{\rightarrow} E + P \qquad (3)$$
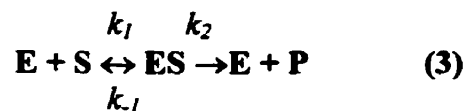
where E is the free enzyme, S is the free substrate, ES is the enzyme-substrate complex and P is the product of the reaction. In its simplest form, protein-mediated membrane drug transport processes could be expressed by equation (3) in the following manner:
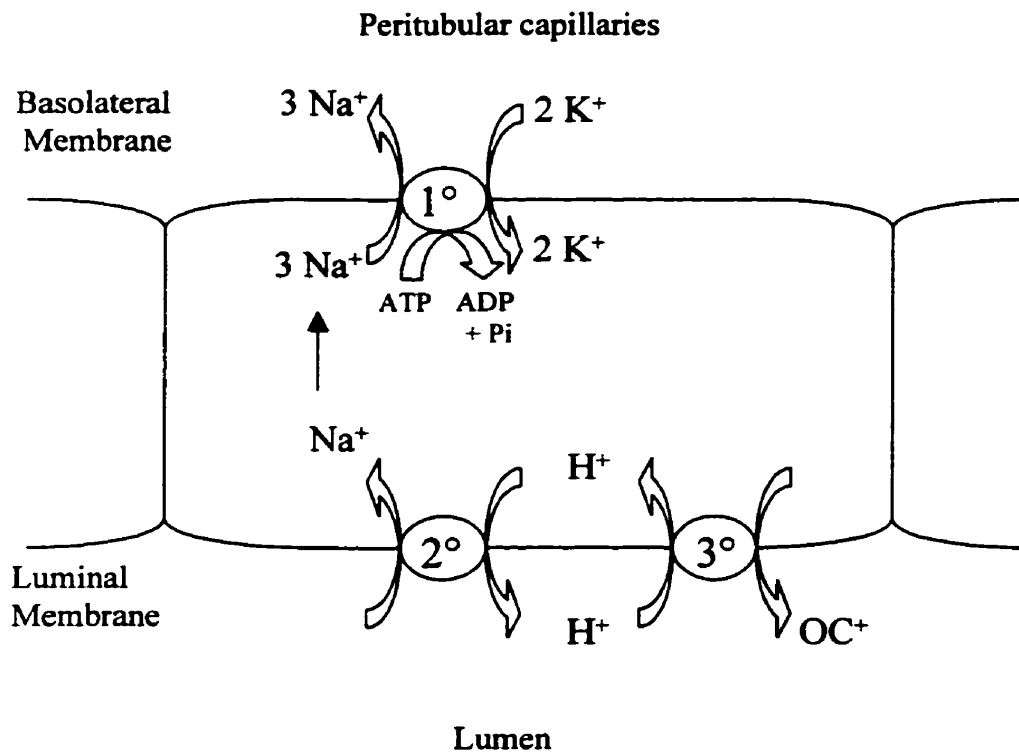
Figure I-2: Examples of primary (Na^+/K^+-ATPase), secondary (Na^+/H^+ exchanger), and tertiary active (OC^+/H^+ exchanger) transport processes. See text for details.

$$M + S_1 \overset{k_1}{\underset{k_{-1}}{\leftrightarrow}} MS \overset{k_2}{\rightarrow} M + S_2 \qquad (4)$$
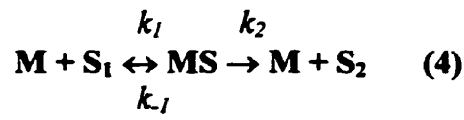
In this instance the transporter (M) mediates the passage of the drug (substrate) across the membrane and into the cell. When initial rates are measured, the second step of the reaction is assumed to be irreversible. However, this reaction could also be written in the reverse direction if efflux of the drug from the cell into the extracellular medium was being studied. The Michaelis-Menten equation (6) can be derived from the above reaction and its equilibrium constants. This derivation can be found in most introductory biochemistry textbooks (Voet and Voet, 1990). This equation is a useful rate equation for the study of-mediated transport reactions. In the derivation of the Michaelis-Menten equation, an important assumption is that the rate of ES formation is equal to its consumption over most of the course of the reaction (Briggs and Haldane, 1925). In other words, a steady-state is reached at which $dMS/dt = 0$. With this assumption and some algebraic work, the initial velocity of the reaction (v) can be expressed as,

$$k_2[MS] = k_1k_2[M]_t[S]/(k_{-1} + k_2 + [S]) \qquad (5)$$

The Michaelis constant $(K_m) = (k_{-1} + k_2)/k_1$ and $V_{max} = k_2[M]_t$ are substituted into equation (3) to give the modern expression of the Michaelis-Menten equation below:

$$v = V_{max}[S]/(K_m + [S]) \qquad (6)$$

where, as described above, v is the measured rate of product formation and S is the substrate concentration. V_{max} is the maximum rate of product formation and occurs when [S] is very large. It is important to note that V_{max} is not a fundamental property of an enzyme, because it depends on enzyme concentration (Cornish-Bowden, 1979). K_m (the Michaelis constant) is the substrate concentration at which the reaction proceeds at 0.5 V_{max}. An enzyme-mediated reaction with a low K_m has maximal catalytic activity at a low substrate concentration, whereas an enzyme-mediated reaction with a high K_m requires a larger amount of substrate to reach its optimal catalytic activity. Although K_m is a constant that represents the dependence of v on [S], K_m is often considered to be a constant that represents the affinity of the enzyme for the substrate. This approximation is only acceptable if $k_2 \ll k_{-1}$ in reaction (3 or 4) is true (Hofstee, 1952). In our renal tubule drug transport studies, initial rates of transport were measured and the Michaelis-Menten equation (6) was used to characterize these rates in terms of the rate constants K_m and V_{max}. We were unable to determine if $k_2 \ll k_{-1}$; thus, the use of the term of "affinity" to describe K_m throughout this thesis is only for descriptive purposes and is not absolute.

I.4   *Graphical representation of the Michaelis-Menten equation*

For enzyme-mediated reactions or transport mediated membrane diffusion, the four graphical methods described below have been used most commonly for the determination of K_m and V_{max} values.

9

1) The Michaelis-Menten plot: (**fig. I-3a**): A plot of a series of initial reaction rates (v) versus [S] produces a rectangular hyperbola, which can be divided into three distinct regions. 1) When S $\ll$ K_m, the equation (6) simplifies to v = V_{max}[S]/K_m, v is in direct proportion to [S] and V_{max}/K_m is the 1st order rate constant. 2) When S is near K_m equation (6) applies, and the reaction is said to follow mixed order kinetics. 3) When S $\gg$ K_m, v = V_{max}, the enzyme is saturated, and v is zero order with respect to S; that is with increasing substrate concentration there is no further increase in reaction velocity. Prior to the advent of computer technology, this plot was not very useful because it was very difficult to extrapolate to V_{max}. As such, V_{max} estimates and resultant K_m values would be highly variable. With the advent of computer non-linear regression programs, this plot has become more useful in determining K_m and V_{max}. The Michaelis-Menten plot is also advantageous because the saturable characteristics of the transport-mediated process can be observed directly from the graph.

2) The Lineweaver-Burk plot (**fig. I-3b**) (Lineweaver and Burk, 1934): This plot has been probably the most extensively but inappropriately used transformation of the Michaelis-Menten equation for the determination of K_m and V_{max}. (Cornish-Bowden, 1979) This transformation is obtained simply by taking the reciprocal of equation (6) to give:

$$1/v = K_m/V_{max} \times 1/[S] + 1/V_{max} \qquad (7)$$

By plotting 1/v versus 1/[S] a straight line with slope equal to K_m/V_{max}, a y-intercept equal to 1/V_{max} is obtained, and the x-intercept is equal to -1/K_m. The major advantage of this transformation is that K_m and V_{max} can be determined from discrete points on the graph.

Its major disadvantage is that the K_m and V_{max} determination are heavily influenced by the rates at low substrate concentrations. Due to the reciprocal nature of the plot, at low substrate concentrations small errors in v lead to large errors in 1/v and thus, large errors in K_m and V_{max}. If the data fit is not extremely good, then data point weighting such as described by Wilkinson (1961) must be used to produce meaningful K_m and V_{max} determinations.

3) The Eadie-Hofstee plot (**fig. I-3c**) (Eadie, 1942; Hofstee, 1952): This transformation is obtained by muliplying both sides of equation (7) by v × V_{max} and rearranging to give:

$$v = Vmax - Km \ v/[S] \qquad (8)$$

Plotting v versus v/[S] gives a straight-line plot with slope equal to $-K_m$, y-intercept equal to V_{max}, and an x-intercept equal to K_m/V_{max}. This plot gives good results in practice; however, because v appears in both coordinates, variation in v leads to deviations toward and away from the origin (Cornish-Bowden, 1979). With the Eadie-Hofstee transformation, errors in v at small substrate concentration lead to deviations in v/[S] and thus K_m and V_{max}.

4) The Hanes plot (**fig. I-3d**) (Hanes, 1932; Lineweaver and Burk, 1934). This final transformation is obtained by multiplying both sides of equation (7) by [S] to give:

$$[S]/v = [S]/V_{max} + K_m/V_{max} \qquad (9)$$

A plot of [S]/v versus [S] gives a straight-line plot with slope equal to $1/V_{max}$, y-intercept equal to K_m/V_{max}, and x-intercept equal to $-K_m$. This is the preferred linear transformation
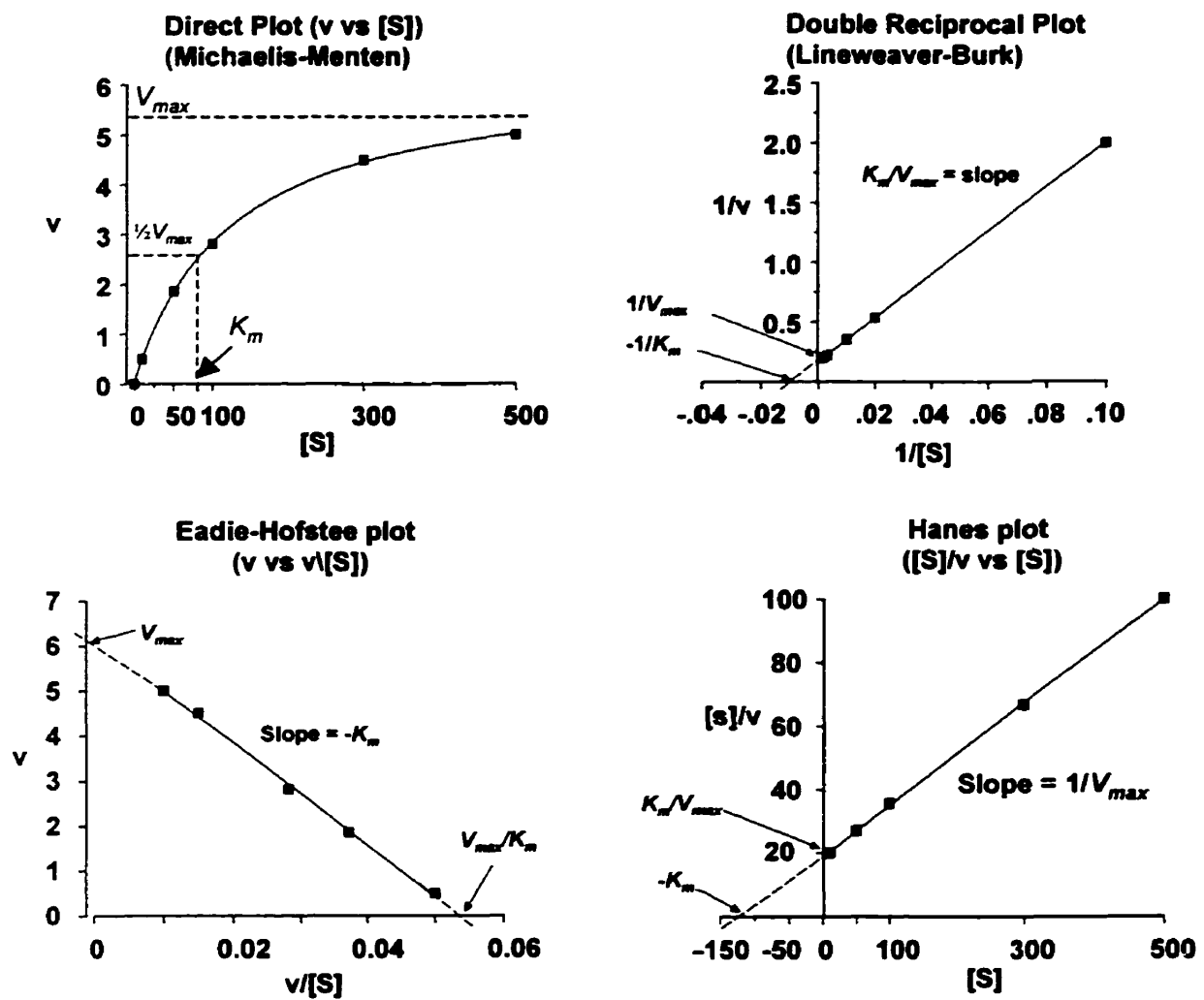
Figure I-3: Graphical representation of protein-mediated transport by: a) Michaelis-Menten plot, b) Lineweaver-Burk plot c) Eadie-Hofstee plot and d) Hanes plot.

of the Michaelis-Menten equation because errors in [S]/v are reflective of v over a wide range in [S] (Cornish-Bowden, 1979).

For the present studies the hyperbolic v versus [S] plot was used for graphical representation for all kinetic determinations and a non-linear regression program was used to estimate K_m and V_{max}. The Hanes and Eadie-Hofstee transformations were useful for initial kinetic estimates and to determine if single or multiple sites were responsible for the observed membrane transport of the substrates under study and for initial estimates of K_m and V_{max}. A straight line would represent a single transport site, whereas a biphasic plot would represent dual transport sites. For K_m and V_{max} determinations, choice of substrate concentration is critical and should be between 0.2× – 5× K_m (Cornish-Bowden, 1979). A minimum of five points; two below K_m (linear portion of the curve); one point at or near K_m and 2 points above K_m (approaching the zero order portion of the curve) gave reproducible fits to this kinetic model.

I.5   *Enzyme Inhibition*

Substances that bind to enzymes and decrease their affinity for substrates or the rates of the enzyme-mediated reaction are known as inhibitors. Inhibitors can be reversible or irreversible. Reversible inhibitors bind and release from the enzyme in an equilibrium process, and alter enzyme function temporarily while they are bound to it. An irreversible inhibitor (e.g. cholinesterase inhibitors) covalently binds to the enzyme and permanently inactivates it. In the present studies the enzyme inhibition is of the reversible type, and thus no further mention of irreversible inhibition will be made. A

13

single substrate transport-mediated reaction in the presence of a reversible inhibitor (I) is displayed by the general reaction in **fig. I-4a**. MI is the enzyme-inhibitor complex, MIS is the enzyme-substrate-inhibitor complex, K_i is the dissociation constant of the MI complex and K_i' is the dissociation constant for the MIS complex. The general equation for linear inhibition is shown in **fig. I-4b**. The four types of reversible inhibition include competitive, non-competitive, uncompetitive and mixed inhibition, and all are variations of the general equation for linear inhibition.

Competitive inhibition is the most common type of inhibition observed in practice (Cornish-Bowden, 1979). In competitive inhibition, the inhibitor competes directly with the substrate for the free enzyme's active site. In competitive inhibition, K_i' approaches infinity and thus $(1+ I/K_i')$ approaches 1 and can be removed from the general equation to give the formula for competitive inhibition in **fig. I-4c**. The net effect of competitive inhibition is that apparent K_m is increased by the factor $(1+I/K_i)$. In competitive inhibition, increasing the substrate concentration will overcome the presence of inhibitor, and thus V_{max} remains constant; however, a higher substrate concentration is required to reach saturation.

Uncompetitive inhibition is the opposite situation compared to competitive inhibition. In this type of inhibition the inhibitor only binds to the MS complex; K_i approaches infinity; and the factor $(1+I/K_i)$ can be removed from the general equation to give the equation for uncompetitive inhibition (**fig. I-4d**). In the presence of an uncompetitive inhibitor both V_{max} and K_m are decreased by the factor $(1+ I/K_i')$.

14

Uncompetitive inhibition occurs almost exclusively as a type of product inhibition that is common in reactions with several substrates and products (Cornish-Bowden, 1979).

Non-competitive inhibition is a pattern of inhibition where the inhibitor alters the catalytic activity of the enzyme by binding to the enzyme at an alternate site, and does not directly compete with the substrate for the active site. In non-competitive inhibition, K_i is equal to K_i' and the equation shown in **fig. I-4b** applies. It is characterized by a decrease in V_{max} by the factor $(1+ I/K_i')$ and no change in K_m. In other words the presence of a non-competitive inhibitor has the effect of reducing the amount of active enzyme available to catalyze the reaction but does not disrupt the enzyme's affinity for the substrate. This type of inhibition is not often observed in practice (Cornish-Bowden, 1979).

The last type of general linear inhibition is mixed-inhibition. This type of inhibition is characterized by variable changes in both V_{max} and K_m depending on the degree of K_i and K_i'. The equation in **fig. I-4b** is applicable to mixed inhibition.

I.6   *Approach for determining inhibition constants*

Two complementary analyses should be used for the determination of the inhibitory constants K_i and K_i' and the type of inhibition (e.g. competitive versus uncompetitive etc.). These are the Cornish-Bowden analysis and Dixon analysis (Dixon, 1953; Cornish-Bowden, 1974). Both analyses require the measurement of reaction rates in the presence of varying concentrations of inhibitor and in the presence of at least two

a)

$$S_1 + M \rightleftharpoons SM \longrightarrow M + S_2$$

$$I \rightarrow \quad K_i \qquad \qquad K_i'$$

$$MI \qquad \qquad MIS$$

$$K_i = [M][I]/[MI] \text{ and } K_i' = [SM][I]/[MIS]$$
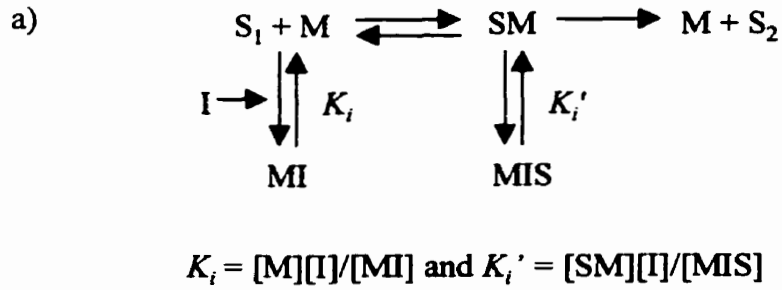
b)

$$v_{app} = \frac{V_{max}[S]}{K_m(1 + I/K_i) + [S](1 + I/K_i')} \quad \text{(general linear inhibition)}$$

c)

$$v_{app} = \frac{V_{max}[S]}{K_m(1 + I/K_i) + [S]} \quad \text{(competitive inhibition)}$$

d)

$$v_{app} = \frac{V_{max}[S]}{K_m + [S](1 + I/K_i')} \quad \text{(uncompetitive inhibition)}$$

Figure I-4: General reaction formula (a) and equations for the different types of linear inhibition (b,c and d).

different starting substrate concentrations. In the Dixon analysis 1/v versus [I] is plotted for two or more substrate concentrations. For each value of S the points lie on a straight line and the point where the two lines intersect is equal to - K_i (**fig. I-5 a, c, e and g**). The linear equation for this plot is derived from the equation for competitive inhibition (Dixon, 1953). The Dixon plot does not distinguish between competitive and mixed inhibitors and does not provide a measure of K_i' (**fig. I-5 a, e**) (Cornish-Bowden, 1974). For the Cornish-Bowden analysis [S]/v versus [I] is plotted for two or more substrate concentrations. It is derived from the general equation for linear mixed inhibition. Like the Dixon plot, for each value of S the points lie on a straight line and their point of intersection is equal to - K_i' (**fig. I-5 b, d, f and h**). However, the Cornish-Bowden plot does not distinguish between uncompetitive and mixed inhibition (**fig. I-5 d, f**) and K_i cannot be determined (Cornish-Bowden, 1974). When these plots are used complementary to each other (**fig. I-5**) the type of inhibition can be identified unambiguously and values for both K_i and K_i' can be determined. Competitive inhibition (**fig. I-5 a, b**) is indicated when the lines on the Dixon plot intersect above the negative x-axis (K_i converges) and the lines on the Cornish-Bowden plot are parallel (K_i' approaches ∞). Uncompetitive inhibition (**Fig. I-5 c, d**) is the opposite situation of competitive inhibition. Here the lines in the Dixon plot remain parallel (K_i approaches ∞) and those in the Cornish-Bowden plot intersect above the negative x-axis (K_i' converges). For mixed inhibition (**fig. I-5 e, f**), the lines in both plots intersect either above or below the negative x-axis depending on the values for K_i and K_i'. Finally, for non-competitive inhibition (**fig. I-5 g, h**), the lines on both plots intersect at the same point on the negative x-axis and both K_i and K_i' are equal.
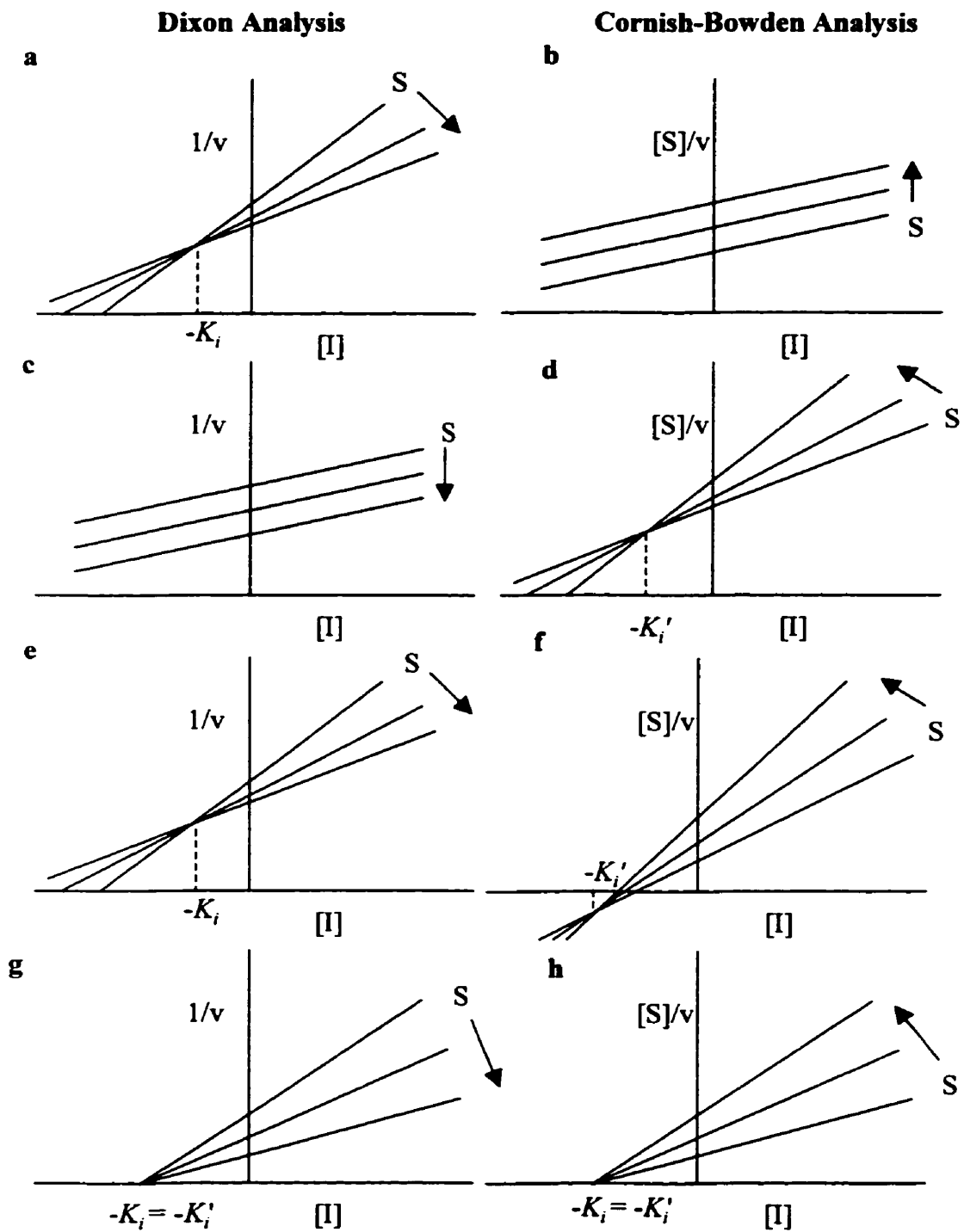
Figure I-5: Dixon and Cornish Bowden Analysis for determination of type of enzyme inhibition. a,b) competitive; c,d) uncompetitive; e,f) mixed; g,h) non-competitive inhibition (Cornish Bowden, 1974).

a

b
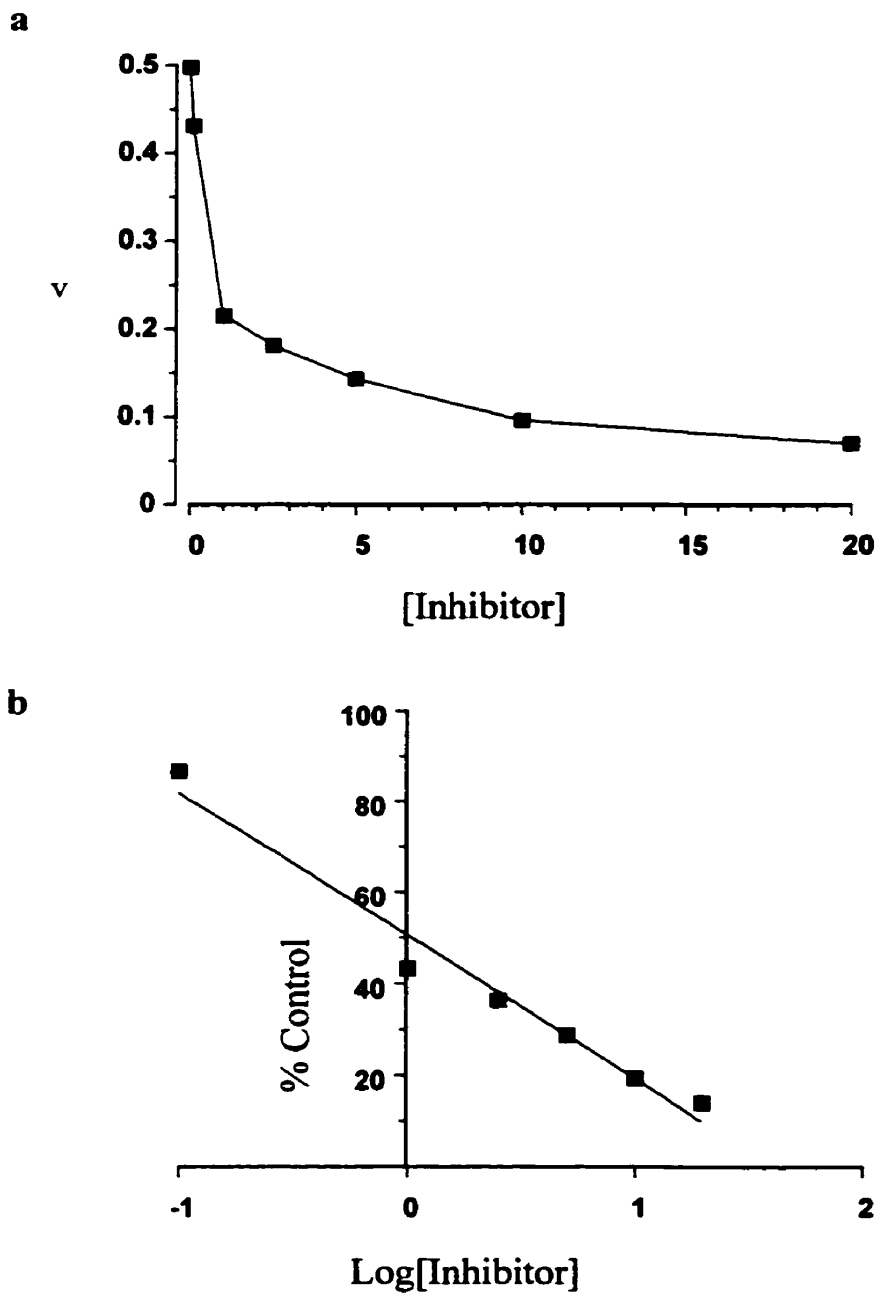
Figure I-6: Demonstration of data conversion for calculation of IC_{50} values. a, reaction rate versus inhibitor concentration; b, reaction rate as % percent control versus log inhibitor concentration.

19

An alternative approach for determining enzyme inhibition is the method of Cheng and Prusoff (1973). The Cheng-Prusoff equation allows for the determination of the concentration of the inhibitor that is required to decrease the rate of the enzyme-catalyzed reaction by 50 percent. Unlike the assays described for the determination of K_i and K_I', IC_{50} calculations only require the measurement of reactions rates in the presence of different inhibitor concentrations at one substrate concentration. For this analysis, reaction rates at different inhibitor concentrations (**fig. I-6a**) are converted to percent control and plotted versus log [I] to give a straight line (**fig. I-6b**). IC_{50} is then determined from the equation of the straight line when Y = 50 %. The major advantage of the IC_{50} determination is that the assays are much smaller than for the Dixon and Cornish-Bowden assays. The major disadvantage with IC_{50} determinations are that they are dependent on substrate concentration and assay conditions, and they cannot identify the type of inhibition (Cheng and Prusoff, 1973). However, if the type of inhibition is known, then IC_{50} can be converted to K_I using the following formulas:

If inhibition is competitive,

$$K_i = IC_{50}/(1+S/K_m) \quad (10)$$

and if inhibition is noncompetitive or uncompetitive

$$IC_{50} = K_I \quad (11)$$

(Cheng and Prusoff, 1973).

The methods for graphical analysis of enzyme inhibition can all be applied to the analysis of inhibition of protein-mediated membrane transport processes such as were carried out in the present studies.

Part II. The kidney and renal tubule drug transport

II.1 *Basic renal processes and anatomy*

The functional unit of the kidney is the nephron. Each human kidney is comprised of about one million nephrons (Vander, 1995; Tisher and Madsen, 1996). There are three types of nephrons: superficial, midcortical and juxtaglomerular nephrons (Kriz and Bankir, 1988). All nephrons consist of a renal corpuscle (filtration apparatus) which is connected to a tubule structure. The renal corpuscle is composed of a tuft of capillaries (glomerulus) which is enclosed within a hollow space called the Bowman's capsule. The tubule portion of the nephron consists of a single layer of epithelial cells attached to a basement membrane along its entire length. The tubule portion is heterogeneous in terms of cell type and function, and can be anatomically divided into four distinct components starting with the proximal tubule, followed by the loop of Henle, the distal tubule and finally the collecting duct (Kriz and Bankir, 1988; Tisher and Madsen, 1996). As shown in **fig. II-1** the main divisions of the tubule can be divided further into smaller subsections. Of importance for this communication, the proximal and distal tubules can be subdivided into the proximal convoluted tubule and straight tubule, and distal convoluted tubule and straight tubule respectively. Furthermore, based on cell morphology, the beginning and the middle portion of the proximal convoluted tubule are referred to as the S_1 segment. The final portion of the proximal convoluted tubule and
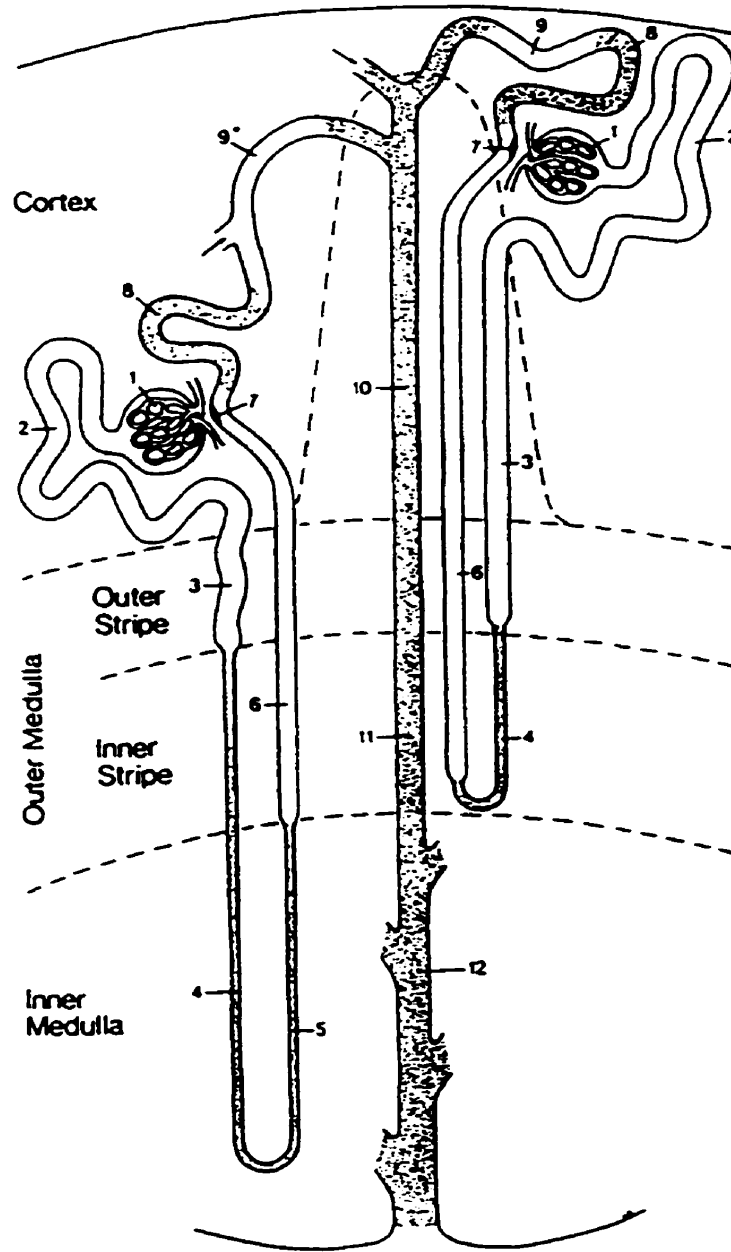
Figure II-1: Diagramatic representation of a superficial and a juxtaglomerular nephron. 1, Renal corpuscle including Bowman's capsule and glomerulus; 2, proximal convoluted tubule; 3, proximal straight tubule; 4, descending thin limb; 5, ascending thin limb; 6, distal straight tubule; 7, macula densa; 8, distal convoluted tubule; 9, connecting tubule; 10, cortical collecting duct; 11 and 12, outer and inner medullary collecting ducts respectively (Kriz and Bankir, 1988)

22

the beginning of the proximal straight tubule is known as the S_2 segment and the remainder of the proximal straight tubule is the S_3 segment.

Via the afferent arterioles, blood enters the glomerular capillaries where a portion of the plasma is filtered into the Bowman's capsule. The fluid entering the Bowman's capsule is essentially a protein free plasma ultrafiltrate, which then passes into the proximal tubule. The composition of the ultrafiltrate is modified along the length of the tubule through secretion and reabsorption of electrolytes, organic compounds and H_2O, resulting in urine formation. Tubular reabsorption defines the process of transferring compounds from the ultrafiltrate to the circulation, whereas tubular secretion defines the process in which a compound is transferred from the peritubular capillaries into the tubule lumen. The amount of a substance that is removed in the urine depends on the extent of its filtration, secretion and reabsorption.

The major function of the kidney is to regulate the volume, osmolarity, mineral composition and acidity of the body by excreting water and electrolytes in amounts adequate to maintain their normal concentrations in the extracellular fluid (Vander, 1995). A second function of the kidney is as an endocrine organ, secreting the hormones renin, erythropoietin and 1, 25-dihydroxyvitamin D_3 (Vander, 1995). The kidney also has an important function in eliminating metabolic wastes or foreign chemicals from the blood into the urine. Through the elimination of potentially harmful exogenous and endogenous compounds by glomerular filtration and renal tubule secretion, the kidney is

able to protect the body from the toxic insult that would otherwise result from their accumulation.

Many of the foreign chemicals that we are exposed to are organic cations and anions. In addition, both foreign and endogenous compounds are metabolized to cations and anions in the body (Pritchard and Miller, 1993). Carrier-mediated transport systems for organic anions and cations have been demonstrated in several tissues, including the kidney, liver, intestines and brain, and may largely affect the rate of drug distribution and elimination (Meijer *et al.*, 1990; Koepsell *et al.*, 1998). With respect to drug elimination, the kidney preferably eliminates smaller more hydrophilic compounds, whereas the larger and more hydrophobic compounds are better candidates for biliary excretion by the liver (Bessighir and Roch-Ramel, 1987). The majority of evidence suggests that the renal tubule secretion of organic cations and anions occurs by distinct transport pathways (Pritchard and Miller, 1993; Sica and Schoolworth, 1996). However, some evidence suggests that there are bisubstrates that can be transported by both organic cation and organic anion transport systems (Ullrich *et al.*, 1993a; Ullrich *et al.*, 1993b; Ullrich, 1994). In addition a new family of drug transporters has been identified which mediates the transport of organic anions, organic cations and neutral steroid molecules (Bossuyt *et al.*, 1996). In following sections the common technical approaches for studying mechanisms or renal tubule secretion and drug elimination by the kidney will be described followed by a review of the characteristics and function of the renal tubule organic anion and organic cation transport systems.

II.2 *Experimental techniques for studying renal tubule drug transport and elimination*

Early studies of organic cation or anion secretion consisted mainly of in vivo renal clearance experiments performed in anaesthetized or conscious dogs (Marshall and Vickers 1923; Marshall, 1931; Rennick *et al.*, 1947; Beyer *et al.*, 1950; Peters *et al.*, 1955; Rennick and Farrah, 1956; Rennick *et al.*, 1956). In more recent years the use of in vivo techniques for studying organic cation transport has lost favor to a variety of in vitro methodologies such as renal cortical slices, isolated perfused and nonperfused renal tubules, cell culture and molecular biology. The in vitro procedures are powerful in determining mechanisms and constitution of the organic cation transport system and each technique has associated advantages and disadvantages. However, caution must be used when extrapolating in vitro results to the in vivo situation. The use of in vivo models remains a necessity to confirm the functional importance of the in vitro observations and should not be overlooked as a valuable tool for studying organic cation transport. Some of the commonly used methods for studying organic cation transport and their advantages and disadvantages are described below.

II.2.a *In vivo renal clearance*

These experiments have been performed generally in anaesthetized or conscious dogs, chickens and rats. In the simplest model, organic cation drugs such as TEA are given orally or intravenously in the presence and absence of potential transport modulators (e.g. other organic cations, change in urine pH) followed by urine collection from a bladder or ureter catheter. Amount of drug cleared in the urine per unit time is divided by inulin or creatinine clearance over the same time interval to determine the

extent of tubule secretion of the drug in question. The most obvious benefit from these types of studies is that the effects of manipulating the organic cation transport system on renal tubule secretion and overall renal drug elimination can be determined. One of the major drawbacks of early in vivo studies was that many of the organic cations under study (potential ganglionic blocking agents) had profound vascular effects and thus hindered the interpretation of experimental results.

II.2.b   *The Sperber Technique*

Sperber developed a model to study in vivo renal clearance of organic compounds which takes advantage of the renal portal circulation of chickens and minimizes systemic effects of the compounds under study (Sperber, 1949; 1959). In this model, "The Sperber Technique", a drug can be infused into the saphenous leg vein through which blood returns to the peritubular capillaries of the ipsilateral kidney before reaching the systemic circulation. Drug excretion in the urine from the ipsilateral kidney (test kidney) and contralateral kidney (control kidney) are then measured. The excess of drug excreted by the test kidney compared to the control kidney can then be attributed to tubule secretion. However, the studies in chickens must be viewed with caution, as extrapolation to mammalian renal tubule transport is questionable.

II.2.c   *Stop-flow analysis*

Stop-flow analysis in anaesthetized dogs has also been used to study in vivo renal tubule organic cation and anion transport (Malvin *et al.*, 1958; Rennick and Moe, 1960; Pilkington and Keyl 1963). In stop-flow analysis, the ureter is cannulated and then

26

occluded to stop urine flow and glomerular filtration. This is followed by intravenous infusion of a test organic cationic or anionic substrate, along with PAH (a marker of proximal tubule secretion) and creatinine (a marker of glomerular filtration). These infused compounds are allowed to equilibrate in the plasma for a short period of time before the ureter occlusion is removed. During the occlusion, substances may enter the renal tubule cells and lumen by secretion mechanisms only. The ureter occlusion then is removed and glomerular filtration and urine flow are reestablished. Several small urine samples are collected from the ureter and measured for the compounds described. The appearance of the test substrate in the urine fractions relative to the appearance of PAH and creatinine allows for relative identification of tubular location of the organic ion transport machinery. The main limitations of this technique are that the determined locations of secretion along the nephron are relative to other substrates and cannot be determined exactly. Second, the effect of mixing of the tubule fluid once the occlusion is removed may impart ambiguity to the interpretation of the data (Rennick and Moe, 1960).

II.2.d *Tubule and capillary micropuncture and microperfusion*

Microperfusion and microinfusion are powerful in situ techniques for defining sites of renal tubular secretion and reabsorption (Moller and Sheikh, 1982). These methods have been used extensively to study mechanisms of organic cation and anion transport across the basolateral and luminal membranes in the proximal tubule (Ullrich *et al.*, 1991, 1992; 1993a, 1993b; Ullrich and Rumrich, 1992; David *et al.*, 1995). Micropuncture experiments are performed in surgically exposed kidneys of anaesthetized

rats. As an example, in continuous flow microperfusion (Ullrich and Rumrich, 1990), a microcapillary pipette is inserted into an oil-blocked tubule lumen, at an upstream site of an accessible cortical nephron (e.g. beginning of the proximal convoluted tubule). From this capillary, a perfusate containing the substance of interest (e.g. radiolabled organic cation) along with ^{14}C-inulin (a volume marker) are infused at a constant rate. The tubule fluid is then collected from a second pipette that is inserted at a more distal location of the tubule (e.g. the end of the proximal convoluted tubule). The disappearance of the test substance relative to that of inulin can then be used to determine the extent of luminal membrane transport of the substance along that segment of the nephron. Capillary microperfusion is a similar procedure and can be used to study mechanisms of organic ion transport across the basolateral membrane (Ullrich and Rumrich, 1990; Ullrich *et al.*, 1991, 1992, 1993a, 1993b). Other variations of the continuous flow microperfusion are available and include stop-flow microperfusion, microinjection and microinfusion (Ullrich and Rumrich, 1990; Shafik and Quamme, 1990; Dahlmann *et al.*, 1998). The major advantage of the micropuncture techniques is that the secretory and reabsorptive function of specific sections of intact nephrons in the whole animal can be studied. Apart from the technical difficulty, a major drawback is that only surface nephron segments can be accessed. In addition, non-physiological perfusates and injection of Lissamine green (a dye used to identify tubule sections of the same nephron) might possibly change tubule function (Ullrich and Rumrich, 1990).

II.2.e   *Isolated plasma membrane vesicles*

Basolateral and luminal membrane vesicles have been prepared from human, dog, rabbit and rat kidney cortex homogenates, separated by Ca^{2+} and Mg^{2+} precipitation, followed by differential centrifugation methods (Kinsella *et al.*, 1979b). The use of isolated membrane vesicles has been important for separating and individually studying the basolateral and apical membrane components of renal tubule organic anion and cation secretion. The effects of membrane potential, intracellular and extracellular pH, inhibitors on organic ion transport, and identification of substrates and driving forces for the organic cation and anion transporters in the respective membranes have readily been determined using this methodology (Kinsella *et al.*, 1979a; Holohan and Ross, 1980, 1981; Takano *et al*, 1984; McKinney and Kunnemann, 1985; Rafizadeh *et al.*, 1987; Wright and Wunz, 1987, 1988; Jung *et al.*, 1989; Montrose-Rafizadeh *et al.*, 1989; Dantzler *et al.*, 1991; Ott *et al.*, 1991; Sokol and McKinney, 1990; Katsura *et al.*, 1991, 1993; Gross and Somogyi, 1994). Disadvantages of this preparation include a small tissue yield. Also, vesicles are heterogeneous in terms of nephron segments because they are prepared from cortical tissue, which contains both proximal and distal convoluted tubules. The polarity of the basolateral membranes is variable, and thus interpretation of data may be difficult. Luminal membrane vesicles are formed with brush borders facing out. Thus, luminal membrane uptake studies do not reflect transport in the direction of secretion.

II.2.f *Cultured renal cells*

LLC-PK$_1$, IHKE-1 and OK cells, proximal tubule cell lines from porcine, human and opposum kidney respectively and MDCK cells, a distal tubule cell line from dog have been used to study the transepithelial transport and accumulation of organic cations (Fouda *et al.*, 1990; McKinney *et al.*, 1990; Saito *et al.*, 1992; Bendayan *et al.*, 1994; Chan *et al.*, 1996; Takami *et al.*, 1998; Hohage *et al.*, 1994, 1998). A unique feature of cultured renal epithelial cells is that when they are grown on a solid support, they form polarized monolayers that have many structural characteristics (microvilli and tight junctions) of epithelia in situ (Handler *et al.*, 1980). Thus, a substrate under study can be applied to one side of the monolayer (basolateral or luminal side) in the presence of transport inhibitors or modulators followed by washing and sampling from the side opposite of substrate administration. Using this process, the directional transport of several organic compounds in the direction of secretion (basolateral → luminal side) has been determined. (Fouda *et al.*, 1990; Saito *et al.*, 1992; Chan *et al.*, 1996; Takami *et al.*, 1998). The major concern when using cell culture is that the cells may not be functionally identical to normal renal cells. For example, activation of protein kinase A, C and G have dramatically different effects on organic cation accumulation in LLC-PK$_1$ cells compared to IHKE-1 cells (Hohage *et al.*, 1998).

II.2.g *Isolated perfused renal tubule segments*

Burg and coworkers (Burg *et al.*, 1969) developed methodology to dissect, incubate and perfuse specific segments of rabbit nephrons. Using this procedure, rabbit tubules fragments are dissected from kidneys in a buffered medium with the aid of a

stereoscopic microscope. Intact fragments of proximal convoluted and straight tubules, distal convoluted and straight tubules, collecting tubules and ascending limbs can be obtained. The isolated tubule fragments are suspended in a bathing medium and capillary pipettes are attached to each end of the tubule, one for administration and one for collection of perfusate. Reabsorption of a substrate is studied by adding it to the perfusate and measuring the substrate's concentration after passage through the tubule. Alternatively, a radioactive organic cation or anionic substrate can be added to the extracellular bathing medium and its recovery in the perfusate can be determined. Thus, this preparation has been advantageous for studies of organic cation and anion secretion because it allows for measurement of transtubular transport and comparison of transport in different nephron segments (Burg and Orloff, 1969; Tune *et al.*, 1969; McKinney, 1982; McKinney and Speeg, 1982; Schali *et al.*, 1983; McKinney 1984). The major disadvantages of the isolated perfused tubules are that the dissection technique is very difficult, varies between animals, and requires several months to learn (Burg, 1972).

II.2.h *Renal cortical slices and isolated renal tubules in suspension*

The renal cortical slice procedure simply involves slicing thin sections of renal cortex from the dissected kidney using a microtone knife, followed by suspension in an appropriate buffer for transport assays (Cross and Taggart, 1950; Wong *et al.*, 1990, 1991). The preparation of proximal and distal tubules from renal cortex requires additional steps of collagenase digestion to break the tissue into fragments, followed by density gradient centrifugation to purify fractions of proximal and distal tubules (Vinay *et al.*, 1981; Gesek *et al.*, 1987). Alternatively, a manual microdissection method to isolate

cortical proximal tubule segments without the use of digestive enzymes has been described (Schali and Roch-Ramel, 1980; Schali et al., 1983; McKinney, 1984). However, this is a tedious and time-consuming technique with a low tissue yield. The cortical slice technique and the isolation of renal tubules by collagenase digestion and centrifugation are relatively simple techniques that produce high tissue yields. Isolated tubules and cortical slices have been used by our laboratory and others to study aspects of organic cation and anion transport (Burg and Orloff, 1969; Sheikh and Moller, 1970; Schali et al., 1983; McKinney, 1984; Wong et al., 1990,1991,1992a 1992b, 1993; Dantzler et al., 1991; Escobar et al., 1994, 1995; Escobar and Sitar 1995; 1996). The major advantage of renal slices and isolated tubules is that the uptake, exit or accumulation of radioactive substrates can be easily studied under a variety of tightly controlled assay conditions that are not otherwise possible in vivo. For example, assays can be carried out in the presence of higher concentrations of inhibitors, under conditions of membrane depolarization, and with altered medium pH to address substrate specificity and energetics of transport. Proximal and distal convoluted tubules are the main components of renal cortical slices and may have differences in the ability to transport organic substances (Malvin et al., 1958; Rennick and Moe, 1960; Pilkington and Keyl 1963; Vinay et al., 1981; Gesek et al., 1987; Wong et al., 1991). Thus, the use of isolated tubules is advantageous because it allows for the determination of transport properties in specific tubule segments as opposed to cortical slices, which will produce results that represent an overall average of the different tissues that make up the slice. In addition, rates of uptake into cortical slices have been reported to be lower than tubules, and may be due to incomplete penetration of substrate and O_2 into deeper regions of the

32

slice (Wedeen and Weiner, 1973; Wong *et al.*, 1990). Disadvantages of renal tubule suspensions are that proximal tubule suspensions are a mixture of primarily S1 and S2 segments, which may have different transport characteristics. Although we believe the observations using the renal tubule preparations reflect basolateral membrane events, luminal transport may also take place, and may affect the kinetic data and interpretations. For example enhanced efflux across the luminal membrane and inhibition of transport at the basolateral membrane may both be reflected as inhibition of uptake. The isolated renal tubule preparation has been used as the in vitro tissue preparation of choice for the present study.

II.3   *Renal tubule organic anion transport*

Historically, the study of organic anion transport has contributed greatly to the understanding of renal physiology. For example, the first convincing reports that mammalian renal convoluted tubules could secrete organic compounds was demonstrated through renal tubule accumulation and clearance studies of the anion dye phenol red in anaesthetized and conscious dogs (Marshal and Vickers 1923; Marshall, 1931). Several endogenous compounds, including bile acids, cyclic nucleotides, prostaglandins and vitamins, and pharmacological compounds such as antibiotics, diuretics and non-steroidal anti-inflammatory are secreted by the renal tubule organic anion transport system **(table II-1)**. Although the renal tubule organic anion transport system has been deemed multispecific, the majority of organic anion secretion studies have incorporated the compound *p*-aminohippurate (PAH) as the prototypical organic anion substrate. This use stems from the fact that PAH is efficiently secreted; it undergoes limited metabolism and

33

renal tubule reabsorption; and it is easily determined chemically (Moller and Sheikh, 1982). The transport system for PAH has become known as the "classical organic anion transport system". The affinities of substrates for the PAH transport system are influenced by charge density, charge number and by position and placement of hydrophobic regions (Fritzsch *et al.*, 1989)

II.3.a. *Tubule localization of organic anion transport*

Through stop-flow and microperfusion studies in the dog and rat, the proximal tubule has been indicated as the primary site for organic anion secretion (Malvin *et al.*, 1958; Courtney *et al*, 1965). In superficial and juxtamedullary nephrons, axial heterogeneity exists for PAH transport in the different proximal tubule segments. It was first demonstrated that PAH secretion in isolated perfused rabbit proximal tubules was greater in the *pars* recta as compared to the *pars* convoluta (Tune *et al.*, 1969). Subsequent studies then demonstrated that secretion of PAH was much greater in proximal S_2 segments compared to S_1 and S_3 segments which had a similar capacity to secrete PAH (Woodhall *et al.*, 1978). The apparent reason for the different PAH secretory capacity of the different proximal tubule segments, was related to a difference in transporter density in the different segments and not transporter type (Shimomura *et al.*, 1981). No reports of distal tubular organic anion transport have been made.

II.3.b *Mechanisms Mediating organic anion transport*

The classical organic anion transport pathway requires energy to move the organic anion uphill across the basolateral membrane against an inside negative

34

Table II-1: Endogenous and exogenous organic anions that are secreted by the renal tubules.

Endogenous compounds	Xenobiotics	
Bile Acids	**Antibiotics**	
Cholate	Carbenecillin	Penicillin G
Taurocholate	Sulfisoxazole	
Cyclic nucleotides	**Diuretics**	
cAMP, cGMP	Acetazolamide	Bumetanide
Metabolites	Furosemide	Metolazone
Hippurate	**NSAIDS**	
Oxalate	Indomethacin	Phenylbutazone
Prostaglandins	Salicylate	
PGE_2	**Miscellaneous**	
Vitamins	Methotrexate	PAH
Ascorbate	Phenol red	Probenecid
Folate	2,4-Dinitrophenol	

Information for this table was obtained from the following references, (Moller and Sheikh, 1982; Besseghir and Roch-Ramel, 1987; Pritchard and Miller, 1993; Sica and Schoolworth, 1996).

membrane potential. The majority of evidence from isolated basolateral membranes and intact tissue from mammalian and non-mammalian kidney indicates that the mechanism of basolateral entry of organic anions is a tertiary active process that is indirectly coupled to Na^+ transport (Pritchard, 1987; Shimada *et al.*, 1987; Pritchard and Miller, 1993; Sweet *et al.*, 1997). In the first step of this model (**fig. II-2**) ATP is hydrolyzed to drive electrogenic $3Na^+/2K^+$ exchange, creating a concentration difference for Na^+ (out > in). The resulting Na^+ concentration difference drives the transport of one dicarboxylate anion across the basolateral membrane in exchange for one Na^+ creating an in > out anion concentration difference (site 2). In the final step (site 3), the downhill transport of the dicarboxylate anion out of the cell stimulates the uphill transport of an organic anion (e.g. PAH) into the cell. The net anionic charge moving into the cell in step 2 is counteracted by the net anionic charge moving out of the cell in step 3 and results in an overall electroneutral process for organic anion transport across the basolateral membrane. Based on its abundance, α-ketoglutarate is the most likely endogenous dicarboxylate that drives the PAH organic anion transport process (Pritchard and Miller, 1993). Once within the cell, organic anions may be sequestered (site 4) within vesicular structures or bind to intracellular proteins (Holohan *et al.*, 1975; Miller *et al.*, 1993). Transport of the organic anion across the luminal membrane is the final step in secretion and is a mediated process. Initial studies performed using brush border membrane vesicles from rat and dog indicated the presence of a potential sensitive, saturable, probenicid-inhibitable, transporter for PAH transport across this membrane (site 5) (Berner and Kinne, 1976; Kinsella *et al.*, 1979a). How electroneutrality is maintained at this site has not been established. An electroneutral anion/anion exchanger (site 6) is also present in the

36

luminal membrane, and may mediate secretion or reabsorption of organic anions such as urate and PAH in exchange for hydroxyl or bicarbonate ions (Blomstedt and Aronson, 1980; Pritchard and Miller, 1993).

II.4   *Renal tubule organic cation transport*

The renal tubule secretion of organic cations was first demonstrated through renal excretion studies of TEA in dogs and humans (Rennick *et al.*, 1947; Rennick and Farrah, 1956, Rennick *et al.*, 1956) and N^1-methylnicotinamide (NMN) in the chicken and dog (Sperber, 1949; Beyer *et al.*, 1950; Peters *et al.*, 1955). Transport maximum for TEA and inhibition of renal excretion of TEA and NMN by cyanine863 were demonstrated, indicating that a carrier mediated transport process was responsible for the secretion of these two compounds (Peters *et al.*, 1955; Rennick and Farrah, 1956; Rennick *et al.*, 1956). In addition, both compounds appeared to describe a renal tubule secretion mechanism that was different from that of the prototypical organic anion (PAH) secretion system, as evidenced by the inability of PAH to inhibit NMN and TEA renal excretion (Peters *et al.*, 1955; Rennick and Farrah, 1956). This pathway has now become known as the "organic cation transport system". Since these early studies, TEA and NMN have gained the status of prototypical substrates for the characterization of renal tubule organic cation transport mechanisms, with TEA being used most frequently.

Although TEA has been used most often for organic cation transport studies, renal tubule organic cation transport has been demonstrated to play an important role in the renal handling of many other important endogenous and exogenous cationic compounds.

37
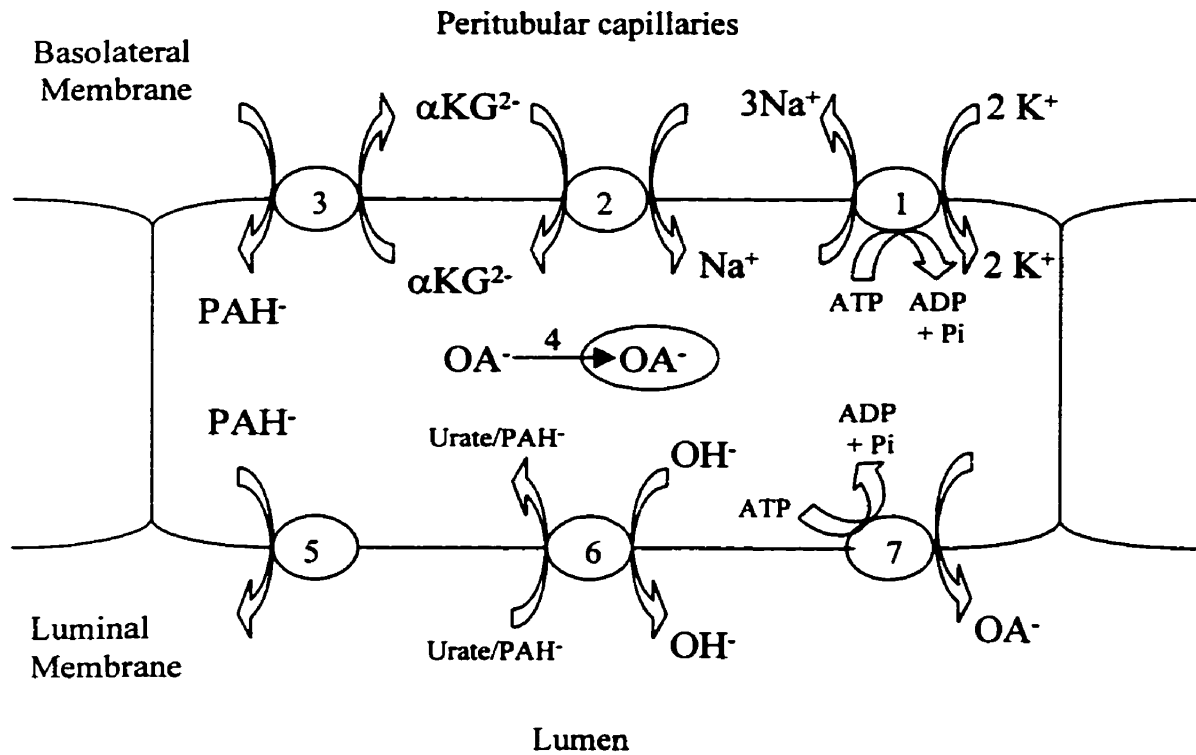
Figure II-2: Current model of organic anion transport in the renal proximal tubule as adapted and modified from Sweet *et al.*(1997).

The group of endogenous compounds (**table II-2**) includes several biogenic amines, acetylcholine and endogenous cationic metabolites (Beyer *et al.*, 1950; Peters, 1960; Quebbemann and Rennick; 1969; Acara and Rennick, 1972a; Acara and Rennick, 1972b; Rennick, 1981; Pritchard and Miller, 1993). The group of exogenous compounds (**table II-2**) comprises several that are therapeutically used, including antiviral agents, anticholinergic agents, H_2 receptor blockers, sympathomimetic agents, opioids, antiarrhythmic agents, α and β–adrenergic receptor blocking agents, diuretic agents and ganglionic blocking agents (Rennick and Moe, 1960; Pilkington and Keyl, 1963; Acara and Rennick, 1972b; Aoki *et al.*, 1979; Weiner and Roth, 1981; Rennick, 1981; McKinney and Speeg, 1982; Pritchard and Miller, 1993; Ullrich *et al.*, 1993a, 1993b). These compounds represent many structurally different classes of molecules and all are primary, secondary, or tertiary amines or quaternary ammonium salts, and most are positively charged at physiological pH. The apparent structural requirements that are required for a substrate to be transported by this system are the presence of a hydrophobic organic backbone and a charged nitrogen group (Rennick, 1981, Ullrich *et al.*, 1991). Substrate affinity for the organic cation transporters increase with increasing hydrophobicity and increased pKa (Ullrich, 1994). There are exceptions to this rule, as several non-ionizable steroid hormones interact with this system, indicating that H-bonding groups on the substrate also affect affinity for the transporters (Ullrich *et al.*, 1993b, Ullrich, 1994).

Table II-2: Endogenous and exogenous organic bases that are secreted by the renal tubules.

Endogenous Substances
1) **Monoamine neurotransmitters:** acetylcholine, dopamine, epinephrine, histamine and 5-hydroxytryptamine
2) **Metabolites:** choline, creatinine and NMN
3) **Vitamins:** riboflavin and thiamine

Xenobiotics
1) **Anticholinergic agents:** atropine 2) **Antiviral agents:** amantadine
3) **Antibiotics:** trimethoprim
4) **Antiarrhythmic agents:** procainamide, quinidine and verapamil
5) **β-adrenergic receptor blockers:** pindolol, nadolol
6) **Diuretics:** amiloride, triamterene 7) **Ganglionic blocking agents:** TEA
8) **Opioids:** morphine, meperidine and dihydromorphine
9) **Sympathiomimetic agents:** ephedrine and isoproterenol
10) **Miscellaneous:** cisplatin, gaunfacine, mepiperphenidol and quinine

Information for this table was obtained from the following references, (Beyer *et al.*, 1950; Peters, 1960; Rennick and Moe, 1960; Pilkington and Keyl, 1963; Quebbemann and Rennick, 1969; Acara and Rennick, 1972a, 1972b; Aoki and Sitar, 1979; Rennick, 1981; Weiner and Roth, 1981; McKinney and Speeg, 1982; Pritchard and Miller, 1993; Ullrich *et al.*, 1993a, 1993b).

II.4.a *Tubule localization of organic cation transport*

Original stop-flow excretion studies using TEA, mepiperphenidol and mecamylamine as organic cation substrates suggested that the proximal tubule is the location in the nephron where organic cation secretion is primarily mediated (Rennick and Moe, 1960; Pilkington and Keyl 1963). In the Pilkington and Keyl report (1963), the authors claim that secretion of mecamylamine and mepiperphenidol occur in the proximal tubule; however, their data do suggest a smaller distal tubule contribution to secretion. Based on the results of these studies, it has been generally accepted that the proximal tubule is the only component of the nephron that has the capacity for transport and secretion of organic cations. Thus, most subsequent in vitro studies of organic cation transport have been performed in tissue preparations of the proximal tubule. Aside from the proximal tubules, little attention has been given to the distal tubules or other portions of the nephron and their ability to transport organic cationic compounds. However, previous studies from our laboratory have demonstrated that the distal tubule is an important site of organic cation transport (Wong *et al.*, 1991, 1992a, 1992b, 1993; Escobar *et al.*, 1994, 1995; Escobar and Sitar 1995, 1996). The presence of distal tubule organic cation transporters is further supported by recent molecular biology evidence which demonstrates the presence of mRNA transcripts of the cloned human (hOCT2) and rat (rOCT2) organic cation transporters in the distal tubule (Gorboulev *et al.*, 1997; Koepsell *et al.*, 1998). In the proximal tubule, there also exists axial heterogeneity of secretion of certain organic cations in different segments of the tubule. TEA and procainamide are secreted primarily in the early segments of the proximal tubule (S1 > S2 > S3), and NMN in the later portions of the proximal tubule (S1 < S2 = S3)

41

(McKinney, 1982; Schali *et al.*, 1983; Besseghir *et al.*, 1990). The difference in secretory rate between the three proximal tubule segments has been attributed to differences in luminal membrane permeability (Schali *et al.*, 1983). It should be pointed out that the data for TEA are inconsistent with the stop-flow studies performed by Rennick and Moe (1960) which suggests that the major site of TEA secretion is distal to the major site of PAH secretion (S_2 segments).

II.4.b   *The classical organic cation secretion pathway*

fig II-3 outlines the steps involved in the generally accepted model of renal tubule organic cation secretion in the proximal tubule. The net secretion process involves transport steps across the basolateral and luminal membranes of the proximal tubules. Experiments studying TEA and NMN transport using isolated basolateral membrane segments demonstrated that the first step in the classical organic cation secretion pathway (passage across the basolateral membrane) is via a saturable carrier-mediated process (transport site 2) (Kinsella *et al.*, 1979a; Takano *et al.*, 1984 Montrose-Rafizadeh *et al.*, 1989). Uptake of organic cations across the basolateral membrane via this transporter is independent of Na^+ concentration in the medium and extracellular pH. The driving force for transport is the inside negative membrane potential that is maintained by the Na^+/K^+ ATPase (transport site 1) (Takano *et al.*, 1984; Wright and Wunz, 1987; Jung *et al.*, 1989; Ullrich *et al.*, 1991). In addition, an organic cation/organic cation exchange system (transport site 3) in the basolateral membrane has also been reported (Montroze-Rafizadeh *et al.*, 1989; Sokol and McKinney, 1990; Dantzler *et al.*, 1991). However, the facilitated transport mechanism and the exchange transport mechanism may represent

dual functional modes of the same transporter rather than two separate carriers with different energetics (Montrose-Rafizadeh *et al.*, 1989; Sokol and McKinney, 1990). The existence of an organic cation/organic cation exchange transporter would appear to be counterproductive in regards to secretion. However, it would be of significance to both reabsorption and secretion of organic cations if it coupled the elimination of harmful cationic xenobiotics or metabolites to the reabsorption of useful endogenous cations. Once in the cell, it has been reported that organic cations may undergo intracellular accumulation or protein binding (site 4) (Pritchard and Miller, 1993; Pritchard *et al.*, 1994). In the final step of secretion, the organic cation passes across the luminal membrane from the cell to the lumen. There are several reports indicating that the transport processes in the luminal and antiluminal membranes differ with respect to mechanism of action and in substrate specificity (Kinsella *et al.*, 1979a; Holohan and Ross, 1980; Takano *et al.*, 1984; Wright and Wunz, 1987; Jung *et al.*, 1989). In the classical organic cation transport pathway, the Na^+/K^+-ATPase (transport site 1) creates a favorable gradient for Na^+/H^+ exchange in the luminal membrane (transport site 5). The resulting proton gradient (pH lumen $\rightarrow$ pH cell) then drives the extrusion of the organic cation from the cell by the action of the saturable H^+/organic cation exchanger (transport site 6) (Takano *et al.*, 1984; Wright and Wunz, 1988; Rafizadeh *et al.*, 1987). Overall this is a tertiary active transport process. This luminal transport process has been demonstrated for a variety of organic cations including TEA, NMN, procainamide and cimetidine, primarily using luminal membrane vesicle preparations from dogs and rabbits (Kinsella *et al.*, 1979a; McKinney and Kunnemann, 1985; Sokol *et al.*, 1985; McKinney and Kunnemann, 1987; Rafizadeh *et al.*, 1987; Wright and Wunz, 1987).

Also shown in this model is the ATP-dependent P-glycoprotein or multidrug resistant protein (transport site 7). In the human kidney P-glycoprotein is localized to the luminal membrane in renal proximal tubules and distal nephron segments, including the collecting ducts and thick ascending limb of Henle's loop (Thiebaut *et al.*, 1987; Ernest *et al.*, 1997). Some transported substrates include the endogenous steroids cortisol, aldosterone, and dexamethasone (Ueda *et al.*, 1992), the cardiac glycoside digoxin (de Lannoy and Silverman,1993) and several lipophilic cationic drugs including daunomycin, colchicine, verapamil, procainamide, quinidine, cimetidine and vinblastine (Beck, 1987; Speeg *et al.*, 1992; Dutt *et al.*, 1994). Based on its location in the luminal membrane and its substrate specificity, P-glycoprotein has been proposed to be important in the renal secretion of certain organic cationic compounds (Thiebaut *et al.*, 1987; Nelson, 1988). As indicated in the above list and in **table II-2**, P-glycoprotein can transport similar substrates as the classical luminal organic cation transporter. However, P-glycoprotein and the luminal organic cation transporter have been confirmed as separate entities based on differences in energetics mediating transport by each system and the observation that TEA is a substrate for the organic cation transport system but not P-glycoprotein (Dutt *et al.*, 1994; Nelson *et al.*, 1995). Organic cations may also be reabsorbed in the renal tubules (transport site 8), thereby preventing the urinary excretion of important physiological molecules such as monoamine neurotransmitters and choline (Koepsell, 1998).
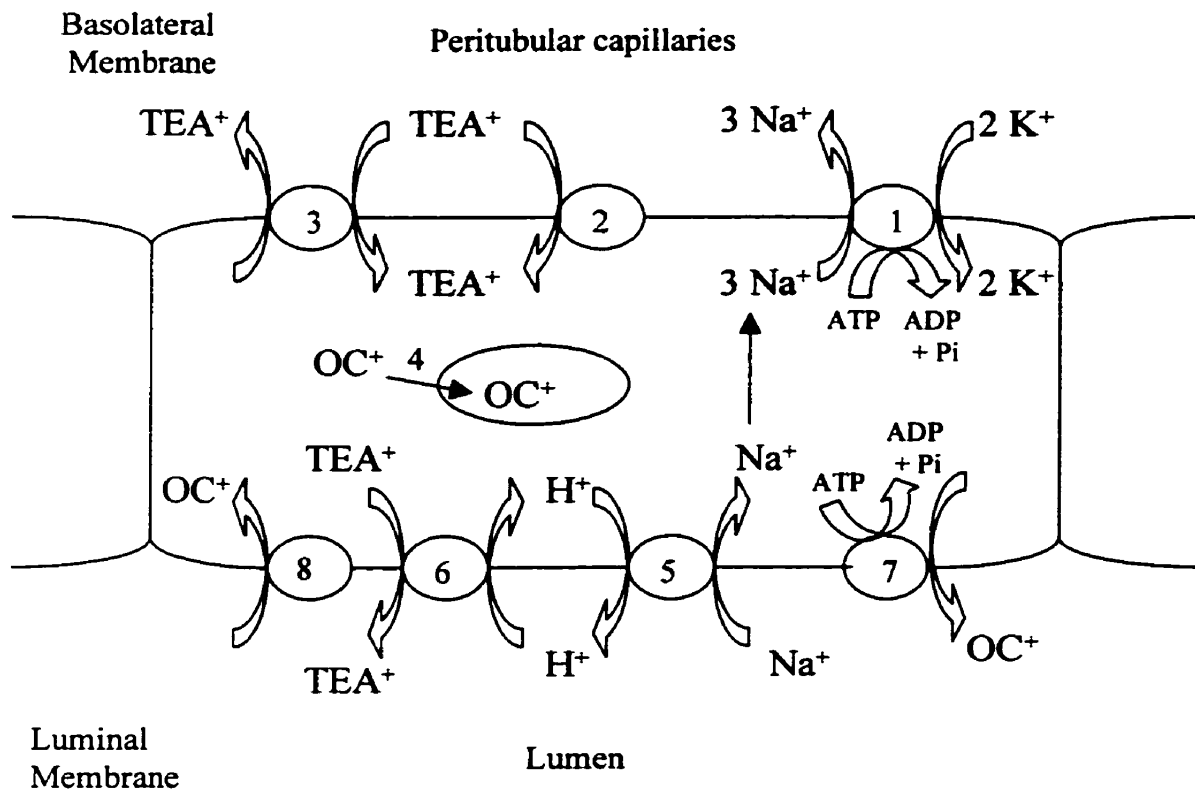
Figure II-3: Classical model of organic cation transport in the renal proximal tubule as adapted and modified from Pritchard and Miller (1993) and Koepsell (1998).

II.4.c *Amantadine as a substrate for renal tubule organic cation transport studies*

Unique to our laboratory, amantadine has been used as a prototype organic cation for characterizing mechanisms that mediate organic cation secretion by the kidney. Amantadine has several properties that make it useful in this regard. It is a nonchiral, primary, aliphatic amine, and exists primarily in the cationic form at physiological pH (pKa = 10.2). It is used therapeutically in the treatment of Parkinson's disease and for prophylaxis against influenza A (Shwab *et al.*, 1969; Parks, 1974; Aoki and Sitar, 1988). In humans, amantadine is eliminated primarily unchanged by the kidney and renal tubule secretion is important in this process (Bleidner *et al.*, 1965; Tilles, 1974; Aoki *et al.*, 1979; Sitar *et al.*, 1997).

From the known data on amantadine renal tubule transport (Wong *et al.*, 1990,1991,1992a 1992b, 1993; Escobar *et al.*, 1994, 1995; Escobar and Sitar, 1995, 1996), we proposed an alternative model to describe the renal tubule energy dependent transport of organic cations **fig. II-4**. The basolateral membrane transport sites for energy-dependent amantadine uptake in proximal tubules can be subdivided into bicarbonate-dependent sites (high-affinity, high-capacity) which are responsible for the majority of amantadine uptake, and less efficient bicarbonate-independent sites (lower-affinity, lower-capacity) (Escobar *et al.*, 1994, Escobar and Sitar, 1995). The bicarbonate-dependent and bicarbonate-independent transport sites are represented by transport site 2 and 3 respectively in **fig. II-4**. Membrane potential and activity of the basolateral membrane Na^+/K^+-ATPase are not rate limiting for the renal tubule uptake of amantadine (Escobar and Sitar, 1995; Escobar and Sitar 1996). These findings suggest

that the majority of amantadine uptake occur as a nonelectrogenic step at the basolateral membrane as opposed to electrogenic uptake demonstrated for TEA. If bicarbonate were transported into the cell along with amantadine, an electroneutral process for amantadine uptake would be maintained. However, this remains to be demonstrated experimentally. Acetozolamide did not inhibit bicarbonate-dependent amantadine uptake suggesting that luminal bicarbonate was not important for the observed effect on amantadine transport (Escobar *et al.*, 1994). The $Na^+/HCO_3^-/CO_3^{2-}$ transporter and the Cl^-/HCO_3^- exchanger (not shown) are basolateral membrane transporters normally involved in bicarbonate reabsorption process along the nephron (Alpern and Preisig, 1997). The $Na^+/HCO_3^-/CO_3^{2-}$ transporter exists in proximal tubules and the thick ascending limb of Henle's loop, whereas various isoforms of Cl^-/HCO_3^- exchangers have been identified in proximal and distal regions of the nephron (Seki *et al.*, 1996; Soleimani and Bizal, 1996; Alpern and Preisig, 1997). 4-acetamide-4'-isothiocyanatostilbene-2-2'-disulfonic acid (SITS) is an inhibitor of the $Na^+/HCO_3^-/CO_3^{2-}$ transporter and Cl^-/HCO_3^- exchanger (Alpern and Preisig, 1997). In proximal tubules SITS only weakly inhibited (20%) bicarbonate-dependent amantadine uptake and more potently inhibited (75%) distal tubule amantadine uptake (unpublished observations). These data suggest that the Cl^-/HCO_3^- exchanger and the $Na^+/HCO_3^-/CO_3^{2-}$ transporter may play a role in maintaining electroneutrality in the bicarbonate-dependent amantadine transport process, but the exact relationship must be further evaluated. At this time, the driving force for the bicarbonate-independent amantadine transport site has not been identified. The bicarbonate-dependent and independent transport sites may be further identified by their differences in sensitivity to inhibition by other compounds. For instance, quinine has a more potent K_i value for

47

inhibition of amantadine uptake via bicarbonate-dependent transport sites as opposed to the bicarbonate-independent transport sites (Escobar and Sitar, 1995). Second, the cardiac glycoside ouabain inhibits bicarbonate-dependent amantadine transport but not bicarbonate-independent transport (Escobar and Sitar, 1996). At this time, it was also not known whether the basolateral transporters described by amantadine are the same as those described by TEA.

Although mechanisms of amantadine basolateral membrane transport in the distal tubule are similar to the proximal tubule (fig. II-4), several notable differences exist. For example, stereoselective inhibition of amantadine uptake by quinine more potent than its enantiomer quinidine is present in proximal tubules but not distal tubules (Escobar and Sitar, 1995). Second, low concentrations of the organic cations cimetidine, nicotine and cotinine stimulate proximal tubule uptake but not distal tubule uptake of amantadine (Wong et al., 1991, 1992b). Third, ouabain more potently inhibits distal tubular amantadine uptake (Escobar and Sitar, 1996). Finally, these data further indicate the purity of the proximal and distal tubule segments that are used in the transport assays.

The basolateral membrane amantadine transporters appear to be multispecific in terms of their substrate specificity as identified by uptake inhibition studies. Several pharmacologically important organic cations interact with the basolateral membrane amantadine transporters, including quinine and quinidine (Wong et al., 1990, 1992a, 1993; Escobar and Sitar, 1995), cimetidine and ranitidine (Wong et al., 1991), nicotine and cotinine (Wong et al., 1992b), several β–blockers (Stupack et al., 1999) and
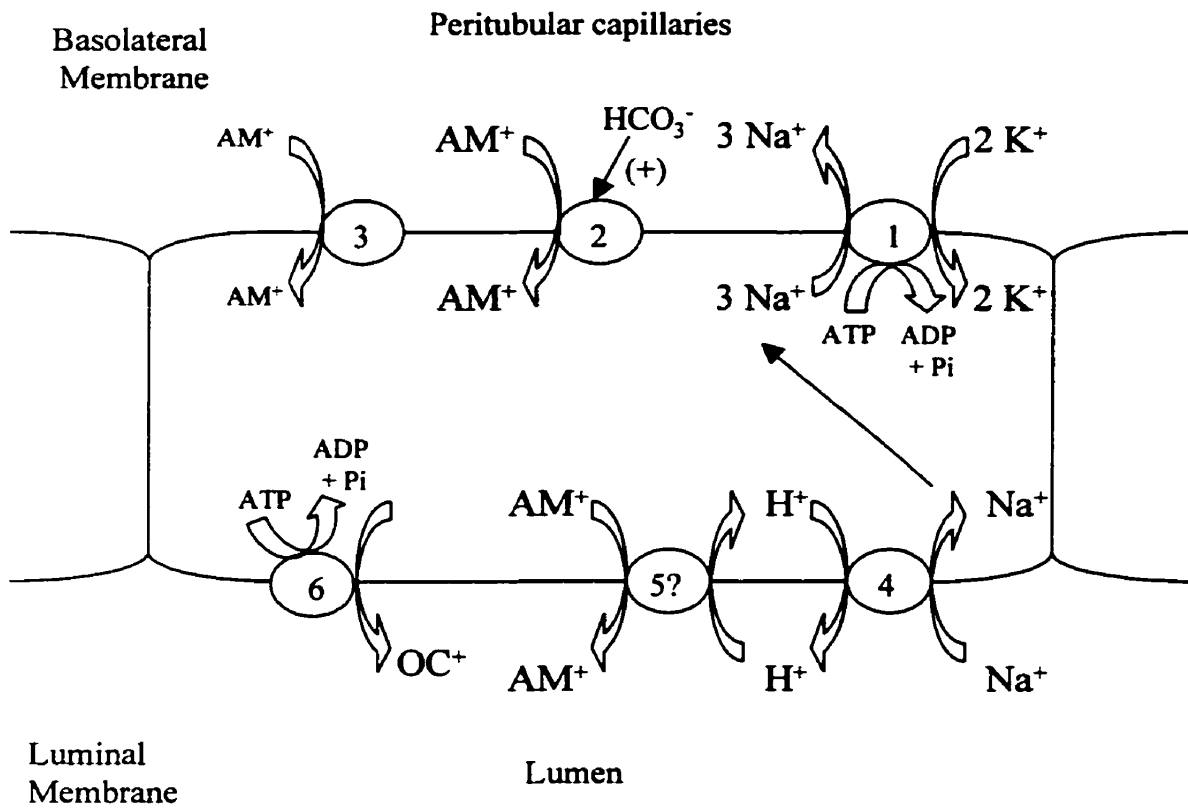
Figure II-4: Renal proximal tubule organic cation secretion model as developed using the organic cation amantadine (Escobar *et al.*, 1994).

verapamil (unpublished data). The fact that many other organic cations interact with the amantadine may translate into clinically important drug interactions in the kidney and possibly altered drug elimination rates. For example, the in vivo observation that both quinine and quinidine administration reduce the rate of renal elimination of amantadine in human males may be explained by drug-drug interactions at the level of the basolateral membrane amantadine transporter (Gaudry *et al.*, 1993). Second, the renal elimination of amantadine in an elderly male was reportedly decreased and amantadine toxicity was observed (ataxia, agitation) by concurrent ingestion of the cationic diuretic triamterene (Wilson and Rajput, 1983). The bicarbonate-dependent basolateral transport and renal elimination of amantadine is also inhibited by pathophysiological levels of the endogenous organic anion L-lactate (Escobar *et al.*, 1995; Sitar *et al.*, 1997). This interaction may have clinical importance in modulating renal elimination of organic cations in metabolic acidosis due to the accumulation of L-lactic acid (Escobar *et al.*, 1995). Bulky uncharged compounds may also interfere with amantadine renal tubule transport as demonstrated by the sensitivity of bicarbonate-dependent amantadine transport by the cardiac glycoside ouabain (Escobar and Sitar, 1996).

The mechanisms mediating the brush border transport of amantadine have not been examined extensively. Thus, it is not known if exit of amantadine across the brush-border is mediated by the classical organic cation/proton exchanger (transport site 5), P-glycoprotein (transport site 6), other unidentified transport sites, or a combination of these processes.

50

The amantadine transport experiments described in the previous paragraphs have been carried out primarily in male rats. Thus extrapolation of these data to the female gender and to humans are important concerns. Studies of amantadine uptake in renal tubules from female rats demonstrate that there are gender differences in kinetic parameters for distal tubule uptake of amantadine compared to males (Wong et al., 1993). More recently amantadine uptake studies in the presence of lactate unmask gender differences in renal proximal tubule amantadine transport (Bobby and Sitar, 1997). In humans, renal clearance of amantadine is about 1.5 times greater in males than in females and may be related to the gender differences in tubule transport mechanisms (Wong et al., 1995). Clinically, the sex difference in renal amantadine transport and clearance may contribute to the observation that adverse events associated with therapeutic amantadine doses are higher in females than males (Somani et al., 1991). A second important gender difference in renal amantadine elimination in humans is that quinine and quinidine inhibit amantadine renal elimination in males but not females (Gaudry et al., 1993). In regard to extrapolation of findings from rat to human, amantadine transport and accumulation and sensitivity to inhibition by the diastereomers quinine and quinidine have been demonstrated to be qualitatively similar in renal cortical slices from male rats and humans (Wong et al., 1990, 1992b). These finding support the continued use of the rat as a model for organic cation transport studies using amantadine.

Part III. Molecular biology of organic anion, cation and neutral drug transporters

In recent years, the molecular cloning and functional characterization of proteins that mediate the transport of drugs and endogenous compounds across cell membranes

have been a dominant area of focus in studies of organic anion and cation transport. The molecular information has great potential to advance the understanding of whole-body drug disposition, drug elimination by the kidney and liver, and access or removal of drugs to and from other tissues. Several families of drug transporters have now been identified in a variety of mammalian species, and have been at least partially characterized with respect to tissue location, substrate specificity and function. The objective of this section is to summarize and clarify the rapidly accumulating experimental molecular data and carefully interpret it with respect to drug transporter function in vivo.

III.1   *The organic anion transporter (OAT) family*

In 1997 two organic anion transporters (OAT1 and ROAT1) were cloned and functionally studied simultaneously by two independent laboratories (Sekine *et al.*, 1997; Sweet *et al.*, 1997). Both groups isolated and cloned cDNA from rat kidney that codes for an identical 551 amino acid peptide with 12 putative transmembrane domains. Northern blot analysis revealed that the mRNA expression was restricted to the kidney. Sekine and coworkers further localized mRNA expression of OAT1 to the convoluted portion of the proximal tubule, which is consistent with the location of the classical PAH secretion machinery (Tune *et al.*, 1969; Sekine *et al.*, 1997). When expressed in Xenopus oocytes, both groups demonstrated saturable uptake of PAH with similar K_m values. Transport was not dependent on membrane potential, and could be stimulated by an outwardly directed dicarboxylate gradient, suggesting that OAT1 and ROAT1 identify the electroneutral basolateral membrane PAH/dicarboxylate exchanger (**fig. II-2**). OAT1 was demonstrated to transport known substrates of the PAH/dicarboxylate exchanger

including methotrexate, cAMP, cGMP, PGE_2, urate and α-ketoglutarate and both OAT1 and ROAT1 were inhibited by the classical organic anion transport inhibitor probenecid. Overall, these initial molecular data provide evidence that OAT1 and ROAT1 were identical transport proteins. Functionally ROAT1 and OAT1 most closely resemble the putative proximal tubule basolateral membrane PAH/dicarboxylate transporter and are thus likely important in renal secretion of organic anions by the kidney.

Proteins from the OAT family have also been cloned from other species including mouse and human and from other tissues in the rat. In the mouse, a protein (NKT) that is expressed in the kidney and is highly homologous to ROAT1 has been cloned. It has been suggested that NKT is the mouse equivalent of ROAT1 because of the highly similar amino acid sequence of these transporters. However, initial functional studies in NKT-expressing Xenopus oocytes have failed to demonstrate that it can mediate uptake of PAH (Lopez-Nieto *et al.*, 1997; Sweet *et al.*, 1997). More recently, an OAT2 has been cloned from rat liver (Sekine *et al*, 1998). OAT2 appears to be identical to the previously cloned novel liver transporter (NLT) which was not previously characterized with respect to its ability to transport organic compounds (Simonson *et al.*, 1994; Sekine *et al*, 1998). OAT2 is highly homologous to OAT1, and has similar functional characteristics; however, its mRNA is expressed to a greater extent in the liver than in the kidney. OAT2 is thought to be responsible for mediating sinusoidal uptake of organic anions into hepatocytes in the liver.

In humans, the molecular cloning and functional expression of two highly similar human kidney organic anion transporters (hOAT1 and hPAHT) have also been achieved recently by two groups (Lu *et al.*, 1999; Hosoyamata *et al.*, 1999). When expressed in Xenopus oocytes, both transporters mediate PAH uptake. Like OAT1, hOAT1 and hPAHT mRNA was strongly expressed in the kidney. Unlike OAT1, hOAT1 mRNA was also detected in skeletal muscle, brain and placenta, and hPAHT mRNA was detected in the brain, suggesting the importance of organic anion transporters in mediating access or extrusion of drugs in other tissues of the body. In the kidney, immunohistochemistry reveals that hOAT1 protein is detected in the basolateral membrane of proximal tubules, and is consistent with the location of the PAH/dicarboxylate exchanger. Similar to OAT1, hOAT and hPAHT-mediated PAH uptake could be inhibited by a variety of other organic anions. Overall hOAT1 and hPAHT are likely identical proteins based on their amino acid sequence and functional characteristics. Both appear to be the functional equivalent of OAT1 in rat, although some differences in substrate specificity have been reported to exist between hPAHT and OAT1 (Hosoyamata *et al.*, 1999).

III.2 The organic anion transport polypeptide (oatp)

The oatp transporters are a family of Na^+ independent organic anion transporters that are about 670 amino acids in length and have 12 predicted transmembrane segments. Presently, three members (oatp1, oatp2 and oatp3) of the oatp gene family have been isolated from rat tissues, cloned and studied in vitro (Jacquemin *et al.*, 1994; Noe *et al.*, 1997; Abe *et al.*, 1998; Kakyo *et al.*, 1998). Oatp1 mRNA is detected in several tissues

in rat, including liver, kidney, brain, lung, skeletal muscle and large intestine (Jacquemin et al., 1994). In the liver, oatp1 is located in the sinusoidal (basolateral) membrane whereas in the kidney, oatp1 is located on the luminal membrane in S_3 segments of the proximal tubule (Bergwerk et al., 1996; Eckhardt et al, 1999). When expressed in Xenopus oocytes, oatp1 mediates the uptake of several exogenous and endogenous organic acids (sulfobromophthalein, bile acids, estrogen conjugates), neutral steroids (aldosterone, dexamethasone, digoxin and ouabain) and some bulky cationic compounds (Jacquemin et al., 1994; Bossuyt et al., 1996; Kanai et al., 1996; Eckhardt et al, 1999). Several substrates of the classical organic anion transport pathway, including PAH and phenol red, failed to inhibit oatp mediated transport of sulfobromophthalein, indicating that the oatp transporters are unique in their substrate specificity compared to the OAT transporters (Kanai et al., 1996). Based on the location of oatp protein in the liver and its substrate specificity, oatp is thought to be important in the sinusoidal uptake and hepatic clearance of endogenous neutral steroid molecules and anionic bile acids (Jacquemin et al., 1994; Bossuyt et al., 1996). In the kidney, the luminal oatp transporter may be important in the secretion or reabsorption of bile acids or anionic conjugates that are handled by this transporter; however, the exact function is not known (Kanai et al., 1996). Oatp2 tissue distribution is restricted to the liver, kidney and brain, and it transports similar substrates compared to oatp1 (Noe et al., 1997). However, unlike oatp1, oatp2 has a very high affinity for digoxin, about 0.2 μM, and may be important in brain CNS accumulation and toxicity of digoxin (Noe et al., 1997).

III.3   *The organic cation transporter (OCT) family*

Recent studies have identified a new family of proteins (OCTs) that have the ability to mediate the electrogenic transport of organic cations across cell membranes. The organic cation transporters (OCTs) belong to a superfamily of proteins that includes multi-drug resistance proteins, facilitative diffusion systems and proton/cation antiporters (Koepsell, 1998). The first transporter to be identified from this family was rOCT1, which was cloned from rat kidney and studied in the Xenopus oocytes expression system (Grundemann *et al.*, 1994). Soon after, structurally homologous proteins with similar properties to rOCT1 were cloned from rat (rOCT1a, rOCT2 and rOCT3), from rabbit (rbOCT1), from the pig kidney proximal tubule cell-line LLC-PK$_1$ (pOCT2), and human (hOCT1 and hOCT2) (Okuda *et al.*, 1996; Grundemann *et al.*, 1997; Gorbulev *et al.*, 1997; Zhang *et al.*, 1997a, 1997b; Kekuda *et al.*, 1998; Terashita *et al.*, 1998). The OCTs are between 553-600 amino acids in length with either 11 or 12 predicted transmembrane helical segments, a large extracellular loop, a large intracellular loop and intracellular NH$_2$ and COOH termini, (fig. III-1). The one exception, rOCT1a, appears to be a splice-variant of rOCT1 and has 430 amino acids and 10 predicted transmembrane domains (Zhang *et al.*, 1997a). The OCTs contain several conserved intracellular phosphorylation sites that may be important in the regulation of transporter function. In fact, it has been demonstrated that inhibitors of protein kinase C can modulate renal tubule organic cation transport in rabbit proximal tubules and a cell line (LLC-PK$_1$) of proximal tubule origin (Hohage *et al.*, 1994, 1998).
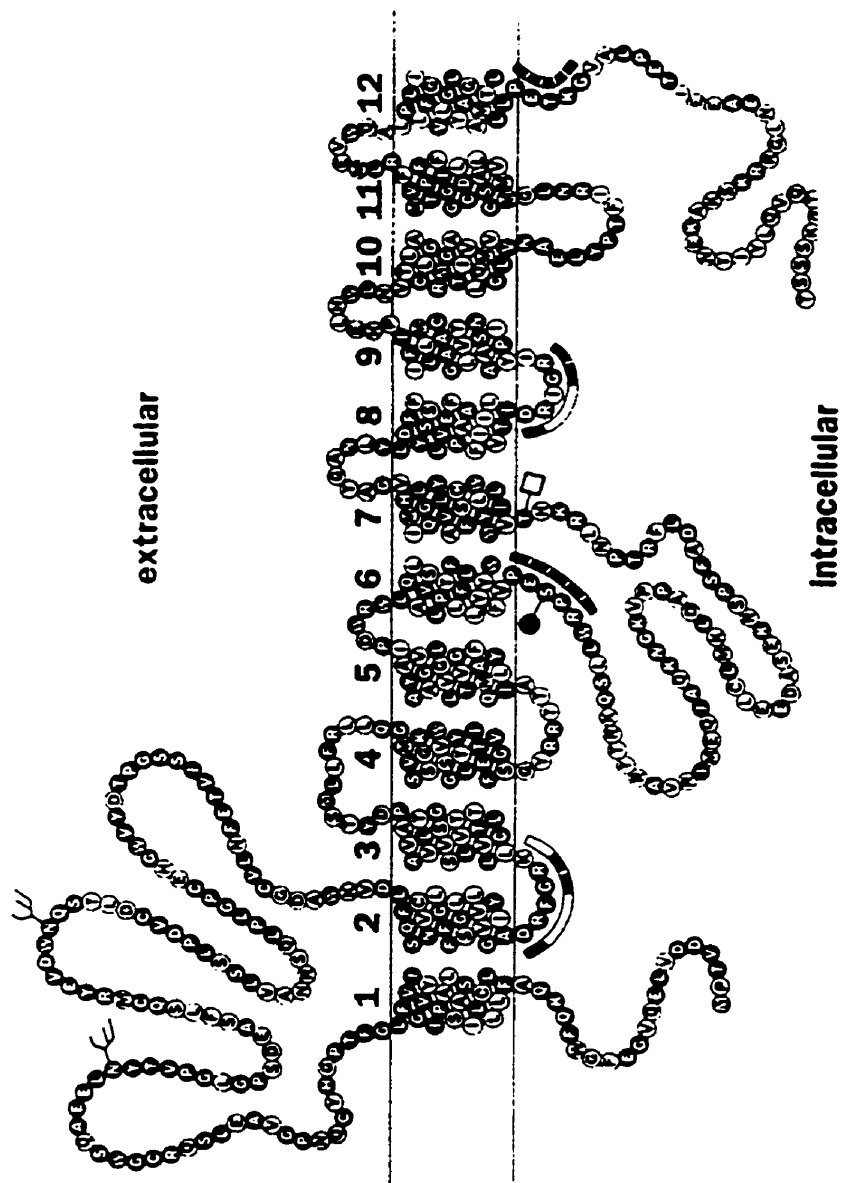
Figure III-1: The primary sequence and proposed membrane topology of rOCT1. Aminoacids that are conserved between rOCT1, rOCT2, mOCT1, hOCT1, hOCT2 and OCT2p are shown in black. Two conserved potential glycosylation sites are marked with a fork. Conserved protein kinase C- and A-dependent phosphorylation sites are marked by a filled circle and an open square respectively (Koepsell 1998).

III.3.a *Tissue distribution of organic cation transporters*

The known members of the OCT family all appear to have unique tissue distribution.

Notable differences also exist between the tissue distribution of the rat OCTs compared to

their human homologues (Zhang *et al.*, 1997b; Koepsell, 1998). Northern blot analysis and

reverse transcriptase PCR have been used to determine which tissues contain OCT mRNA,

and in situ hybridization has been used to detect tissue-specific location of OCT mRNA

expression. It should be kept in mind that mRNA expression does not predict protein level or

location; therefore, until protein can be determined immunochemically, the interpretation of

the presence or absence of specific mRNA in certain tissues should be interpreted with

caution. rOCT1 mRNA is detected in samples of kidney cortex and medulla, liver, intestine

and colon of the rat. Conversely, in peripheral tissues, rOCT2 mRNA expression is confined

to cortex and medulla of the kidney as determined by Northern blot after PCR amplification

(Okuda *et al.*, 1996). More recently, rOCT2 mRNA has also been detected in various

regions of the rat brain, including the nucleus accumbens, substantia nigra and the striatum

(Grundemann *et al.*, 1997). In the liver and small intestines, rOCT1 mRNA is expressed in

hepatocytes and enterocytes respectively (Grundemann *et al.*, 1994). In the kidney, the exact

locations in which these proteins are expressed are questionable. The available data show the

rOCT1 mRNA is detected in proximal tubules, glomeruli and cortical collecting ducts, but

not distal tubules, whereas rOCT2 is transcribed in all of the above mentioned segments

(Grundemann *et al.*, 1994; Koepsell, 1998). By immunohistochemical detection, rOCT1

protein is detected in the basolateral membrane of proximal tubules and in the sinusoidal

membrane of hepatocytes (Meyer-Wentrup *et al.*, 1998; Urakami *et al.*, 1998). rOCT3

mRNA is most abundantly expressed in the placenta, moderately expressed in the intestine,

heart and brain, weakly expressed in the kidney and lung, and is undetectable in the liver by Northern blot analysis (Kekuda *et al*, 1998). The human organic cation transporter hOCT1 is transcribed ubiquitously, and hOCT2 is transcribed in the kidney, brain, spleen, placenta and intestine (Gorboulev *et al.*, 1997). Interestingly, hOCT mRNA transcripts are found in the distal tubules and were located in the luminal membrane by immunochemical methods (Gorboulev *et al.*, 1997).

III.3.b *Functional characteristics*

Similar to the classical studies of organic cation transport, TEA has been predominantly used as the prototype organic cation for the functional characterization of the cloned OCTs. When the OCTs are expressed in Xenopus oocytes or cell lines, they mediate the saturable uptake of TEA with widely varying values of K_m (**table III-1**). The 10-fold difference in K_m for TEA uptake mediated by rOCT2 expressed in Xenopus oocytes versus MDCK cells (Madin-Darby canine kidney cells) suggests that the choice of cell expression system may dramatically affect K_m values for organic cation transport. The OCT mediated uptake of TEA is dependent on membrane potential and is independent of Na^+ and extracellular pH. These properties are all characteristic of the classical proximal tubule basolateral membrane organic cation transporter (Takano *et al.*, 1984; Wright and Wunz, 1987; Jung *et al.*, 1989; Ullrich *et al.*, 1991). Detailed functional studies demonstrate that rOCT1, rOCT2 and hOCT2 expressing Xenopus oocytes can mediate the uptake of several substrates for the classical organic cation transport system including MPP, NMN, choline, dopamine, (Martel *et al.*, 1996; Busch *et al.*, 1996a, 1996b; Gorboulev *et al.*, 1997; Koepsell *et al.*, 1998; Busch *et al.*, 1998; Okuda *et al.*, 1999). In

addition, rOCT1 mediates uptake of serotonin, acetylcholine and epinephrine (Busch *et al.*, 1996b) and hOCT2 mediates uptake of serotonin, histamine and norepinephrine (Busch *et al.*,1998). hOCT1 has been demonstrated to mediate uptake of TEA, NMN, MPP and cimetidine (Gorboulev *et al.*, 1997; Zhang *et al.*, 1997b, 1998). Other substrates for rOCT3 and rOCT1a have yet to be reported. There are likely more substrates for these transporters, but due to the infancy of the molecular studies, only very few have been identified at present. Similar to the classical organic cation transport system, OCT mediated organic cation transport can be inhibited by many structurally distinct organic cations (**Table III-2**). Interestingly, from this list of inhibitors, amantadine has been shown to inhibit hOCT1 mediated TEA uptake and hOCT2 mediated dopamine uptake (Zhang *et al.*, 1998; Busch *et al.*, 1998). When comparing the OCT isoforms within species and between species, there appears to be similarities in substrate affinity (K_m) and inhibitory potency (K_i and IC_{50}) for some compounds, whereas considerable differences in substrate specificity and inhibitory potency exist for other compounds (Gorboulev *et al.*, 1997; Koepsell, 1998; Urakami *et al.*, 1998; Zhang *et al.*, 1998; Okuda *et al.*, 1999). The diverse range of substrates that the OCTs can accept, and the growing list of inhibitors provide convincing evidence that the OCTs are multispecific organic cation transporters.

Based on the localization in the kidney and the functional characteristics of rOCT1 and rOCT2, it is most likely that they are the functional equivalent of the basolateral membrane organic cation transporters that mediate the first step in organic cation secretion in the proximal tubule (**fig II-3**). The exact function of hOCT1 and

Table III-1: Reported K_m values for TEA transport into Xenopus oocytes or cell lines expressing various isoforms of OCTs.

Transporter	Km	Expression System	Reference
rOCT1	95 ± 10 μM 38 μM	Xenopus oocytes MDCK cells	Grundemann *et al.*, 1994 Urakami *et al.*, 1998
rOCT1a	42 ± 12 μM	Xenopus oocytes	Zhang et al., 1997
rOCT2	45 μM 500 μM	MDCK cells Xenopus oocytes	Urakami *et al.*, 1998 Koepsell, 1998
rOCT3	2.5 ± 0.2 mM	HeLa cells	Kekuda *et al.*, 1998
hOCT1	229 ± 79 μM	HeLa cells	Zhang *et al.*, 1998
hOCT2	76 ± 13 μM	Xenopus oocytes	Gorboulev *et al.*, 1997
pOCT2	20 and 620 μM	LLC-PK$_1$ cells	Grundemann *et al.*, 1997
OCTN1	436 ± 41 μM	HEK293 cells	Tamai *et al.*, 1997

Data are reported as mean ● SE.

Table III-2: Reported inhibitors of OCT mediated organic cation transport

Acebutolol	Amantadine	Choline
Cimetidine	Clonidine	Corticosterone
Cyanine$_{863}$	Decynium-22	Desipramine
± disopyramide	Dopamine	Gaunidine
Mepiperphenidol	Midazolam	MPP
± Nicotine	NMN	3-O-Methylisoprenalin
Procainamide	Quinidine	Quinine
Tetrabutylammonium	Tetrapentylammonium	Tetrapropylammonium
Tetrahexylammonium		

Information for this table was obtained from the following references, (Grundemann *et al.*, 1994; Busch *et al.*, 1996a, 1996b, 1998; Martel *et al.*, 1996; Okuda *et al.*, 1996, 1999;Gorboulev *et al.*, 1997; Zhang *et al.*, 1997a, 1997b, 1998, 1999; Kekuda *et al.*, 1998; Koepsell *et al.*, 1998; Urakami, 1998).

hOCT2 in the kidney has not been determined, but it is also likely that they play a role in the basolateral membrane transport of organic cations. The expression of rOCT2 mRNA and the localiztion of hOCT2 protein in the distal tubule also suggest that this portion of the nephron as well as the proximal tubule is important in drug transport in the human kidney. The expression of the OCT mRNA in other tissues including liver, brain, intestines and placenta suggests that this family of drug transporters has a fundamental importance in mediating drug distribution to various parts of the body and in drug elimination.

III.3.c *The OCTN transporters*

Two additional transporters (hOCTN1 and hOCTN2) have been cloned from human fetal liver and human placental trophoblast cell lines (Tamai *et al.*, 1997; Wu *et al.*, 1998; Yabuuchi *et al.*, 1999). Both hOCTN1 and hOCTN2 belong to the OCT family based on their amino acid similarity to OCT1, OCT2 and OCT3 (Tamai *et al.*, 1997; Wu *et al.*, 1998). hOCTN1 and hOCTN2 are 551 and 557 amino acids in length and have 11 and 12 predicted transmembrane segments respectively. Their predicted structure is much like that for the OCTs (**fig III-1**). hOCTN1 mRNA is strongly detected in the kidney, fetal liver, trachea and bone marrow, but is not expressed in adult liver (Tamai *et al.*, 1997). hOCTN2 mRNA is also expressed strongly in the kidney, heart, skeletal muscle and placenta and weakly expressed in the adult liver, brain and lung (Wu *et al.*, 1998). When expressed in Xenopus oocytes or HEK 293 cells, both transporters mediate the pH dependent, saturable uptake of TEA. In addition, hOCTN1 mediated TEA efflux was demonstrated to be stimulated by a proton gradient (out → in) and was independent

of membrane potential (Yabuuchi et al., 1999). Similar to the OCTs, several organic cations could inhibit TEA transport by the OCTN transporters, including cimetidine, methamphetamine, MPTP, nicotine, procainamide, quinidine, quinine, pyrilamine and verapamil (Tamai et al., 1997; Wu et al., 1998; Yabuuchi et al., 1999). Although the exact location of OCTN in the kidney has not been determined, the functional data are consistent with that of the organic cation/proton exchanger of the luminal membrane (Fig II-3) which mediates the second step in renal tubule organic cation secretion.

SUMMARY OF STUDY OBJECTIVES

The compound tetraethylammonium has been used as the prototypical organic cation for studying mechanisms of organic cation transport. We may be able to better define and identify the mechanisms and function of the organic cation transport system by performing detailed studies using multiple organic cation substrates. Thus, the first goal of the present dissertation was to identify that the renal tubule bicarbonate-dependent organic cation (amantadine) transporter previously characterized by our laboratory (Escobar et al., 1994; Escobar and Sitar 1995) has different properties as compared to the organic cation transporters identified by TEA.

As described in the introduction, several proteins that have the ability to transport organic cations have been cloned and studied in isolated cell systems. The molecular biology alone has not unequivocally identified if the cloned and isolated transporters are functionally important in renal tubules, or in vivo. However, these data do prove useful in the design of our in vitro organic cation transport experiments, which are carried out in

isolated renal tubules. The second goal of this project was to perform in vitro renal tubule transport studies that may provide insight as to which cloned organic cation transporters are functionally important for amantadine and TEA transport in the kidney.

Previous characterization of organic cation transport in our laboratory has been accomplished almost entirely using in vitro preparations of isolated tubules or renal slices from healthy animals. In addition, to the best of our knowledge, effects of pathological conditions on renal tubule organic cation transporters have not been studied. Clearly this is an important oversight, because altered renal drug elimination becomes even more apparent in persons with decreased renal function. The third objective was to determine if two conditions (diabetes and unilateral nephrectomy) that alter renal function might modify function of the renal tubule bicarbonate-dependent amantadine transporter, and thus have implications for altered organic cation elimination.

Chronic NH_4^+ administration (as NH_4Cl) has been demonstrated to increase the renal elimination of amantadine and several other organic cations. This effect has been attributed to acidification of the urine and decreased pH dependent passive reabsorption of the uncharged form of the organic cation back into the peritubular capillaries. The objective of this series of experiments was to demonstrate that NH_4^+ modulates renal tubule amantadine transport through direct pH-independent effects on the bicarbonate-dependent amantadine transporter as an alternate explanation of this phenomenon.

It has previously been identified that in vitro renal proximal and distal tubule uptake of amantadine is bicarbonate-dependent with an apparent K_m of 22 mM (Escobar et al., 1994). The final goal of the present studies was to determine the in vivo importance of increased plasma bicarbonate levels on the function of the bicarbonate-dependent organic cation (amantadine) transporter as it relates to renal clearance.

GENERAL METHODS

M.1   In vitro renal tubule transport assays

M.1.a   *Renal tubule preparation*

All experimental protocols were approved by the Protocol Management and Review Committee (University of Manitoba) according to the guidelines of the Canadian Council on Animal Care. All in vitro organic cation transport studies were carried out in isolated rat renal proximal and distal tubules. Separation of proximal and distal tubules was performed by the Percoll density gradient centrifugation method (Vinay *et al.*, 1981; Gesek *et al.*, 1987) as modified by Wong *et al.* (1990) and current modifications to improve the tissue preparation. The modified procedures are as follows. Normally, four male Sprague-Dawley rats (University of Manitoba, Canada, Charles River breeding stock) weighing 250-300g were anesthetized with sodium pentobarbital (50 mg/kg). Frequently, kidneys were obtained from male Sprague-Dawley rats during uninephrectomy procedures performed under ether anesthesia. It is our experience that there are no differences in organic cation transport in kidneys harvested from either method. Kidneys were removed, immediately decapsulated, and then were placed in ice-cold Krebs-Henseleit solution (KHS), pH 7.4. KHS contained (in millimolar concentrations): NaCl, 118; KCl, 4.7; $MgCl_2$, 1.2; KH_2PO_4, 1.4; $NaHCO_3$, 25; $CaCl_2$, 2.5 and glucose, 11. Renal cortical sections were then dissected from the medullary tissue approximately 1 mm from the corticomedullary junction and placed in ice-cold KHS buffer (20 ml). Next, the cortical sections were finely minced with a tissue chopper (Mickle Lab. Engineering Co. Ltd., Gomshall, Surrey, UK). Minced tissue was placed in

67

10 ml of cold KHS and was added to a KHS-collagenase solution containing 15 ml KHS, 1 ml of 10% bovine serum albumin and 10 mg of low trypsin collagenase A (0.23 U/ mg lysozyme) and oxygenated for 2 min with 95/5% O_2/CO_2. The tissue was then incubated at 31°C with shaking (100 oscillations per min) in a Dubnoff incubator (Precision Scientific Co., Chicago, IL). During the digestion, the tissue was gently pipetted for 5 min with a large bore pipette (5 ml) at intervals of 15 min to assist in breaking up the tissue. To ensure adequate digestion of the tissue, the progress of the digestion was monitored at intervals of 5 min (beginning 30 min after the start of the incubation) by light microscopy (100× magnification) of a small aliquot of tissue from the digestion mixture. The duration of the digestion was consistently between 35-45 min. The digestion procedure was terminated by the addition of 30 ml of ice-cold KHS and the tissue was filtered through a polyethylene mesh filter (pore size, 292 μm) to remove any large undigested fragments. The tissue was then washed 3 times by sequential resuspension in KHS followed by low-speed centrifugation (4°C, 60 × g for 1 min). The final pellet was resuspended in 40 ml of a 50 % Percoll solution (20 ml each of Percoll and double strength KHS at pH 7.4) and centrifuged for 30 min at 27,000 × g (4°C). Proximal and distal tubules were removed from the gradient (bands IV and II from the top of the centrifuge tube, respectively) and were washed 3 times by sequential resuspension in KHS followed by low-speed centrifugation at (4°C, 60 × g for 1 min). After the final wash, proximal and distal tubule fractions were normally resuspended in the desired volume of KHS. If the transport assays included measurements in the absence of bicarbonate, the last wash and the final resuspension of the tubule fragments would be done with Cross-Taggart (CT) buffer. The CT buffer contained (in millimolar

concentrations) NaCl, 132; KCl, 4.7; MgCl$_2$, 1.2; KH$_2$PO$_4$, 1.4; sodium phosphate buffer (pH 7.4) 15; CaCl$_2$, 1.0; glucose, 11 and was pH adjusted with NaOH. Tissue protein was determined prior to the transport assays by the Biuret method (Gornall *et al.*, 1949). At this point the resuspension volume was adjusted to give a final protein concentration of 6 − 8 mg/ml. The proximal and distal tubule suspensions were kept on ice until just prior to the start of the transport assays at which time they were warmed to room temperature by 20 min incubation in a 25°C water bath. The purity of tubule fractions was assessed by measuring levels of enzyme markers (alkaline phosphatase for proximal and hexokinase for distal tubules) and by microscopic examination as previously reported (Scholer and Edelman, 1979; Vinay *et al.*, 1981; Wong *et al.*, 1991).

M.1.b *Renal tubule organic cation transport studies*

Amantadine and TEA were used as prototype organic cations for the transport studies. The uptake or efflux of amantadine and TEA in different buffer systems and in the presence and absence of transport modulators were performed to characterize mechanisms of organic cation transport in the isolated renal tubules. The general methods followed for the transport assays are presented below. The detailed methodologies and the substrates, inhibitors and buffers used for specific experiments are reported in each respective chapter.

M.1.c *Amantadine and TEA influx experiments*

Linear rates for the energy-dependent renal tubule uptake of amantadine and TEA were determined in the presence of bicarbonate (KHS buffer) or in the absence of

bicarbonate (CT buffer). For the amantadine and TEA influx assays, tubes were prepared (in triplicate) that contained a fixed amount of ^{3}H-amantadine (10 nM) or TEA (10μM) in a volume of 150 μl of either KHS or CT buffer. These tubes also contained various amounts of unlabeled amantadine or TEA (K_m and V_{max} determinations) and/or transport modulators (influx inhibition experiments) in various concentrations. Isolated proximal or distal tubule suspensions (50 μl in the appropriate buffer) were added to each assay tube to begin the influx reaction. After addition of the tubule suspension, the assay tubes were incubated for 30 s (amantadine) and for 60 s (TEA) in a 25°C water bath with shaking (100 oscillations/min). Incubations for TEA were 60 s in duration as opposed to 30 s for amantadine to insure the linearity of initial uptake rates. The influx reactions were terminated by the addition of 2 × 4 ml of ice-cold KHS, followed by rapid filtration under negative pressure, through glass fiber filters (No. 32, Schleicher and Schuell, Inc., Keene, NH). The filters were immediately placed into scintillation vials containing 4 ml of Ready Safe scintillation fluid (Beckman, Beckman Instruments Inc., Fullerton, CA) and counted in a Beckman model LS5801 scintillation counter. Non-specific uptake of radioactivity to tissue and filters was determined by measuring uptake of ^{3}H-amantadine or ^{14}C-TEA in the presence of a saturating amount of unlabeled amantadine (10 mM) or TEA (10 mM), respectively. Non-specific uptake was subtracted from total radioactivity to determine the energy-dependent uptake of these compounds.

M.2 In vivo renal clearance of amantadine and kynurenate:

The methods for the in vivo experimentation are described in their entirety in chapter five.

M.3 Data analysis:

For the individual experiments, each data point for the transport and inhibition studies was performed in triplicate. Data are expressed as mean $\pm$ SE of at least 4 experiments unless otherwise stated. Transport rates for uptake are reported as specific uptake (nonspecific uptake subtracted) of amantadine or TEA by the tubules in nmol mg^{-1} protein min^{-1}. Efflux is normally characterized as the % of amantadine or TEA remaining in the tissue after the efflux period. Apparent K_m and V_{max} values were determined by fit to the Michaelis-Menten equation and K_i by fit to the equation for competitive inhibition using a non-linear regression program, Leonora, (Cornish-Bowden, 1995). IC_{50} values were determined from the amantadine inhibition profiles by regressive probit analysis of increasing inhibitor concentrations (Cheng and Prusoff, 1973). Dixon (1953) and Cornish-Bowden (1974) analyses were used to determine the nature of inhibition. An unpaired t-test was used for statistical analysis of differences between two groups. ANOVA models were used for analysis of significant differences among multiple groups. Multiple comparisons of the significant ANOVA were performed by Tukey's HSD test. Specific differences between means with a p value of 0.05 or less were considered to be significant. All statistical analyses were performed using Systat for Windows 6.0.1 (SPSS Inc., Chicago, IL). Information regarding specific data analysis methods are reported in the methods sections of the individual chapters.

M.4 Chemicals

^{3}H-amantadine (28 Ci/mmol) was obtained from Amersham International (Buckinghamshire, UK). ^{14}C-TEA was obtained from American Radiolabeled Chemicals, Inc. (St. Louis, MO). ^{3}H-Kynurenic acid (14 Ci mmol^{-1}) was obtained from Amersham Canada (Oakville, Ontario, Canada). Collagenase was obtained from Boehringer, Mannheim (Laval, Quebec, Canada). Unlabeled amantadine was obtained from Dupont Canada Inc. (Mississauga, Ontario, Canada). Unlabeled TEA, kynurenic acid, quinine, quinidine, procainamide, cyanine$_{863}$, N^1-methylnicotinamide, dopamine, digoxin and verapamil were obtained from Sigma Chemical Co. (St Louis, MO, USA). Physiological saline (0.9 % w/v) was obtained from Baxter Corporation (Toronto, Ontario, Canada). NaHCO$_3$ for intravenous injection (8.4 %) was obtained from Abbott Laboratories Limited (Montreal, Quebec, Canada). Creatinine assay kits (procedure #555) were obtained from Sigma Chemical Co. (St. Louis, MO, USA). BCECF and BCECF-AM was purchased from Molecular Probes (Eugene OR). All other chemicals were of the highest grade available from commercial suppliers.

Chapter 1: Amantadine-Selective Versus Tea-Selective Organic Cation Transporters (Part I)

Section Hypothesis: Multiple organic cation transporters exist in the kidney and may be identified by selective transport of amantadine and TEA..

Introduction

As described earlier, an abundance of information pertaining to the renal tubule organic cation transport system comes from studies using tetraethylammonium (TEA) as a prototypical organic cation substrate. Transport of TEA across the basolateral membrane of proximal tubules is a saturable, energy-dependent, carrier-mediated process that is driven by the inside negative membrane potential and is independent of pH **fig. II-3** (Sokol and McKinney, 1990; Takano *et al.*, 1984). Efflux from the tubule cell into the lumen is mediated by a saturable H^+/organic cation exchanger that uses a proton gradient derived from the Na^+/H^+ exchanger also located in the luminal membrane, **fig. II-3** (Takano *et al.*, 1984; Rafizadeh *et al.*, 1987). However, the TEA model alone may not be sufficient to account for the renal tubule secretion pathways of other organic cations.

The mechanisms controlling amantadine secretion by the kidney appear different than for TEA. Transport sites for amantadine in proximal and distal tubules can be subdivided into bicarbonate-dependent sites (high-affinity, high-capacity) which are responsible for the majority of amantadine uptake and less efficient bicarbonate-independent sites (lower-affinity, lower-capacity) (Escobar *et al.*, 1994, Escobar and Sitar, 1995). Although a bicarbonate-dependent basolateral transport component has

been reported for the cation NMN (Ullrich *et al.*, 1991), a similar transport phenomenon has not been demonstrated for TEA. Membrane potential and activity of the basolateral membrane Na^+/K^+-ATPase are not rate limiting for the renal tubule uptake of amantadine (Escobar and Sitar, 1995, 1996). These findings suggest that the majority of amantadine uptake occurs as a nonelectrogenic step at the basolateral membrane as opposed to electrogenic uptake for TEA. Considering these apparent differences in amantadine and TEA renal tubule transport characteristics, we hypothesize that amantadine and TEA identify distinct basolateral membrane organic cation transporters in the kidney. Identifying distinct renal organic cation transporters and their substrate specificity by using TEA and amantadine as organic cation probes may allow for the prediction of potential drug interactions in the kidney.

Methods

Amantadine and TEA Uptake Studies

Linear rates for the energy-dependent renal tubule uptake of amantadine and TEA were determined in the presence of bicarbonate (KHS buffer) and in the absence of bicarbonate (CT buffer). These experiments were performed as described in the general methods and were designed to determine and compare the K_m and V_{max} for renal tubule amantadine uptake with that of renal tubule TEA uptake in the presence and absence of bicarbonate at pH 7.4.

Amantadine and TEA Inhibition studies

The inhibition of ^{14}C-TEA (10 µM) energy-dependent uptake by unlabeled amantadine and NMN (10-1000 µM) and inhibition of ^{3}H-amantadine uptake (10µM) by

74

TEA and NMN (10 – 1000 μM) were determined in proximal and distal tubules in KHS and CT buffer (pH 7.4). The same procedures as described for the transport assays were used for the inhibitor studies.

Results

TEA and amantadine uptake studies

TEA uptake was linear for at least 60 seconds (r^2 for linear regression ranged from 0.89 – 0.98) in proximal tubules and distal tubules in the presence and absence of bicarbonate, as shown in (**fig. 1-1**). Amantadine uptake into proximal and distal tubules was linear for at least 30 seconds (data not shown) as previously reported from our lab (Wong *et al.*, 1990). Both proximal and distal tubule segments accumulated ^{14}C-TEA and ^{3}H-amantadine in a saturable manner (**fig. 1-2**). Eadie-Hofstee plots for energy dependent amantadine and TEA uptake versus concentration are shown in (**fig. 1-3**). The linear nature of the amantadine plots indicated that a single site is mediating amantadine uptake in both KHS and CT buffers. The biphasic nature of the TEA plots revealed that TEA uptake into proximal and distal tubules may be characterized by two transport sites, a high-affinity transport site, and a lower-affinity transport site. TEA concentrations between 10 and 60 μM were used to characterize the high affinity TEA transport site, and 100 to 500 μM to characterize the lower-affinity transport site. (**fig. 1-4**) shows $K_{m\ TEA\ 1}$ and $V_{max\ TEA\ 1}$ (K_{m} and V_{max} for TEA uptake at the high affinity site). $K_{m\ TEA\ 1}$ and $V_{max\ TEA\ 1}$ were similar in CT and KHS buffer in both proximal and distal tubules. The lack of a difference in kinetic parameters between buffer groups allowed us to combine the data from each buffer group such that we could increase the power (n = 16 compared to 8) of

detecting a difference in K_m or V_{max} between proximal and distal tubules. Comparing proximal and distal tubules when data from both buffer groups were combined indicated that $K_{m\ TEA\ 1}$ was less (higher affinity) in proximal (33.4 ± 4.8 μM) compared to distal tubules (49.4 ± 4.8 μM), $p < 0.05$. The difference in $V_{max\ TEA\ 1}$ in proximal tubules (0.295 ± 0.034 nmol mg^{-1} min^{-1}) compared to distal tubules (0.209 ± 0.034 nmol mg^{-1} min^{-1}) approached statistical significance ($p < 0.08$). For the observed difference between mean proximal and distal tubule $V_{max\ TEA\ 1}$ a power calculation with grouped standard deviation (0.133 nmol mg^{-1} min^{-1}) indicated that a minimum of 37 replicates would be required to detect a significant difference when $\alpha = 0.05$ and $\beta = 0.20$ and thus was not pursued. For the lower-affinity site, $K_{m\ TEA\ 2}$ and $V_{max\ TEA\ 2}$ were similar between tubule fragments and were not dependent on the presence of bicarbonate in the medium (**fig. 1-5**). K_m and V_{max} for the lower-affinity TEA uptake sites were respectively between 5 to 10 fold greater, and 3 to 4 fold greater than for the high-affinity sites. Kinetic parameters for amantadine uptake are shown in **fig. 1-6**. $K_{m\ A}$ (K_m for amantadine uptake) was similar in both proximal and distal tubules and was increased when CT was substituted for KHS buffer ($p < 0.001$). $V_{max\ A}$ (V_{max} for amantadine uptake) was greater in proximal tubules compared to distal tubules in both buffers ($p < 0.001$). In both tubule fragments V_{max} was reduced in CT buffer compared to KHS buffer ($p < 0.001$).

Inhibition studies

We first evaluated the ability of TEA to inhibit the energy-dependent renal tubule uptake of amantadine (**fig. 1-7**). TEA concentrations ranging from 10 – 1000 μM were unable to impede the uptake of amantadine into isolated renal proximal and distal tubules

in bicarbonate or phosphate buffer at pH 7.4. Conversely, amantadine was able to inhibit TEA uptake into proximal and distal tubules ($p < 0.05$) compared to the respective control (**fig. 1-8**). The inhibition profiles were similar in both bicarbonate and phosphate buffer.

Subsequently, we analyzed the ability of another prototypical organic cation substrate (NMN) to inhibit amantadine and TEA uptake (**fig. 1-9**). In proximal tubules NMN was not able to inhibit amantadine uptake, but at higher concentrations it reduced TEA uptake by 60-70% ($p < 0.05$). A similar NMN inhibition profile for TEA was observed in distal tubules. In distal tubules NMN had no effect on amantadine uptake in CT buffer but inhibited amantadine uptake by 30-40% in KHS buffer ($p < 0.05$).

Table 1-1 shows IC_{50} and inhibitor dissociation constant (K_i) values for amantadine inhibition of TEA uptake. Dixon and Cornish-Bowden analysis confirmed that amantadine inhibition of TEA uptake was consistent with that of competitive inhibition (data not shown) and justifies the determination of K_i from IC_{50} values by the Cheng-Prusoff competition method (Cheng and Prusoff, 1973). K_i values were similar in proximal and distal tubules and did not differ between KHS and CT buffer. The ratios of K_m for amantadine uptake versus K_i for amantadine inhibition of TEA uptake were calculated (**Table 1-1**). In both proximal and distal tubules the ratios of $K_{m\,A}/K_i$ were greater than one. The $K_{m\,A}/K_i$ ratio was greater in CT buffer compared to KHS buffer.
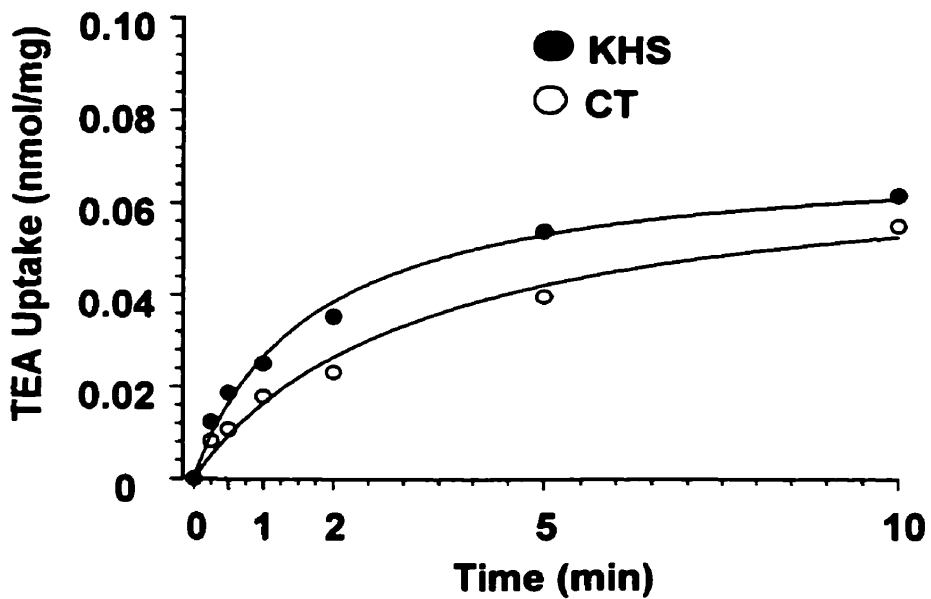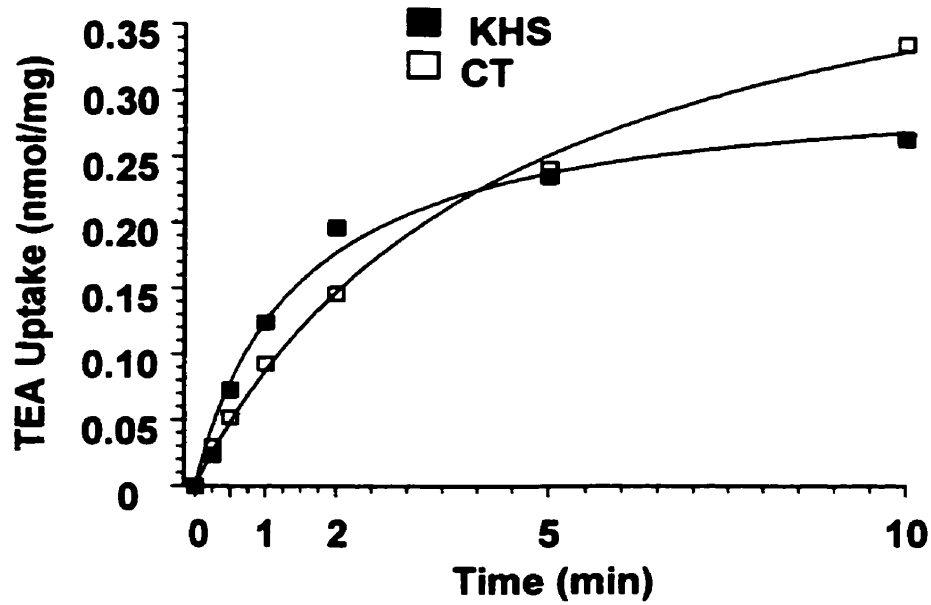
Figure 1-1: Representative plots of a single experiment showing TEA (10μM) uptake versus time into isolated renal cortical proximal (upper panel) and distal (lower panel) tubules in the presence (KHS) and absence (CT) of bicarbonate at pH 7.4. Total TEA uptake is expressed as nmol per mg of protein.
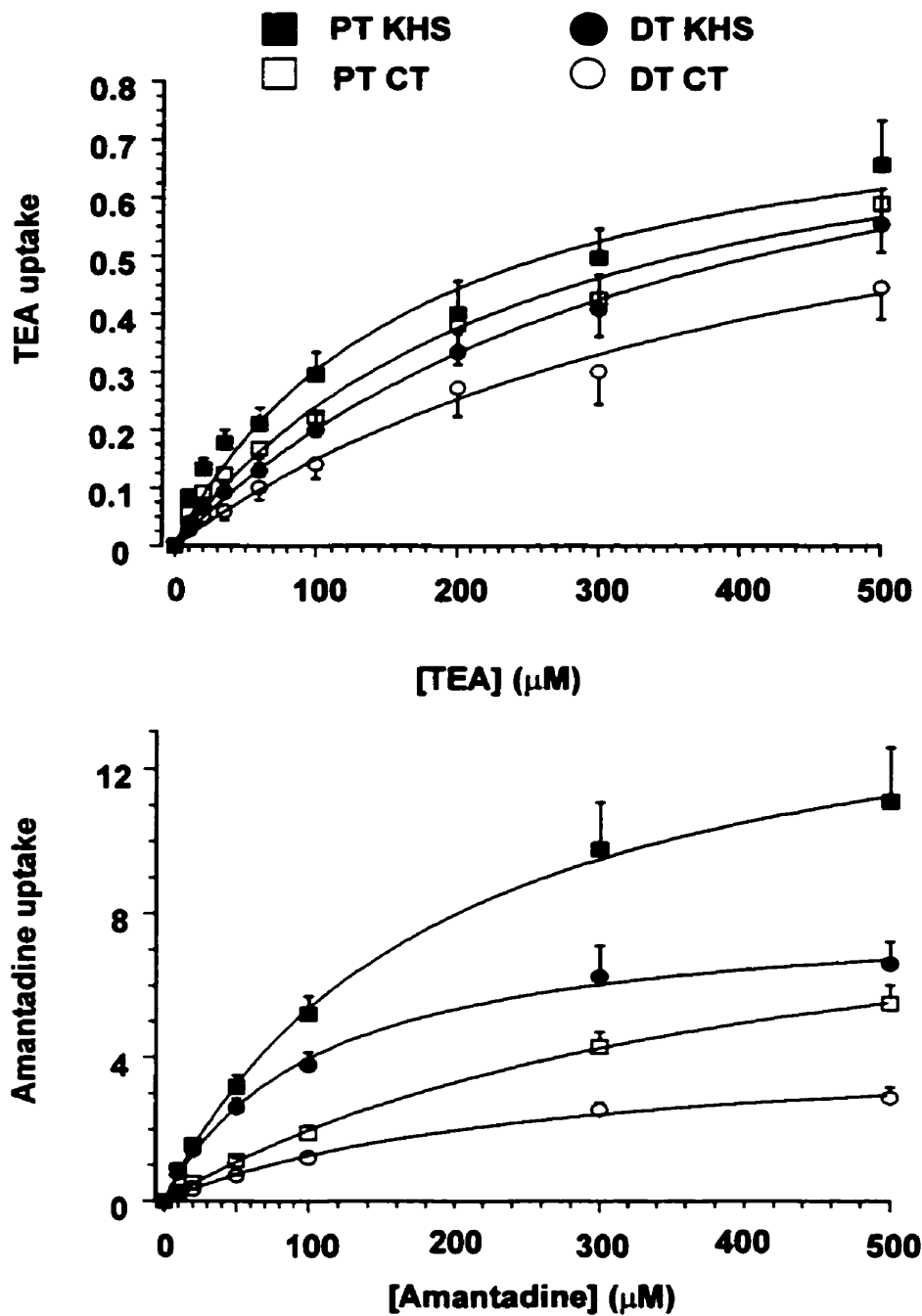
Figure 1-2: Saturation curves for TEA (upper panel) and amantadine (lower panel) uptake into isolated proximal (PT) and distal (DT) tubules in the presence (KHS) and absence of bicarbonate (CT). Amantadine and TEA uptake rates (nmol mg^{-1} min^{-1}) are expressed as mean ± SE of 5 to 8 separate determinations.
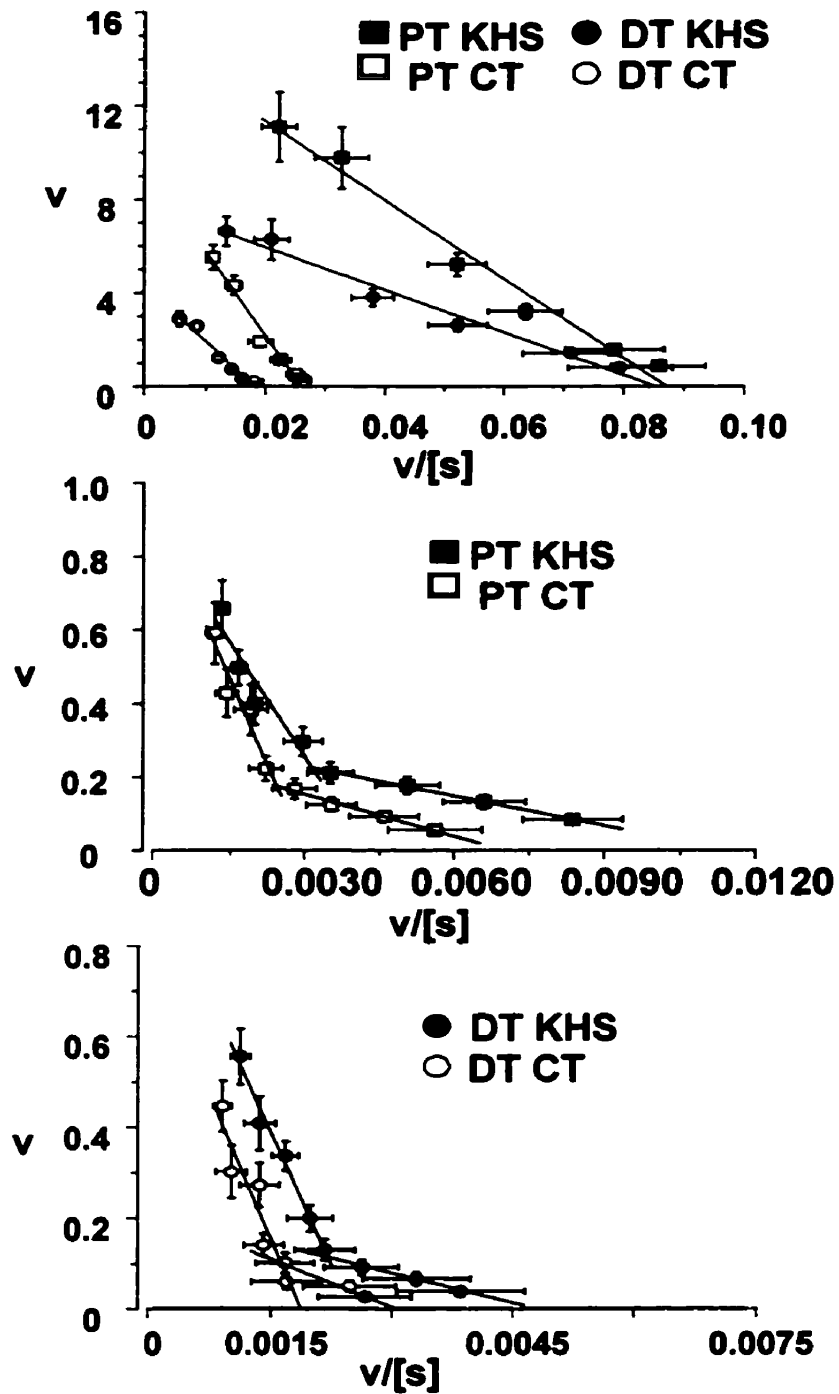
Figure 1-3: Eadie-Hofstee plots for amantadine (top) and TEA (middle and bottom) uptake into isolated proximal (PT) and distal (DT) tubules. v is the rate of amantadine or TEA uptake (nmol mg^{-1} protein min^{-1}) and [s] is the concentration of amantadine or TEA (μM). Each data point is representative of the mean $\pm$ SE of 5 to 8 separate determinations.

80
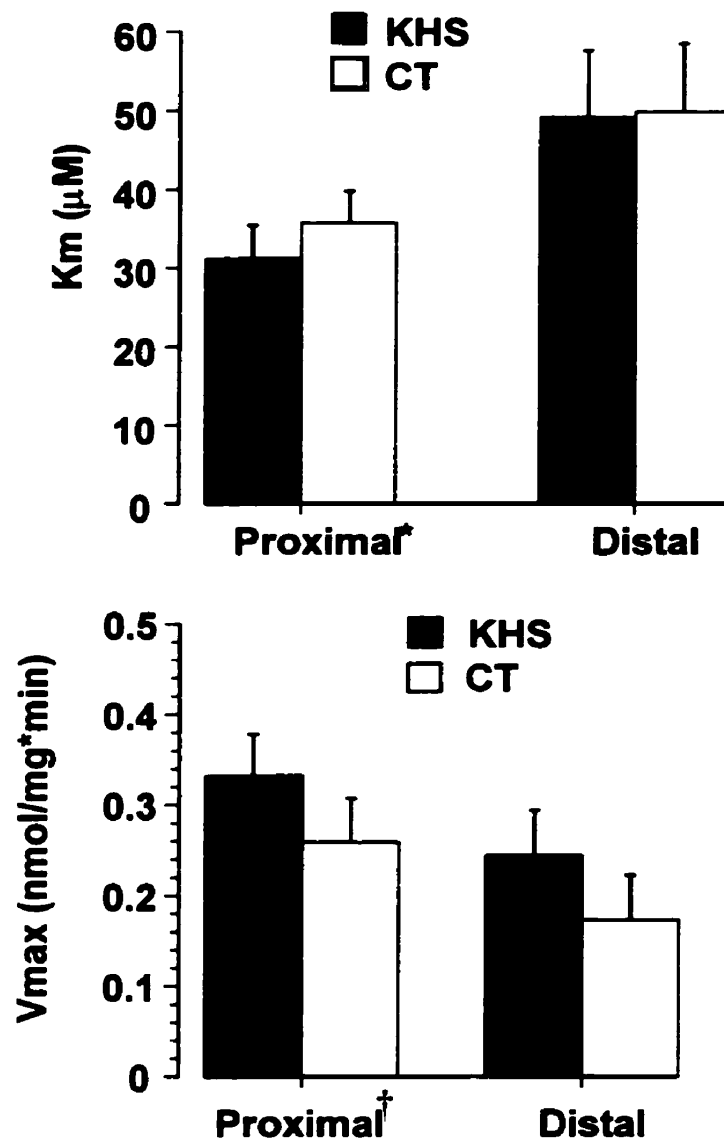
Figure 1-4: Calculated apparent K_m (upper panel) and V_{max} (lower panel) values for ^{14}C-TEA uptake by high-affinity transport site in proximal and distal tubules in the presence (KHS) and absence (CT) of bicarbonate at pH 7.4. Values are reported as mean ± SE from 8 separate determinations. Treatment groups were compared by two-way ANOVA with tubule and buffer as the grouping variables. * $p < 0.05$ and † $p < 0.08$ proximal tubules compared to distal tubules when data from KHS and CT groups are combined.
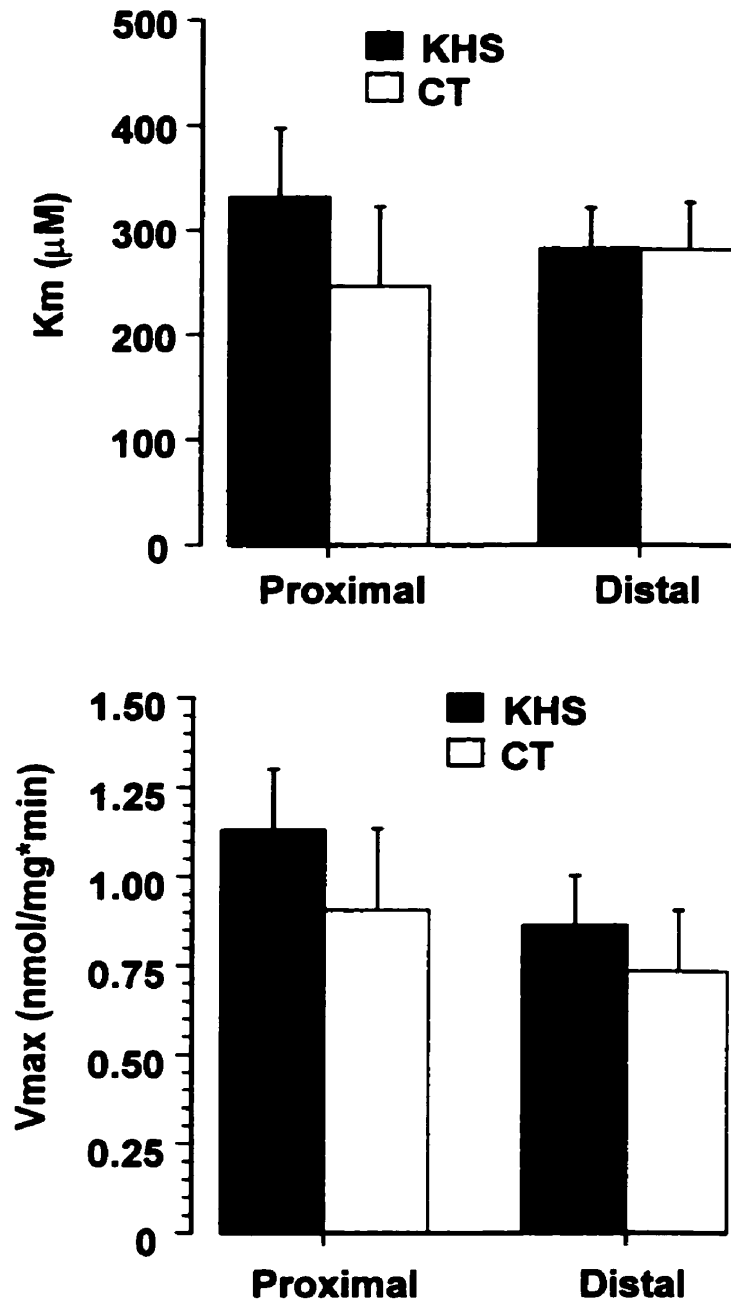
Figure 1-5: Calculated apparent K_m (upper panel) and V_{max} (lower panel) values for ^{14}C-TEA uptake by lower-affinity transport site in proximal and distal tubules in the presence (KHS) and absence (CT) of bicarbonate at pH 7.4. Values are represented as mean ● SE of 4 to 6 separate determinations. Treatment groups were compared by two-way ANOVA with tubule and buffer as the grouping variables.
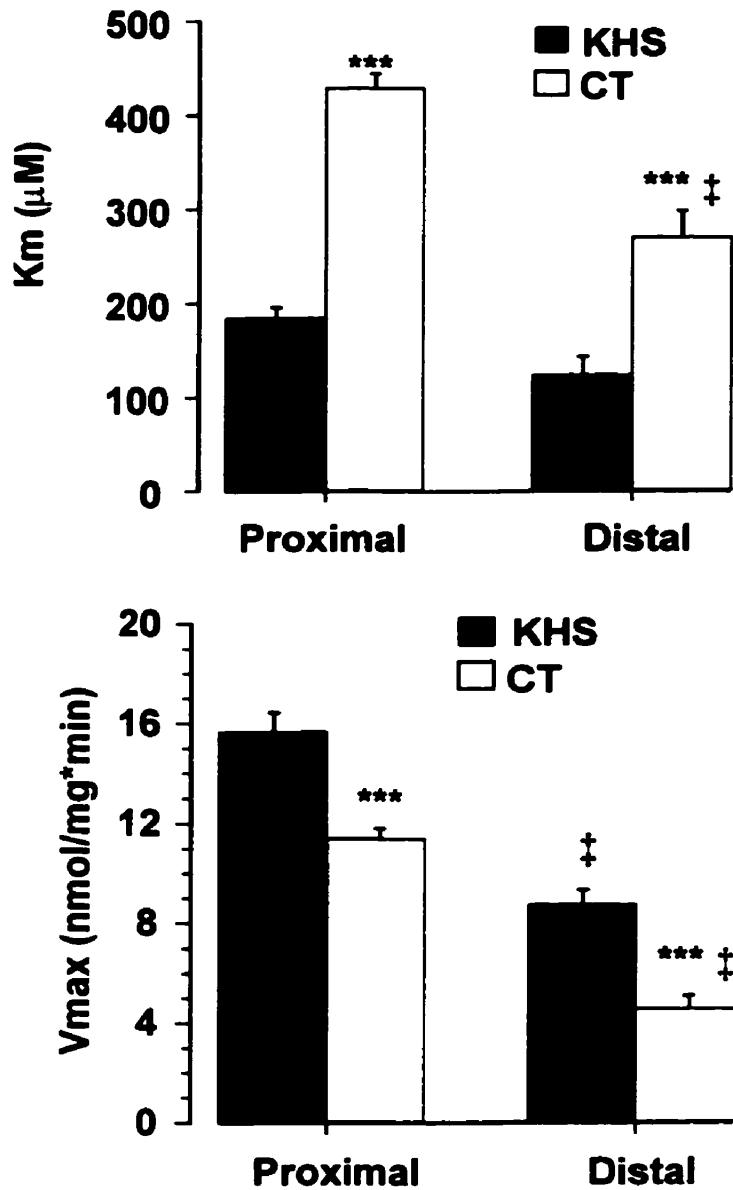
Figure 1-6: Calculated apparent K_m (upper panel) and V_{max} (lower panel) values for ^{3}H-amantadine uptake by isolated renal proximal and distal tubules in the presence (KHS) and absence (CT) of bicarbonate at pH 7.4. Values are represented as mean ● SE of 5 separate determinations. Treatment groups were compared by two-way ANOVA with tubule and buffer as the grouping variables. *** $p < 0.001$ compared to KHS within tubule group. $^‡ p < 0.001$ proximal compared to distal tubule within same buffer group.
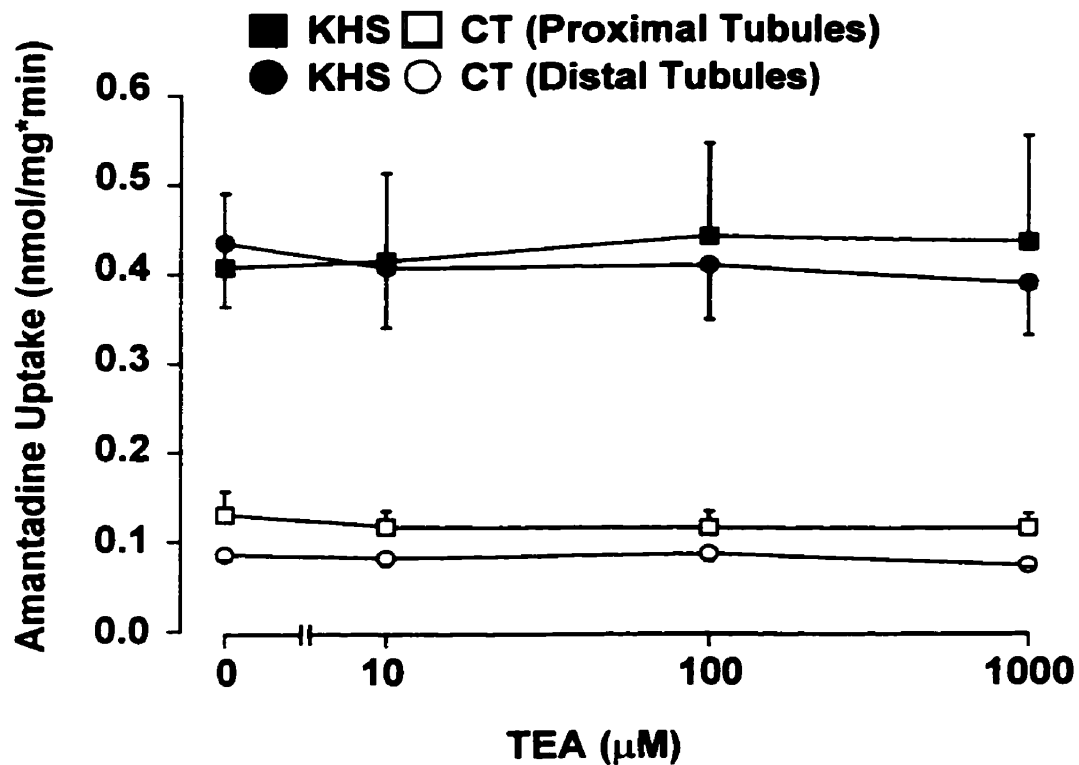
Figure 1-7: Inhibition of 10 µM amantadine uptake into isolated renal cortical proximal and distal tubules by TEA in the presence (KHS) and absence (CT) of bicarbonate at pH 7.4. Values represent the mean ± SE of 4 separate determinations.
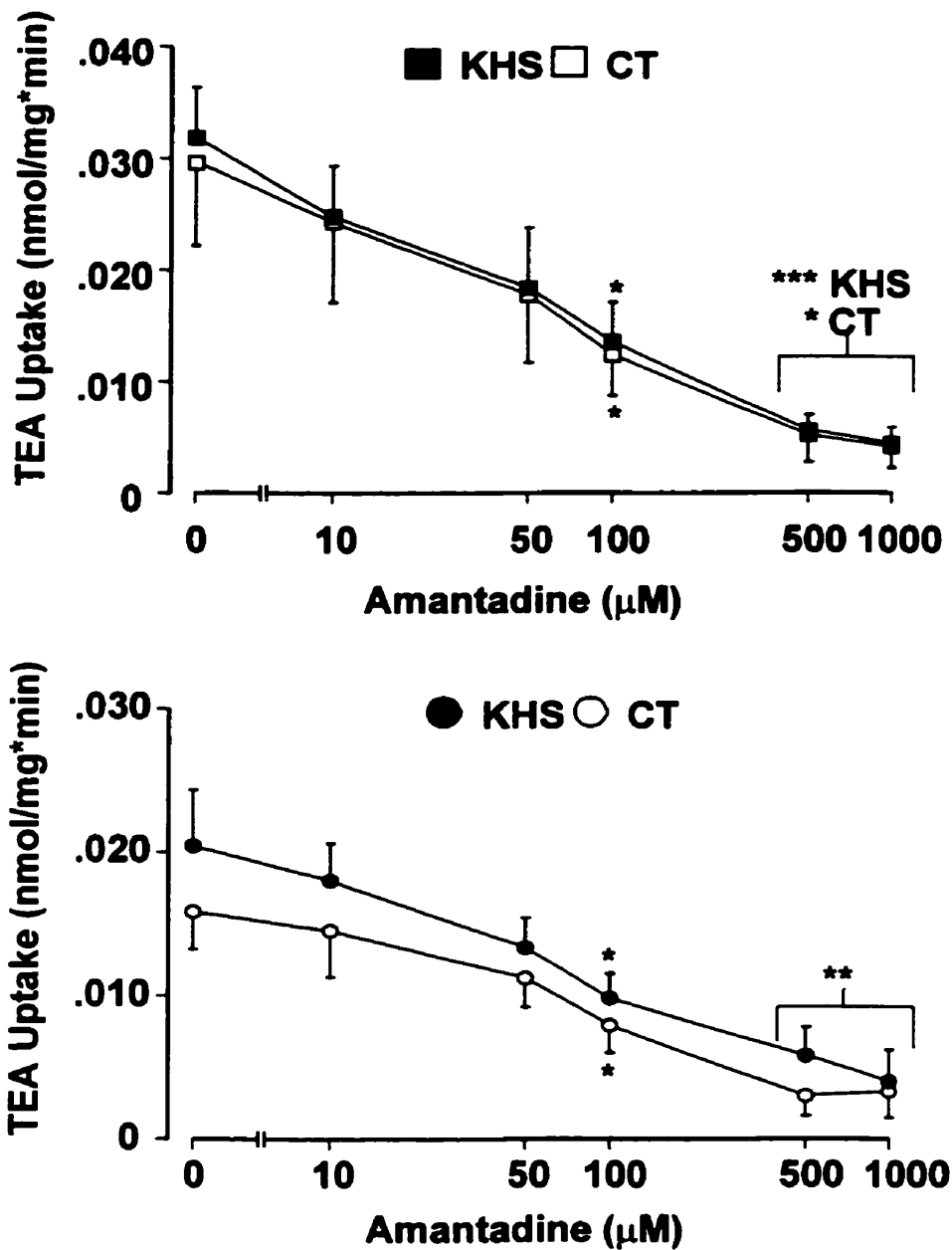
Figure 1-8: Amantadine inhibition of 10 µM TEA uptake into isolated renal cortical proximal (upper panel) and distal tubules (lower panel) in the presence (KHS) and absence (CT) of bicarbonate at pH 7.4. Values represent the mean ● SE of 5 to 7 separate determinations. * $p < 0.05$, ** $p < 0.01$ and *** $p < 0.001$ compared to control (no amantadine present), Repeated measures ANOVA followed by Tukey's HSD Test.
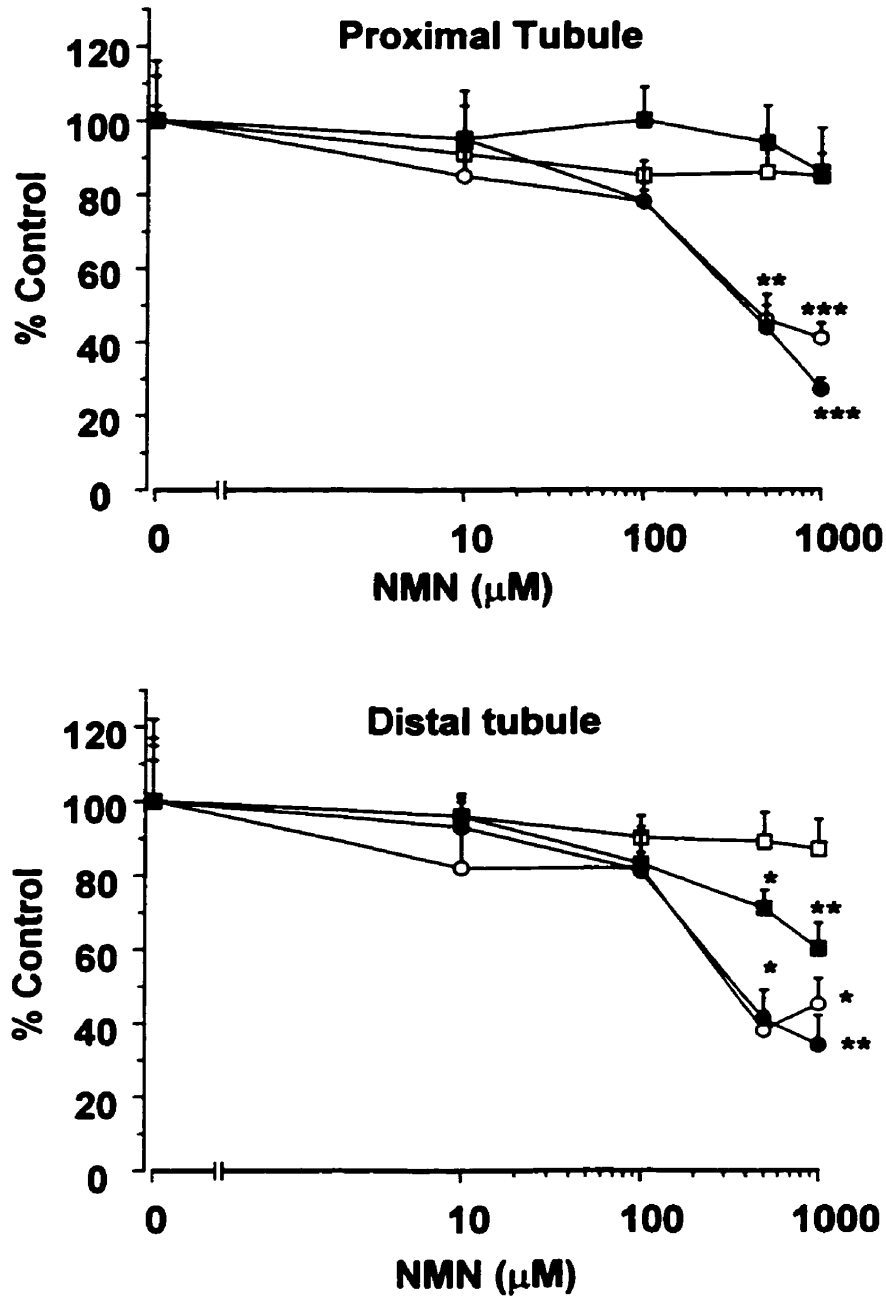
Figure 1-9: NMN inhibition of amantadine (squares) and TEA (circles) uptake into proximal (upper panel) and distal tubules (lower panel). Assays were performed in KHS (solid symbols) and CT buffer (open symbols) at pH 7.4. Values represent the mean ± SE of 4 separate determinations. * $p < 0.05$, ** $p < 0.01$ and *** $p < 0.001$ compared to respective amantadine or TEA control, repeated measures ANOVA followed by Tukey's HSD Test.

Table 1-1. Derived IC_{50} and K_i values for amantadine inhibition of energy-dependent uptake of TEA by isolated rat renal cortical proximal and distal tubules with comparison to the apparent K_m values calculated for amantadine transport under the same conditions.

All concentrations are expressed in $\mu M \pm SE$ of 4 to 7 experiments.

Tubule	Buffer	IC_{50}	K_i	$K_m A^{+}$ [1]	$K_m A^{+}/K_i$
Proximal	KHS	56 ± 12	40 ± 9	190 ± 11^{c}	4.8
Proximal	CT	52 ± 11	41 ± 8	$412 \pm 23^{c\,d}$	10.0
Distal	KHS	82 ± 14	60 ± 11	102 ± 11^{c}	1.7
Distal	CT	48 ± 8	38 ± 7	$245 \pm 34^{c\,d}$	6.4

[1] A^{+}, amantadine, [b] K_i values were similar in all four groups, two-way ANOVA with tubule and buffer as grouping factors. [c] $p < 0.01$, K_m compared to K_i within the same tubule and buffer group, [d] $p < 0.01$ compared to K_m in KHS buffer within the same tubule group.

Discussion

Amantadine uptake into proximal and distal tubules from the rat could be described by a high-affinity-capacity, bicarbonate-dependent transport site and a lower-affinity-capacity, bicarbonate-independent transport site and is concordant with previous studies (Escobar et al., 1994; Escobar and Sitar, 1995). The previously calculated K_m and V_{max} for amantadine uptake were (76 µM and 4.83 nmol mg^{-1} min^{-1}) and (68 µM and 4.58 nmol mg^{-1} min^{-1}) for proximal and distal tubules respectively. The current K_m values in KHS were about two-fold higher than those calculated by Escobar et al, 1994. K_m values for amantadine uptake in CT were similar to those calculated by Escobar et al, 1994. Our calculated V_{max} values in both KHS and CT and in proximal and distal tubules were about 3 fold higher than reported by Escobar et al., 1994. In spite of the differences in K_m and V_{max}, the same qualitative effects on amantadine transport were maintained namely a decrease in $V_{max\,A}$ and an increase in K_m in the absence of bicarbonate.

The uptake of TEA into isolated proximal and distal tubules was best characterized by a high-affinity, low-capacity component and a lower-affinity, higher-capacity component. To the best of our knowledge, this is the first report to describe energy-dependent distal tubule transport of TEA. Unlike amantadine, the uptake of TEA at these two sites was similar in the presence and absence of bicarbonate. Most others have described only a single transport site for TEA, but with widely varying affinity (Wright and Wunz, 1987; Takano et al., 1984; Schali et al., 1983; Takami et al., 1998; Ullrich et al., 1991; McKinney et al., 1990). The one exception (Grundemann et al., 1997) demonstrated a high-affinity component (20 µM) and a low-affinity component

(620 μM) for TEA uptake by the OCT2p transporter transfected into human 293 cells. We believe that the failure of others to detect two transport sites for TEA relates to the selection of TEA concentrations used in attempts to characterize its transport properties. The difference in $K_{m\ TEA\ /}$ and possibly $V_{max\ TEA\ /}$ between proximal and distal tubules suggests that the composition of transporters involved in uptake of TEA is different between the tubule segments, with a higher affinity-capacity component existing in the proximal tubules. The observed differences in the bicarbonate effect on amantadine versus TEA transport further supports the division of basolateral membrane organic cation transporters into ones that are bicarbonate-dependent and others that are independent of bicarbonate (Escobar *et al.*, 1994).

The inhibition studies showed that TEA could not inhibit amantadine uptake. The highest concentration of TEA (1000 μM) was greater than the high-affinity and lower-affinity K_m values for TEA uptake in proximal and distal tubules. This saturating concentration of TEA would be expected to inhibit amantadine uptake if the two compounds entered the tubules via identical transporters. Conversely, amantadine is essentially able to block completely TEA uptake. The fact that amantadine inhibited TEA uptake but TEA didn't inhibit amantadine uptake indicates a number of possibilities. TEA is not transported and doesn't interact with the bicarbonate-dependent and bicarbonate-independent amantadine transporters. Amantadine interacts with the TEA transporters but is not transported. The TEA transporters also transport amantadine but, the proportion of uptake at this site is very small such that any inhibition of

amantadine uptake by TEA is masked by the larger bicarbonate-dependent amantadine transport component.

In addition to TEA, NMN has been used to characterize organic cation transport in the kidney (Kinsella *et al.*, 1979a; Holohan and Ross, 1980). NMN has been demonstrated to inhibit renal tubule transport of TEA (Ullrich *et al.*, 1991; Montrose-Rafizadeh *et al.*, 1989) but, interactions with amantadine uptake have not been reported. The fact that NMN does not inhibit amantadine uptake in proximal tubules at concentrations that inhibit TEA uptake strengthens the argument that TEA and amantadine may represent transport at different sites.

The distinctness of the organic cation transport sites for TEA and amantadine is further supported by the difference in K_m for amantadine uptake versus the K_i for amantadine inhibition of TEA transport. Theoretically, the K_m/K_i ratio should be near one if TEA transport sites are the same as those previously identified for amantadine and competitive inhibition is assumed. The observed K_m/K_i ratio is substantially greater than one for both proximal and distal tubules, and is greater in CT compared to KHS buffer. Thus, the bicarbonate-dependent and bicarbonate-independent amantadine transport sites may be different than those described by TEA.

Our previous model to explain organic cation transport by renal proximal tubules (Escobar and Sitar, 1995) has been revised to reflect the present findings (fig. 1-10). Transport site 1 represents the high-affinity-capacity, bicarbonate-dependent amantadine

transporter that is responsible for approximately 80% of basolateral amantadine uptake into the tubule cell. Transport site 2 represents a lower-affinity-capacity, bicarbonate-independent amantadine transporter responsible for about 20% of amantadine uptake. Our present data show that TEA is not a substrate for transport site 1 or 2. Basolateral uptake of TEA may be characterized best by two additional bicarbonate-independent transport sites, a high-affinity, low-capacity site (site 3) and a lower-affinity, higher-capacity site (site 4). Sites 3 and 4 may also represent higher-affinity, lower-capacity transport sites for amantadine, as identified by amantadine inhibition of TEA uptake. In proximal tubules, NMN appears to interact with the TEA but not the amantadine transport sites. On the luminal membrane, exit of TEA is mediated by an H^+/organic cation exchanger (transport site 5) that uses the H^+ gradient (out $\rightarrow$ in) created by the Na^+/H^+ exchanger (Takano *et al.*, 1984; Rafizadeh *et al.*, 1987). Transport of certain organic cations (not including TEA) across the luminal membrane may also be mediated by the ATP dependent P-glycoprotein (transport site 7) (Dutt *et al.* 1994). Further studies are required to evaluate whether the mechanisms of luminal transport of amantadine are similar to that of TEA and whether amantadine is a substrate for P-glycoprotein. Our data suggest that similar organic cation transport mechanisms for amantadine and TEA exist in the distal tubule. However, for both amantadine and TEA sufficient in vivo evidence is lacking to determine the relative contribution of the proximal and distal tubules to total renal secretion of these compounds.

rOCT1, rOCT1a, rOCT2 and rOCT3 are four members of the organic cation transporter family that are expressed in the rat kidney and have been demonstrated to

Peritubular Capillaries

Basolateral
Membrane

HCO₃⁻

A⁺

(-)   (-) ?

Na⁺

(+)

1   2   3   4

K⁺

AM⁺   AM⁺   TEA⁺   TEA⁺

ATP   ADP + P₁   H⁺   Na⁺

7   5   6

OC⁺   TEA⁺   H⁺
         AM⁺ ?

Luminal
Membrane

Tubule Lumen
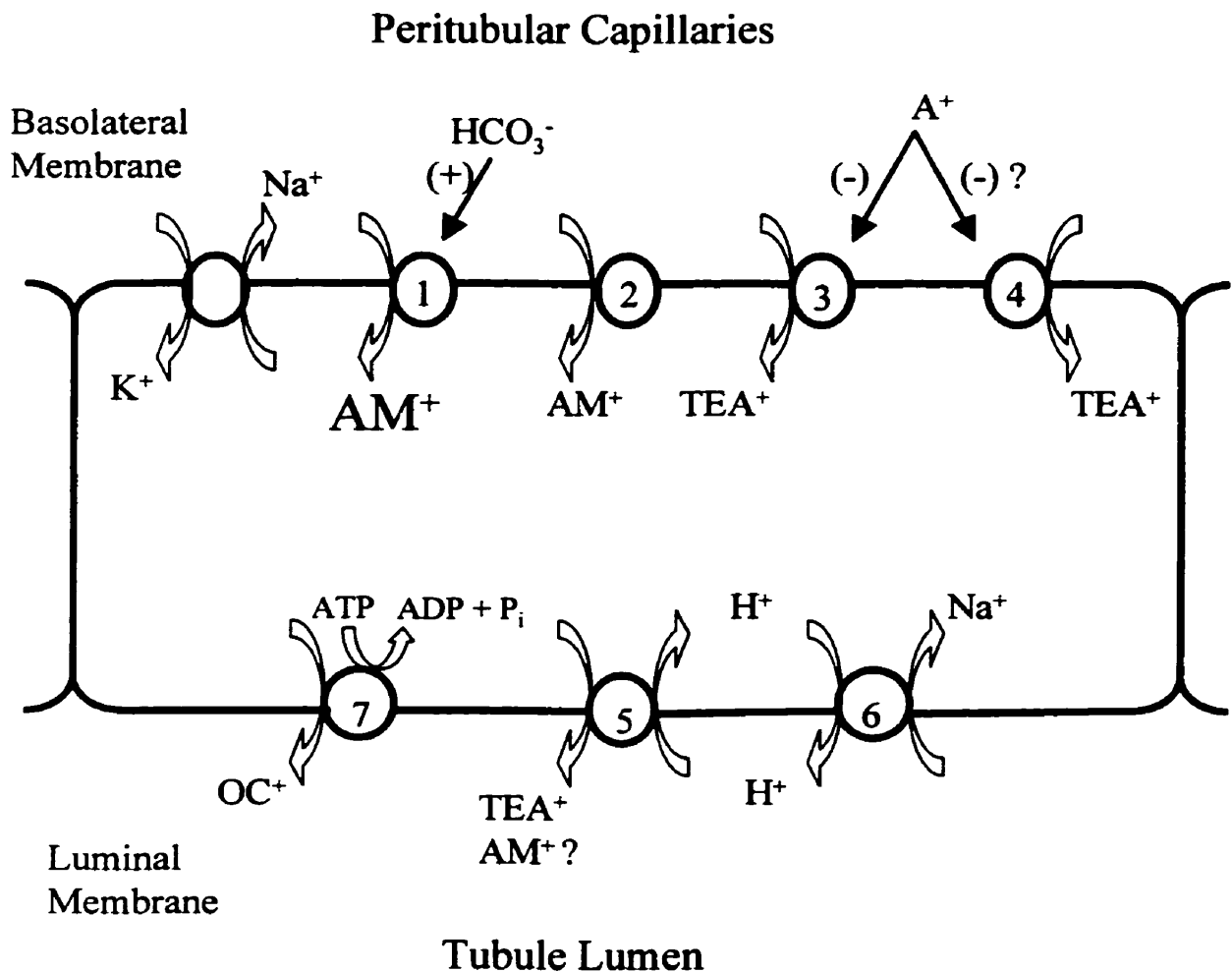
Figure 1-10: Revised model for organic cation transport by rat renal proximal tubules when amantadine and TEA are used as prototypical substrates to characterize this system. AM^+, amantadine; OC^+, organic cation. Site 1: high-affinity-capacity, bicarbonate-dependent amantadine transporter. Site 2: low-affinity-capacity, bicarbonate-independent amantadine transporter. Site 3: High-affinity, low-capacity TEA transporter (inhibited by amantadine). Site 4: Low-affinity, high-capacity TEA transporter (possibly inhibited by amantadine). Site 5: Luminal membrane Na^+/H^+ exchanger. Site 6: H^+/organic cation exchanger. Site 7: P-glycoprotein. (+) refers to activation and (-) refers to inhibition.

92

transport TEA (Grundemann *et al.*, 1994; Zhang *et al.*, 1997a; Okuda *et al.*, 1996; Kekuda *et al.*, 1998). Of the cloned rat organic cation transporters, rOCT1 is thought to be localized in basolateral membranes of S1 rat proximal tubule segments (Koepsell, 1998). rOCT2 is located in the basolateral membranes of S2 and S3 rat proximal tubule segments and possibly distal tubules (Koepsell, 1998). It is likely that our data reflect TEA uptake by at least two of these transporters. For the proposed high-affinity TEA transport site, our K_m $_{TEA\ 1}$ values (33 μM for proximal tubules and 49 μM for distal tubules) closely corresponded to those estimated for rOCT1a (42 μM) expressed in Xenopus oocytes (Zhang *et al.*, 1997a), and rOCT1 (38 μM) and rOCT2 (42 μM) expressed in MDCK dog kidney distal tubule cell lines (Urakami *et al.*, 1998). For the proposed lower-affinity TEA transport site, our K_m $_{TEA\ 2}$ values (246-331 μM) were intermediate between those reported for TEA uptake by rOCT1 (Km = 95 μM) and rOCT2 (Km = 500 μM) (Grundemann *et al.*, 1994; Koepsell, 1998). The estimated K_m for TEA uptake by rOCT3 was 2.5 mM by tracer uptake studies (Kekuda *et al.*, 1998). Thus, rOCT3 should not be a major contributor to TEA uptake in our preparation. Our K_m $_{TEA\ 1}$ and K_m $_{TEA\ 2}$ values are similar to those reported for rOCT1, rOCT1a and rOCT2, and suggest that basolateral TEA uptake into isolated renal tubules may be mediated by some combination of uptake by these transporters. The fact that expression of rOCT1 and rOCT2 in Xenopus oocytes (Grundemann *et al.*, 1994; Koepsell, 1998) and MDCK cells (Urakami *et al.*, 1998) gives different estimates of K_m suggests the cell expression system used may influence kinetic determinations. It is not known which expression system is most comparable to that of normal renal tubule cells. Therefore, our ability to identify the two TEA transporters detected in the present study is limited. Since TEA

doesn't inhibit amantadine uptake, rOCT1, rOCT1a and rOCT2 may be excluded as the bicarbonate dependent amantadine transporters. This hypothesis remains to be tested by evaluating the ability of specific inhibitors of rOCT1 and rOCT2 to block amantadine and TEA uptake into the renal tubule preparations.

NKT, NLT and RST are kidney-expressed proteins that are highly homologous to the OCT family and have been speculated to transport organic cations (Mori *et al.*, 1997; Lopez-Nieto *et al.*, 1997; Simonson *et al.*, 1994). It is possible that these proteins may contribute to amantadine transport in the kidney. However, more recent reports have indicated that NKT and NLT are likely organic anion transporters (Sweet *et al.*, 1997; Sekine *et al*, 1998).

In summary, it has been proposed that the basolateral uptake of type I organic cations (small, more hydrophilic cations) in the proximal tubule is mediated by a single, multispecific, saturable component of the membrane, namely OCT1 (Koepsell, 1998). Using different prototypical type 1 organic cation substrates (amantadine versus TEA) gives a vastly different depiction of organic cation transport in the kidney. This discrepancy suggests that multiple transporters with dissimilar controlling mechanisms may mediate the renal tubule basolateral transport of type 1 organic cations in proximal and distal tubules. Considering the observed differences in amantadine and TEA renal tubule transport, we conclude that amantadine and TEA identify distinct organic cation transport sites in the kidney. Identifying substrate specificity for the different renal

organic cation transporters may allow us to predict potential drug interactions in the kidney.

Chapter 2: Amantadine-Selective Versus Tea-Selective Organic Cation Transporters (Part II)

Section Hypothesis: Cloned transporters OCT1 and OCT2 may not be sufficient to explain the phenomena of organic cation transport by the kidney.

Introduction

It has been hypothesized that the initial step in secretion of organic cations may be mediated by multiple transporters in the basolateral membrane (Sokol and McKinney, 1990; Pritchard and Miller, 1993; Takami *et al*, 1998). In support of this hypothesis, I demonstrated in the preceding chapter that amantadine and TEA characterize different basolateral membrane organic cation transporters in renal proximal and distal tubules. The transporters appear to have different mechanisms of control and possibly substrate specificity. The major difference in mechanism is that amantadine transport into renal proximal and distal tubules is primarily bicarbonate-dependent, whereas TEA transport is independent of bicarbonate in the medium (Escobar *et al*., 1994; Escobar and Sitar 1995). Distinct substrate specificity for amantadine-selective and TEA-selective organic cation transporters was indicated inhibition of TEA but not amantadine uptake in the proximal tubule by NMN.

Transport studies and immunological evidence both suggest that rOCT1 and rOCT2 are renal basolateral membrane transporters and are responsible for the first step in organic cation secretion (Grundemann *et al*., 1994; Urakami *et al*., 1998). In the previous chapter, we demonstrated two sites for basolateral membrane uptake of TEA in proximal and distal tubules that had calculated K_m values similar to those reported for

rOCT1, rOCT1a and rOCT2. These data suggested that basolateral TEA uptake into isolated renal tubules may be mediated by some combination of uptake by these transporters. Since TEA does not inhibit amantadine uptake into renal proximal and distal tubules, rOCT1, rOCT1a and rOCT2 may be excluded as the bicarbonate dependent amantadine transporters. This hypothesis was tested in the present study by evaluating the ability of substrates or inhibitors of rOCT1 and rOCT2 to block amantadine and TEA uptake into the renal tubule preparations. The compounds chosen for the present study have been reported to have substantially different K_m or IC_{50} values for the inhibition of TEA uptake into rOCT1- or rOCT2-expressing Xenopus oocytes (Koepsell, 1998; Okuda et al., 1999). Although two of the inhibitors used in this study (procainamide and NMN) have been reported to inhibit OCT1a mediated TEA uptake (Zhang et al., 1997a) there presently exists insufficient kinetic data to further evaluate the potential contribution of OCT1a to the TEA and amantadine transport process.

In summary, the major objectives of this study were to: further identify that amantadine and TEA characterize different organic cation transporters, identify substrate specificity for the amantadine-selective and TEA-selective organic cation transporters, and to compare the amantadine and TEA transporters in an intact tubule preparation with the already cloned organic cation transporters rOCT1 and rOCT2.

Methods

Amantadine and TEA Inhibition studies

The effects of known inhibitors (procainamide, dopamine, cyanine863, quinine and corticosterone) of organic cation transport on the uptake of 10 μM ^{14}C-TEA and ^{3}H-amantadine in proximal and distal tubules in the presence and absence of bicarbonate were evaluated. The transport reactions were carried out as described in chapter 1, except that the incubation medium also contained various concentrations of the transport inhibitors. Although it was demonstrated in chapter 1 that TEA transport was independent of bicarbonate, it was important to rule out the possibility that bicarbonate-dependent and bicarbonate-independent transport sites with similar kinetics for mediated TEA uptake. Therefore, inhibition assays were carried out in both KHS and CT buffers. Due to the hydrophobic nature of corticosterone it was dissolved in a 95 % v/v ethanol. After necessary dilutions for the inhibition assay, each corticosterone assay tube contained a final ethanol concentration of 0.95 % v/v.

Amantadine and TEA efflux studies

For these studies, 50 μl of ^{3}H-amantadine or ^{14}C-TEA dissolved in KHS (final concentration 10 μM) were added to 150 μl of proximal or distal tubule suspension in KHS and were incubated in a 25°C water bath with shaking (100 oscillations/min) for 15 min (amantadine) and 20 min (TEA) to achieve tissue loading of amantadine and TEA, respectively. Amantadine (30 s) and TEA (60 s) efflux was then carried out by adding 50 μl ($\times$ 3 replicates) of each tissue suspension to 950 μl of KHS (controls) or 950 μl KHS with 10, 100 and 1000 μM amantadine or TEA. The reactions were terminated and

samples were counted as indicated for the uptake studies. To determine total amantadine and TEA that was preloaded, 50 µl (x 3 replicates) of tissue suspension were added after the 15 min (amantadine) and 20 min (TEA) pre-incubation period to tubes that contained no buffer and were then immediately washed and filtered to terminate the reaction.

Results

Amantadine and TEA inhibition experiments

We evaluated a series of structurally distinct compounds (quinine, cyanine$_{863}$, procainamide, dopamine and corticosterone) for their ability to inhibit the uptake of the organic cations TEA and amantadine into isolated renal proximal and distal tubules. Control rates of 10 µM amantadine and TEA renal tubule uptake in the absence of inhibitors are shown in (fig. 2-1). Consistent with previous data, uptake of amantadine into proximal and distal tubules is greater in the bicarbonate-containing medium (KHS) opposed to the non-bicarbonate medium (CT), $p < 0.001$. Alternatively, 10 µM TEA uptake into proximal and distal tubules was similar in the presence and absence of bicarbonate. The rate of TEA uptake but not amantadine uptake into proximal tubules was greater than into distal tubules, $p < 0.01$. Also, the rates of amantadine uptake were 5 (CT) to 10 (KHS) times greater than those reported for TEA.

Rates of amantadine and TEA uptake (expressed as a percentage of control values fig. 2-1) in the presence of increasing inhibitor concentrations are shown in figs. 2-2, 2-3, 2-4, 2-5 and 2-6. Cyanine$_{863}$, quinine and procainamide inhibited (in a concentration dependent manner) amantadine and TEA uptake into proximal and distal tubules in KHS

and CT buffers (**figs. 2-2, 2-3 and 2-4**). Calculated IC_{50} values for inhibition of amantadine and TEA uptake by these compounds are shown in **table 2-1**. As determined from the IC_{50} data, TEA uptake was more potently inhibited than amantadine uptake into proximal and distal tubules in KHS and CT buffer by cyanine863, (500-1000 fold, $p <$ 0.001), quinine (30-200 fold, $p < 0.001$) and procainamide (15-150 fold, $p < 0.05$). Corticosterone dose-dependently inhibited TEA but not amantadine uptake into proximal and distal tubules in KHS and CT (**fig. 2-5**). For the corticosterone inhibition assay, the rates of amantadine or TEA uptake in vehicle control solutions that contained 0.95 % v/v ethanol were not different from the buffer (KHS or CT) controls that did not contain ethanol (data not shown). Dopamine also inhibited TEA uptake but not amantadine uptake into proximal tubules in KHS and CT buffers (**fig. 2-6**). In distal tubules IC_{50} for dopamine inhibition was only calculable for TEA in KHS (**table 2-1**). Dose-response curves for NMN inhibition of amantadine and TEA were presented in the previous chapter, but IC_{50} data was not included. The calculated IC_{50} values for NMN inhibition of TEA uptake are now included in the present section and were similar in proximal and distal tubules, and in the presence and absence of bicarbonate (**table 2-1**). NMN did not inhibit amantadine uptake, with the exception of distal tubules in bicarbonate buffer. However, the extent of inhibition in this case was not large enough to calculate IC_{50} values and was estimated to be greater than 1mM based on the inhibition profile. For all the inhibitors tested, IC_{50} values were similar in proximal and distal tubules with the exception of dopamine inhibition of TEA where the IC_{50}'s appeared more potent in proximal tubules than in distal tubules (**table 2-1**). Based on IC_{50} values, the rank order of inhibitory potency for TEA uptake was cyanine863 $\cong$ quinine > corticosterone >

procainamide > NMN $\cong$ dopamine. The rank order of inhibitory potency for amantadine

uptake (quinine > cyanine$_{863}$ > procainamide) was different than for TEA.

The K_i (dissociation constant) values for these inhibitors were calculated from the

IC_{50} values by the method of Cheng and Prusoff (1973) assuming that they were all

competitive inhibitors of transport (**table 2-2**). The calculated K_i values provided a

similar interpretation, as did the IC_{50} values described above. When possible, the

inhibitor dissociation constant (K_i) was used for the purpose of comparing the results of

our inhibition studies with previously reported data in the literature (**table 2-3**). In

situations where K_i values have not been reported previously, we used comparison of our

IC_{50} data with those reported in the literature. It is appreciated that IC_{50} comparisons

should only be accepted as tentative in nature because of the dependence of calculated

IC_{50} on substrate concentration and assay conditions (Cheng and Prusoff, 1973).

However, in our experiments it is valid to compare IC_{50} for inhibition of amantadine and

TEA uptake because the same assay conditions were used, and the concentration of TEA

and amantadine were the same (10 μM). In addition, our IC_{50} values give a close

estimate of K_i because amantadine and TEA concentrations used were substantially lower

than K_m for their uptake. In this situation the denominator in the equation (K_i =

$IC_{50}/(1+s/K_m)$ approaches one and IC_{50} approaches K_i.

Amantadine and TEA efflux experiments

We performed amantadine and TEA efflux experiments to determine if exit of

amantadine and TEA from the tubules occurs by independent mechanisms. All efflux

studies were performed in the presence of bicarbonate, at pH 7.4. Efflux of both amantadine (30 s) and TEA (60 s) from renal proximal and distal tubules was observed under trans-zero conditions (**fig. 2-7**). Efflux of amantadine from proximal and distal tubules was stimulated in a concentration dependent manner by the presence of amantadine in the efflux medium whereas TEA (10-1000 μM) had no effect on amantadine efflux. Likewise, efflux of TEA from proximal and distal tubules was stimulated in a concentration dependent manner by the presence of TEA in the efflux medium whereas the presence of amantadine (10-1000 μM) in the efflux medium had no effect on TEA efflux.
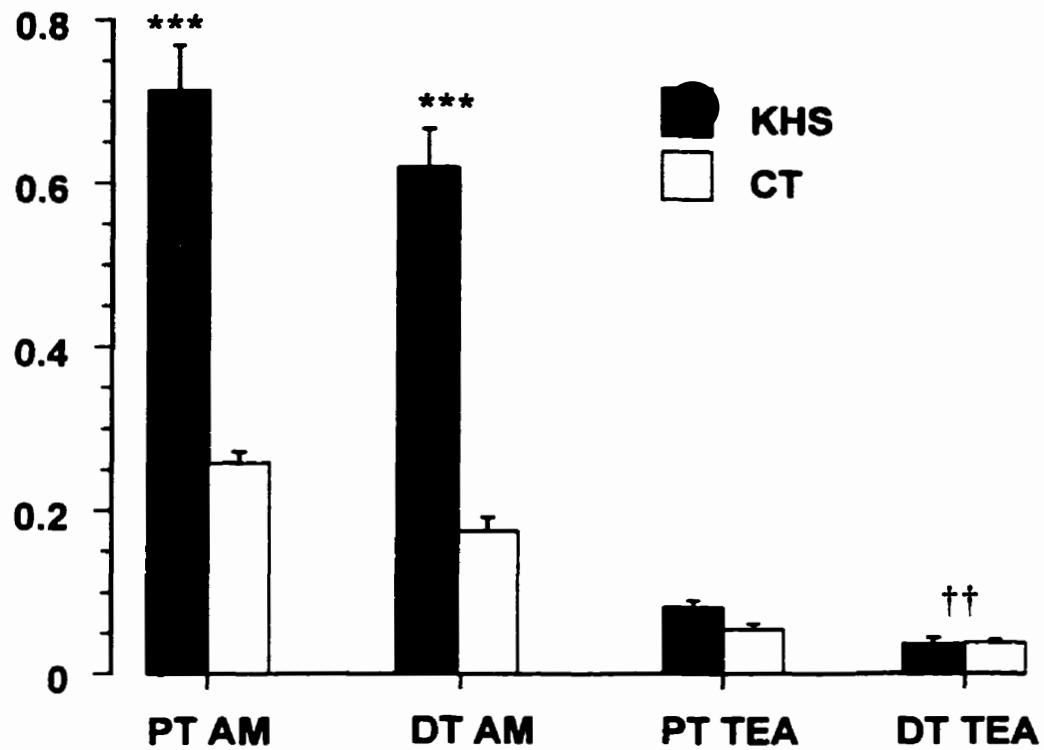
Fig. 2-1. Control rates (nmol mg^{-1} protein min^{-1}) of 10 μM amantadine (AM) and TEA uptake into isolated renal proximal (PT) and distal tubule (DT) segments. Each symbol represents the mean ± s.e. mean of 6-11 separate determinations. *** p < 0.001 compared to amantadine uptake CT, †† p < 0.01 compared to TEA uptake in proximal tubules, ANOVA followed by Tukey's HSD.
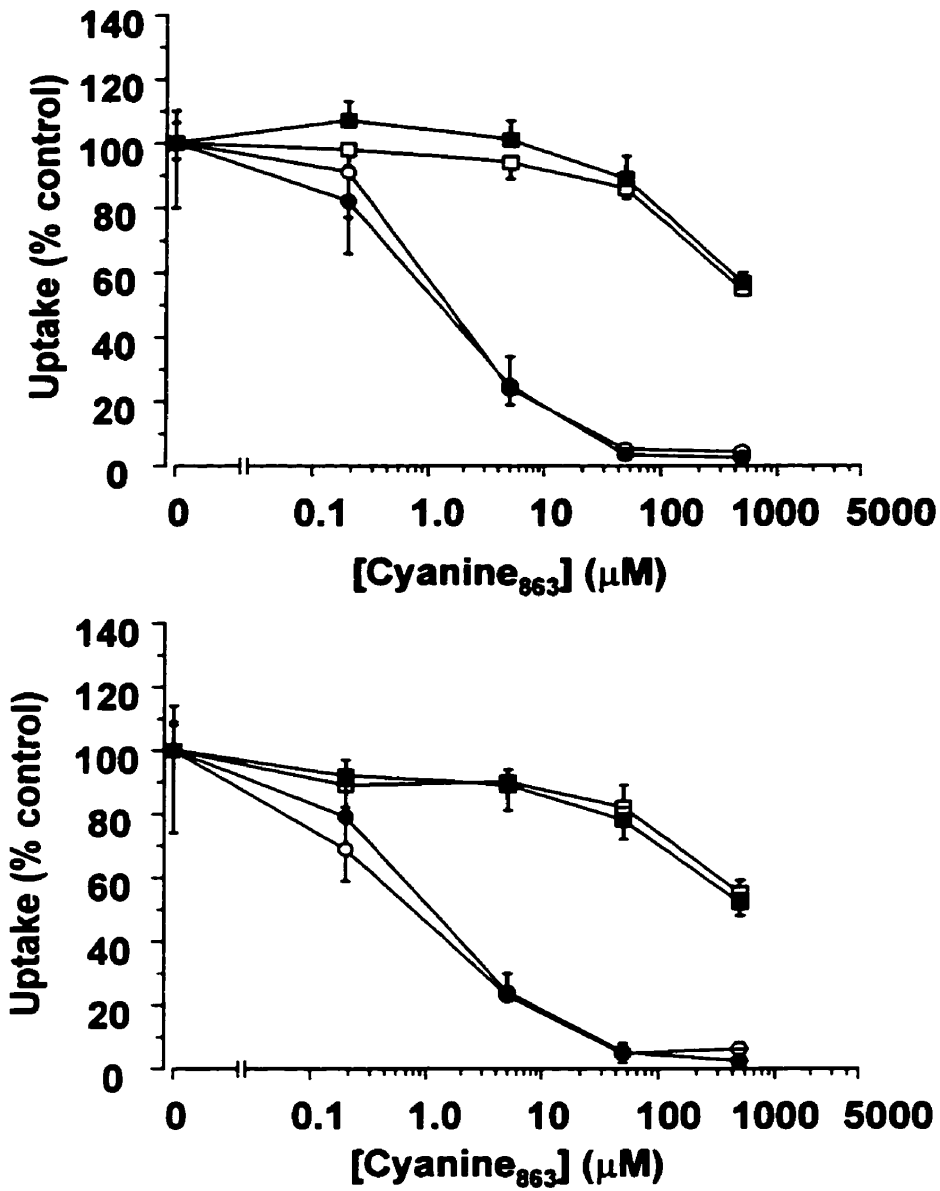
Figure 2-2. Cyanine$_{863}$ inhibition of amantadine (squares) and TEA (circles) uptake into isolated proximal (upper panel) and distal (lower panel) tubules in KHS (closed symbols) or CT (open symbols) buffer. The concentrations of cyanine$_{863}$ used were 0.2, 5, 50 and 500 μM. Inhibition data are represented as uptake as a percentage of control. Each symbol represents the mean ± SE of 4 to 5 separate determinations.
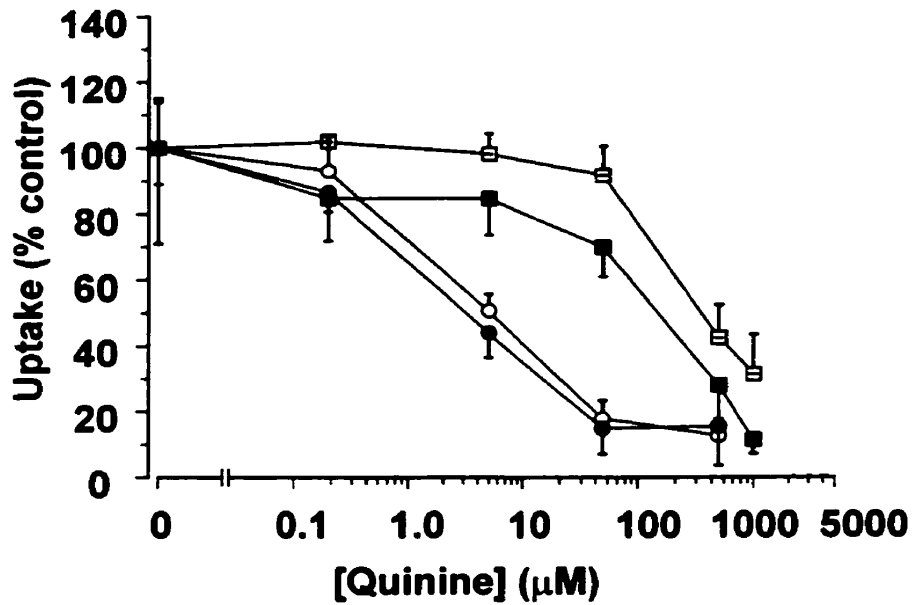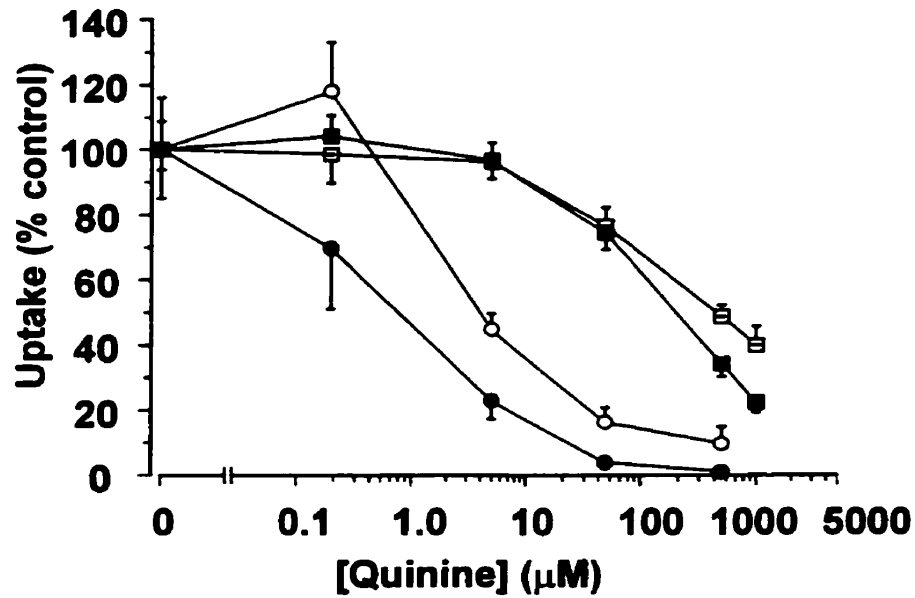
Figure 2-3. Quinine inhibition of amantadine (squares) and TEA (circles) uptake into isolated proximal (upper panel) and distal (lower panel) tubules in KHS (closed symbols) or CT (open symbols) buffer. The concentrations of quinine used were 0.2, 5, 50 and 500 and 1000 µM. Inhibition data are represented as uptake as a percentage of control. Each symbol represents the mean ± SE of 4 to 6 separate determinations.
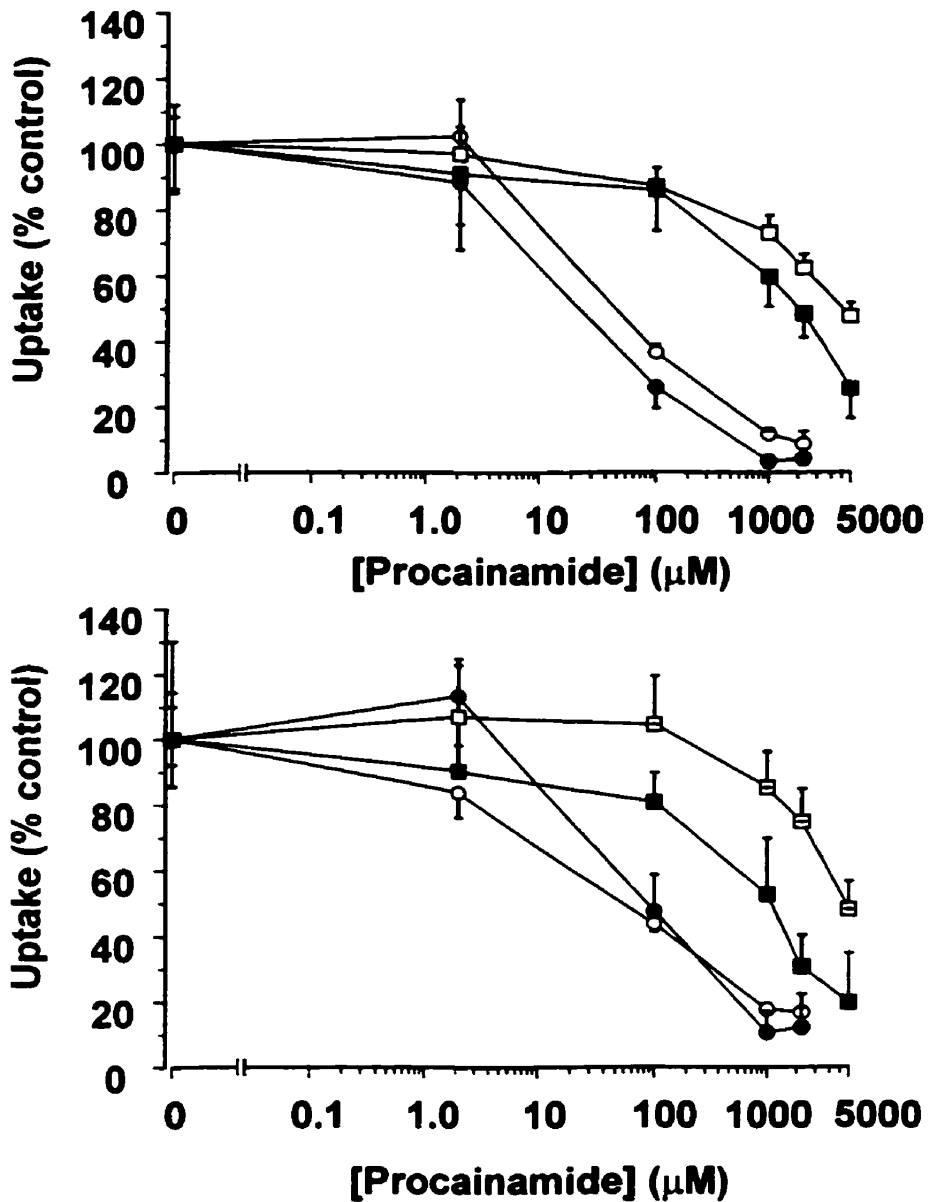
Figure 2-4. Procainamide inhibition of amantadine (squares) and TEA (circles) uptake into isolated proximal (upper panel) and distal (lower panel) tubules in KHS (closed symbols) or CT (open symbols) buffer. The concentrations of procainamide used were 2, 100, 1000, 2000 and 5000 μM. Inhibition data are represented as uptake as a percentage of control. Each symbol represents the mean ± SE of 4 to 6 separate determinations.
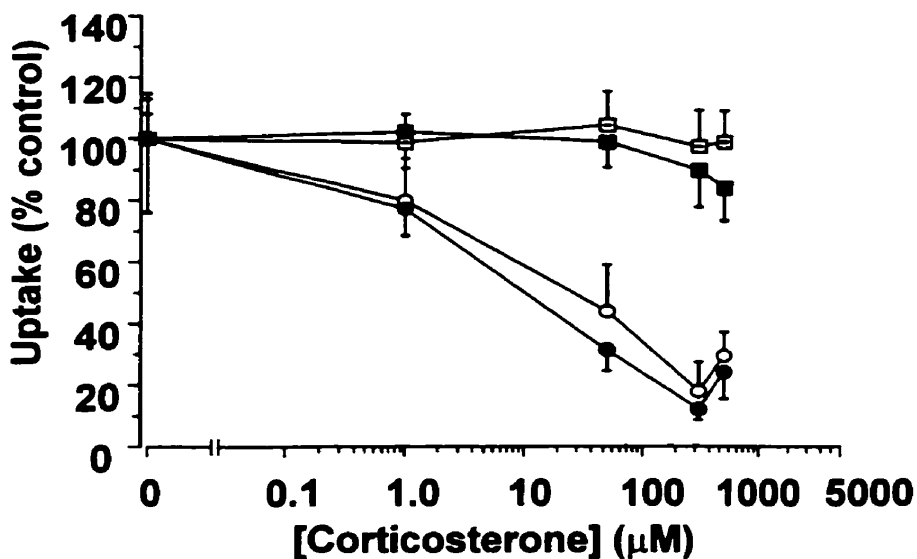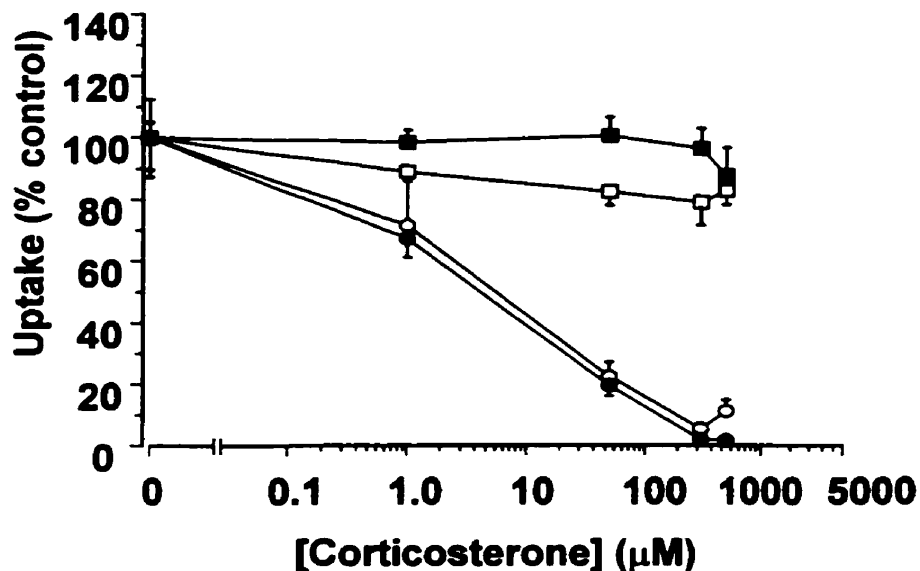
Figure 2-5. Corticosterone inhibition of amantadine (squares) and TEA (circles) uptake into isolated proximal (upper panel) and distal (lower panel) tubules in KHS (closed symbols) or CT (open symbols) buffer. The concentrations of corticosterone used were 1, 50, 300 and 500 µM. Corticosterone was dissolved in 95% v/v ethanol and the final assay solutions contained an ethanol concentration of 0.95 % v/v. Inhibition data are represented as uptake as a percentage of vehicle control, which contained (0.95 % v/v ethanol). Each symbol represents the mean ± SE of 4 to 5 separate determinations.
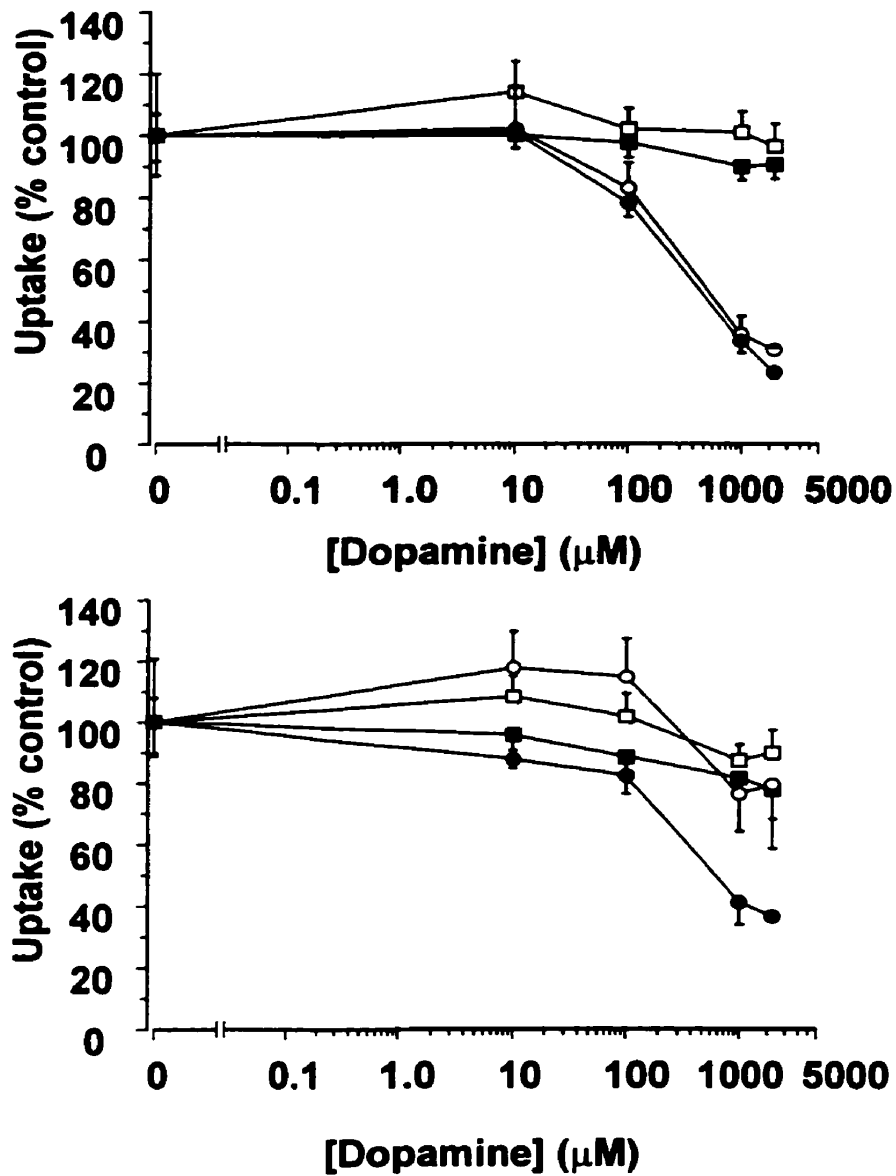
Figure 2-6. Dopamine inhibition of amantadine (squares) and TEA (circles) uptake into isolated proximal (upper panel) and distal (lower panel) tubules in KHS (closed symbols) or CT (open symbols) buffer. The dopamine concentrations used were 10, 100, 1000 and 2000 μM. Inhibition data are represented as uptake as a percentage of control. Each symbol represents the mean ± SE of 4 to 5 separate determinations.
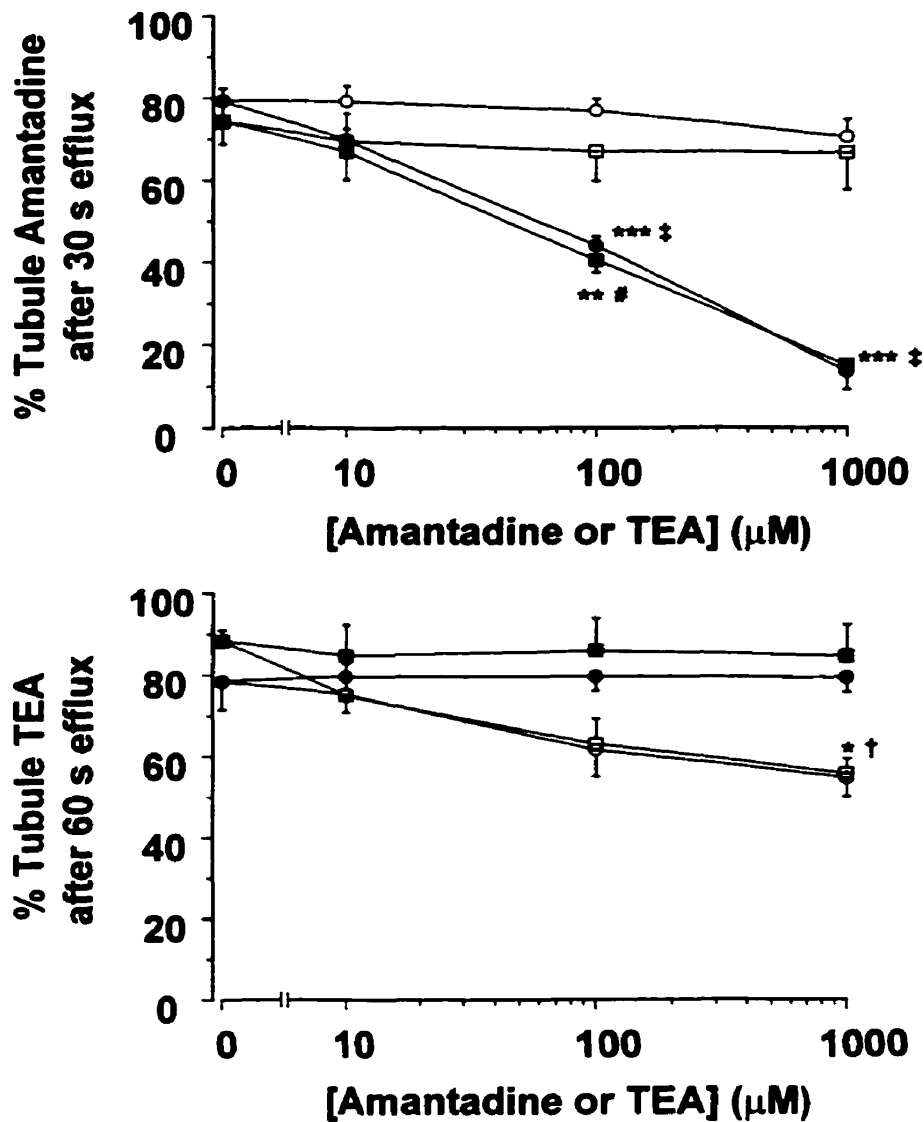
Figure 2-7. Efflux of amantadine (upper panel) and TEA (lower panel) from proximal (squares) and distal (circles) tubules into KHS (trans-zero conditions) or KHS with 10, 100 and 1000 μM amantadine (closed symbols) or 10, 100 and 1000 μM TEA (open symbols). The efflux period was 30 s for amantadine and 60 s for TEA. Each point represents the mean $\pm$ SE of 5 separate determinations. * $p < 0.05$, ** $p < 0.01$ and *** $p < 0.001$ compared to trans-zero conditions within tubule group. # $p < 0.01$ and ‡ $p < 0.001$ compared to efflux in the presence of TEA at the same concentration and within the same tubule group. † $p < 0.05$ compared to efflux in the presence of amantadine at the same concentration and within the same tubule group.

109

Table 2-1: IC_{50} values (μM) for inhibition of renal proximal and distal tubule uptake of amantadine and TEA

Inhibitor		Proximal (KHS)	Proximal (CT)	Distal (KHS)	Distal (CT)
Cyanine[863],	AM [1]	930 ± 300^c	880 ± 170^c	1400 ± 800^c	820 ± 230^c
	TEA	1.6 ± 0.8	1.0 ± 0.3	2.6 ± 1.4	0.80 ± 0.30
Quinine	AM	180 ± 20^c	350 ± 90^c	91 ± 14^c	440 ± 150^c
	TEA	1.6 ± 0.2	1.6 ± 0.4	2.9 ± 1.2	4.7 ± 2.0
Procainamide	AM	2200 ± 800^c	6400 ± 2000^c	1100 ± 700^a	6700 ± 2900^c
	TEA	19 ± 7	42 ± 17	75 ± 42	65 ± 26
Dopamine	AM	DNI	DNI	DNI	DNI
	TEA	490 ± 60	300 ± 100	$1.1 \bullet 0.4$	> 1 mM
Corticosterone	AM	DNI	DNI	DNI	DNI
	TEA	4.9 ± 1.9	3.0 ± 0.7	7.0 ± 3.8	20 ± 10
NMN	AM	DNI	DNI	> 1 mM	DNI
	TEA	320 ± 130	590 ± 120	410 ± 130	340 ± 80

[1] AM, amantadine. IC_{50} values are reported as mean ± SE of 4 or 5 individual experiments. DNI = did not inhibit. In some instances inhibition was present but not to the extent required for IC_{50} determinations. Therefore, these values were indicated as being greater than the highest concentration of inhibitor used in the dose response curve

(e.g. > 1mM). The IC_{50} data were transformed by the factor $[\log_{10}(IC_{50} \times 10)]$ to produce similar variance in the amantadine and TEA groups for ANOVA followed by Tukey HSD, [a] $p < 0.05$, and [c] $p < 0.001$.

Table 2-2: K_i (μM) values for inhibition of renal proximal and distal tubule uptake of amantadine and TEA

Inhibitor		Proximal (KHS)	Proximal (CT)	Distal (KHS)	Distal (CT)
Cyanine$_{863}$	AM [1]	890 ± 290^c	860 ± 170^c	1300 ± 700^c	790 ± 220^c
	TEA	1.3 ± 0.6	0.76 ± 0.25	2.2 ± 1.2	0.66 ± 0.27
Quinine	AM	170 ± 20^c	340 ± 90^c	80 ± 10^c	420 ± 40^c
	TEA	1.3 ± 0.4	1.2 ± 0.3	2.4 ± 1.0	3.9 ± 1.6
Procainamide	AM	2100 ± 800^c	6200 ± 2000^b	1000 ± 700^b	6400 ± 2800^a
	TEA	16 ± 5	32 ± 13	62 ± 35	53 ± 22
Dopamine	TEA	400 ± 50	230 ± 70	880 ± 400	
Corticosterone	TEA	4.1 ± 1.6	2.3 ± 0.6	5.8 ± 3.1	16 ± 8
NMN	TEA	260 ± 110	460 ± 90	340 ± 110	280 ± 62

[1] AM, amantadine. K_i values are reported as mean ± SE of 4 or 5 individual experiments. K_i values were determined from IC_{50} values using the conversion $K_i = IC_{50}/(1 + s/K_m)$ and assuming competitive inhibition (Cheng and Prusoff, 1973) For this conversion we used our K_m values for TEA and amantadine uptake in proximal and distal tubules, in KHS and CT buffer that were reported in chapter 1. The K_i data were transformed by the factor $[\log_{10}(IC_{50} \times 10)]$ to produce similar variance in the amantadine and TEA groups for ANOVA followed by Tukey HSD, $^a p < 0.05$, $^b p < 0.01$ and $^c p < 0.001$.

Table 2-3: Reported K_m [K_i] or (IC_{50}) values for substrates or inhibitors of rOCT1 and rOCT2.

Compound	rOCT1 K_m, [K_i] or (IC_{50})	rOCT2 K_m, [K_i] or (IC_{50})	Expression System	Reference
Cyanine$_{863}$	(0.13 μM) [0.67 μM] [0.13 μM]	(8.5 μM)	Xenopus oocytes HEK 293 cells Xenopus oocytes	Koepsell, 1998 Martel *et al.*, 1996 Grundemann *et al.*, 1994
Quinine	(0.9 μM) [4.3 μM] [0.93 μM]	(14 μM)	Xenopus oocytes HEK 293 cells Xenopus oocytes	Koepsell, 1998 Martel *et al.*, 1996 Grundemann *et al.*, 1994
Procainamide	(13 μM) (44 μM) [13 μM]	(1500 μM) (257 μM)	Xenopus oocytes Xenopus oocytes Xenopus oocytes	Koepsell, 1998 Okuda *et al.*, 1999 Grundemann *et al.*, 1994
Corticosterone	(160 μM) [72 μM]	(5 μM)	Xenopus oocytes HEK 293 cells	Koepsell, 1998 Martel *et al.*, 1996
Dopamine	51 μM	650 μM	Xenopus oocytes	Koepsell, 1998
NMN	340 μM (2420 μM) [669 μM] [1000 μM]	800 μM (1560 μM) [403 μM]	Xenopus oocytes Xenopus oocytes MDCK cells Xenopus oocytes	Koepsell, 1998 Okuda *et al*, 1999 Urakami *et al*, 1998 Grundemann *et al.*, 1994

K_i values are shown in square brackets, IC_{50} values in round brackets and K_m values are not bracketed.

Discussion

The present studies were designed to determine if amantadine-selective and TEA-selective transporters, previously identified in intact tubule preparations, could be associated with the cloned organic cation transporters rOCT1 and rOCT2. It is apparent from the reported literature data (**table 2-3**) that rOCT1 and rOCT2 may have substantially different affinities for some organic cations and similar affinities for other organic cations. We attempted to choose inhibitors with different specificity for the two transport systems such that we may predict, based on our IC_{50} and K_i data, which transporters may be responsible for mediating TEA and amantadine uptake into isolated proximal and distal tubule segments. The major findings of this study are consistent with the idea that amantadine and TEA characterize different organic cation transporters, and that rOCT1 and rOCT2 may be insufficient to explain in its entirety, the renal tubule basolateral transport of organic cations.

Cyanine$_{863}$ and quinine are known inhibitors of renal tubule transport and secretion of organic cations (Rennick *et al.*, 1956; Wong *et al.*, 1990; Gaudry *et al.*, 1993). Procainamide has been used to characterize mechanisms of the renal tubule organic cation transport system (McKinney and Speeg, 1982; McKinney 1983). It was quite evident from our data that cyanine$_{863}$, quinine and procainamide interact with the amantadine-selective and the TEA-selective transporters; however, they more potently inhibit TEA uptake as compared to amantadine uptake in proximal and distal tubules. Our reported K_i values for cyanine$_{863}$, quinine and procainamide inhibition of TEA uptake

are in close agreement with those reported for inhibition of TEA transport by rOCT1 expressed in Xenopus oocytes or HEK 293 cells (**table 2-3**). Conversely, our K_i values for inhibition of amantadine uptake are much greater than those reported for rOCT1, suggesting that rOCT1 does not mediate amantadine transport in isolated renal tubules. Detailed K_i values for inhibition of rOCT2 mediated uptake by these compounds have not been published; however, cyanine$_{863}$, quinine and procainamide were all reported to have more potent IC_{50} values for inhibition of TEA transport by rOCT1 than rOCT2 (**table 2-3**). Compared to these data, our IC_{50} values for inhibition of TEA uptake by cyanine$_{863}$, quinine and procainamide more closely resemble inhibition of rOCT1 mediated TEA uptake, whereas the IC_{50} values for inhibition of amantadine uptake are much greater than those reported for inhibition of rOCT1 or rOCT2 mediated TEA uptake. These data suggest that the transport of TEA into renal proximal and distal tubules is more closely associated with the characteristics of rOCT1, whereas bicarbonate-dependent and independent amantadine transport is not associated with rOCT1 or rOCT2. The similarity for inhibition of TEA uptake in KHS and CT is consistent with our previous data that indicate renal tubule uptake of TEA is via bicarbonate-independent transporters.

Studies in rats and rOCT1-expressing HEK 293 cells indicate that the catecholamine dopamine is a substrate for the renal tubule organic cation transport system and rOCT1 (Brandle *et al.*, 1992; Busch *et al.*, 1996b). In our study, dopamine specifically blocked TEA uptake and had little or no effect on amantadine uptake into the proximal and distal tubules. Our K_i values for dopamine inhibition of proximal tubule TEA uptake are in close agreement with those determined by Brandle *et al* (1992), and

were intermediate between the reported K_m values for dopamine transport by rOCT1 and rOCT2 (**table 2-3**). Distal tubule IC_{50} values for dopamine inhibition of TEA uptake were estimated as greater than 1mM, and suggest a difference in the proximal versus distal tubule distribution of TEA-selective organic cation transporters. Amantadine has been shown to inhibit the uptake of dopamine by hOCT2 (the human homologue of rOCT2) with a K_i of about 30 µM (Busch *et al.*, 1998). Therefore, it is interesting that in our experiments dopamine did not inhibit the renal tubule transport of amantadine. A similar phenomenon was observed in the previous chapter and showed amantadine inhibits TEA uptake into renal tubules but TEA does not inhibit amantadine uptake. With respect to dopamine inhibition, the experimental data suggest that the TEA-selective transporters may accept catecholamines such as dopamine for transport but the amantadine-selective transporters do not.

The endogenous steroid corticosterone is an inhibitor of TEA uptake mediated by the rat organic cation transporters rOCT1 and rOCT2, the porcine organic cation transporter OCT2p, and the human organic cation transporter hOCT1 (Grundemann *et al.*, 1994; Grundemann *et al.*, 1997; Koepsell, 1998; Zhang *et al.*, 1998). According to reported IC_{50} values corticosterone more potently inhibits TEA uptake by rOCT2-expressing oocytes than rOCT1-expressing oocytes (**table 2-3**). Our experimental data indicate that the TEA-selective transporters in the kidney may also transport hydrophobic uncharged steroid molecules, whereas the amantadine-selective transporters do not. Corticosterone has also been shown to interact with the rat organic anion transporter oatp (Kanai *et al.*, 1996; Bossuyt *et al.*, 1996); thus, we may exclude oatp as being the

amantadine-selective transporter(s). The ability of corticosterone to inhibit TEA uptake without preincubation suggests that it is acting directly on the TEA transporter(s) and is consistent with the findings of others (Grundemann *et al.*, 1997). Our *Ki* values for corticosterone inhibition of TEA uptake are lower than those estimated for rOCT1 expressed in HEK 293 cells (**table 2-3**). Our IC_{50} values more closely resemble those published for rOCT2 than those for rOCT1 (**table 2-3**).

The endogenous metabolite NMN undergoes renal tubule secretion and has been used as a substrate to characterize the renal tubule organic cation transport system (Beyer *et al.*, 1950; Kinsella *et al.*, 1979a; Holohan and Ross, 1980; Ullrich *et al.*, 1991). NMN had a reported lower K_m for rOCT1 than rOCT2 (**table 2-3**). Other reports have also demonstrated that K_i and IC_{50} values for NMN inhibition of TEA uptake in MDCK cells or Xenopus oocytes expressing rOCT1 or rOCT2 were similar (**table 2-3**). Our calculated K_i values for NMN inhibition of TEA were similar to the K_m reported by Koepsell (1998) and the K_i values reported by Urakami *et al.* (1998). The overall inhibition data from NMN, dopamine and corticosterone failed to provide a clear indication of which of the transporters (rOCT1 or rOCT2) is more responsible for TEA transport in intact proximal and distal tubule segments.

In the present study, extracellular amantadine stimulated its efflux only and extracellular TEA similarly stimulated TEA efflux only. The apparent "trans-stimulation" of organic cation efflux by the presence of the same compound or a similar compound in the efflux medium is a well known phenomenon. Trans-stimulation of

efflux occurs when the transport mediated influx of an extracellular compound stimulates the efflux of its intracellular analogue by the reverse action (or exchange mechanism) of the transporter (Christensen, 1975). Another possibility to explain this apparent observed increase in efflux is cis-inhibition. Cis-inhibition of efflux occurs when the presence of a compound in the efflux medium causes an apparent increase in the efflux of an intracellular analogue not by stimulating increased intracellular to extracellular flux but by inhibiting reclamation of the already effluxed analogue (Cristensen, 1975). Renal tubule transport has been shown to be directional (basolateral to luminal transport) for some organic cations (Saito et al., 1992; Chan et al., 1996; Takami et al., 1998). Therefore, a third possible explanation for the enhancement of amantadine and TEA efflux is that the saturating concentrations of amantadine and TEA in the extracellular medium stimulate by mass action the efflux of the preloaded amantadine or TEA across the luminal membrane. The contribution of these three factors to the observed increase in amantadine or TEA exit from the tubule cells cannot be determined from the present study. However, the results of the efflux studies are consistent with our uptake data, and suggest that exit of amantadine and TEA from renal tubule cells also occurs by independent mechanisms. Furthermore, the fact that amantadine inhibits TEA uptake but does not stimulate TEA efflux suggests that amantadine interacts with but is not transported by the TEA transporter(s).

In summary, the inhibition and efflux studies strengthen support for our previous suggestion that the renal tubule transport of amantadine and TEA are mediated by different transport systems. The differences in the inhibition profiles for amantadine and

TEA uptake support our contention that amantadine transport is not consistent with rOCT1- and rOCT2- mediated organic cation transport as they are presently characterized. From these data, we propose that amantadine identifies a renal tubule organic cation transporter system that is novel from that previously characterized with TEA. Further in vitro and in vivo characterization of the amantadine-selective transporter(s) is required to more clearly identify its substrate specificity and importance in drug elimination by the kidney.

Chapter 3: Bicarbonate-Dependent Organic Cation Transport In Disease

Section hypothesis: Disease conditions that affect the kidney may alter organic cation transport and thus have implications for reduced renal drug elimination and consequential drug accumulation and toxicity.

Introduction

In the previous two chapters we provided evidence that supports the division of renal tubule basolateral membrane organic cation transporters into those that are amantadine-selective and those that are TEA-selective. In this section the focus is on describing the effects of Streptozotocin (STZ)-induced diabetes mellitus and uninephrectomy on the bicarbonate-dependent organic cation transporter and its implications for altered drug elimination.

Nephropathy and end-stage renal failure are major complications observed in long-term diabetes mellitus (Deckert *et al.*, 1978; Andersen *et al.*, 1983). However, structural and functional changes in the kidney are already present at the onset of clinically obvious diabetes mellitus (Morgensen *et al*, 1983). The early stages of diabetes mellitus in humans and in experimentally induced diabetes mellitus in rats are characterized by microalbuminurea, hyperfiltration, and hypertrophy of the kidney and are not associated with any clinically overt signs of decreased renal function (Seyer-Hansen *et al.*, 1980; Jensen *et al*, 1981; Morgensen *et al.*, 1983; Cortes *et al.*, 1987). Despite the ample evidence concerning altered renal structure and function, few data are available regarding

the effects of diabetes complications on the clearance of drugs that are eliminated predominantly unchanged by the kidney (Gwilt *et al.*, 1991, Preston and Epstein, 1999). The primary objective of this study was to evaluate if early-stage untreated streptozotocin (STZ)-induced diabetes mellitus can disrupt or alter the function of the renal tubule organic cation transport system. Uninephrectomy results in compensatory renal hypertrophy and hyperplasia similar to that observed in early-stage untreated STZ-induced diabetes mellitus (Seyer-Hansen, 1978). For the present study the uninephrectomized (UNX) rats provided a non-disease control in which to study the effects of renal hypertrophy on renal tubule organic cation transport mechanisms. Second, studies in UNX rats may provide information about adaptive physiological response in how the kidney maintains secretory function in face of decreased renal mass. This has not been studied in regards to organic cation secretion by the kidney. Finally, the ensuing hypertrophy after uninephrectomy may be associated with increased expression of one or more organic cation transporters in the remaining kidney, thus possibly providing a useful experimental model to study components of the organic cation transport pathway that are not otherwise visible in a two-kidney rat.

In the previous two chapters we have identified that amantadine characterizes a unique organic cation transporter in the kidney that may be important for cationic drug elimination. In humans, it is known that the renal elimination of amantadine is reduced with impaired renal function and can lead to amantadine toxicity (Bleidner *et al.*, 1965; Ing *et al.*, 1979; Horadam *et al.*, 1981; Armbruster *et al.*, 1974; Aoki and Sitar, 1988). However, it is not well known whether pathophysiological conditions that affect renal

function (such as diabetes mellitus) affect the renal tubule organic cation transport system and thus the excretion of amantadine or other organic cations by the kidney. We hypothesized that the renal changes associated with diabetes mellitus and the compensatory renal growth after uninephrectomy result in modulation of the renal organic cation transport system and thus may have implications for drug elimination by the kidney. In particular, we investigated the bicarbonate-dependent amantadine transporter(s) which is/are the primary mediator(s) for the energy-dependent passage of amantadine across the basolateral membrane into proximal and distal tubule cells (the first step in secretion) (Escobar et al., 1994; Escobar and Sitar, 1995).

In untreated or poorly regulated diabetes mellitus, a major complication is the development of ketoacidosis which is primarily due to the overproduction and accumulation of acetoacetate and β-hydroxybutyrate (Foster and McGarry, 1983). Previous studies from our laboratory indicate that lactate (similar in structure to β-hydroxybutyrate) inhibits bicarbonate-dependent amantadine transport in vitro and decreases renal amantadine elimination in vivo (Escobar et al., 1995; Sitar et al., 1997). Thus, it is possible that overproduction of β-hydroxybutyrate in untreated diabetes may have a similar effect as lactate in disrupting bicarbonate-dependent organic cation transport. We analyzed β-hydroxybutyrate and other lactate and bicarbonate-like anions (glycolate, propionate, α–hydroxybutyrate and γ–hydroxybutyrate) for the ability to modulate amantadine transport via the bicarbonate-dependent transporter and to determine the structural requirements for the anionic component of this transport process.

Methods

Experimental design and animal preparation

Male Sprague-Dawley rats (150-200 g) were obtained from the University of Manitoba (Charles River breeding stock). The rats were housed in plastic cages at 22°C, with a twelve-hour light/dark cycle. Rats had free access to food and water. Three separate experimental series were performed as part of this study.

     Experiment 1: We compared transport properties of amantadine in renal proximal and distal tubules isolated from control male Sprague-Dawley rats (group 1) versus STZ induced diabetic rats with (group 2) or without insulin treatment (group 3). The preparation of diabetic animal and confirmation of the diabetic state were performed according to the methods of Hatch *et al.*, (1995). After an overnight fast, rats (groups 2 and 3) were injected in the tail vein with STZ (75 mg/kg body wt.) dissolved in freshly prepared citrate buffer (pH 4.5). Control rats (group 1) were injected with 0.1 M citrate only. At 24 hours post STZ injection, glucosuria was confirmed in the diabetic rats by using Ames Diastix®. Urine glucose levels in diabetic rats were greater than 111 mM (estimated from the Diastix). One group of diabetic animals (group 2) was injected daily (14:00 h) with 3 units of NPH insulin. Within 24 h of insulin treatment, the diabetic rats had no glucosuria. Five days post-STZ injection the kidneys were removed and renal tubule transport studies were performed. On the day of experimentation, blood glucose levels of rats were estimated, by using Chemstrip bG (glucose oxidase). Only animals that had blood glucose levels greater than 21 mM were used in the diabetic group (group 3). At a later date, kidneys from an additional control group and hyperinsulemic group

were made available for amantadine transport studies. Hyperinsulemic rats were prepared by injecting normal rats with NPH insulin (daily, four 4 days) as described above for the diabetic rats. The control rats received daily saline injections in place of insulin. On the day of the experiment blood glucose levels (7-8 mM) were similar in hyperinsulinemic rats compared to control.

Experiment 2: We compared transport properties of amantadine in the renal proximal and distal tubules isolated from two-kidney rats (group 4) versus similar age uninephrectomized rats (group 5). For the uninephrectomized rats (group 5), the right kidney was removed under ether anaesthesia via a flank incision and a minimum one-week recovery period was imposed. Renal tubule transport studies were performed on tubules isolated from the remaining kidney 7-14 days after the unilateral nephrectomy was performed.

Experiment 3: We examined a series of lactate-like organic anion metabolites (glycolate, racemic lactate, propionate or racemic α, racemic β and γ–hydroxybutyrate) to determine if ketoacid formation can modulate organic cation transport by the kidney and to determine the structural requirements for the anion component of the bicarbonate-dependent organic cation transporter. These series of experiments were performed in renal tubules isolated from normal male Sprague Dawley rats.

Amantadine transport studies

These studies were aimed at evaluating the function of the bicarbonate-dependent amantadine transport process. Therefore, all amantadine transport assays were performed in the presence of 25 mM bicarbonate (KHS buffer). To determine K_m and V_{max} for amantadine uptake, tubules were prepared (in triplicate) that contained a fixed amount of ³H-amantadine (1 nM) and unlabeled amantadine (final assay concentrations 10 to 500 μM) in a volume of 150 μl of KHS buffer. For the anion inhibition studies, the assay tubes contained 10 μM amantadine, 0.4 – 50 mM of either glycolate, lactate, propionate or α, β or γ–hydroxybutyrate in 150 μl KHS buffer. Proximal or distal tubule suspensions (50 μl in KHS buffer) were then added to each assay tube to begin the transport reaction. The remainder of the assay was carried out as described in the general methods.

Results

Diabetic rat study

In our first series of experiments, we analyzed the effects of early-stage STZ-induced diabetes on the renal tubule transport of the organic cation amantadine by the bicarbonate-dependent organic cation transporter. All diabetic rats were confirmed diabetics by urine glucose measurements prior to insulin treatment. In these rats urine glucose were greater than 111 mmol L^{-1}. On the day of the experiment (4 days after induction of diabetes with STZ), rats in the diabetic group had a blood glucose level greater than 21 mM (data not shown). The uptake of amantadine in pH 7.4 KHS was saturable in renal proximal and distal tubules isolated from control rats and the STZ-

induced diabetic rats with or without insulin treatment (**fig. 3-1**). The calculated apparent K_m and V_{max} for amantadine uptake into the tubules are shown in **table 3-1**. Compared to the respective proximal and distal tubule control groups, the K_m (affinity) for amantadine uptake was not altered in diabetic rats that did or did not receive insulin treatment. In the untreated diabetic rats, V_{max} (maximal capacity) for amantadine uptake was selectively increased (70%) in proximal tubule segments compared to control ($p < 0.05$). In the insulin-treated diabetic rats, the V_{max} for amantadine uptake returned to control levels and was significantly lower than for the untreated diabetic rats ($p < 0.05$).

UNX rat study

In the second series of experiments, we examined the bicarbonate-dependent transport of amantadine into proximal and distal tubules isolated from the remaining kidney of UNX rats 7-14 days after the uninephrectomy. Similar to that observed in the diabetic rat experiments, uptake of amantadine with increasing concentration was saturable in proximal and distal tubules isolated from the UNX rats (data not shown). The calculated apparent K_m and V_{max} for amantadine uptake in renal proximal and distal tubules isolated from the remaining kidney of the uninephrectomized rats versus control male Sprague-Dawley rats are shown in **table 3-2**. Similar to the untreated diabetic rats, a selective increase (70 %) in V_{max} was observed in the proximal tubules isolated from the uninephrectomized rats compared to control ($p < 0.01$). The K_m for amantadine uptake into proximal and distal tubules did not differ between the control and UNX rats.

127

Predicted uptake of amantadine

We used the Michaelis-Menten equation and the calculated apparent K_m and V_{max} parameters for each of the individual experiments and treatment groups to predict the rates of renal tubule uptake for a therapeutically relevant plasma concentration of amantadine (5 µM), **table 3-3**. In the untreated diabetic rats, the increased V_{max} was associated with an increase in the predicted uptake of 5 µM amantadine into proximal tubules compared to controls ($p < 0.05$). In the diabetic + insulin treated rats the predicted rate of amantadine uptake into proximal tubules approached control levels. There were no differences in predicted amantadine uptake into distal tubules from control, diabetic untreated or diabetic insulin treated groups. The predicted rates for 5 µM amantadine were greater in proximal tubules of UNX rats compared to control, but were not different in distal tubules.

Structure/activity studies

We examined the ability of the six structurally similar organic acids (glycolate, lactate, propionate and α, β and γ-hydroxybutyrate) shown in **fig. 3-2** to modulate the bicarbonate-mediated transport of amantadine into isolated proximal and distal tubules from control Sprague-Dawley rats. The single carbon bicarbonate ion is needed for optimal amantadine uptake (Escobar *et al.*, 1994). The 4-carbon hydroxycarboxylic acids, α, β and γ-hydroxybutyrate had no effect on bicarbonate-dependent amantadine uptake in proximal or distal tubules (**fig. 3-3**). Consistent with our previous studies (Escobar *et al.*, 1995), high concentrations of lactate (3-carbon backbone) completely inhibited bicarbonate-dependent amantadine uptake in both proximal and distal tubules

128

(fig. 3-4), ($p < 0.05$) whereas propionate had no effect. Glycolate (2-carbon backbone)

also inhibited amantadine uptake ($p < 0.001$) and was a more potent inhibitor than lactate

(fig. 3-4). Calculated IC_{50} values for inhibition of amantadine uptake by glycolate ($3.53 \pm$

1.36 mM in proximal tubules and 5.73 ± 0.94 mM in distal tubules) were lower than

lactate (12.5 ± 2.8 mM, proximal tubules and 16.0 ± 1.1 mM, distal tubules) in both

proximal and distal tubules ($p < 0.05$)
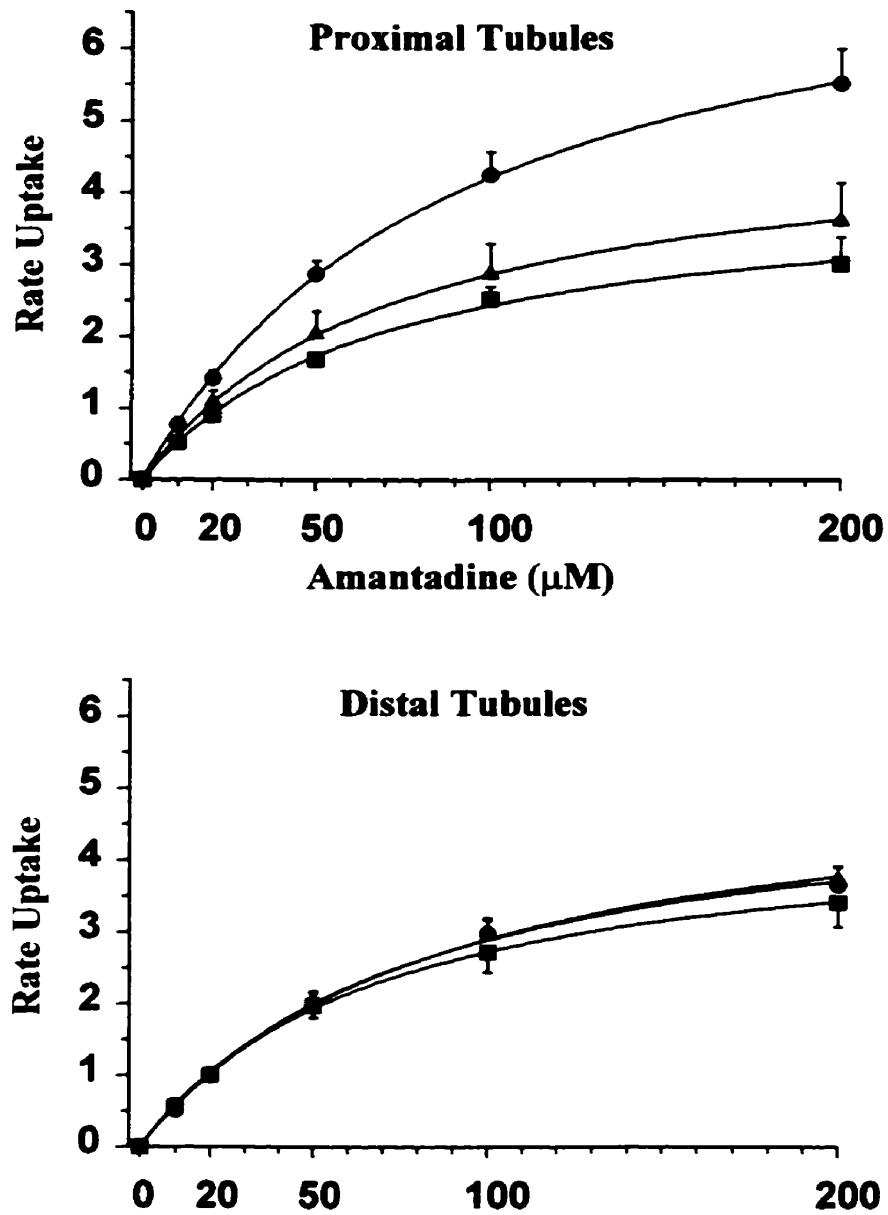
Figure 3-1: Michaelis-Menten curves demonstrating saturable energy-dependent uptake of amantadine with increasing amantadine concentration for proximal tubules (upper panel) and distal tubules (lower panel) isolated from control rats (squares), untreated diabetic rats (circles) and insulin treated diabetic rats (triangles). Each point represents the mean ± SE of 4 or 5 separate determinations.
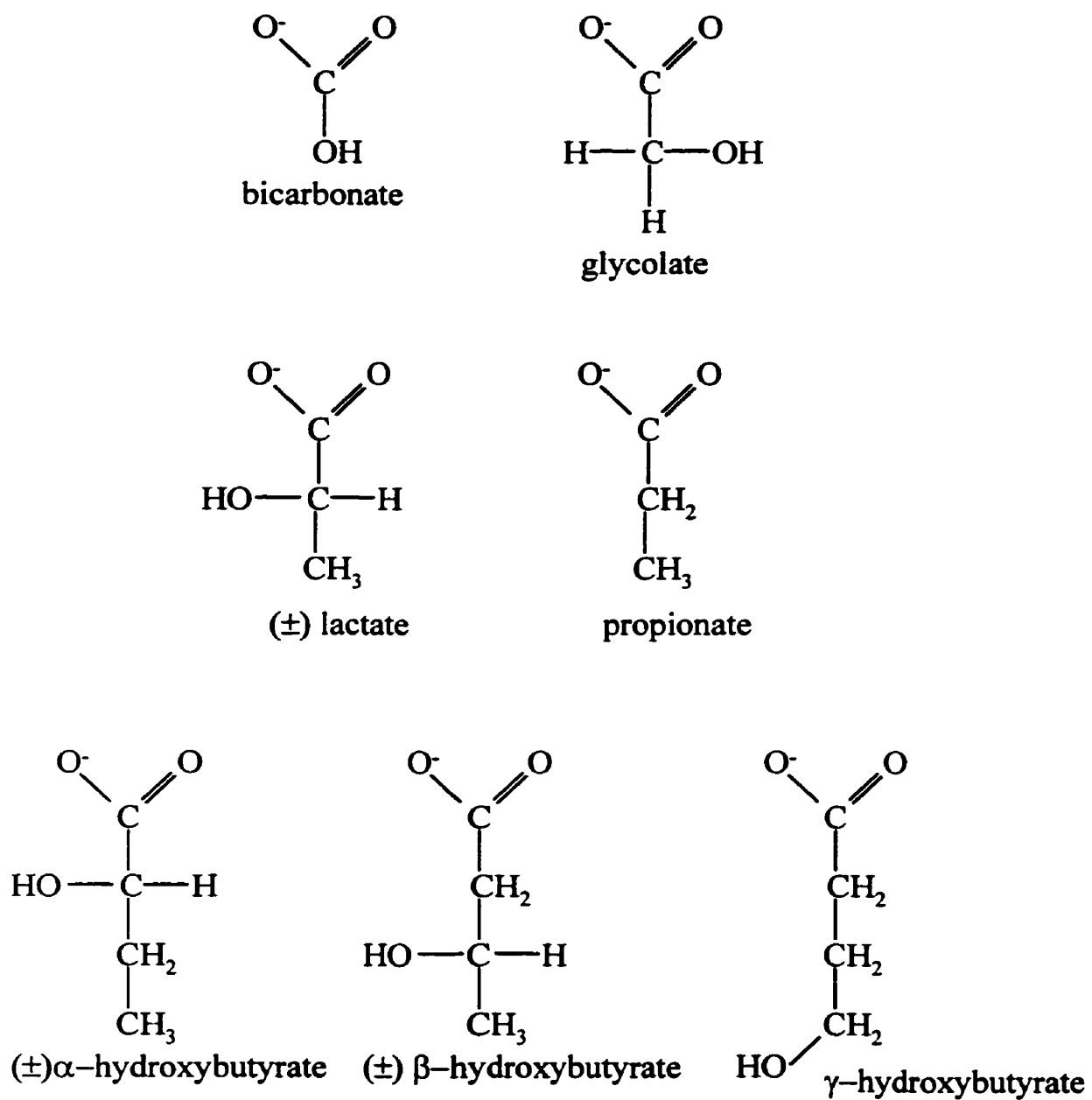
Figure 3-2: Chemical structures of bicarbonate, glycolate, lactate, propionate and α, β and γ-hydroxybutyrate. (±) indicates that a racemic mixture was used

131
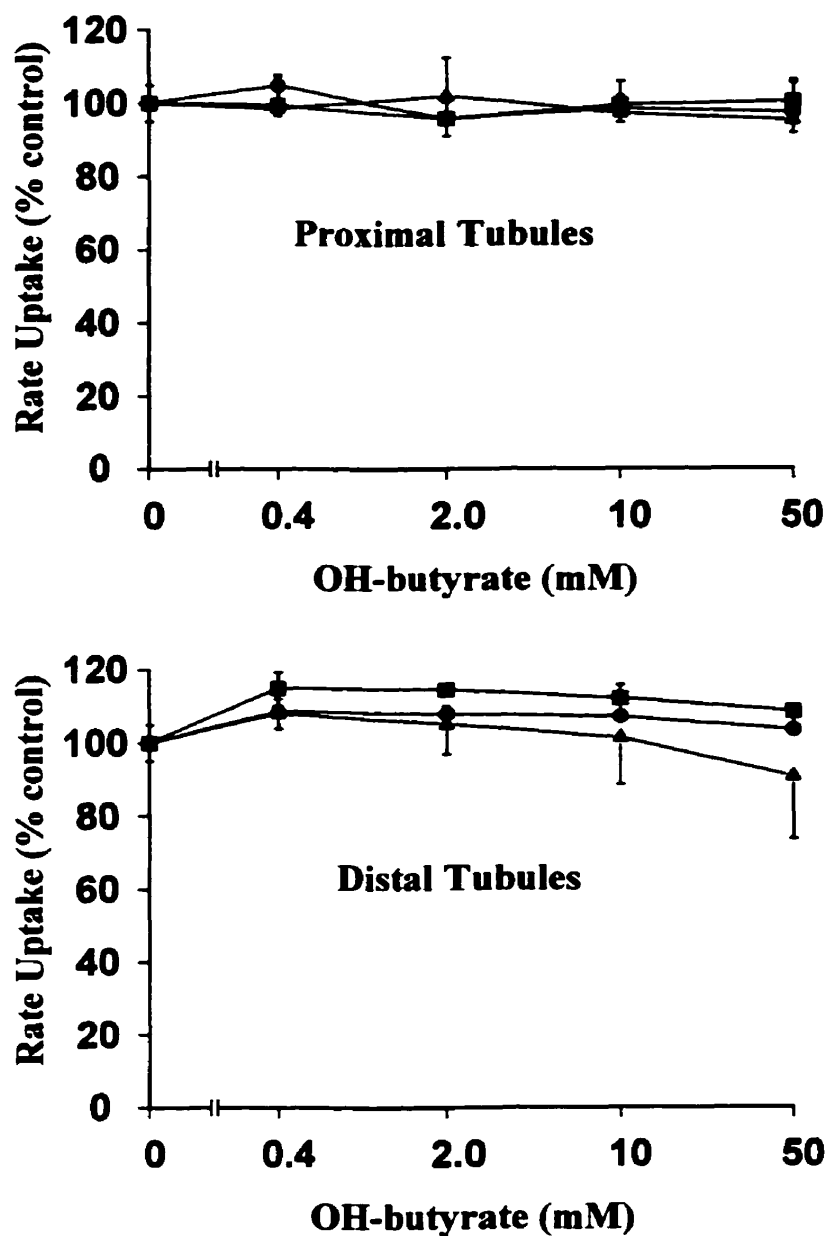
Figure 3-3: Inhibition of 10 µM amantadine uptake into proximal tubules (upper panel) and distal tubules (lower panel) by α-hydroxybutyrate (squares), β-hydroxybutyrate and γ-hydroxybutyrate (triangles). These experiments were performed on proximal and distal tubules isolated from control male Sprague-Dawley rats. The rates of uptake (% control) are expressed as mean ± SE of 3 separate experiments.
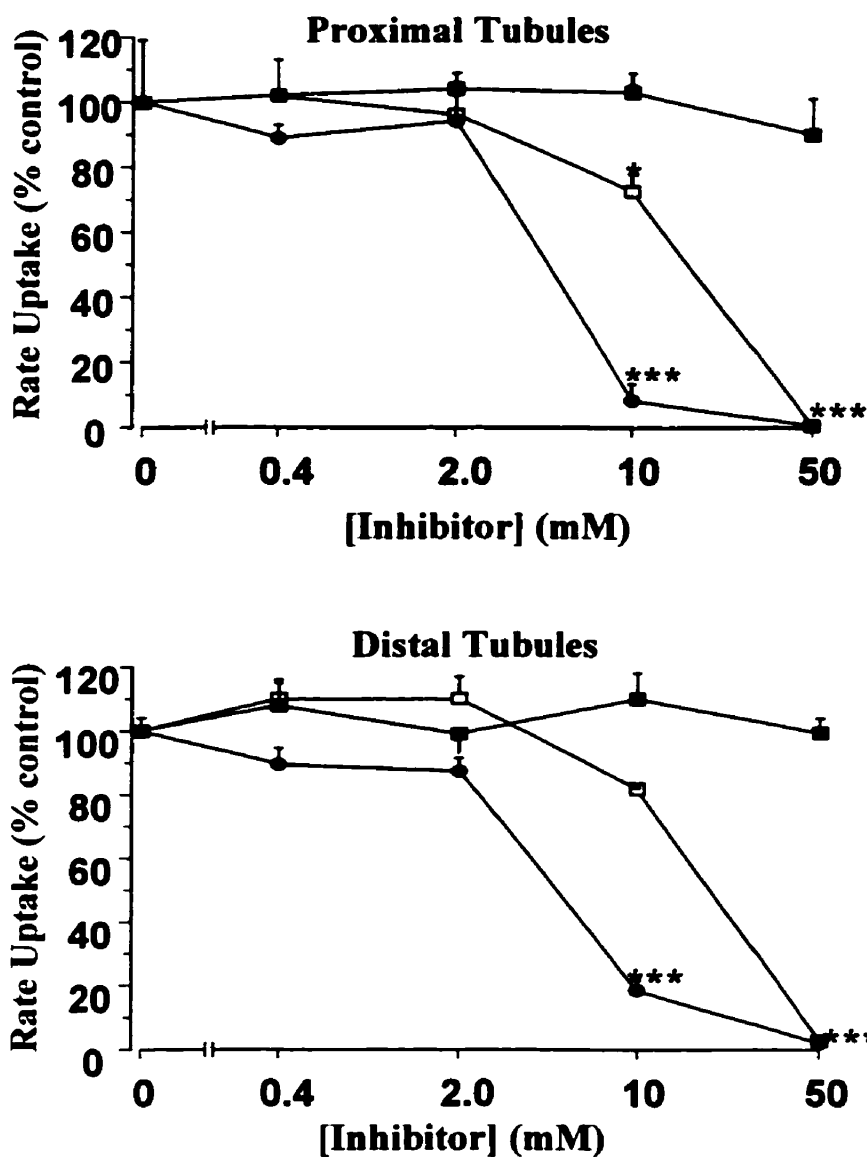
Figure 3-4: Inhibition of 10 μM amantadine uptake into proximal tubules (upper panel) and distal tubules (lower panel) by propionate (solid squares), lactate (open squares) and glycolate (solid circles). These experiments were performed on proximal and distal tubules isolated from control male Sprague-Dawley rats. The rates of uptake (% control) are expressed as mean ± SE of 3 separate experiments. * $p < 0.05$ and *** $p < 0.001$ compared to control, two-way ANOVA followed by Tukey's HSD.

Table 3-1: Comparison of Apparent K_m and V_{max} for amantadine uptake into proximal and distal tubules between control, diabetic untreated and insulin treated diabetic rats.

Tubule	Control	Diabetic	Insulin	Control	Diabetic	Insulin
	K_m (μM)			V_{max} (nmol mg^{-1} min^{-1})		
Proximal	91 ± 17	97 ± 17	73 ± 10	4.8 ± 0.7	8.2 ± 0.7*†	5.0 ± 0.8
Distal	65 ± 9	99 ± 14	90 ± 11	4.4 ± 0.5	6.0 ± 0.8	5.4 ± 0.8

Renal tubule transport studies were performed 4 days after the induction of diabetes by STZ. Each value represents the mean ± SE of 4 or 5 separate experiments. * $p < 0.05$, ** $p < 0.01$ compared to the respective control and † $p < 0.05$ compared to the insulin treated diabetic rats, one-way ANOVA followed by Tukey's HSD test.

Table 3-2: Comparison of Apparent K_m and V_{max} for amantadine uptake into proximal and distal tubules between control and UNX rats.

Tubule	Control	UNX	Control	UNX
	K_m (μM)		V_{max} (nmol mg^{-1} min^{-1})	
Proximal	102 ± 16	115 ± 13	6.9 ± 1.1	12.4 ± 1.9*
Distal	92 ± 13	83 ± 9	5.7 ± 0.6	6.4 ± 0.9

Renal tubule transport studies were performed 7-14 days after the unilateral nephrectomy for the UNX rats. Each value represents the mean ± SE of 8 separate experiments. * $p < 0.05$ compared to the respective control, unpaired t-test.

Table 3-3: Predicted rates of renal tubule uptake of 5 μM amantadine based on calculated apparent *Km* and *Vmax*.

Experiment 1: comparison between control, untreated diabetic and Insulin treated diabetic rats.

Tubule	Control	Diabetic	Diabetic + Insulin
Proximal	0.262 ± 0.019	0.421 ± 0.039*	0.321 ± 0.050
Distal	0.323 ± 0.035	0.290 ± 0.014	0.298 ± 0.037

Experiment 2: comparison between control and UNX rats.

Tubule	Control	UNX
Proximal	0.324 ± 0.014	0.534 ± 0.075*
Distal	0.308 ± 0.024	0.371 ± 0.054

For each individual experiment, apparent K_m and V_{max} and the Michaelis-Menten equation were used to calculate the predicted rate of 5 μM amantadine uptake for each treatment group. The predicted uptake rates (nmol mg $^{-1}$ min^{-1}) as expressed as mean ● SE of 4 to 8 separate determinations. ● The predicted uptake of 5 μM amantadine into proximal tubules was greater in the untreated diabetic rats (one-way ANOVA followed by Tukey's HSD test) and UNX rats (unpaired t-test) compared their respective controls ($p < 0.05$).

Discussion

The present studies were designed to evaluate whether early-stage untreated STZ-diabetes mellitus and UNX (as a non-disease control of renal hypertrophy) can modify the function of the renal tubule organic cation transport system. To the best of our knowledge, the present study represents the first specific description of the effects of experimentally induced diabetes mellitus and uninephrectomy on the renal tubule organic cation transport system. The major finding of the present study was that both early-stage untreated diabetes mellitus and UNX caused a selective increase proximal tubular amantadine transport capacity. In the diabetic rats, this change in transport could be reversed by daily insulin treatment.

We have reported previously that amantadine uptake across the basolateral membrane into proximal and distal tubules is primarily mediated via a bicarbonate-dependent transport component (Escobar *et al.*, 1994, Escobar and Sitar 1995). Thus, our present studies were carried out in the presence of 25 mM bicarbonate to address the effects of diabetes mellitus and UNX on the bicarbonate-dependent organic cation transporters. The basic kinetic data demonstrated that amantadine uptake is saturable in the untreated and insulin treated diabetic rats as well as the UNX rats. This finding indicates that the carrier mediated transport process for amantadine uptake that is present in normal male (Wong *et al* 1993, Escobar *et al* 1994) is maintained in the diabetic and UNX rats.

STZ-induced diabetes mellitus has been demonstrated to modulate the hepatic, biliary and renal clearance of certain organic anionic, cationic and uncharged drugs and bile acids (Watkins and Dykstra, 1987; Nadai *et al.*, 1990; Stone *et al.*, 1997). It has been suggested that alteration of drug clearance in diabetes mellitus may be mediated to some extent by alterations in membrane drug transport systems (Watkins and Dykstra, 1987; Nadai *et al.*, 1990). Our data provide novel evidence that STZ-induced diabetes mellitus alters function of the renal organic cation transport system in renal proximal tubules. STZ-induced diabetes mellitus has also been shown to decrease renal cortical slice accumulation of the organic cation gentamicin, but was without effect on N^{I}-methylnicotinamide (Elliot *et al.*, 1985) and may be related to changes in organic cation transport mechanisms. Gentamicin (unpublished data) and N^{I}-methylnicotinamide (**fig. 1-9**, chapter 1) show only weak affinity for the bicarbonate-dependent amantadine transporter. Thus, effects of diabetes mellitus on organic cation transport may be highly variable, depending on the transporters involved.

Functional changes in the kidney during the early stage of diabetes mellitus include hypertrophy and hyperfiltration (Seyer-Hansen *et al.*, 1980; Jensen *et al*, 1981; Morgensen *et al.*, 1983; Cortes *et al.*, 1987). Compensatory growth following uninephrectomy results in changes to the kidney (hypertrophy and hyperplasia) that is similar to that of early-stage diabetes mellitus (Seyer-Hansen, 1978). The similar changes in transport capacity in early-stage untreated diabetes mellitus and UNX rats suggest that there is a similar mechanism present that is responsible for the changes in amantadine renal tubule transport kinetics. In early-stage untreated diabetes mellitus and

after UNX, there is a similar increase in renal cellular protein, mRNA and DNA content (Seyer-Hansen, 1978). Thus, it is possible that there could be increased synthesis and expression of the bicarbonate-dependent amantadine transporter in these two conditions. The increased capacity for amantadine uptake is suggestive of increased amounts of functional bicarbonate-dependent amantadine transporters or possible enhanced efficiency of existing transporters in proximal tubules but not in distal tubules.

As demonstrated by our theoretical calculations using the Michaelis-Menten equation, the change in V_{max} would be predicted to significantly increase the transport rate of therapeutically relevant concentrations of amantadine in the untreated diabetic rats and UNX rats. It is assumed that the hypertrophy after UNX is an adaptive response to decreased renal mass. On the other hand, in diabetes mellitus, early structural and functional changes may be precursors to the development of nephropathy (Morgensen *et al.*, 1983). Thus, in vivo studies must be performed to determine the consequence of increased amantadine uptake in these two models. For it is possible that increased renal tubule uptake of amantadine in these two conditions is manifested by different changes in renal elimination of amantadine in vivo.

Insulin administration to STZ-induced diabetic rats prevents renal growth (Seyer-Hansen, 1978). Thus, if the increase in amantadine transport is related to renal growth after the onset of diabetes mellitus, the presence of insulin should attenuate the change. This effect in fact was observed. In the insulin treated diabetic rats, the V_{max} for amantadine uptake was similar to control levels and significantly lower than the untreated

139

diabetic rats. Insulin is important in the regulation of protein synthesis (Kimball *et al.*, 1994) and insulin receptors are found in the renal tubules (Meezan and Freychet, 1979). It has been suggested that insulin may regulate the synthesis or function of organic ion transport proteins in the kidney (Nadai *et al*, 1990). However, because both the untreated diabetes mellitus and UNX result in similar increases to V_{max}, this explanation appears to be unlikely for the bicarbonate-dependent amantadine transporter. As additional evidence, we were able to perform a single experiment comparing amantadine kinetics in 4-day, non-diabetic, hyperinsulinemic rats to control rats. In this experiment, the K_m and V_{max} for proximal and distal tubule amantadine uptake were similar between the two groups (data not shown). This finding suggests further that insulin per se is not directly influencing expression or function of the bicarbonate-dependent amantadine transporter, or that any effect of insulin is already maximized.

Nephrotoxicity with proximal tubule damage has been reported in cancer patients receiving chronic STZ treatment (Ries and Klastersky, 1986). In rats, it has been demonstrated that STZ results in a transient depression of GFR 30-120 min following STZ administration (Carney *et al.*, 1979). Other parameters of renal function such as Na^+, Cl^-, K^+ and PO_4^{3-} excretion were similar between controls and the STZ-induced diabetic rats. Thus, it has been concluded that the STZ-induced diabetes mellitus provides a good animal model to evaluate the effects of diabetes mellitus on renal function (Carney *et al.*, 1979). We cannot be 100% sure that the effects on amantadine uptake in the diabetic rats were due only to the diabetic condition and not possible toxic effects of STZ. However, the fact that insulin administration attenuated amantadine

uptake must also indicate that the observed increase in V_{max} in the diabetic rats is more likely due to the diabetic condition and not acute STZ-induced renal tubule toxicity. Concerns of renal tubule toxicity caused by STZ may be alleviated in future studies by using the genetically susceptible diabetic BB-Wistar rats of which 30-40% spontaneously develop type-1 like diabetes mellitus after about 13 weeks of age (Verhaeghe et al., 1999).

In untreated or poorly regulated diabetes mellitus, a common complication is the development of ketoacidosis, which is characterized by high levels of acetoacetate and D-β-hydroxybutyrate (Foster and McGarry, 1983). Both L- and D-Lactate, which are similar in structure to β-hydroxybutyrate, has been demonstrated to inhibit bicarbonate-dependent amantadine transporters (Escobar et al., 1995). Thus, we investigated whether pathologically relevant levels of β-hydroxybutyrate may alter renal tubule transport as an explanation for the increase in V_{max} in the diabetic rats. The results demonstrated that even very high levels of β-hydroxybutyrate were unable to modulate amantadine uptake. Thus it is unlikely that overproduction of β-hydroxybutyrate would contribute to altered amantadine transport in our in vitro studies and renal elimination in the in vivo situation. Other plasma metabolite abnormalities that occur in ketoacidosis, such as low bicarbonate combined with high lactate levels (Foster and McGarry, 1983) may be more relevant to altered renal organic cation elimination than β-hydroxybutyrate, as it is known that changes in lactate and bicarbonate levels modulate renal tubule transport and renal elimination of amantadine (Escobar et al., 1994; Escobar et al., 1995; Sitar et al., 1997).

Bicarbonate is the conjugate base of carbonic acid. We analyzed the series of bicarbonate-related hydroxycarboxylic acids and the carboxylic acid propionate (**fig. 3-2**) for their ability to modulate bicarbonate-dependent amantadine transport. These compounds all exist predominantly in the ionized form at physiological pH of 7.4. From these analyses, it appears that the position of the hydroxyl group and the length of the carbon backbone are important in determining how these anions access and modulate the bicarbonate-dependent amantadine transport system. The effect of chain length of the anion is demonstrated by the fact that the two-carbon glycolate was more potent than the three-carbon lactate as an inhibitor of the bicarbonate-dependent transport process, whereas four-carbon hydroxybutyrate compounds had no effect. The importance of the hydroxyl group was demonstrated by the fact that lactate, an α-hydroxy compound, inhibited the bicarbonate-dependent amantadine uptake but the structural related carboxylic acid propionate (no hydroxyl group present) had no effect. These data suggest that the bicarbonate-dependent amantadine uptake system may represent a cation/anion cotransport system that most efficiently accepts bicarbonate as its substrate.

In summary, these data do show that diabetes mellitus and UNX alter the renal tubule transport kinetics for amantadine uptake via the bicarbonate-dependent amantadine transporter. Our theoretical calculations indicate the potential for increased renal tubule accumulation and possibly renal elimination of therapeutic amantadine levels in the early-stage untreated diabetic and UNX rats. Diabetes mellitus is a long-term disease that has several clinically defined stages (Morgensen *et al.*, 1983). To fully characterize the effects of diabetes mellitus on renal organic cation transport mechanisms

and their potential for contributing to altered drug elimination and/or efficacy and toxicity

our observations must be extended to multiple time points which that reflect the different

stages of diabetes mellitus.

Chapter 4: Amantadine Transport: Interaction With Ammonium Ion

Section hypothesis: NH_4^+ is a substrate and/or inhibitor of the bicarbonate-dependent amantadine transporter(s), and thus can alter organic cation renal elimination through competitive inhibition of these transporters.

Introduction

We have attempted to identify endogenous and exogenous compounds that are substrates or modulators for the bicarbonate-dependent organic cation transport process, to further our understanding of its physiological importance, to determine its potential for altering renal organic cation elimination under pathophysiological conditions, and the potential for drug interactions at this transport site. In the present chapter, we present further mechanistic and functional characteristics of the bicarbonate-dependent amantadine transport process through the use of NH_4^+ as a transport modulator.

From a physiological standpoint, NH_4^+ represented a relevant molecule for these studies, as it is an endogenously produced cationic metabolite. NH_4^+ production occurs predominantly in the proximal tubule cells of kidney, mainly via metabolism of glutamine (Good and Burg, 1984; Vinay *et al.*, 1986). Its renal elimination is necessary for generation of new bicarbonate ions by the kidney and maintenance of acid-base balance (Halperin *et al.*, 1990; Dubose *et al.*, 1996). The efficient transfer of NH_4^+ from its major site of synthesis (proximal tubules) to the final urine is reliant on a number of transport processes for NH_4^+ and NH_3 along the length of the nephron (Good and Knepper, 1985; Knepper, 1991).

144

Pathophysiologically, its production in the proximal renal tubules, and its excretion are increased in acute and chronic acidosis (Vinay *et al.*, 1980, 1982, Good and Burg, 1984; Brosnan *et al.*, 1987).

The administration of NH_4^+ as NH_4Cl (a systemic and urine acidifier) has been demonstrated to greatly enhance the renal excretion of several organic bases in humans. Some examples include amantadine (pKa 10.1), memantine (pKa 10.3), pseudoephedrine (pKa 9.4), methamphetamine (pKa 11) and flecainide (pKa 9.3) (Beckett and Rowland, 1965; Geuens and Stephens, 1967; Brater *et al.*, 1980; Muhiddin *et al.*, 1984; Freudenthaler *et al.*, 1998). It has been generally accepted that NH_4Cl increases renal excretion of the organic bases by acidifying the urine, which subsequently leads to increased ionization and decreased passive reabsorption of the organic base that has gained access to the tubule lumen by filtration and secretion (for review, see Vander, 1995). However, the renal elimination of other organic bases by humans, such as cimetidine (pKa 6.8) and procainamide (pKa 9.3), has been demonstrated to be unaffected by NH_4Cl administration (Galeazzi *et al*, 1976; Somoygi and Gugler, 1985), suggesting other possible mechanisms at work. Furthermore, other investigators have reported that the ratio of unionized/ionized as predicted by the Henderson-Hasselbalch equation is a poor predictor of renal reabsorption of organic bases (Randhawa *et al.*, 1995). In addition to the decrease in urine pH that occurs with chronic NH_4Cl administration, NH_4^+ production in the kidney, and concentration in the plasma and urine increase (Good and Dubose, 1987). The possibility that interaction of NH_4^+ with renal tubule organic base transporters contributes to the observed effects of NH_4Cl administration on the renal elimination of organic bases has not been considered previously. Bearing in

145

mind that many substrates for renal tubule organic cation transport system contain charged amine or ammonium groups (for review see, Besseghir and Roch-Ramel, 1987; Sica and Schoolworth, 1996) and that ammoniumexists predominantly in the charged form (NH_4^+) at physiological pH, this seemed like a reasonable hypothesis. The results presented in this chapter suggest that NH_4^+ may contribute to alter renal organic cation clearance via direct interactions with organic cation transporters.

From a mechanistic standpoint, high concentrations of NH_4^+ are known to alkalinize pH_i transiently without affecting pH_o in several tissues, including snake renal proximal tubules (Roos and Boron, 1981; Bose, 1995; Kim and Dantzler, 1995, 1997). Therefore, the use of NH_4^+ as a transport modulator in this series of experiments also allowed us to address the effects of pH_i on the basolateral amantadine-selective organic cation transporter.

Methods

NH_4^+ Inhibition studies

The effects of various concentrations of NH_4^+ on the energy-dependent uptake of ^3H-amantadine into isolated renal proximal and distal tubules from male and female rats was evaluated in KHS, 5mM lactate buffer and CT buffer. Lactate buffer contained (in mM concentrations): Na lactate, 5; NaCl, 135; KCl, 4.7; $MgCl_2$, 1.2; KH_2PO_4, 1.4; $CaCl_2$, 1.0, glucose, 11, and was pH adjusted to 7.4 with NaOH. We examined four different ammonium salts NH_4Cl, NH_4NO_3, $(NH_4)_2HPO_4$ and $(NH_4)_2SO_4$ to ensure that any potential effects on amantadine transport were due to NH_4^+ and not the negative counter ion. For initial NH_4^+ inhibition studies, assays tubes were prepared (in triplicate)

146

that contained a fixed amount of ^{3}H-amantadine (1nM) and unlabeled amantadine (final assay concentrations 10 μM) and various concentrations (0.1, 1.0, 2.5, 5.0, 10 and 20 mM) of NH_4^+ in a volume of 150 μl of either KHS, lactate or phosphate buffer. Proximal or distal tubule suspensions (50 μl, in the appropriate buffer) were added to each assay tube to begin the transport reaction. The remainder of the assay was carried out as described in the general methods.

Determination of K_i values for NH_4^+ by Dixon analysis

NH_4^+ (0.1, 0.5, 1.0, 1.5 and 2.0 mM) inhibition of amantadine (10 and 50 μM) was performed such that K_i values for NH_4^+ inhibition of amantadine uptake into proximal and distal tubules in the presence of KHS could be determined by the method of Dixon (Dixon, 1953). The 30 s transport assays were carried out as described above for the NH_4^+ inhibition assays. Cornish-Bowden plots (Cornish-Bowden, 1974) were also used complementary to the Dixon plots to aid in the determination of type of inhibition (e.g. competitive, non-competitive, uncompetitive or mixed linear inhibition).

Effects of NH_4^+ on apparent K_m and V_{max} for amantadine uptake

We determined the apparent K_m and V_{max} of amantadine in normal KHS buffer and KHS buffer that contained 0.5, 1.0 and 2.0 mM NH_4Cl. For each concentration of NH_4^+ and control, the rates of 10, 20, 50, 100, 300 and 500 μM amantadine uptake were determined. The 30 s transport assays were carried out as described in the general methods.

147

Measurement of pH_i in proximal tubule segments by fluorescence microscopy

We used the pH-sensitive fluorescent dye 2'7'-bis-(2-carboxyethyl)-5-(and-6)-carboxyfluorescein (BCECF) to measure the effects of 20 mM NH_4^+ and 30 mM propionate on pH_i in proximal tubules isolated as described above. Similar procedures have been used by others to study changes in pH_i in isolated renal tubules (Martinez *et al.*, 1997; Kim and Dantzler, 1997). Fluorescence microscopy experiments were performed with a Nikon Diaphot TMD inverted microscope equipped with an epifluorescence attachment and a Nikon fluor oil immersion objective (50x) (Nikon Inc. Melville NY, USA). The excitation light was generated by a super high-pressure mercury vapor light source with a liquid light wave-guide. Specific wavelengths were selected by a Lambda 10-2 filter changer. Wavelength-specific filters for measuring pH were set at 440 (isosbestic wavelength for BCECF) and 490 nm (the excitation maxima). The selected excitation light was directed to the sample with a matched dichroic mirror. The emitted fluorescence light passed through the dichroic mirror and a (540 nm) emission filter. Emitted fluorescent light from the sample was captured and digitized by a SensiCam VGA 12-bit, cooled High Performance Digital Imaging Camera (The Cooke Corporation, Auburn Hills, MI, USA). Axon Ion Imaging Workbench software (Axon Instruments Inc., Foster City, CA, USA) installed on a microcomputer with a Pentium 350 MHz processor and Windows 98 operating system was used for acquisition and processing of images, ratiometric and non ratiometric imaging, full control of the camera and automatic filter changer. All software, camera and instruments were supplied by Optikon Corporation Ltd. (Kitchener, Ontario, Canada).

The pH studies were carried out in HEPES buffer as well as KHS (at pH 7.4) as a control to compare our data to previous studies which predominantly report the use of HEPES and not KHS in their experimental procedures. HEPES contained (in mM concentrations) NaCl, 118; KCl, 4.7; $MgCl_2$, 1.2; KH_2PO_4, 1.4; HEPES, 25; $CaCl_2$, 2.5 and glucose, 11, and was adjusted to pH 7.4 with NaOH. In these initial pH_i assays, experiments were carried out using a single concentration of NH_4^+ (20 mM) and propionate (30 mM), and only in proximal tubule fragments from male rats. To prepare tissue for imaging, 50 µl of proximal tubule suspension (8-10 mg/ml) were diluted into 930 µl of KHS or HEPES. The dilute tubule suspension was than dispensed overtop of an ultra thin fluorescent grade coverslip inside a temperature-controlled bathing chamber (Biophysica TCV-2 digital temperature regulator and chamber, Baltimore, MD, USA) on the stage of the microscope. The dilute tubule suspension was allowed to incubate for 15 min during which time the tubules normally adhered to the glass coverslip without any further treatment or manipulation of the slide surface. 20 µl of 1mM BCECF-AM (final concentration 20 µM) was added to the bathing chamber and the tubules were allowed to incubate for 45 min at 25 °C to load the dye. The ester form of the dye (BCECF-AM) enters the cells readily, where it is then hydrolyzed by nonspecific esterases to the impermeable fluorescent dye BCECF. Upon completion of the dye-loading period, the extraneous dye was washed off with KHS or HEPES buffer by a gravity-fed flow through system set at a flow rate of 5ml/min for 5 min. The buffer flow was then shut off and the system was allowed to equilibrate for 15 min. A 5 min control baseline was then established prior to the administration of 20 mM NH_4^+ or 30 mM propionate in KHS or HEPES buffer. The NH_4^+ or propionate treatments were administered via the flow

through system (5 ml/min for 2 min), after which the flow was shut off and the tissue was allowed to incubate for a further 10 min. The NH_4^+ and propionate were then washed out with fresh KHS or HEPES buffer via the flow through system (5ml/min for 5) min followed by an additional 15 min equilibration period, control baseline, second treatment period (NH_4^+ or propionate) and washout. Thus, each tissue preparation was exposed to both 20 mM NH_4^+ and 30 mM propionate treatments. During the imaging period, pH of the KHS buffer was maintained at 7.4 by continuous bubbling of O_2/CO_2 (95/5 %) into the flow through system.

Calibration of intracellular BCECF sensitivity to pH

At the end of each experiment, a ratiometric R_{max} and R_{min} fluorescence calibration was performed as follows to determine the pH sensitivity of the intracellular BCECF (Yu *et al.*, 1991; Guia and Bose, 1994). KCl (final concentration, 140 mM) and the K^+/H^+ ionophore nigericin (10 μl of a 5 mM solution, final concentration, 25 μM) were added to the bathing chamber to equilibrate pH_o and pH_i. pH was first titrated to 9.0 by addition of Tris, and the maximum 490/440 nm BCECF fluorescence ratio is determined, followed by acidification to pH 4.0 with acetic acid and the determination of the minimum 490/440 nm BCECF fluorescence ratio. The internal BCECF fluorescence ratio ($R_{490/440}$) can be then converted to pH_i using the following equation:

$$pH_i = 7.14 - log[(R_{max} - R)/(R - R_{min})] \qquad (12)$$

where 7.14 is the pKa of BCECF and R_{max} and R_{min} are the maximum and minimum BCECF fluorescence ratios respectively (Yu *et al.*, 1991; Guia and Bose, 1994).

Effects of NH₄⁺ and propionate preincubation on amantadine uptake

20 mM NH_4Cl, 30mM propionate or KHS (control tubes) were added as a 20 μl

solution to assay tubes that contained 50 μl of the tubule suspension and 110 μl of KHS,

and was allowed to incubate for 5 min. To initiate the 30 s transport assay after the

incubation period, ^{3}H-amantadine (20 μl) in KHS (to give a final amantadine

concentration of 10 μM) was added and the transport assays were carried out as described

earlier. The 30 s inhibition assays for 20 mM NH_4Cl and 30 mM propionate without

preincubation were performed as described previously.

Results

NH_4^+ Inhibition studies

The first series of experiments were performed to determine if NH_4^+, at constant

medium pH, modulates the function of the renal tubule amantadine transporter(s). Initial

rates of energy-dependent amantadine uptake into isolated proximal tubules from male

rats suspended in KHS (pH 7.4), in the presence of various concentrations of four

different ammonium salts NH_4Cl, NH_4NO_3, $(NH_4)_2HPO_4$ and $(NH_4)_2SO_4$, are shown in

(fig. 4-1). All NH_4^+ salts inhibited proximal tubule uptake of amantadine in a similar

fashion. These data suggested that the observed inhibition effects on amantadine uptake

were due to NH_4^+ and not the negative counter ion. Similar results were observed in

distal tubules (data not shown).

The next series of NH_4^+ inhibition experiments were performed to determine the

effect of the buffer medium on the ability of NH_4^+ to inhibit amantadine uptake into

proximal and distal tubules from male and female rats. Inhibition assays were carried out in bicarbonate buffer (KHS), phosphate buffer (CT) or 5 mM lactate buffer, all at pH 7.4. Consistent with previous data, control uptake of 10 μM amantadine in KHS was substantially greater than in CT or lactate buffers (Escobar *et al.*, 1994). For male and female proximal tubules, it is apparent from the absolute inhibition data that the presence of bicarbonate (KHS) in the medium is required for maximal NH_4^+ inhibition of amantadine uptake (**fig. 4-2**). Furthermore, at high NH_4^+ concentrations the rates of amantadine uptake in KHS approached those in CT and lactate buffer. These data suggest that NH_4^+ was predominantly interacting with the bicarbonate-dependent transport process. Similar results were obtained in distal tubules from male and female rats (data not shown). As such, all subsequent analyses were carried out in the presence of bicarbonate.

NH_4^+ inhibition studies were carried out in both proximal and distal tubules of male and female rats to address potential for gender and tubule related heterogeneity in organic cation transport mechanisms. NH_4^+ inhibited amantadine uptake more potently in distal tubules as compared to proximal tubules in male rats and female rats at all concentrations tested (**fig. 4-3**). In addition, amantadine uptake into proximal and distal tubules from female rats was more sensitive to inhibition by NH_4^+ than proximal and distal tubules from male rats at $NH_4^+ \geq 1.0$ mM (**fig. 4-4**). Calculated IC_{50} (mM) values supported the interpretation that NH_4^+ more potently inhibited amantadine uptake in distal compared to proximal tubules, in male rats (1.7 ± 0.3 versus 16.3 ± 6.1, $p < 0.05$), but not female rats (0.6 ± 0.2 versus 1.3 ± 0.5). IC_{50} values for NH_4^+ inhibition were

lower in female PT compared to male PT (0.6 ± 0.2 versus 16 ± 6 $p < 0.01$), but were similar in DT from both genders (female, 1.3 ± 0.5 versus male, 1.7 ± 0.3).

Dixon and Cornish-Bowden analyses were performed to determine the nature of NH_4^+ inhibition of amantadine uptake into proximal and distal tubules. For both male (fig. 4-5a, c) and female (fig 4-5b and d) proximal tubules, the lines in the Dixon and Cornish-Bowden plots intersect either above or below the negative x-axis. These profiles are consistent with that of mixed inhibition and should be characterized by changes in K_m and decrease in V_{max} in the presence of the inhibitor (Cornish-Bowden, 1974). Similar plots were obtained for the distal tubules (data not shown). The calculated K_i values were 1.1 ± 0.2 and 0.47 ± 0.09 for male proximal and distal tubules respectively and 1.0 ± 0.1 and 0.39 ± 0.06 for female proximal and distal tubules respectively. K_i values were similar between males and females, but were lower in distal tubules compared to proximal tubules for both male and female rats ($p < 0.01$).

To confirm that NH_4^+ modulates the kinetics of renal tubule amantadine transport we determined the apparent K_m and V_{max} of amantadine in normal KHS buffer and KHS buffer that contained various concentrations of NH_4^+ (table 4-1). The presence of 1.0 mM and 2.0 mM NH_4^+ in the extracellular medium resulted in an increase in apparent K_m for amantadine uptake in proximal and distal tubules from both male and female rats. However, the presence of NH_4^+ had no effect on apparent V_{max} for amantadine uptake into any of the tubule preparations. The increased apparent K_m and non-changing V_{max} is

153

consistent with competitive inhibition of amantadine uptake by NH_4^+ at these concentrations.

Effect of NH_4Cl and Na propionate on pH_i of proximal tubule cells

In our amantadine uptake experiments pH_o was buffered at pH 7.4. However, it was not known if the observed NH_4^+ inhibition could be explained by changes in pH_i resulting from incubation of the renal tubules with NH_4^+. We used fluorescence imaging studies with the pH sensitive dye BCECF to determine if 20 mM NH_4^+ alters pH_i in renal proximal tubule cells. As a control, we monitored pH_i after exposure to 30 mM propionate which is known to produce intracellular acidification (De Hemptinne *et al.*, 1983; Bose, 1995; Kim and Dantzler, 1997), but does not inhibit amantadine transport (fig. 3-4, chapter 3). Typical tracings for intracellular proximal tubule pH_i before and after treatment with NH_4^+ and propionate are shown in **fig. 4-6**. In both HEPES (**fig. 4-6a**) and KHS (**fig. 4-6b**) buffer the 20 mM NH_4^+ pulse generally resulted in an initial intracellular alkalinization in proximal tubule cells followed by a more gradual acidification. Exposure of the proximal tubules to 30 mM propionate resulted in a rapid intracellular acidification in both HEPES (**fig. 4-6c**) and KHS buffer (**fig. 4-6d**). However, in KHS, pH_i remained acidic, whereas in HEPES, pH_i gradually returned towards normal values over time. We compared the pH_i values at time zero (control), to 30 sec (the length of our amantadine transport assay time) and 5 min (a time significantly longer than for our transport assays (**table 4-2**). pH_i 30 s or 5 min after NH_4^+ or propionate treatment was not different from controls in KHS or HEPES buffer. However, pH_i at 5 min, was lower than 30 s after the NH_4^+ pulse in both KHS and HEPES

buffer ($p < 0.05$). Although pH$_i$ generally decreased in the propionate treated rats in KHS, the acidification at these specific time points was not significantly different from control. Based on the pH$_i$ determinations from the fluorescence imaging experiments, we performed an additional series of experiments in which we analyzed the ability of NH$_4^+$ and propionate to inhibit 30 s amantadine uptake with and without a 5 min pre-incubation period (**fig. 4-7**). The 20 mM NH$_4^+$ treatment showed similar inhibition of amantadine uptake with and without the 5 min preincubation period. In proximal tubules, the 5 min preincubation with 30 mM propionate resulted in a slightly decreased level of amantadine uptake compared to the 30 s propionate treatment. However, amantadine uptake in proximal and distal tubules, after exposure to 30 mM propionate, with and without the 5 min preincubation, were similar to the respective controls.
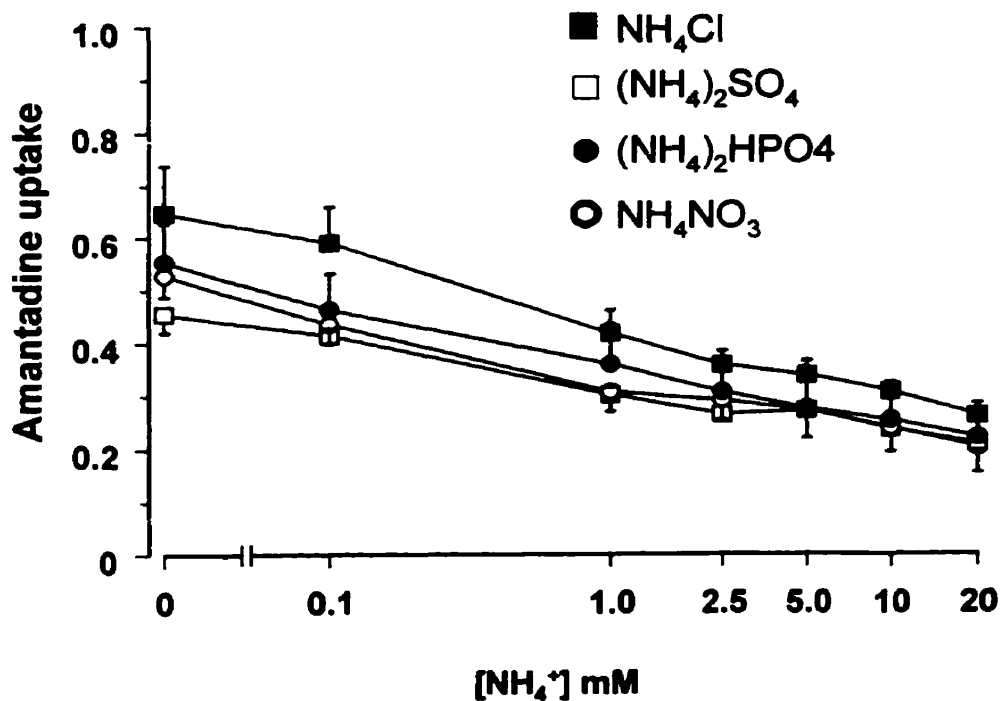
Figure 4-1: The 30 s uptake of amantadine (10 μM) into proximal tubules from male rats in KHS buffer was determined in the presence of NH_4Cl, NH_4NO_3, $(NH_4)_2HPO_4$ and $(NH_4)_2SO_4$ (0.1, 1.0, 2.5, 5.0, 10 and 20 mM). Rates of amantadine uptake are expressed as nmol mg $^{-1}$ protein min^{-1}. Each point represents the mean ± SE from 3 or 4 separate determinations. Inhibition of amantadine uptake was not dependent on NH_4^+ salt at any of the tested concentrations, two-way ANOVA.
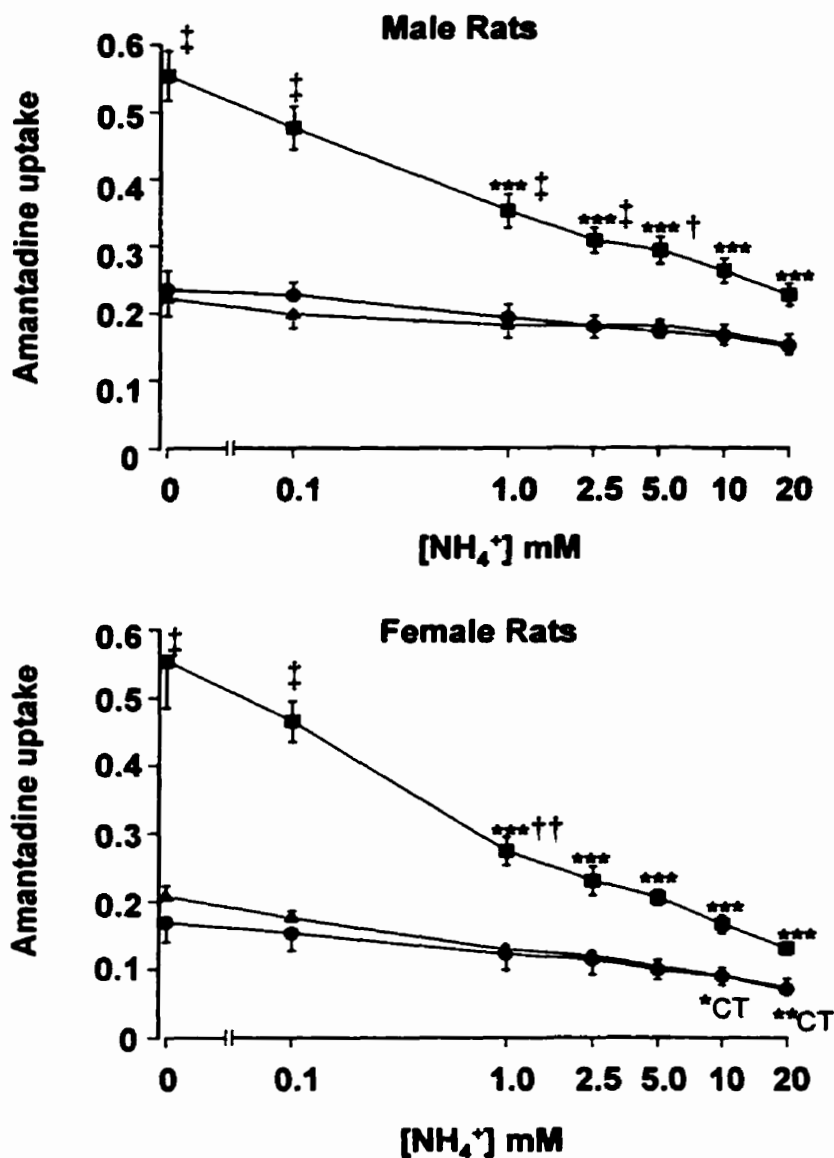
Figure 4-2: The effect of NH_4^+ (0.1, 1.0, 2.5, 5.0, 10 and 20 mM) on 30 s uptake of amantadine (10 μM) into proximal tubules from male (upper panel) and female rats (lower panel) suspended in KHS (squares), 5 mM lactate (triangles) and CT buffers (circles). Rates of amantadine uptake are expressed as nmol mg $^{-1}$ protein min^{-1}. Each point represents the mean $\pm$ S.E. from 4-13 separate determinations. $^{*}p < 0.05$, ** $p <$ 0.01 and *** $p < 0.001$ compared to within group control. $^{\dagger}p < 0.05$, †† $p < 0.01$ and ‡ p < 0.001 compared to uptake in CT or lactate at the same NH_4^+ concentration, two-way ANOVA followed by Tukey's HSD.

157
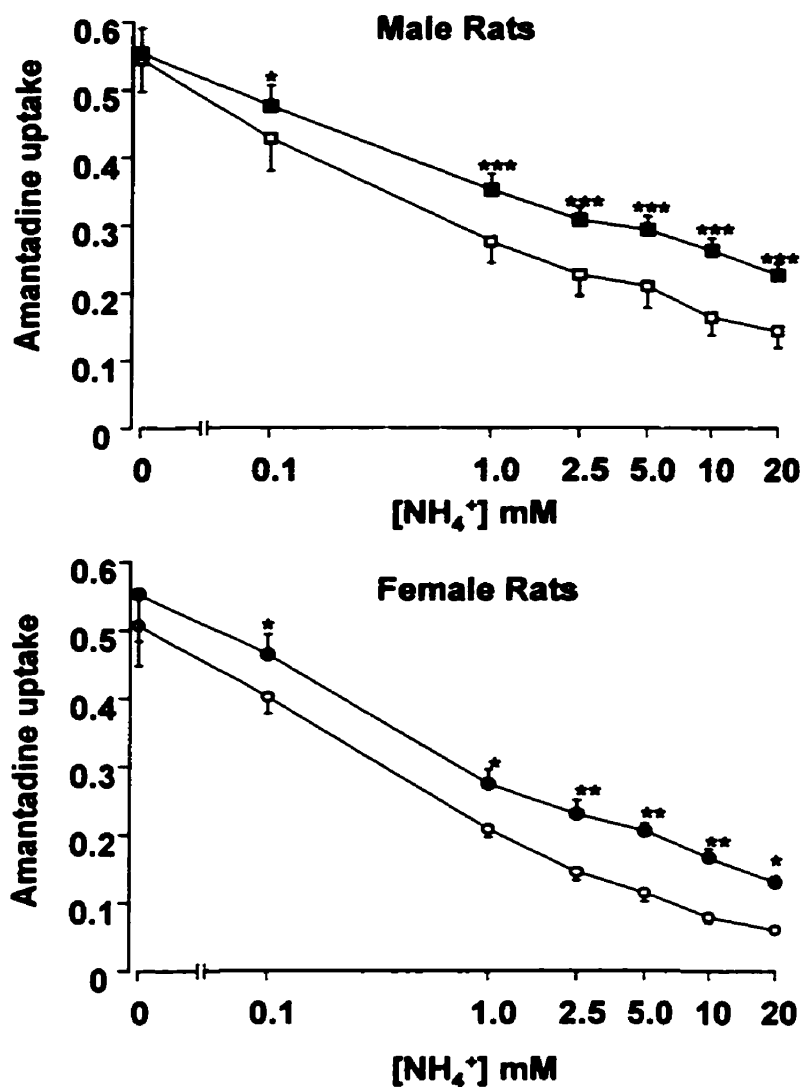
Figure 4-3: The effect of NH_4^+ (0.1, 1.0, 2.5, 5.0, 10 and 20 mM) on 30 s uptake of amantadine (10 μM) into proximal (solid squares and circles) and distal tubules (open squares and circles) from male (upper panel) and female rats (lower panel). All assays were performed in KHS buffer. Rates of amantadine uptake are expressed as nmol mg^{-1} protein min^{-1}. Each point represents the mean $\pm$ SE from 4-13 separate determinations. Data were compared by a three-way ANOVA with tubule and NH_4^+ concentrations as grouping factors, followed by Tukey's HSD. $*$ $p < 0.05$, $**$ $p < 0.01$ and $***$ $p < 0.001$ proximal compared to distal tubules at the same NH_4^+ concentration.

Proximal Tubules

Amantadine uptake

0.6
0.5
0.4
0.3
0.2
0.1
0

*** *** *** *** *** ***

0   0.1   1.0   2.5 5.0 10   20

[NH$_4^+$] mM

Distal Tubules

Amantadine uptake

0.6
0.5
0.4
0.3
0.2
0.1
0

** ** *** *** **

0   0.1   1.0   2.5 5.0 10   20

[NH$_4^+$] mM
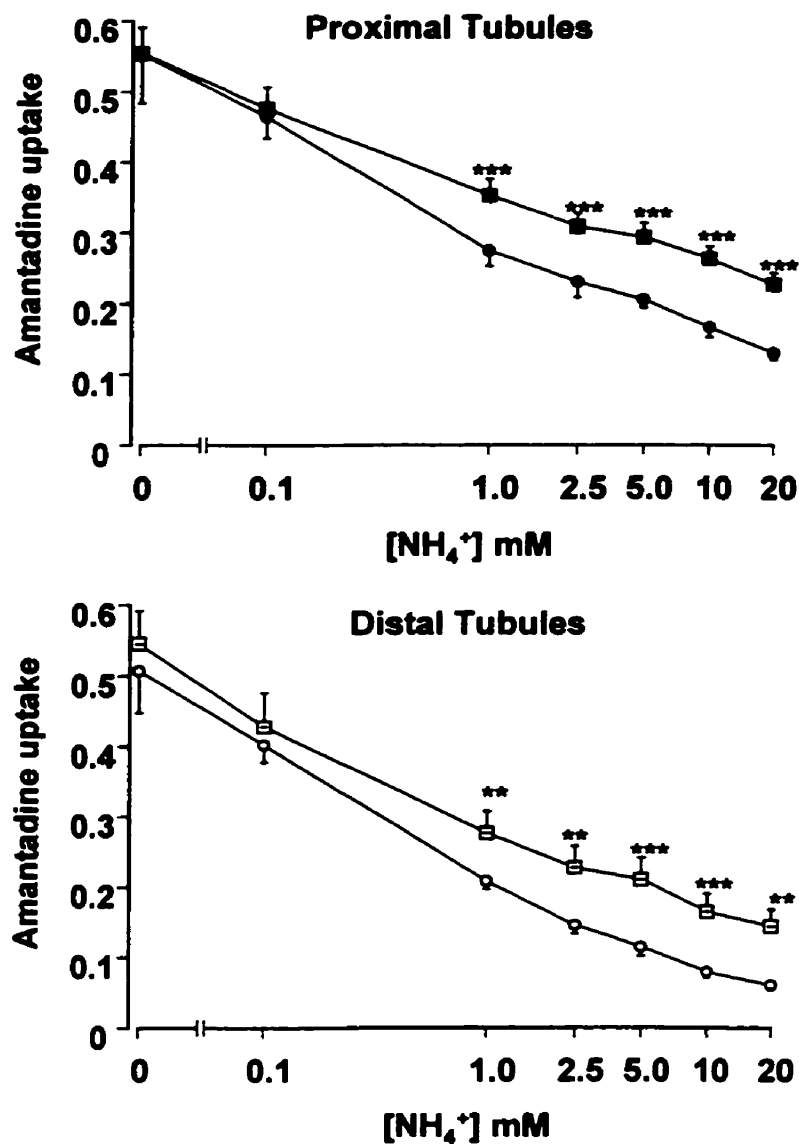
Figure 4-4: The effect of NH$_4^+$ (0.1, 1.0, 2.5, 5.0, 10 and 20 mM) on 30 s uptake of amantadine (10 μM) into proximal (upper panel) and distal tubules (lower panel) from male (solid squares and circles) and female rats (open squares and circles). All assays were performed in KHS buffer. Rates of amantadine uptake are expressed as nmol mg^{-1} protein min^{-1}. Each point represents the mean ± SE from 4-13 separate determinations. Data were compared by a three-way ANOVA with gender and NH$_4^+$ concentrations as grouping factors, followed by Tukey's HSD. * $p < 0.05$, ** $p < 0.01$ and *** $p < 0.001$ male compared to female proximal and distal tubules at the same NH$_4^+$ concentration.
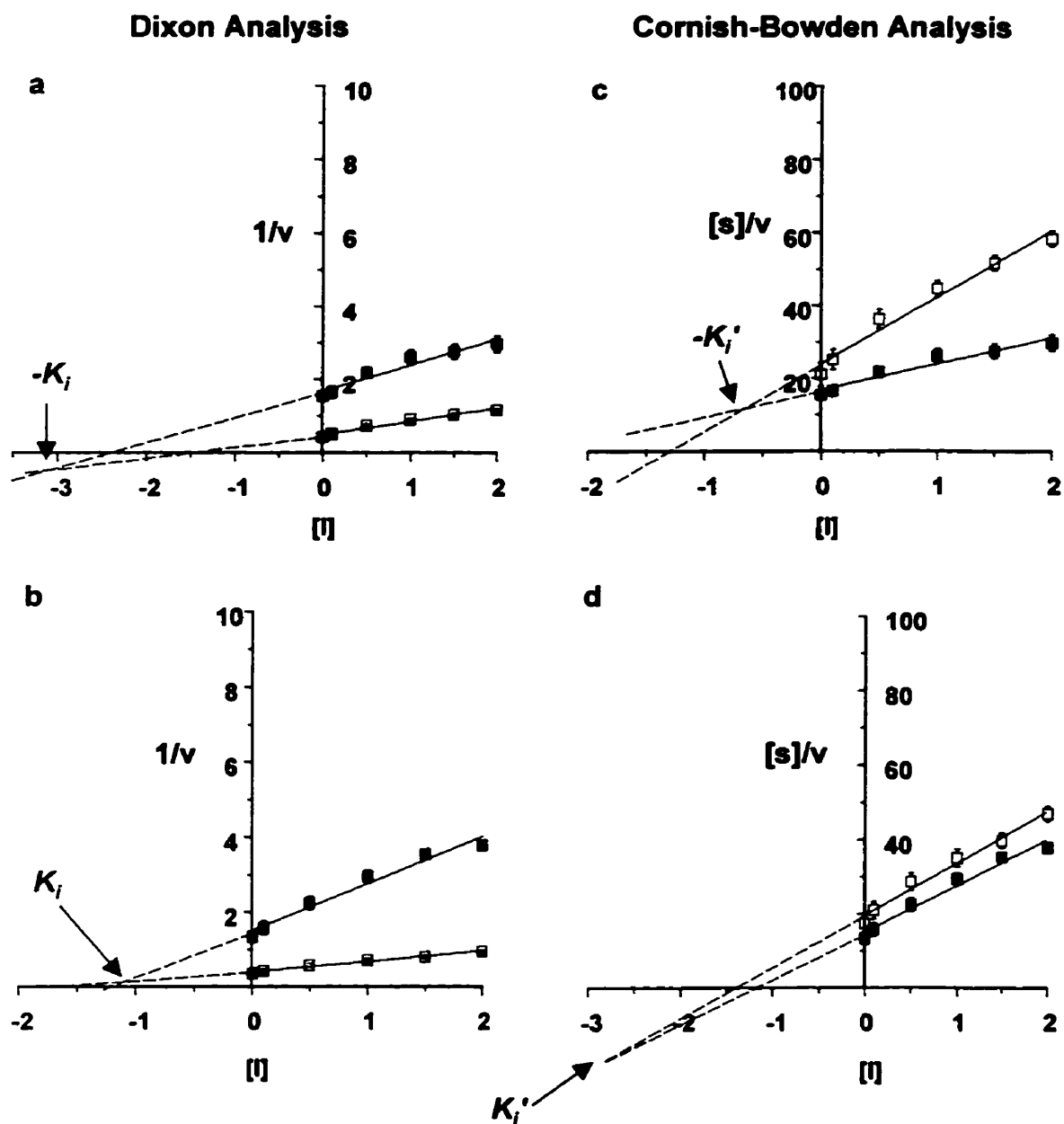
Figure 4-5: Representative Dixon (a,b) and Cornish-Bowden (c,d) analyses for NH_4^+ (0.1, 0.5, 1.0, 1.5 and 2.0 mM) inhibition of 30 s amantadine uptake into proximal tubules from male (a,c) and female (b,d) rats in the presence of KHS. Amantadine concentrations used were 10 μM (solid squares) and 50 μM (open squares). All data points represent mean ± SE of 3-4 separate determinations.
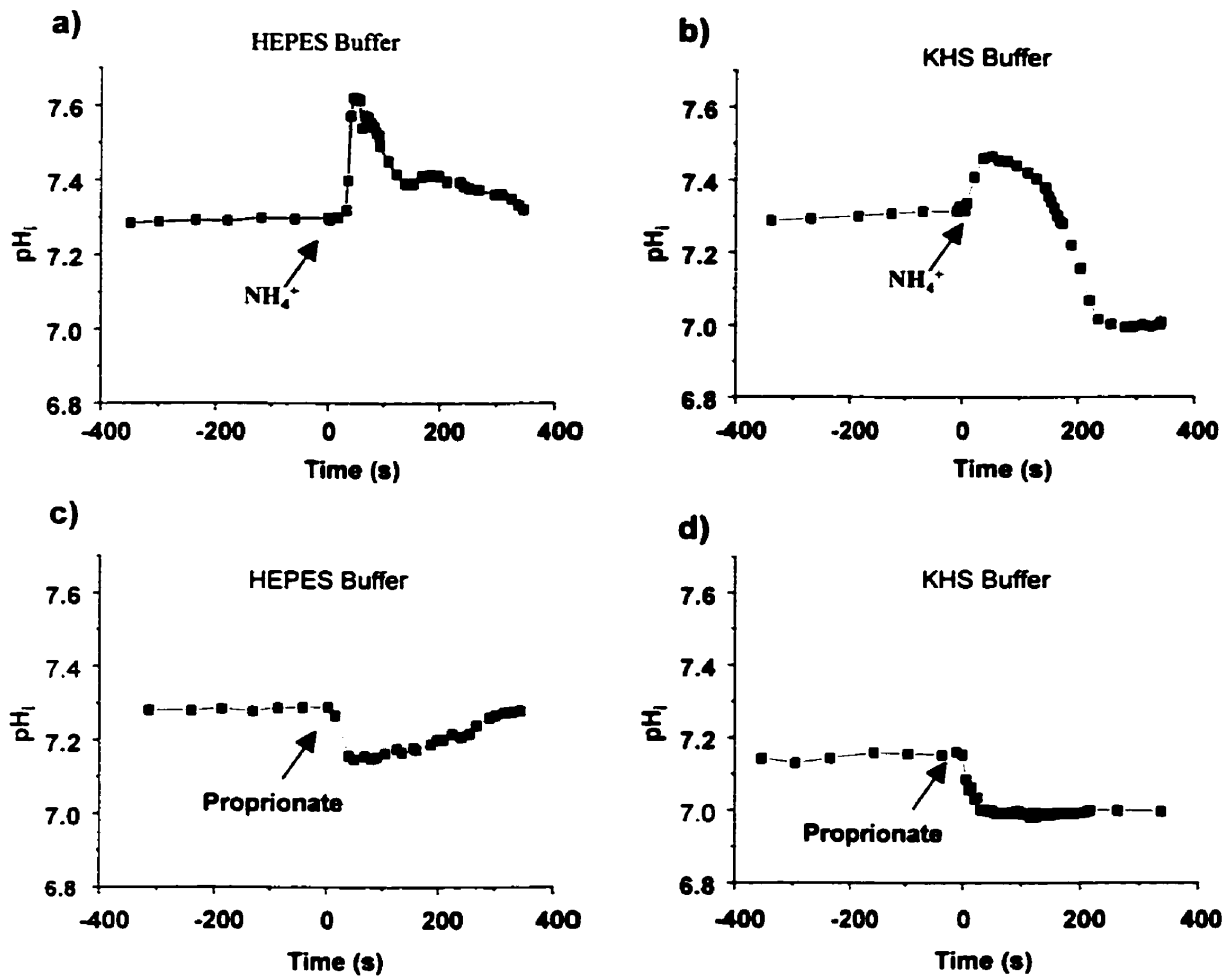
Fig. 4-6. Representative tracings of proximal tubule pH$_i$ before and after incubation with 20 mM NH$_4^+$ (a, b) or 30 mM propionate (c, d). Assays were carried out in the presence (KHS) or absence of bicarbonate (HEPES). NH$_4^+$ and propionate administration was started at time = 0.
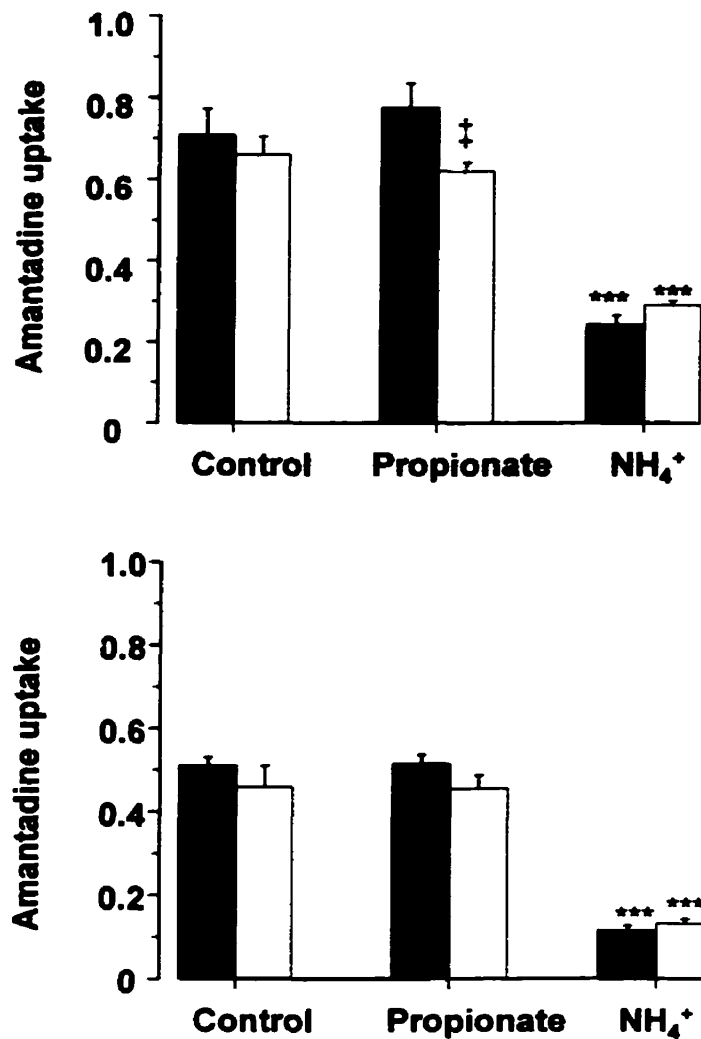
Fig. 4-7. Amantadine uptake (30 s) into male proximal and distal tubules in KHS alone (control), in KHS with 30 mM propionate, and in KHS with 20 mM NH_4^+ with (open bars) and without (solid bars) a 5 min preincubation period. Each bar represents the mean $\pm$ SE from 4 separate determinations. A mixed model ANOVA with repeated measures for treatment (control, propionate or NH_4^+), followed by Tukey's HSD test, was used for statistical analysis. *** $p < 0.001$ compared to the within group control rats and ‡ p < 0.01 compared to 30 mM propionate treatment without preincubation.

Table 4-1: Apparent K_m and V_{max} for amantadine uptake into isolated male and female rat renal proximal (PT) and distal tubules (DT) in the presence of bicarbonate buffer and increasing concentrations of NH_4^+.

Apparent K_m (μM) — NH_4^+ Concentration (mM)

	Control	0.5 mM	1.0 mM	2.0 mM
Male PT	147 ± 6	205 ± 24	370 ● 93*	367 ± 48*
Male DT	177± 29	335 ● 82	601 ● 95***	643 ± 45***
Female PT	126 ± 18	216 ± 44	409 ● 72**	494± 82***
Female DT	103 ± 20	213 ± 27	275 ± 28*	461 ± 83***

Apparent V_{max} (nmol mg^{-1} protein min^{-1})

	Control	0.5 mM	1.0 mM	2.0 mM
Male PT	11.6 ± 1.6	10.4 ± 1.3	10.6 ± 2.0	10.2 ± 0.7
Male DT	8.1 ± 1.9	6.5 ● 0.8	9.7 ± 1.4	9.3 ● 1.6
Female PT	9.1 ± 1.5	9.1 ± 2.0	9.7 ± 1.3	8.9 ± 1.1
Female DT	6.1 ± 0.9	5.2 ± 1.1	4.2 ● 1.0	4.5 ±0.8

K_m and V_{max} values are represented as mean ● SE of 4-8 separate determinations. * $p <$ 0.05, ** $p < 0.01$ and *** $p < 0.001$ compared to control within tubule and gender group, one-way ANOVA followed by Tukey's HSD test.

Table 4-2. Changes in pH$_i$ in proximal tubule cells in response to incubation with 20 mM NH$_4^+$ or 30 mM propionate.

Treatment and Time	KHS pH$_i$	Hepes pH$_i$
20 mM NH$_4^+$		
Control	7.29 ± 0.03	7.31 ± 0.09
30 s	7.40 ± 0.07	7.60 ± 0.12‡
5 min	7.13 ± 0.06*	7.17 ± 0.09***
30 mM propionate		
Control	7.12 ● 0.11	7.27 ± 0.17
30 s	7.05 ± 0.09	7.17 ● 0.12
5 min	6.85 ± 0.15	7.25 ± 0.17

Extracellular pH in the buffering medium was maintained at 7.4. Each value represents the mean ± SE of 5 separate experiments. For each experiment, pHi was reported as the average of 4 simultaneous measurements from different areas of the same tubule. The control measurement was recorded at time 0 immediately prior to the NH$_4^+$ or propionate pulse. Observed pH$_i$ values were compared by mixed model ANOVA with repeated measures for time. Multiple comparisons of the significant ANOVA were performed by Tukey's HSD test.

Discussion

The study presented in this chapter addressed the potential importance of NH_4^+ as a modulator of renal tubule, energy-dependent organic cation transport. In particular, we have focused our studies on the previously identified bicarbonate-dependent renal tubule amantadine transport process (Escobar et al., 1994; Escobar and Sitar 1995). The major finding of the present study was that NH_4^+ directly modulates the access of amantadine to the bicarbonate-dependent organic cation transporters, apparently independent of changes in pH_i. The NH_4^+ inhibition effect was present in both proximal and distal tubules from male and female rats, with some variation.

The initial inhibition experiments were carried out to determine if NH_4^+ was a potential modulator of renal tubule transport of amantadine. The similarity in the inhibition profiles for the four different NH_4^+ salts indicated that the inhibition effect on energy-dependent amantadine transport was independent of the counter anion (Cl^-, NO_3^-, SO_4^{2-}, or HPO_4^{2-}). Therefore, the observed inhibition of amantadine uptake in the presence of the various NH_4^+ salts was most likely due to the presence of NH_4^+.

Amantadine transport assays in KHS define its uptake via the bicarbonate-dependent amantadine transporter(s) (Escobar et al., 1994). Assays in CT define amantadine uptake via the bicarbonate-independent amantadine transporter(s); whereas lactate is a less effective mediator of amantadine uptake via the bicarbonate dependent transporter (Escobar et al., 1994; 1995). The fact that NH_4^+ inhibition was more predominant in the presence of bicarbonate suggested that NH_4^+ was modulating

predominantly the bicarbonate-dependent amantadine transport process. Using in situ peritubular micropuncture procedures, it has been demonstrated that NH_4^+ did not inhibit the contraluminal transport of the organic cation NMN (Ullrich *et al.*, 1991). However, in chapters 1 and 2 we have demonstrated that contraluminal transport of NMN is more likely mediated by bicarbonate-independent TEA-selective transporters rather than bicarbonate-dependent amantadine-selective organic cation transporters. Thus, the present inhibition data suggest that NH_4^+ may interact specifically with bicarbonate-dependent amantadine-selective transporters in the renal tubules. This idea is further supported by the fact that the renal elimination of two organic cations that are only weak inhibitors of the bicarbonate-dependent amantadine transport process (cimetidine and procainamide) (Wong *et al.*, 1991; results, chapter 2) have been shown to be unaffected by NH_4Cl administration (Galeazzi *et al*, 1976; Somoygi and Gugler, 1985).

Detailed kinetic experiments were performed to establish by what method $NH_4^+$was inhibiting the renal tubule uptake of amantadine. The combined Dixon and Cornish-Bowden methods of inhibition analyses suggested that NH_4^+ was acting as a mixed inhibitor. In mixed inhibition, the inhibitor can bind both to the free enzyme to give an MI complex with a dissociation constant K_i and to the MS complex to give an unreactive MIS complex with dissociation constant K_i' (Cornish-Bowden, 1979). In the presence of a mixed inhibitor apparent K_m and V_{max} are expected to change by the factors $K_m[(1 + i/K_i)/(1 + i/K_i')]$ and $V_{max}/(1 + i/K_i')$ (Cornish-Bowden, 1979). Upon analysis of the effect of NH_4^+ on apparent K_m and V_{max} for the renal tubule uptake of amantadine (via the bicarbonate-dependent transporter) into proximal and distal tubules from male and

female rats, we found that at low NH^+ concentrations (1.0 and 2.0 mM) only K_m increased, whereas V_{max} remained unchanged. This finding was consistent with NH_4^+ being a competitive type inhibitor of renal tubule amantadine transport at these concentrations. From these findings, it seems likely that NH_4^+ may modulate access of the organic cation to bicarbonate-dependent amantadine transporters by direct competition for the active site. These data also suggest a potential role for certain organic cation transporters in the mediation of NH_4^+ secretion and homeostasis in the kidney.

It is has been reported that high concentrations of NH_4^+ lead to alkalinization of pH_i in several tissues including proximal tubule cells (Roos and Boron, 1981; Bose, 1995; Kim and Dantzler, 1995, 1997; Martinez et al., 1997). In renal proximal tubules, it has been reported that transport-mediated basolateral uptake of the organic cation TEA decreases as pH_i shifts up or down from the normal resting pH_i (about 7.1) (Kim and Dantzler, 1997). Therefore, it was important for us to confirm whether or not the observed effects of NH_4^+ on renal tubule amantadine transport could be explained by changes in pH_i. Consistent with other reports (Kim and Dantzler 1995, 1997; Martinez et al., 1997), incubation of renal proximal tubules with NH_4^+ caused an initial intracellular alkalinization, whereas incubation with propionate caused intracellular acidification. The one major difference that we observed was that intracellular acidification to levels below baseline occurred, even prior to wash-out of the extracellular NH_4^+. This observation was compared to other reports in which pH_i remained elevated until the NH_4^+ was removed from the media (Kim and Dantzler 1995, 1997; Martinez et al., 1997). Aside from these differences, it was clear that NH_4^+ and propionate caused changes in pH_i.

Comparison of pH_i at 0, 0.5 and 5 min after NH_4^+ and propionate administration was not statistically different in KHS compared to HEPES. However, the overall response of pH_i in proximal tubules to NH_4^+ and propionate administration appeared to be quite different in physiological KHS compared to non-physiological HEPES buffer, as shown by the individual pH_i tracings. The fact that NH_4^+ produced similar inhibition of amantadine uptake at two time points, one with alkaline pH_i (30 s) and one with acidic pH_i (5 min preincubation) suggested that a change in pH_i was not rate limiting to the observed inhibition. This notion was confirmed by the propionate data in which there was a trend towards acidification of pH_i in KHS to similar levels observed with NH_4^+, but no inhibition of amantadine uptake. Thus, the results of our pH_i studies in relation to our amantadine transport assay times suggested that a change in pH_i was not contributory to the observed amantadine inhibition upon incubation with NH_4^+. Furthermore these experiments suggested that the bicarbonate-dependent amantadine transporter might function independently of moderate changes in pH_i.

Plasma NH_4^+ levels have been reported to be between 50 and 100 μM in both rats and humans and they can increase during chronic acidosis (Glabman *et al.*, 1963; Lockwood *et al.*, 1979; Good and Dubose, 1987). If measured carefully, plasma NH_4^+ are in the range of 10 – 40 μM (personal communication with Dr. Mitchell Halperin). In our experiments, NH_4^+ inhibition was observed in proximal and distal tubules from both male and female rats at concentrations as low as 100 μM, thus, inhibition of amantadine uptake by lower concentrations of NH_4^+ may be relevant to physiological and pathophysiological levels in the plasma. The higher concentrations of NH_4^+ (above 100

μM) used in our assays are not physiological with respect to levels of NH_4^+ found in the plasma. However, the use of high NH_4^+ concentrations may further help elucidate mechanisms in organic cation transport and identify gender and tubule differences in organic cation transport. For instance, even at high concentrations of NH_4^+, amantadine transport was not completely inhibited. This could indicate the presence of organic cation transporters that are sensitive to NH_4^+ and those that are not, and may be useful as another method of characterizing organic cation transporters. Furthermore, the absolute sensitivity of amantadine transport to inhibition by NH_4^+ appeared to be different between males and females (females more sensitive than males) and between proximal and distal tubules (distal more sensitive than proximal). The direct inhibition of basolateral organic cation transporters would not be predicted to increase organic cation elimination as is observed in vivo after administration of NH_4Cl. Although not studied in the present report, we may propose a modified postulate that any inhibitory effects of NH_4^+ on the basolateral transporters are masked by a more predominant effect on luminal transporters. Considering that concentrations of NH_4^+ in the tubules can reach very high levels, 2 mM in proximal and about 20 mM in distal tubules (Glabman *et al.*, 1963) this modified postulate appears to be a more attractive hypothesis.

In summary, the major finding of the present study was that NH_4^+ directly modulates the access of amantadine to the bicarbonate-dependent organic cation transporters independent of changes in pH_i or pH_o. We propose that direct competition of NH_4^+ for organic cation transporter sites in the kidney may help explain the fact that NH_4Cl administration is associated with increased renal elimination of certain organic

cationic drugs in healthy individuals. Clinically, increased NH_4^+ production and elimination by the kidney becomes important in ketoacidosis of chronic fasting, chronic renal insufficiency and gastrointestinal loss of bicarbonate (Tizianello *et al.*, 1980; Halperin *et al.*, 1989). Thus, if increased NH_4^+ levels alter renal elimination of organic cations, these conditions may also represent situations in which drug elimination can be affected. The effect of NH_4^+ on luminal amantadine transport remains to be evaluated using efflux studies, isolated luminal membrane preparations or directional transport studies in cell culture.

Chapter 5: In Vivo Functional Importance of Bicarbonate Dependent Organic Cation Transport

Section hypothesis: The bicarbonate-dependent amantadine transporter has implications for impaired renal elimination of organic cations in the face of changing plasma bicarbonate concentrations.

Introduction

When human volunteers taking oral amantadine were given chronic oral sodium bicarbonate, a decrease in amantadine excretion followed by an increase in plasma amantadine concentration was observed (Geuens and Stephens, 1967). From their study, it was inferred that bicarbonate decreased amantadine excretion by increasing urine pH and thus passive reabsorption of amantadine. In contrast, in vitro rat experiments have demonstrated that at constant pH, the energy-dependent uptake of the organic cation amantadine into proximal and distal tubules, is primarily mediated by bicarbonate-dependent transport sites (Escobar *et al.*, 1994; Escobar and Sitar, 1995).

In the study by Geuens and Stephens (1967), no attempts were made to address the possibility that the depression in renal elimination of amantadine might be mediated by bicarbonate driven changes in secretion or filtration, in addition to or rather than pH mediated passive reabsorption. The novelty of the present study is our extension of the importance of secretion and filtration components of amantadine clearance as a function of an acute exposure to bicarbonate. The objective of the current study was to determine if the modulating effects of bicarbonate on the renal tubule amantadine (organic cation)

transport system that is located in proximal and distal tubules (Wong *et al.*, 1991, 1992a; Escobar *et al.*, 1994, 1995; Escobar and Sitar 1995, 1996) contribute to the previous observation that sodium bicarbonate dosing decreases amantadine renal excretion. The K_m value (about 22 mM) for bicarbonate at these transport sites is close to normal plasma bicarbonate concentrations (25 mM). Therefore, we proposed that increases in plasma bicarbonate above physiological levels (or above the transporter K_m for bicarbonate) would be expected to increase amantadine renal tubule uptake at the bicarbonate-dependent organic cation transport sites. The increased amantadine uptake might then be reflected as a measurable change in the amantadine renal clearance in vivo. Disorders in which plasma bicarbonate concentration rises above normal are quite common in humans and include metabolic alkalosis and metabolic compensation to respiratory acidosis (Dubose *et al.*, 1996). These may represent potential conditions in which organic cation elimination by the kidney may be compromised.

It has also been suggested that organic cation and anion transport in the kidney may be facilitated by common transporters (Ullrich *et al.*, 1993a, 1993b; Ullrich, 1994). Therefore, the effects of bicarbonate on renal elimination of kynurenate (an organic anion) was evaluated to determine if bicarbonate effects on tubule transport are specific for organic cations. Kynurenate is a minor end product of tryptophan metabolism (Stone and Connick, 1985). In rats, kynurenate is rapidly eliminated predominantly unchanged by the kidneys (Turski and Schwarcz, 1988). It therefore represents a good organic anion model substrate for these studies.

172

Methods

Experimental Design

The use of the UNX rat model has been established and characterized previously (Intengan and Smyth, 1996). Rats were initially assigned to one of five groups. Control rats (group 1) received intravenous physiological saline only. Treatment groups received amantadine + saline (group 2), amantadine + sodium bicarbonate (group 3), kynurenate + saline (group 4), and kynurenate + sodium bicarbonate (group 5). Two additional groups were added to the experimental protocol to analyze blood gases, urine electrolytes and urine pH in animals receiving amantadine + saline (group 6) and amantadine + sodium bicarbonate (group 7). The detailed methods that we used are presented below.

Preparation of amantadine and kynurenate solutions

Solutions for the infusion of amantadine HCl and kynurenate were prepared on the day of the experiment from stock solutions. Amantadine HCl was dissolved in physiological saline. Kynurenic acid (kynurenate) was dissolved in 1 M NaOH; the solution was back titrated with 0.1 M HCl to pH 7.4 and its volume was adjusted with physiological saline. ^{3}H-Amantadine or ^{3}H-kynurenate was added to an aliquot of the stock amantadine and kynurenate solutions respectively, such that the final molar ratio of ^{3}H-label/non-label was consistently 1/10000.

Animal preparation

Males Sprague-Dawley rats (200-225 g) were obtained from the University of Manitoba (Charles River breeding stock). The rats were housed in metal cages, at 22°C,

with a twelve-hour light/dark cycle. They had free access to food (standard Purina rat chow) and tap water. The right kidney was removed under ether anaesthesia via a flank incision and a minimum one-week recovery period was imposed. Renal clearance experiments were performed 7 to 14 days after the unilateral nephrectomy. On the day of the experiment, the rats (270-340 g) were anaesthetized with sodium pentobarbital (50 mg kg^{-1}, i.p.). Body temperature was monitored with a rectal thermometer and maintained at 37.5°C with a thermostatically controlled heating pad. A tracheotomy was performed and the animals were allowed to breathe spontaneously. The left carotid artery was cannulated with PE-50 polyethylene tubing and connected to a Grass polygraph via a Statham pressure transducer (Model P23Dc) for monitoring blood pressure and heart rate. The left jugular vein was cannulated with PE-160 polyethylene tubing for administration of saline, sodium bicarbonate, amantadine or kynurenate. Additional anaesthetic (3.0 mg) as required throughout the experiment was injected through a latex adapter into the main i.v. line. A left flank incision was made; the remaining kidney was exposed; and the ureter was cannulated with PE-50 polyethylene tubing to allow for urine collection.

Amantadine and kynurenate renal clearance experiments

Immediately following completion of the surgical preparation, rats were started on a continuous infusion of 5 IU (international units) heparin in isotonic (300 mOsmol l^{-1}) saline (0.9 % w/v) at 97 µl min^{-1} and were allowed to stabilize for 45 min. The heparin/saline infusion was maintained for the remainder of the procedure, except during amantadine, kynurenate and sodium bicarbonate infusion periods. Immediately following the stabilization period, 3 mg kg^{-1} of ^{3}H-amantadine (groups 2 and 3) or ^{3}H-

174

kynurenate (groups 4 and 5) were infused in a total volume of 200 µl at a rate of 97 µl min^{-1}. The control animals (group 1) received an equivalent volume of physiological saline over the same duration. Five minutes after the completion of drug administration, the first 20 min urine collection was started. At the start of the second urine collection period, groups 3 and 5 were infused with hypertonic (2000 mOsmol l^{-1}) sodium bicarbonate (5 mmol kg^{-1} i.v.) at 111 µl min^{-1}, whereas the remaining groups (groups 1, 2 and 4) were maintained on the heparin/saline infusion. Following the start of the bicarbonate administration, there were five successive 20 min urine collection periods. All urine samples were collected into pre-weighed vials and the urine volume was determined gravimetrically. Blood sampling was done from the carotid artery cannula at the beginning of each urine collection period (7, 27, 47, 67, 87 and 107 min after the start of amantadine or kynurenate infusion). Blood samples (100 µl) were collected into microfuge tubes that contained 1.0 IU of heparin sulfate. A final blood sample (2 ml) was taken at the end of the final urine collection period for determination of plasma creatinine levels, osmolality and plasma ions. Blood was centrifuged immediately to separate the plasma. Two 20 µl aliquots from each plasma and urine sample were placed in plastic scintillation vials, suspended in 5 ml of Beckman Ready-Safe Scintillation Cocktail, vortexed for 30 sec, and counted for radioactivity in a Beckman model LS5801 scintillation counter (Beckman Instruments, Fullerton, CA).

To address the issues of blood gasses, urine electrolytes and urine pH, we performed additional experiments to measure plasma pH, bicarbonate and pCO$_2$, and urine pH in rats treated with amantadine + saline (group 6, n = 4) and rats administered

175

amantadine + sodium bicarbonate (group 7, n = 4). The same procedures were used for these experiments as described above, with the addition of the following minor changes. A slightly larger volume of blood was necessary for blood gas measurements than for measurements of plasma amantadine (140 versus 100 µl). Therefore, to keep the volume of blood withdrawal similar over the duration of the experiment, we reduced the number of blood collections from seven to five. The five blood samples were taken (7 min, 27, 47, 87 and 127 min) after amantadine infusion. To facilitate rapid and efficient withdrawal of blood samples, an arterial-venous loop was inserted connecting the carotid artery and the jugular vein (Xie *et al.*, 1996). Samples were drawn directly from the arterial side of the loop into a capillary tube, sealed, and measured for HCO_3^-, pCO_2 and pH immediately using an Instrumentation Laboratory System 1302 Blood-Gas Analyzer. Saline, bicarbonate and amantadine were all infused through the venous side of the loop. Urine pH was measured using a standard microelectrode. Plasma and urine osmolalities were determined with a Precision System Micro Osmometer. The plasma and urine Na^+ Cl^- and K^+ concentrations were determined using a Nova Electrolyte Analyzer.

Thin-layer chromatography

Thin-layer chromatography was performed according to previously described methods to confirm the presence of unmetabolized ^{3}H-amantadine and ^{3}H-kynurenate in urine samples (Uchiyama and Shibuya, 1969; Turski and Shwarcz, 1988). ^{3}H-Amantadine and ^{3}H-kynurenate standards were dissolved in saline control urine samples and run in parallel with the test urine samples on fluorescent silica gel plates (Analtech Inc. Newark, DE). The developing solvent for amantadine was a mixture of n-butanol :

acetic acid : water (4 : 1 : 5) and for kynurenate a mixture of n-butanol : methanol : water : ammonium hydroxide (60 : 20 : 19 : 1). The developing time ranged between 50 and 60 min. Sections (0.5 cm) from the origin to the solvent front of the plate were scraped and counted for ^{3}H radioactivity. Analysis of plasma was not possible due to the small volume and low specific radioactivity of plasma samples. For calculations, it was assumed that all radioactivity counted in plasma was associated with the parent compounds.

Data analysis

The radioactivity in each plasma and urine sample was recorded as disintegrations per minute (DPM). Background radioactivity, consistently about 20 DPM, was subtracted to obtain the specific DPM value. Plasma and urine amantadine and kynurenate concentrations were determined from the respective DPM values. Thin-layer chromatography demonstrated that for amantadine treated rats, amantadine and an unidentified metabolite were present in the urine. Therefore, all urine DPM values for amantadine treated rats were corrected for the percentage of the ^{3}H-metabolite in the urine as follows. Amantadine DPM (urine) = total DPM (urine) x AUC (amantadine peak on t.l.c.)/AUC (amantadine peak + metabolite peak on t.l.c.). A colorimetric assay based on the Jaffé reaction (Sigma Diagnostic Kit, procedure # 555) was used to quantify urine and plasma creatinine. The renal clearance of amantadine (groups 2 and 3), kynurenate (groups 4 and 5), and creatinine (all groups) was calculated for each of the six collection intervals using the area under the curve method (Gibaldi & Perrier, 1982).

Renal clearance ratios of amantadine and kynurenate to creatinine were calculated in order to evaluate the effect of bicarbonate on their renal tubule secretion. Additional pharmacokinetic analysis was performed by fitting the plasma concentrations of amantadine and kynurenate to the two-compartment open model of drug disposition with intravenous infusion, using a non-linear regression program, WinNonlin version 1.1, (WinNonlin Scientific Consulting, Inc.). The parameters determined were the area under the plasma drug concentration vs. time curve (AUC), half-life of initial drug disposition (t1/2 α), and terminal disposition (t1/2 β), the plasma drug clearance (Cl_p), and the apparent volume of distribution at steady-state (Vd_{ss}). All data are presented as mean $\pm$ SE of a least four experiments. Data were analyzed for treatment and time effects by mixed model repeated measures (for time) analysis of variance using Systat for Windows, version (6.01). Significant differences between means were determined with Tukey's HSD test. Differences between means with a p value ≤ 0.05 were considered to be significant.

Results

Metabolism of amantadine and kynurenate

Urine samples from amantadine treated rats consistently revealed two peaks of radioactivity, indicating metabolism of the parent compound (data not shown). The retention factor (r_f value) for the parent compound and the metabolite were consistently 0.67 and 0.53 respectively. Considering the significant amantadine metabolism observed in our experiments, we attempted to identify the metabolite, but were unsuccessful. By gas chromatographic analysis of urine samples, we did confirm that the metabolite was not acetylamantadine. Urine samples from the kynurenate treated rats displayed one peak

that was consistent with that of the standard (r_f value = 0.80) indicating that the radioactivity recovered in the urine was associated with the parent compound.

Renal clearance measurements

Creatinine clearance was used as a general marker for renal glomerular filtration rate (GFR) (**fig. 5-1a and 5-2a**). For clarity of interpretation of creatinine clearance, the same saline-control data are shown separately in each figure. However, groups 1 - 5 were compared simultaneously for statistical analysis. Increases in creatinine clearance were observed in amantadine treated rats that received bicarbonate and in kynurenate treated rats independent of sodium bicarbonate treatment ($p < 0.05$). Amantadine treatment alone did not alter the creatinine clearance. Creatinine clearance for the saline controls did not decrease with time, indicating maintenance of renal filtration function over the duration of our experiments.

The effect of sodium bicarbonate on the interval renal clearances of amantadine and kynurenate is shown in **fig. 5-1b and 5-2b** respectively. It was important to compare the interval renal clearances rather than just the overall renal clearances so that persistence of any effects of the sodium bicarbonate treatment could be identified. The interval amantadine renal clearance (**fig. 5-1b**) was similar in both amantadine treated groups before sodium bicarbonate administration (collection period 1). After sodium bicarbonate administration (collection periods 2-6) the interval amantadine renal clearances (**fig. 5-1b**) were 30 % to 60 % lower than the respective controls ($p < 0.05$). The interval amantadine renal clearance decreased with time irrespective of treatment (p

< 0.01). The overall mean renal clearance of amantadine was lower in the sodium bicarbonate treated group (0.76 ± 0.04 ml min^{-1} 100g^{-1}) versus the amantadine + saline treated rats (1.16 ± 0.04 ml min^{-1} 100g^{-1}), ($p < 0.01$). In the kynurenate treated rats, the interval kynurenate renal clearance was similar in both groups before and after sodium bicarbonate infusion (fig 5-2b). The mean interval kynurenate renal clearance decreased with time ($p < 0.01$). There was no effect of sodium bicarbonate treatment on overall mean kynurenate clearance (1.11 ± 0.05 ml min^{-1} 100g^{-1}) versus the kynurenate + saline treated rats (1.19 ± 0.05 ml min^{-1} 100g^{-1}).

Renal clearance data were normalized to creatinine clearance for amantadine (fig. 5-1c) and kynurenate (fig. 5-2c). Initially, all amantadine/creatinine and kynurenate/creatinine clearance ratios were substantially greater than one, indicating renal tubule secretion of both amantadine and kynurenate. In the two amantadine treatment groups, the mean amantadine/creatinine clearance ratios were similar before sodium bicarbonate treatment and were 55% to 70% lower than the respective time controls after bicarbonate treatment ($p < 0.01$). The overall amantadine/creatinine clearance ratio was reduced in the sodium bicarbonate treated rats (1.62 ± 0.12) compared to the amantadine + saline treated rats (2.97 ± 0.12), ($p < 0.01$). Similar to amantadine clearance, the amantadine/creatinine clearance ratio decreased with time after amantadine infusion ($p < 0.001$). The kynurenate/creatinine clearance ratio decreased with time after dosing ($p < 0.001$) and was lower only during collection interval 2 for the sodium bicarbonate-treated group compared to the control determination ($p < 0.01$). There was no effect of sodium bicarbonate treatment on the overall mean

kynurenate/creatinine clearance ratio for sodium bicarbonate treated (2.26 ± 0.09) versus for the saline treated (2.31 ± 0.09) rats.

For the current experiments, a direct comparison of amantadine clearance with the clearance of its major metabolite was not possible, because we were unable to determine metabolite concentrations in the plasma. However, it was possible to compare the rates of excretion and total excretion of amantadine versus the amantadine metabolite (**table 5-1**). Before sodium bicarbonate administration, the rate of urinary amantadine excretion was similar in both groups and was reduced after sodium bicarbonate administration (collection periods 2 and 3), ($p < 0.01$), which is consistent with the observed decrease in amantadine clearance. Total amantadine excretion was lower in the sodium bicarbonate treated rats ($p < 0.01$). The rate of amantadine metabolite excretion for all urine collection periods and total amount of amantadine metabolite excreted in the urine was similar in the amantadine + saline and the amantadine + sodium bicarbonate treated rats. In contrast to amantadine, there were no appreciable changes in the rate of kynurenate excretion, or total kynurenate recovered in the urine, for the sodium bicarbonate treated rats compared to controls.

Correlation between urine flow rate and amantadine/creatinine and kynurenate/creatinine clearance ratios

Urine flow rates ($\mu l\ min^{-1}$) for each urine collection period and group of rats are shown in **table 5-2**. Urine flow rates for all groups increased with time ($p < 0.001$) and reached a plateau between 60-100 $\mu l\ min^{-1}$. Initially (collection period 1) the urine flow

rates were similar in all groups. After sodium bicarbonate treatment, the urine flow rate was greater during urine collection periods 2 and 3 compared to the groups that did not receive sodium bicarbonate ($p < 0.05$). The more rapid diuresis in the sodium bicarbonate treated rats is likely due to the greater Na^+ load from the hypertonic $NaHCO_3$ infusion as compared to the isotonic heparin saline infusion. After the third urine collection period, the urine flow rates in the sodium bicarbonate treated rats decreased towards values similar to the groups that did not receive sodium bicarbonate treatment. Amantadine/creatinine and kynurenate/creatinine clearance ratios versus urine flow rates are presented in **fig. 5-3**. The amantadine/creatinine clearance ratio was not correlated with a change in urine flow rate in the amantadine + saline treated rats ($r^2 = 0.092$) and in the amantadine + sodium bicarbonate treated rats after the start of sodium bicarbonate administration ($r^2 = 0.022$). Conversely, the kynurenate/creatinine clearance ratio in kynurenate + saline treated rats was moderately correlated with urine flow rate ($r^2 = 0.421$). However, no effect of urine flow rate on the kynurenate/creatinine clearance in the sodium bicarbonate treated was demonstrated ($r^2 = 0.057$).

Comparison of blood gas, urine pH and urine electrolytes

Blood-gas and urine pH values for group 6 (amantadine + saline) and group 7 (amantadine + sodium bicarbonate) treated rats are shown in **table 5-3**. The blood gas and urine pH measurements were not performed in the kynurenate treated rats because there was no major effect of sodium bicarbonate on kynurenate renal clearance. In the amantadine + saline treated rats blood bicarbonate, pCO_2 and pH, and urine pH were similar over the duration of the experiment. Before the sodium bicarbonate infusion,

plasma bicarbonate, pCO_2 and pH and urine pH were similar between the two groups. After the acute sodium bicarbonate dose: blood bicarbonate increased to a maximum level of 34.6 ± 0.41 mM, which was approximately 8 mM higher than the amantadine + saline treated rats (26.9 ± 0.67 mM) at the same time point ($p < 0.001$). The plasma bicarbonate levels dropped in the last two collection intervals, but remained greater than the respective controls ($p < 0.001$). In contrast to the large increase in blood bicarbonate, the blood pH remained only slightly elevated (7.45 –7.48) compared to control measurements (7.40 –7.41) at the same time points ($p < 0.01$). Blood pCO_2 increased slightly but was not significant. Urine pH in the amantadine + saline treated rats remained constant and slightly acidic (6.6 – 6.8), whereas the urine pH became alkaline immediately following bicarbonate infusion and remained elevated at (pH = 8) in the amantadine + bicarbonate treated rats ($p < 0.001$). The amount of sodium, chloride and potassium excreted in the urine and the cumulative sodium retention (the amount of sodium administered – the amount of sodium excreted in the urine) were similar in both groups prior to sodium bicarbonate treatment (collection period 1) (**fig. 5-4**). After sodium bicarbonate administration, the interval and total sodium excretion in the urine was increased compared to the control ($p < 0.001$). Cumulative sodium retention was increased in the sodium bicarbonate treated rats compared to the controls for collection periods two and three. However, by the final collection period, the total sodium retained was similar in both groups. Increases in potassium and chloride interval and total excretion in the urine were also observed in the sodium bicarbonate treated rats ($p < 0.05$).

Pharmacokinetic determinations

Mean amantadine and kynurenate plasma concentrations versus time are shown in fig. 5-4. The plasma amantadine and kynurenate concentration versus time profiles were similar in the sodium bicarbonate treated and control rats. The amantadine and kynurenate plasma concentrations from the individual experiments were fit to the two-compartment open model of distribution to determine the pharmacokinetic parameters shown in **table 5-5**. The amantadine pharmacokinetic parameters are provisional and highly variable because the experiment must span two $\beta_{t1/2}$ periods for a more reliable determination of pharmacokinetic parameters. In the sodium bicarbonate treated rats Vd_{ss} for amantadine was increased compared to the amantadine + saline treated rats ($p <$ 0.05). AUC and $\beta_{t1/2}$ tended to be higher in the sodium bicarbonate treated rats compared to the saline treated rats however the differences were not significant. For kynurenate the kinetics of disposition were similar in control vs. bicarbonate treated rats.

a

Creatinine Clearance
ml min^{-1} 100g^{-1}

- ■ Saline
- □ Amantadine + Saline
- ▨ Amantadine + Bicarbonate

bicarbonate

Urine collection period

b

Amantadine Clearance
ml min^{-1} 100g^{-1}

- □ Amantadine + Saline
- ▨ Amantadine + Bicarbonate

bicarbonate

Urine collection period
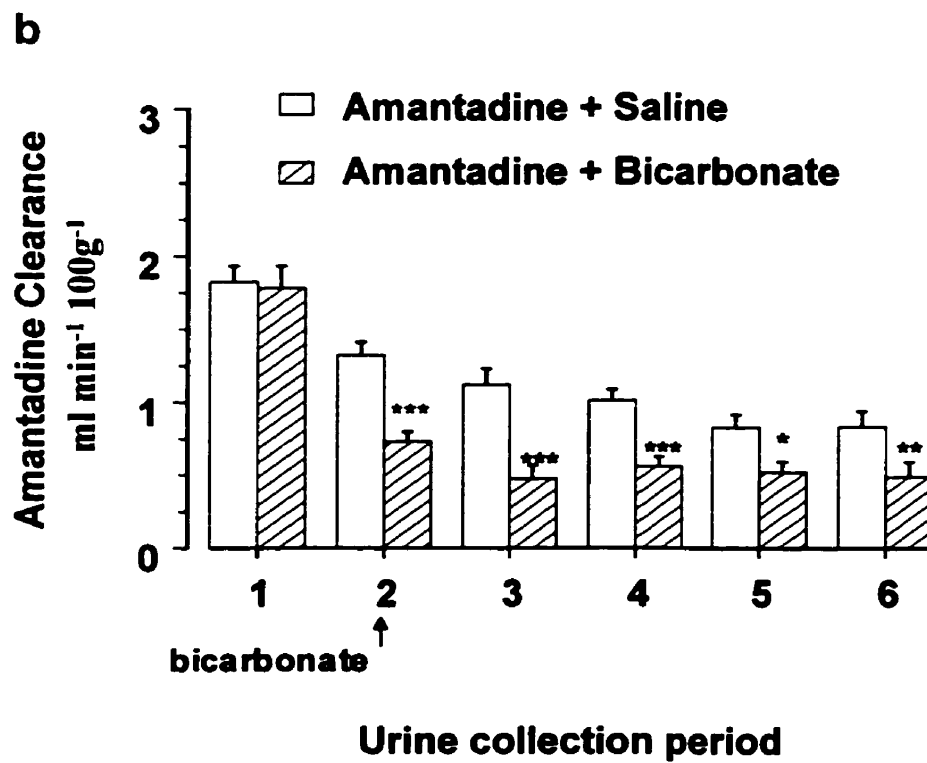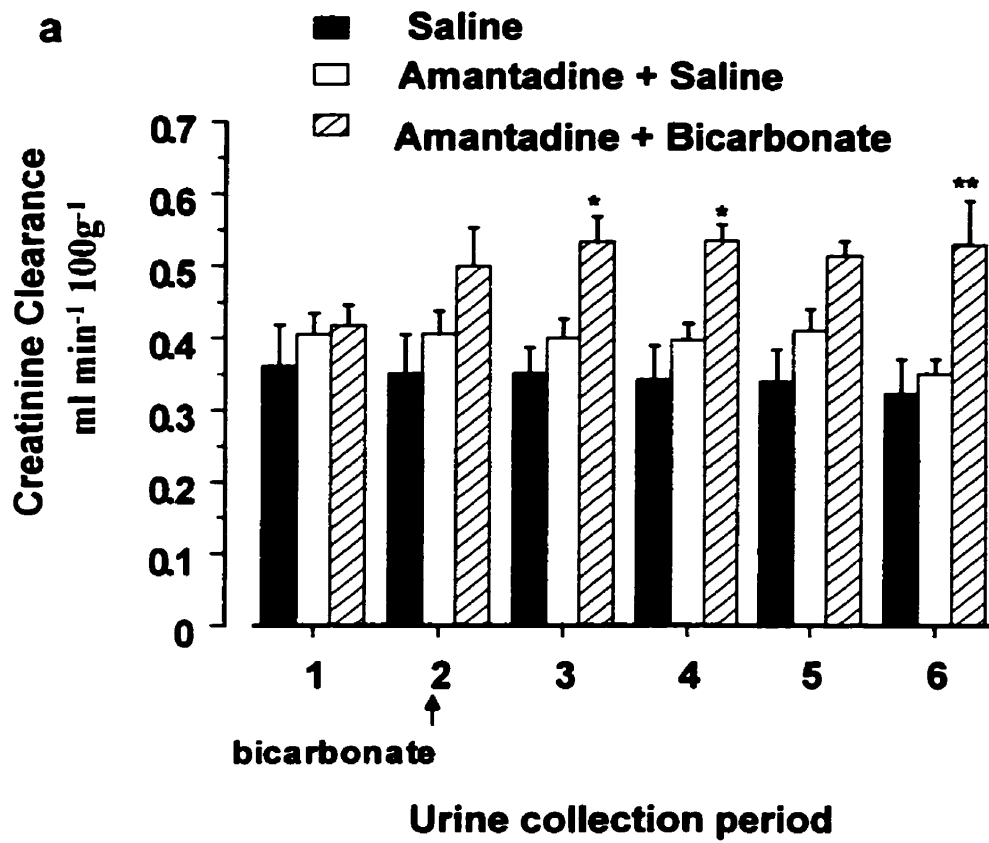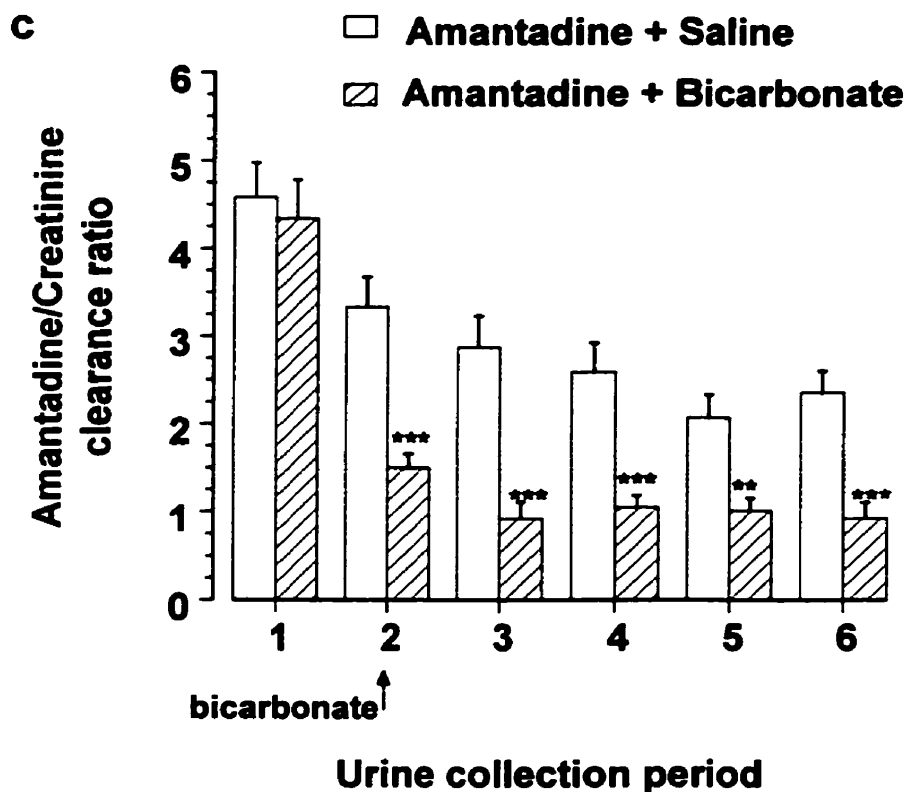
Figure 5-1: The effect of bicarbonate administration on a) creatinine clearance b) renal clearance of amantadine and c) the amantadine/creatinine renal clearance ratio. At the beginning of the first urine collection period rats received 3 mg kg^{-1} amantadine i.v. The bicarbonate-treated rats (hatched bars) received 5 mmol kg^{-1} bicarbonate i.v. at the beginning of the second urine collection and the controls (open bars) received an equivalent volume of saline (0.9 % i.v.). For creatinine clearance, an additional set of controls (solid bars) were maintained on 0.9 % saline only. For each urine collection period the data are expressed as mean ± SE, n = 5 (except saline control n = 4). Mixed model ANOVA with repeated measures for time, followed by Tukey's HSD test were used for statistical analysis. * $p < 0.05$, ** $p < 0.01$ and *** $p < 0.001$, difference from the saline-treated rats (panel a) and the amantadine + saline-treated rats (panels a, b and c) of the same urine collection period.

a

Creatinine clearance
(ml min⁻¹ 100g⁻¹)

Saline
Kynurenate + Saline
Kynurenate + Bicarbonate

bicarbonate

Urine collection period

b

Kynurenate clearance
(ml min⁻¹ 100g⁻¹)

Kynurenate + Saline
Kynurenate + Bicarbonate

bicarbonate

Urine collection period

187
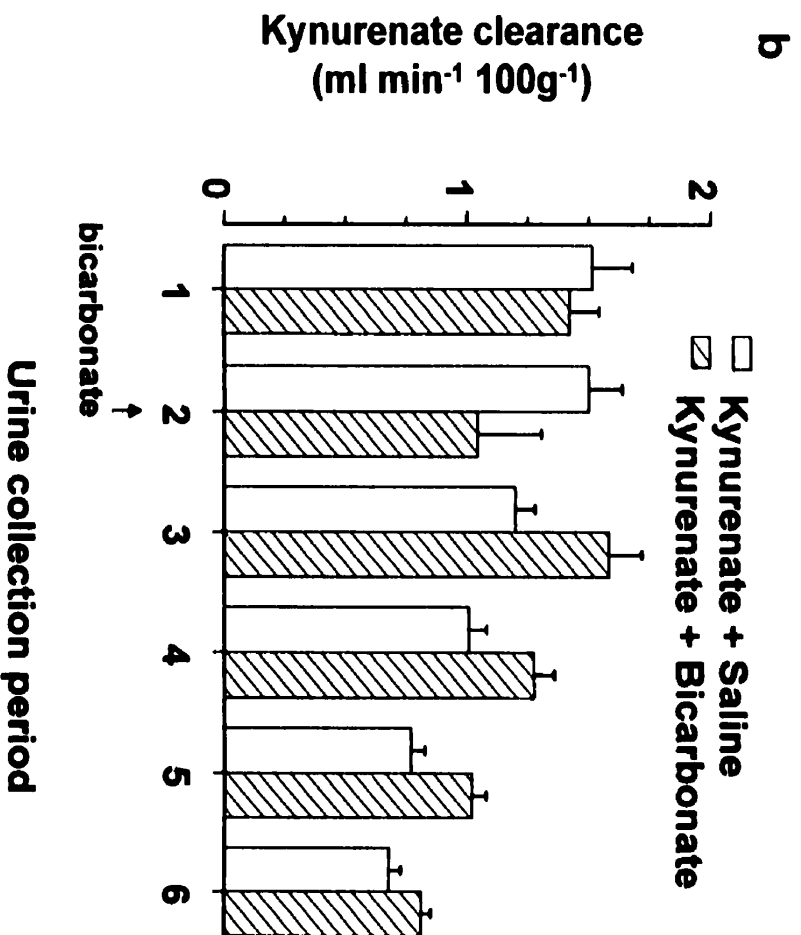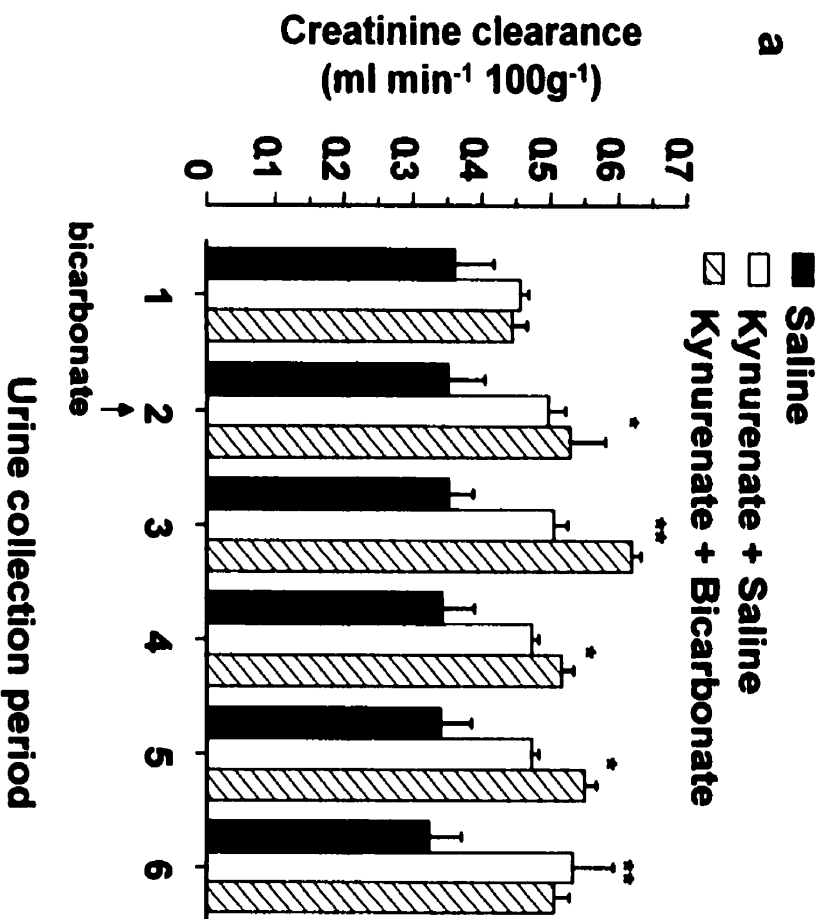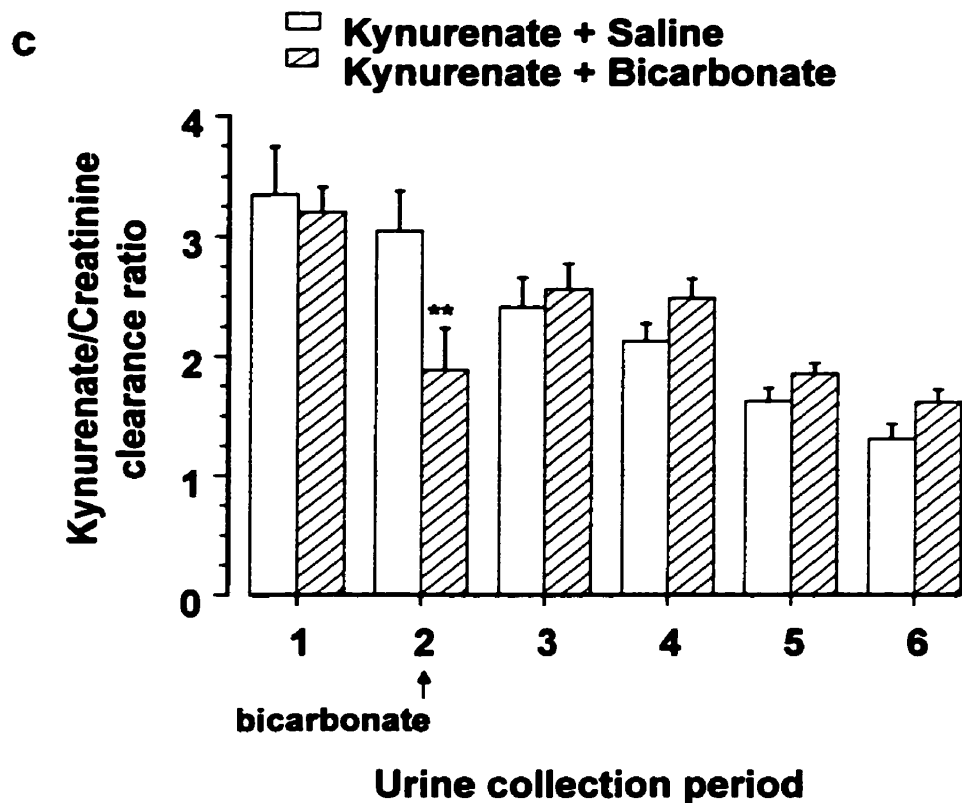
Figure 5-2: The effect of bicarbonate administration on a) creatinine clearance b) renal clearance of kynurenate and c) the kynurenate/creatinine renal clearance ratio. At the beginning of the first urine collection period rats received 3 mg kg^{-1} kynurenate i.v. The bicarbonate-treated rats (hatched bars) received 5 mmol kg^{-1} bicarbonate i.v. at the beginning of time interval 2 and controls (open bars) received an equivalent volume of saline (0.9 % i.v.). For creatinine clearance an additional set of controls (solid bars) were maintained on 0.9 % saline only. For each urine collection period the data are expressed as mean ± SE, n = 5 (except saline control n = 4). Mixed model ANOVA with repeated measures for time, followed by Tukey's HSD test were used for statistical analysis. * $p <$ 0.05 and ** $p <$ 0.01 compared to the saline-treated rats (panel a) and the kynurenic acid + saline-treated rats (panel c) of the same urine collection period.
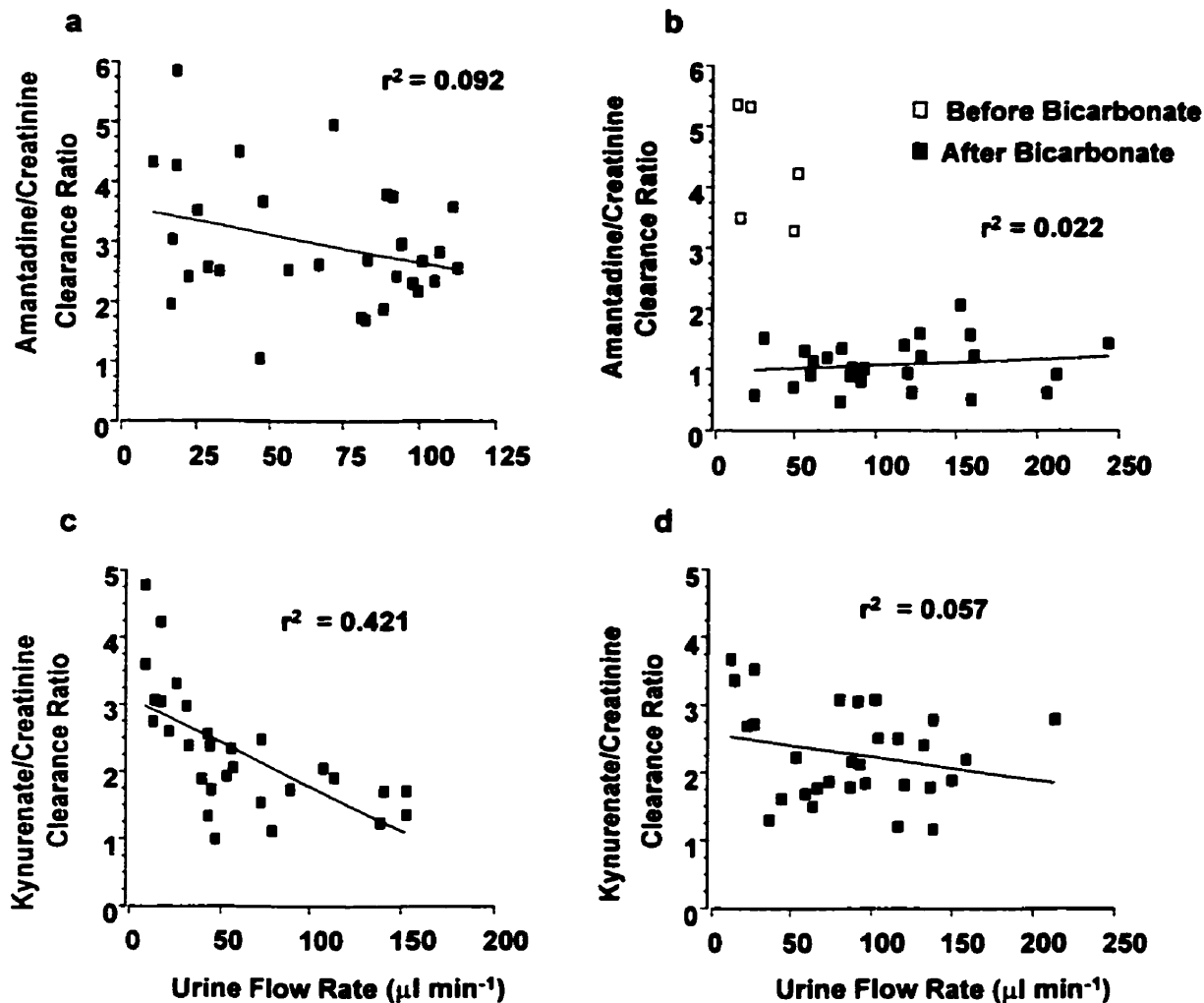
Figure 5-3: Correlation between urine flow rate and the amantadine/creatinine or kynurenate/creatinine clearance ratio. The figures show the combined clearance vs. urine flow rate data for all rats in each group. The solid line represents the least-squares regression for the correlation. a) Amantadine + saline-treated rats b) amantadine + bicarbonate-treated rats c) kynurenate + saline-treated rats and d) kynurenate + bicarbonate-treated rats. In panel b the amantadine/creatinine clearance ratio before bicarbonate administration (open squares) and after bicarbonate administration (solid squares) are identified to emphasize the change in the amantadine/creatinine clearance ratio after bicarbonate administration. For this group the regression fit was performed only on data points after the start of bicarbonate infusion.

189
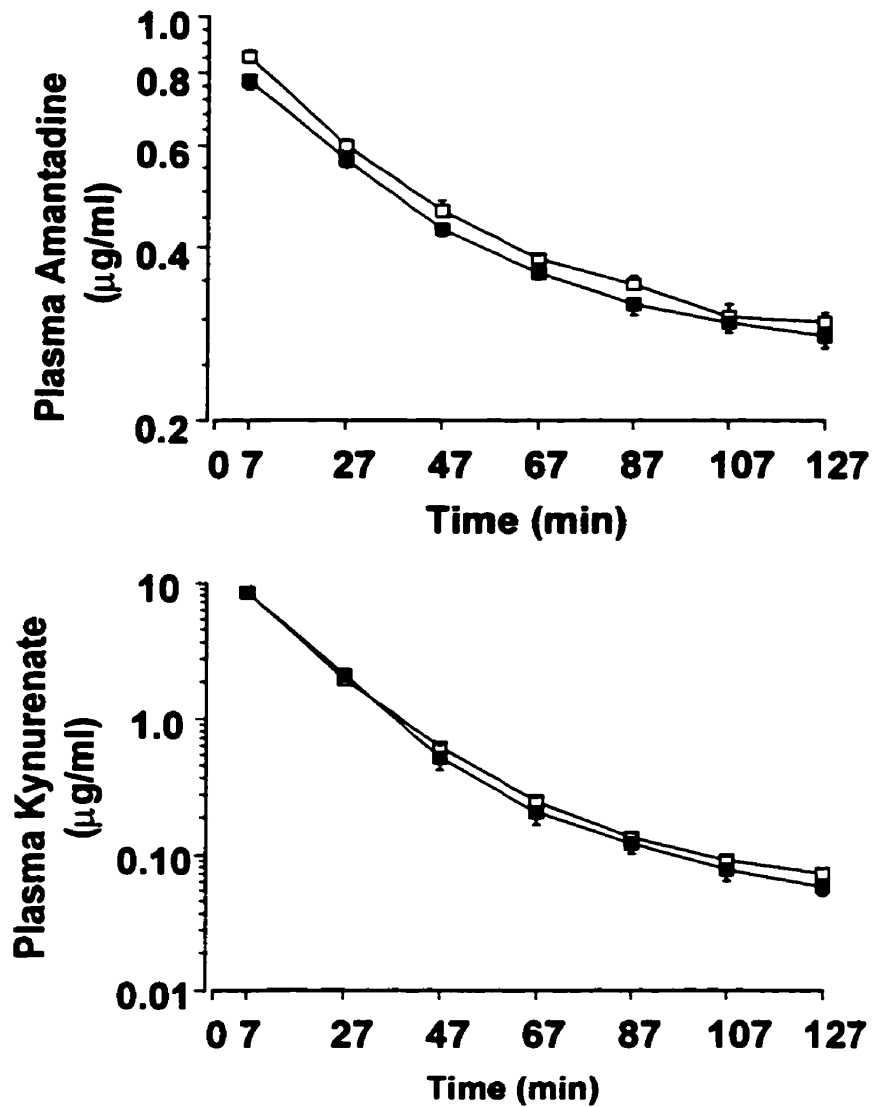
Figure 5-4: Plasma concentration versus time profiles for amantadine (upper panel) and kynurenate (lower panel). Amantadine and kynurenate (3 mg kg^{-1}) were infused starting at time zero and the duration of the infusion was 2 min. Plasma concentrations were measured at the beginning and end of each urine collection. The bicarbonate-treated rats (filled squares) received 5 mmol kg^{-1} bicarbonate i.v. at the beginning of the second urine collection (27 min) and the controls (open squares) received an equivalent volume of saline (0.9 % i.v.). Amantadine or kynurenate concentrations (µg/ml) are represented as the mean ± SE of five separate experiments. Error bars are not visible for all points due to small SE.

Table 5-1: Amantadine, metabolite and kynurenate excretion rate (nmol min^{-1}) in the urine and total excretion (μmol)

Treatment	Urine Collection Period						Total
	(1)	(2)	(3)	(4)	(5)	(6)	
Amantadine Excretion							
Amantadine + Saline	22.1 ± 1.8	11.6 ± 0.7	7.8 ± 0.6	6.1 ± 0.5	4.4 ± 0.4	3.9 ± 0.3	1.12 ± 0.07
Amantadine + NaHCO$_3^-$	21.3 ± 1.4	6.4 ± 0.4***	3.3 ± 0.5***	3.3 ± 0.3	2.8 ± 0.3	2.5 ± 0.6	0.79 ± 0.05[a]
Amantadine Metabolite Excretion							
Amantadine + Saline	13.3 ± 0.7	13.2 ± 0.5	11.9 ± 0.08	9.9 ± 0.3	8.7 ± 0.1	7.2 ± 0.5	1.29 ± 0.04
Amantadine + NaHCO$_3^-$	13.2 ± 1.0	11.6 ± 1.5	11.4 ± 1.0	10.6 ± 0.7	9.0 ± 0.6	8.8 ± 0.6	1.29 ± 0.09
Kynurenate Excretion							
Kynurenate + Saline	133 ± 4	37.1 ± 2.7	11.4 ± 4.4	2.0 ± 0.4	1.2 ± 0.1	3.8 ± 0.2	3.8 ± 0.2
Kynurenate + NaHCO$_3^-$	131 ± 11	23.6 ± 5.6	9.6 ± 1.3	3.6 ± 0.6	1.8 ± 0.3	1.0 ± 0.2	3.2 ± 0.2

Data are expressed as mean ± SE of five separate determinations. *** $p < 0.001$ compared to the amantadine + saline treated group, ANOVA followed by Tukey's HSD test. [a] $p < 0.01$ compared to the amantadine + saline treated rats, unpaired t-test. The amount of metabolite eliminated in μmol was calculated assuming that there was a 1:1 conversion ratio for specific activity between the parent amantadine compound and the metabolite.

Table 5-2. Urine flow rates (μl min^{-1})

Treatment	Urine Collection Period					
	(1)	(2)	(3)	(4)	(5)	(6)
1) Saline	18 ± 5	39 ± 10	86 ± 19	94 ± 24	84 ± 25	73 ± 20
2) Amantadine + Saline	29 ± 11	55 ± 15	86 ± 15	82 ± 13	71 ± 16	67 ± 14
3) Kynurenate + Saline	17 ±4	33 ± 11	55 ± 16	70 ± 12	90 ± 24	93 ± 23
4) Amantadine + NaHCO₃⁻	31 ± 9	157 ± 27***	165 ± 19**	103 ± 13	70 ± 12	60 ± 10
5) Kynurenate + NaHCO₃⁻	21 ± 3	128 ± 12**	144 ± 19*	93 ± 13	83 ± 12	65 ± 10

Data are expressed as mean ± SE of four or five separate determinations * $P < 0.05$, ** $P < 0.01$ and *** $P < 0.001$ compared to the non-bicarbonate treated rats of the same urine collection period, ANOVA followed by Tukey's HSD test.

Table 5-3: HCO_3^-, pCO_2 and pH in rats treated with amantadine + saline or amantadine + $NaHCO_3^-$

Parameter		Blood Sample				
	Group	(1)	(2)	(3)	(4)	(5)
1) HCO_3^-	Control	27.5 ± 0.8	26.7 ± 0.6	26.9 ± 07	26.5 ± 0.6	26.6 ± 0.4
	Treatment	28.4 ± 0.5	28.2 ± 0.3	34.6 ± 0.4***	31.8 ± 0.7***	29.8 ± 0.2***
2) pH	Control	7.41 ± 0.01	7.40 ± 0.01	7.40 ± 0.01	7.41 ± 0.02	7.41 ± 0.01
	Treatment	7.41 ± 0.01	7.41 ± 0.01	7.48 ± 0.01***	7.46 ± 0.01***	7.46 ± 0.01***
3) pCO_2	Control	43.4 ± 2.2	41.8 ± 1.9	42.7 ± 1.6	41.3 ± 1.8	41.2 ± 1.2
	Treatment	44.6 ± 0.9	45.2 ± 1.1	45.7 ± 0.6	43.5 ± 0.4	41.8 ± 0.7

		Urine Collection Period			
	Group	(1)	(2)	(3)	(4)
Urine pH	Control	6.68 ± 0.22	6.73 ± 0.20	6.71 ± 0.13	6.81 ± 0.10
	Treatment	6.45 ± 0.27	8.03 ± 0.08***	8.24 ± 0.03***	8.00 ± 0.11***

Data are represented as mean ± SE of four separate experiments. Control = amantadine + saline treated rats and Treatment = amantadine + sodium bicarbonate treated rats. HCO_3^- is expressed in units of mmol L^{-1} and pCO_2 is expressed in units of mm Hg. ** $p < 0.01$, and *** $p < 0.001$ compared to the control group, ANOVA followed by Tukey's HSD test.

Table 5-4: Na$^+$, Cl$^-$, and K$^+$ excretion (μmol) in the urine and cumulative Na$^+$ retention (μmol) in amantadine + NaCl and amantadine + NaHCO$_3^-$ treated rats

Parameter	Group	Urine Collection Period				Total
		(1)	(2)	(3)	(4)	
1) Na$^+$ excretion	Control	27 ± 6	41 ± 11	140 ± 22	178 ± 35	387 ± 55
	Treatment	61 ± 30	432 ± 64***	614 ± 73***	402 ± 16***	1508 ± 172***
2) Cumulative Na$^+$ retention	Control	264 ± 6	513 ± 14	956 ± 29	1360 ± 56	
	Treatment	230 ± 30	1370 ± 88***	1340 ± 161***	1520 ± 169	
3) K$^+$ excretion	Control	46 ± 7	46 ± 5	88 ± 5	92 ± 9	272 ± 15
	Treatment	59 ± 2	105 ± 7***	141 ± 8***	127 ± 6**	432 ± 18***
4) Cl$^-$ excretion	Control	61 ± 9	74 ± 13	198 ± 23	227 ± 32	552 ± 46
	Treatment	102 ± 28	355 ± 40***	472 ± 48***	363 ± 19*	1291 ± 105***

Data are represented as mean ± SE of four separate experiments. Control = amantadine + saline treated rats and Treatment = amantadine + sodium bicarbonate treated rats. Collection periods 1 and 2 were 20 min whereas 3 and 4 were 40 min in duration. * p < 0.05** p < 0.01, and *** p < 0.001compared to the control group, ANOVA followed by Tukey's HSD test.

Table 5-5: Kinetic parameters for amantadine and kynurenic acid disposition in the rat

Treatment	Amantadine + saline (n = 5)	Amantadine + HCO$_3^-$ (n = 5)	Kynurenic acid + saline[1] (n = 4)	Kynurenic acid + HCO$_3^-$ (n = 5)
AUC (mg min L^{-1})	283 ± 144	1279 ± 938	197 ± 7	189 ± 19
$\alpha_{t1/2}$ (min)	19.7 ± 2.1	23.8 ± 1.9	8.55 ± 0.42	8.01 ± 0.50
$\beta_{t1/2}$ (min)	518 ± 307	3480 ± 2840	34.2 ± 2.6	56.5 ± 20.3
Vd$_{ss}$ (L kg^{-1})	6.35 ± 0.66	9.08 ± 1.0*	0.300 ± 0.006	0.354 ± 0.060
Cl$_p$ (ml min^{-1} 100g^{-1})	1.9 ± 0.4	1.0 ± 0.3	1.53 ± 0.05	1.66 ± 0.20
[2]Cl$_r$ (ml min^{-1} 100g^{-1})	1.16 ± 0.04	0.76 ± 0.04**	1.11 ± 0.05	1.19 ± 0.05
Cl$_r$/Cl$_p$	0.95 ± 0.39 (0.65)	3.3 ± 2.5 (0.78)	0.70 ± 0.03	0.76 ± 0.09

Data are expressed as mean ± SE of four or five separate determinations. The median values for amantadine Cl$_r$/Cl$_p$ are shown in brackets. [1]Model fit was only possible for 4 of 5 animals for this group. [2]Cl$_r$, mean renal clearance over the duration of the experiment. * $p < 0.05$, ** $p < 0.01$ compared to amantadine + saline treated rats, unpaired t-test. All pharmacokinetic parameters for the two kynurenic acid treated groups were similar, unpaired t-test.

Discussion

This study addressed the potential in vivo functional importance of a previously identified in vitro bicarbonate-dependent renal tubule amantadine (organic cation) transport mechanism (Escobar et al., 1994; Escobar and Sitar, 1995). The major finding of the present study was that acute sodium bicarbonate administration decreased amantadine renal clearance, most likely by modulation of renal tubule secretion. Our present in vivo observations in rats are consistent with a previous report that chronic administration of sodium bicarbonate reduced the renal excretion amantadine in humans (Geuens and Stephens, 1967). Similar effects of sodium bicarbonate loading on decreasing the renal clearance of other organic bases in rats and dogs have also been reported (Torretti et al., 1962; Weiner and Roth, 1981). In addition our data demonstrated for the first time that a chronic alteration in circulating bicarbonate is not necessary to result in decreased renal clearance of amantadine.

In the present study, the importance of secretion and filtration components of amantadine clearance as a function of an acute exposure to sodium bicarbonate were determined. The relative contribution of secretion of amantadine and kynurenate to their overall renal clearance was determined by the amantadine or kynurenate/creatinine clearance ratio, respectively. Creatinine has been demonstrated to undergo renal tubule secretion as well as reabsorption (Harvey and Malvin, 1965; Nannum et al., 1983). However, it has been widely accepted clinically for estimating GFR, and in practice, when renal function is normal, it gives estimates of GFR that are similar to those

estimated by inulin (Giovannetti and Barsotti G, 1991). In rats the use of endogenous creatinine clearance (determined by the non-specific alkaline picrate assay) and inulin clearance resulted in similar estimates of GFR as evidenced by the creatinine/inulin clearance ratio near one (Darling and Morris, 1991). For these reasons and the fact that the creatinine determination is very convenient compared to inulin, creatinine clearance was chosen as the method to estimate GFR for these experiments. Creatinine clearance may be decreased by the presence of other organic cations or anions such as cimetidine or probenecid that compete for common tubule secretion pathways (Harvey and Malvin, 1965; Darling and Morris, 1991; van Acker *et al.*, 1992). However, in our experiments amantadine and kynurenate did not depress creatinine clearance. To alleviate concerns regarding the suitability of creatinine as a marker of GFR future studies should incorporate the use of inulin for this purpose.

Initially, amantadine and kynurenate undergo significant renal tubule secretion, as indicated by an amantadine/creatinine and kynurenate/creatinine clearance ratio greater than one. Based on the decrease in the observed amantadine/creatinine clearance ratio in face of a relatively constant creatinine clearance, it appears that sodium bicarbonate dosing is decreasing amantadine clearance through effects on secretion and not filtration. Conversely, kynurenate secretion appears to be only transiently decreased during the period of sodium bicarbonate infusion. This may reflect temporary changes in renal function during the time of the infusion. With reference to our chosen organic cation and anion substrates, the effect of sodium bicarbonate infusion on renal tubule transport

appears to be specific for the organic base as opposed to a general phenomenon affecting both organic acid and base secretion.

In this study, an acute dose of sodium bicarbonate was sufficient to impair the renal clearance of amantadine for an extended period of time. The chosen dose of sodium bicarbonate (5 mmol kg^{-1}) for these studies was based on its apparent volume of distribution (0.4-0.5 L kg^{-1}) in dogs and was expected to increase peak plasma bicarbonate levels by 10 mM (Adrogue *et al.*, 1983). The peak blood bicarbonate concentration observed in our experiments, approximately 5 min after the bicarbonate infusion was stopped, was about 8 mM higher than the respective control blood bicarbonate levels and remained elevated thereafter. Since blood bicarbonate levels remain elevated, it is suggestive that the increase in plasma bicarbonate ion concentration may be responsible for the decreasing amantadine clearance. However, in the present studies the amantadine + saline treated rats received a total of 1.75 mmol Na$^+$ over the duration of the collection periods whereas the amantadine + sodium bicarbonate treated rats received 3.00 mmol of Na$^+$. It was clear from the experiments that Na$^+$ and the cumulative retention of Na$^+$ are increased after sodium bicarbonate infusion compared to the control rats. In vivo, it is not known if the increased Na$^+$ excretion or extracellular fluid volume expansion because of greater Na$^+$ retention may contribute to the observed effect that sodium bicarbonate infusion decreases the renal clearance and excretion of amantadine. Furthermore, the sodium bicarbonate infusion increased K$^+$ and Cl$^-$ excretion compared to controls. At this time we cannot rule out that the increased Na$^+$ retention, Na$^+$ excretion or K$^+$ and Cl$^-$ excretion in the sodium bicarbonate treated rats

contributes to the observed alteration in amantadine renal clearance. We believe that the increased plasma bicarbonate level is the most important factor in explaining the effect on renal clearance of amantadine because previous in vitro studies demonstrated that renal tubule transport of amantadine is dependent on bicarbonate and independent of Na^+ and K^+ concentration (Escobar and Sitar, 1994; 1996). To confirm this hypothesis, future in vivo experiments must incorporate the use of hypertonic sodium chloride infusion to control for the greater Na^+ load in the sodium bicarbonate treated rats.

We believe passive reabsorption is likely to have only minor importance in explaining the decrease in amantadine clearance for the following reasons. Due to the high pKa of amantadine (pKa = 10.1), only a limited gradient for passive reabsorption of amantadine from the tubule lumen to the peritubular capillaries would be established by the increase urine pH. Secondly, with increasing urine flow rates with time in our animals, there would be a predicted increase in net renal drug excretion and increased clearance due to less contact time for passive reabsorption of the drug into the peritubular capillaries. In our model, this effect was not apparent, as a large increase in urine flow rate in the bicarbonate treated rats was not correlated with a substantial increase in the amantadine/creatinine clearance ratio. Furthermore, drug disposition studies in humans showed amantadine renal clearance was not dependent on urine pH (Aoki et al., 1979). The slight increase in blood pH (< 0.1) resulting from the bicarbonate infusion will not significantly change the degree of ionization of amantadine in the plasma. Thus there should be little effect of pH changes on whole body distribution of amantadine.

By studying bicarbonate effects on amantadine and kynurenate, we were able to demonstrate pharmacokinetic data for amantadine and kynurenate in the rat. These parameters have not been previously published. The plasma concentration data do not reflect the dramatic effect of bicarbonate on renal clearance of amantadine. However, pharmacokinetic analysis of these data suggest that bicarbonate administration may have increased amantadine's Vd_{ss}. Although there are species differences in amantadine metabolism and elimination, the distribution characteristics for amantadine in the control rats (Vd_{ss} = 6.35 ● 0.66 L kg^{-1}) is similar to that reported in adult male humans (Vd_{ss} = 6.59 ± 1.49 L kg^{-1}) after i.v. amantadine infusion (Bleidner et al., 1965; Aoki and Sitar, 1988). Our reported control amantadine/creatinine clearance ratio is also similar to amantadine/creatinine ratios previously reported in humans and in dogs (Tilles, 1974; Aoki et al., 1979; Sitar et al., 1997), indicating similar renal secretory capacity for amantadine in these species. The median renal to plasma clearance ratio (Cl_r/Cl_p) for amantadine was about 0.5 and is consistent with additional routes of amantadine elimination (metabolism) as well as renal elimination of the parent compound. The observed Cl_r/Cl_p ratio for kynurenate was about 0.75. This observation may indicate that kynurenate is being metabolized to a small extent but the presence of any metabolite was undetectable by our t.l.c. methods.

In humans, a variety of amantadine metabolites have been identified by mass-spectrometry with the predominant metabolite of amantadine being N-acetylamantadine (Köppel and Tenczer, 1985). To test whether the metabolite profile for amantadine in the rat is similar to that in humans, we did gas chromatography analysis for acetylamantadine

according to previously published methods (Bras *et al.*, 1998). We were unable to detect acetylamantadine in our rat urine samples and thus can exclude acetylamantadine as the major metabolite of amantadine formed in our rat experiments. The fact that the total excretion of amantadine but not the metabolite changes in our experiments suggests that: 1) Amantadine and the metabolite do not interact at an identical point in the renal excretion pathway 2) It is likely that bicarbonate is reducing amantadine clearance solely by modulating renal tubule transport. Since it is likely that amantadine and the metabolite do not interact at a common tubule secretory pathway, the exact identity of the metabolite is not critical for the understanding of the present findings.

The exact mechanism of bicarbonate reduction in net renal secretion of amantadine remains elusive at this time. We may speculate that in order to satisfy in vitro data of increased amantadine renal tubule accumulation in the presence of bicarbonate and in vivo data of decreased secretion, bicarbonate may be able to decrease the luminal efflux of amantadine in addition to its stimulatory effect on amantadine uptake at basolateral membrane. Renal tubule luminal organic cation transporters may mediate the passage of organic cations from the tubule cell into the tubule lumen (Kinsella *et al.*, 1979a; Holohan and Ross, 1980). These organic cation transporters may represent sites for the observed bicarbonate effect. Although we did not measure urinary output of bicarbonate in these studies, upon giving a bicarbonate load luminal delivery of bicarbonate and urinary excretion should increase (Dubose *et al.*, 1996). Thus, there is potential for a luminal bicarbonate effect on transport of amantadine. Evidence for bicarbonate modulation of luminal proximal tubule organic cation transporters as

201

opposed to increased non-ionic diffusion has already been demonstrated for the organic base procainamide (McKinney, 1984). However, aside from the McKinney report, bicarbonate modulation on luminal membrane organic cation transporters has not been studied. Alternatively, evidence exists that indicates secretion of some organic cations across the brush border membrane of proximal tubules is coupled to an inwardly directed proton gradient that is driven by the Na^+/H^+ exchanger located in the brush border membrane (Holohan and Ross, 1981; Takano *et al.*, 1984; Rafizadeh *et al.*, 1987). Therefore, it is also possible that the alkalinization of the tubule fluid that occurs after bicarbonate administration may cause a decrease in the driving force for H^+/organic cation exchange across the brush border membrane of proximal tubules, and thus a decrease in amantadine clearance.

Certain organic cationic drugs such as aminoglycoside antibiotics are highly toxic to the kidney (Bennett, 1989). The finding that the bicarbonate-dependent increase in amantadine uptake in vitro is not linked to increased renal excretion of amantadine in vivo raises the issue of pharmacological consequence of increased renal or serum accumulation of amantadine or potential nephrotoxic organic cations such as aminoglycosides. Our data suggest that acute changes in acid/base status that result in increased plasma bicarbonate levels may compromise renal elimination of amantadine and possibly other organic cation drugs that are specifically handled by bicarbonate-dependent organic cation transporters in the kidney.

GENERAL SUMMARY AND CONCLUDING REMARKS

The initial objective of these studies was to determine whether the previously described bicarbonate-dependent renal tubule amantadine transporter(s) was/were unique from other known renal tubule organic cation transporters. We have shown that the large reliance on one compound, namely TEA has failed with respect to define the renal tubule organic cation transport system in its entirety. Our results in chapter 1 and 2 clearly demonstrate that the once considered "single multispecific transport system" for organic cations appears now to be comprised of a series of organic cation transporters with unique substrate specificity and controlling mechanisms. There appeared to be at least four basolateral organic cation transporters, namely the bicarbonate-dependent and bicarbonate-independent amantadine-selective transporters as well as high-affinity and low-affinity transporters for TEA. The identification of multiple transport sites is important for more thoroughly identifying the possibility for drug interactions of preexisting or novel therapeutic agents in the kidney when multiple medications are consumed simultaneously. In future studies, the use of molecular, immunochemical and in vivo techniques should contribute to further establishing the identity, tissue distribution and function of each of these transporters. Furthermore, using molecular biology information, it would be interesting from a clinical perspective to determine if genetic polymorphisms of the various organic cation transporters are present and result in altered therapeutic effectiveness of drug treatments, drug toxicity and or inherited disease conditions.

Our studies in diabetic and UNX rats (chapter 3) suggested that the function of the bicarbonate-dependent amantadine transporters in the proximal tubule could be modulated by these conditions. Our predictions suggested that the alteration in the kinetics of the bicarbonate-dependent organic cation transporters might be important for in vivo drug elimination by the kidney. Considering the prevalence of diabetes mellitus and end stage renal disease in North America, additional research on the effects of disease on renal tubule secretion of organic cationic drugs by the kidney is necessary. In future studies, the in vivo renal elimination of substrates for the various renal organic cation transporters should be addressed at all stages of diabetes mellitus (controlled and uncontrolled) and in one kidney versus two kidney rats. This approach should aid in the determination of potential long-term effect of these chronic conditions on drug secretion by the kidney tubules, of which there is very little information at present. Our findings would suggest that alteration in organic cation transporter function in disease states, such as diabetes mellitus, could possibly modulate access/elimination of therapeutic agents to/from target organs resulting in decreased drug efficacy or possibly toxicity. Therefore, the study of the organic cation transporters in other tissues, including brain, liver, intestines and heart represents an attractive area for further study.

In chapter four I presented the hypothesis that interactions of NH_4^+ with organic cation transporters may be important in describing the well-known phenomenon that NH_4Cl administration increases the renal elimination of several organic cation drugs. This suggestion was opposed to the well-established thinking that NH_4Cl increases renal excretion of the organic bases by acidifying the urine, which subsequently leads to increased ionization and decreased passive reabsorption of the organic base that had gained access to

the tubule lumen by filtration and secretion. In several literature reports, when healthy subjects received NH_4Cl, the majority of evidence supported an association between urine pH and organic cation elimination by the kidneys but not necessarily the passive diffusion hypothesis. The effects of other parameters that change in acid base disturbances including plasma pH, plasma HCO_3^-, and NH_4^+ production and levels in the kidney have unjustifiably been ignored in regard to drug elimination by the kidney. The evidence presented herein demonstrated that NH_4^+ competitively interacted predominantly with the bicarbonate-dependent amantadine transporters in renal proximal and distal tubules of male and female rats. This interaction was independent of changes in extracellular or intracellular pH and significantly decreased renal tubule transport of amantadine. We have alternatively hypothesized that more pronounced interactions of NH_4^+ with luminal transporters may occur because of the higher NH_4^+ concentrations in the lumen as opposed to the peritubular capillaries. To confirm this hypothesis, future studies must address the effects of NH_4^+ on amantadine efflux from proximal and distal tubules, and on amantadine transport using either isolated luminal membrane preparations or directional transport studies in cell culture. These findings may have clinical importance for drug elimination in conditions where production and excretion of NH_4^+ increases, such as in gastrointestinal loss of bicarbonate, K^+ deficiency, chronic fasting and renal insufficiency.

The final object of this dissertation research (chapter 5) was to develop methodology to study the renal tubule transport of amantadine in an in vivo rat model and to study the implications of bicarbonate on the function of the bicarbonate-dependent

amantadine transporter in vivo. The UNX rat model was successfully used for these studies and provided a reliable model to study organic cation clearance and elimination by the kidney. The initial in vivo study addressed the potential functional importance of a previously identified in vitro bicarbonate-dependent renal tubule amantadine transport mechanism. The major finding was that acute sodium bicarbonate administration decreased amantadine renal clearance, most likely by modulation of renal tubule secretion. However, in order to clarify mechanism of action, additional in vivo studies are required. In vitro studies using membrane vesicles would also be useful to determine the effects of bicarbonate on the luminal transport of amantadine. In addition, our data demonstrated for the first time that a chronic alteration in circulating bicarbonate is not necessary to result in decreased renal clearance of amantadine. Taking into the consideration the results from our in vitro studies of amantadine transport in UNX rats, a future comparison of amantadine renal elimination in two kidney rats versus UNX rats will be important for confirmation of these findings. Secondly, now that the in vivo procedure is developed, it will represent an appropriate model to study and compare amantadine-selective transporters versus TEA-selective transporters with regard to their ability to secrete other organic cation drugs.

206

References

Abe T, Kakyo M, Sakagami H, Tokui T, Nishio T, Tanemoto M, Nomura H, Hebert SC, Matsuno S, Kondo H and Yawo H (1998) Molecular characterization and tissue distribution of a new organic anion transporter subtype (oatp3) that transports thyroid hormones and taurocholate and comparison with oatp2. *J Biol Chem* **273**: 22395-22401.

Acara M and Rennick B (1972a) Renal tubule transport of choline: modifications caused by intrartenal metabolism. *J Pharmacol Exp Ther* **182**: 1-13.

Acara M and Rennick B (1972b) Renal tubule transport of acetylcholine and atropine: enhancement and inhibition. *J Pharmacol Exp Ther* **182**: 14-26.

Alpern RJ and Preisig PA (1997) Renal acid-base transport, in *Diseases of the Kidney, 6th edition* (Schrier RW and Gottschalk CW, eds) pp 189-201, Little, Brown and Co., Boston.

Andersen AR, Christiansen JS, Andersen JK, Kreiner S and Deckert T (1983) Diabetic nephropathy in type 1 (insulin-dependent) diabetes: an epidemiological study. *Diabetologia* **25**: 496-501.

Androgue JH, Brensilver J and Cohen, JJ (1983) Influence of steady-state alterations in acid-base equilibrium on the fate of administered bicarbonate in the dog. *J Clin Invest* **71**: 867-883.

Aoki FY and Sitar DS (1988) Clinical pharmacokinetics of amantadine hydrochloride. *Clin Pharmacokinet* **14:** 35-51.

Aoki FY, Sitar DS and Ogilvie RI (1979) Amantadine kinetics in healthy young subjects after long term dosing. *Clin Pharmacol Ther* **26:** 727-736.

Armbruster KFW, Rahn AC, Ing, TS, Halper IS, Dyama JH et al. (1974) Amantadine toxicity in a patient with renal insufficiency. *Nephron* **13:** 183-186.

Beck WT (1987) The cell biology of multiple drug resistance. *Biochem Pharmacol* **36:** 2879—2887.

Beckett AH and Rowland (1965) Urinary excretion of methylamphetamine in man. *Nature* **206:** 1260-1261.

Bendayan R, Lo B and Silverman M (1994) Characterization of cimetidine transport in LLC-PK₁ cells. *Am J Soc Nephrol* **4:** 74-84.

Bennett WM (1989) Mechanisms of aminoglycoside nephrotoxicity. *Clin Exp Pharmacol Physiol* **16:** 1-6.

Bergwerk AJ, Shi XY, Ford AC, Kanai N, Jacquemin E, Burk RD, Bai S, Novikof PM, Steiger B, Meier PJ, Schuster VL and Wolkoff AW (1996) Immunologic distribution of an organic anion transport protein in rat liver and kidney. *Am J Physiol* **271**: G231-G238.

Berner W and Kinne R (1976) Transport of *p*-aminohippuric acid by plasma membrane vesicles isolated from rat kidney cortex. *Pflugers Arch* **361**: 269-277.

Besseghir K and Roch-Ramel F (1987) Renal excretion of drugs and other xenobiotics. *Renal Physiol* **10**: 221-241.

Besseghir K, Mosig D and Roch-Ramel F (1990) Transport of the organic cation N^1-methylnicotinamide by the rabbit renal proximal tubule: I. accumulation in the isolated nonperfused tubule. *J Pharmacol Exp Ther* **253**: 444-451.

Beyer KH, Russo HF, Gass SR, Wilhoyte KM and Pitt AA (1950) Renal tubular elimination of N^1-methylnicotinamide. *Am J Physiol* **160**: 311-320.

Bleidner WE, Harmon JB, Hewes WE, Lynes TE and Hermann EC (1965) Absorption, distribution and excretion of amantadine hydrochloride. *J Pharmacol Exp Ther* **150**: 484-490.

Blomstedt JW and Aronson PS (1980) pH-gradient-stimulated transport of urate and *p*-aminohippurate in dog renal microvilles membrane vesicles. *J Clin Invest* **65**: 931-934.

Bobby B and Sitar DS (1997) The effect of lactate on sex differences in renal tubular energy-dependent transport of an organic cation. 38th National Student Research Forum, Galveston, Texas, p61 (C-1).

Bose R (1995) Sodium/hydrogen exchange. in *Airways Smooth Muscle: peptide receptors, ion channels and signal transduction* (Raeburn D and Giembycz MA eds) pp 234-254, Birkhauser Verlag, Basel, Switzerland.

Bossuyt X, Muller M, Hagenbuch B and Meier PJ (1996) Polyspecific drug and steroid clearance by an organic anion transporter of mammalian liver. *J Pharmacol Exp Ther* **276:** 891-896.

Brandle E, Fritzsch G and Greven J (1992) Affinity of different local anaesthetic drugs and chatecholamines for the contraluminal transport system for organic cations in proximal tubules of rat kidneys. *J Pharmacol Exp Ther* **260:** 734-741.

Bras APM, Hoff HR, Aoki FY and Sitar DS (1998) Amantadine acetylation may be affected by acetyltransferases other than NAT1 or NAT2. *Can J Physiol Pharmacol* **76:** 701-706.

Brater DC, Kaojarern S, Benet LZ, Lin ET, Lockwood T, Morris RC, McSherry EJ and Melmon KL (1980) Renal excretion of pseudoephedrine. *Clin Pharmacol Ther* **28**: 690-694.

Briggs GE and Haldane JBS (1925) A note on the kinetics of enzyme action. *Biochem J* **19**: 338-339.

Brosnan JT, Lowry M, Vinay P, Gougoux A and Halperin ML (1987) Renal ammonium production – une vue canadienne. *Can J Physiol Pharmacol* **65**: 489-498.

Burg MB (1972) Perfusion of isolated renal tubules. *Yale J Biol Med* **45**: 321-326.

Burg MB and Orloff J (1969) p-Aminohippurate uptake and exchange by separated renal tubules. *Am J Physiol* **217**: 1064-1068.

Burg M, Grantham J, Abramow M and Orloff J (1966) Preparation and study of fragments of single rabbit nephrons. *Am J Physiol* **210**: 1293-1298.

Busch AE, Karbach U, Miska D, Gorboulev V, Akoundova A, Volk C, Arndt P, Ulzheimer JC, Sonders MS, Baumann C, Waldegger S, Lang F and Koepsell H (1998) Human neurons express the polyspecific cation transporter hOCT2, which translocates monoamine neurotransmitters, amantadine and memantadine. *Mol Pharmacol* **54**: 342-352.

Busch AE, Quester S, Ulzheimer JC, Waldegger S, Gorboulev V, Arndt P, Lang F and Koepsell H (1996a) Electrogenic properties and substrate specificity of the polyspecific rat cation transporter rOCT1. *J Biol Chem* **271**: 32599-32604.

Busch AE, Quester S, Ulzheimer JC, Gorboulev V, Akoundova A, Waldegger S, lang F and Koepsell H (1996b) Monoamine neurotransmitter transport mediated by the polyspecific organic cation transporter rOCT1. *FEBS Lett* **395**: 153-156.

Carney SL, Wong NLM and Dirks JH (1979) Acute affects of streptozotocin diabetes on rat renal function. *J Lab Clin Med* **93**: 950-961.

Chan BSH, Lazzaro VA, Seale JP and Duggin GG (1996) Transport of paraquat in a renal epithelial cell line LLC-PK$_1$. *J Pharmacol Exp Ther* **279**: 625-632.

Cheng Y-C and Prusoff WH (1973) Relationship between the inhibition constant (K_i) and the concentration of inhibitor which causes 50 % inhibition (I_{50}) of an enzymatic reaction. *Biochem Pharmacol* **22**: 3099-3108.

Christensen HN (1975) Biological Transport, 2nd ed. W.A. Benjamin, Inc., London.

Cornish-Bowden A (1974) A simple graphical method for determining the inhibition constants of mixed, uncompetitive and non-competitive inhibitors. *Biochem J* **137**: 143-144.

Cornish-Bowden A (1979) Fundamentals of Enzyme Kinetics. Butterworths, London, UK.

Cornish Bowden A (1995) Analysis of enzyme kinetic data. Oxford University Press, Oxford.

Cortes P, Dumler F, Goldman J and Levin NW (1987) Relationship between renal function and metabolic alterations in early streptozotocin-induced diabetes in rats. *Diabetes* **36**: 80-87.

Courtney MA, Mylle M, Lassiter WE and Gottschalk CW (1965) Renal tubule transport of water, solute and PAH in rats loaded with isotonic saline. *Am J Physiol* **209**: 1199-1205.

Cross RJ and Taggart JV (1950) Renal tubular transport: accumulation of p-aminohippurate by rabbit kidney slices. *Am J Physiol* **161**: 181-190.

Dahlmann A, Dantzler WH, Silbernagl S and Gekle M (1998) Detailed mapping of ochratoxin A reabsorption along the rat nephron in vivo: The nephrotoxin can be

reabsorbed in all nephron segments by different mechanisms. *J Pharmacol Exp Ther* **286**: 157-162.

Dantzler WH, Wright SH, Chatsudthipong V and Brokl OH (1991) Basolateral tetraethylammonium transport in intact tubules: specificity and *trans*-stimulation. *Am J Physiol* **261**: F386-F392.

Darling IM and Morris ME (1991) Evaluation of "true" creatine clearance in rats reveals extensive renal secretion. *Pharmaceutical Res* **8**: 1318-1322.

David C, Rumrich G and Ullrich KJ (1995) Luminal transport system for H^+/organic cations in the rat proximal tubule: kinetics, dependence on pH; specificity as compared to the contraluminal organic cation transport system. *Plfugers Arch* **430**: 477-492.

Deckert T, Poulsen JE and Larsen M (1978) Prognosis of diabetics with diabetes onset before age of thirty-one. *Diabetologia* **14**: 363-377.

De Hemptinne A, Marrannes R and Vanheel B (1983) Influence of organic acids on intracellular pH. *Am J Physiol* **245**: C178-C183.

De Lannoy IAM and Silverman M (1993) P-glycoprotein (P-gp) mediates the transport of the cardiac glycoside digoxin. *FASEB J* **7**:A456.

Dixon M (1953) The determination of enzyme inhibitor constants. *Biochem J* **55**: 170-171.

Dubose TD Jr, Cogan MG and Rector FC Jr (1996) Acid-Base Disorders, in *The Kidney, 5th edition* (Brenner BM ed) pp 929-998, W. B. Saunders Co., Philadelphia.

Dutt A, Heath LA and Nelson JA (1994) P-glycoprotein and organic cation secretion by the mammalian kidney. *J Pharmacol Exp Ther* **269**: 1254-1260.

Eadie G (1942) The inhibition of cholinesterase by physostigmine and prostaglandin. *J Biol Chem* **56**: 658-666.

Eckhardt U, Schroeder A, Steiger B, Hochli M, Landmann L, Tynes R, Meier PJ and Hagenbuch B (1999) Polyspecific substrate uptake by the hepatic organic anion transporter oatp1 in stably transfected CHO cells. *Am J Physiol* **276**: G1037-G1042.

Elliot WC, Houghton DC, Gilbert DN, Baines-Hunter J and Bennett WM (1985) Experimental gentamicin nephrotoxicity : effect of streptozotocin induced diabetes. *J Pharmacol Exp Ther* **233**: 264-270.

Ernest S, Rajaraman S, Megyesi J and Bello-Reuss EN (1997) Expression of MDR1 (multidrug resistance) gene and its protein in normal human kidney. *Nephron* **77**: 284-289.

Escobar MR and Sitar DS (1995) Site-selective effect of bicarbonate on amantadine renal transport: quinine-sensitive in proximal vs quinidine-sensitive sites in distal tubules. *J Pharmacol Exp Ther* **273**: 72-79.

Escobar MR and Sitar DS (1996) Use of digitalis glycosides to identify the mechanisms of amantadine transport by renal tubules. *J Pharmacol Exp Ther* **277**: 1189-1194.

Escobar MR, Goralski K and Sitar DS (1995) L(+) and D(-) Lactate modulate rat renal tubule accumulation of amantadine in the presence and absence of bicarbonate. *J Pharmacol Exp Ther* **275**: 1317-1323.

Escobar MR, Wong LTY and Sitar DS (1994) Bicarbonate-dependent amantadine transport by rat renal cortical proximal and distal tubules. *J Pharmacol Exp Ther* **270**: 979-986.

Foster DW and McGarry JD (1983) The metabolic derangements and treatment of diabetic ketoacidosis. *New Engl J Med* **309**: 159-169.

Fouda A-K, Fauth C and Roch-Ramel F (1990) Transport of organic cations by kidney epithelial cell line. *J Pharmacol Exp Ther* **252**: 286-292.

Freudenthaler S, Meineke I, Schreeb K-H, Boakye E, Gundert-Remy U and Gleiter CH (1998) Influence of urine pH and urinary flow on the renal excretion of memantine. *Br J Clin Pharmacol* **46**: 541-546.

Fritzsch G, Rummich G and Ullrich KJ (1989) Anion transport through the contraluminal cell membrane of renal proximal tubule. The influence of hydrophobicity and molecular charge distribution on the inhibitory activity of organic anions. *Biochim Biophys Acta* **978**: 249-256.

Galeazzi RL, Sheiner LB, Lockwood T and Benet LZ (1976) The renal elimination of procainamide. *Clin Pharmacol Ther* **19**: 55-62.

Gaudry SE, Sitar DS, McKenzie JK and Aoki FY (1993) Gender and age as factors in the inhibition of renal clearance by quinine and quinidine. *Clin Pharmacol and Ther* **54**: 23-27.

Gesek FA, Wolff DW and Strandhoy JW (1987) Improved separation method for rat proximal and distal renal tubules. *Am J Physiol* **253**: F358-F365.

Geuens HF and Stephens RL (1967) Influence of the pH of urine on the rate of excretion of 1-adamantane amine. 5th International Congress of Chemotherapy, Vienna, June 26-July 1, 1967, p703-713, Verlag der Wiener Medizinischen Akademie, Vienna.

Gibaldi M and Perrier D (1982). Clearance Concepts. in *Pharmacokinetics, 2nd edition* (Swarbrick J ed) pp 319-351, Marcel Dekker Inc, New York.

Giovannetti S and Barsotti G (1991) In defense of creatinine clearance. *Nephron* **59:** 11-14.

Glabman S, Klose RM and Giebisch G (1963) Micropuncture study of ammonia excretion in the rat. *Am J Physiol* **205:** 127-132.

Good DW and Burg MB (1984) Ammonia production in individual segments of the rat nephron. *J Clin Invest* **73:** 602-610.

Good DW and Dubose TD Jr (1987) Ammonia transport by early and late proximal convoluted tubule of the rat. *J Clin Invest* **79:** 684-691.

Good DW and Knepper MA (1985) Ammonia transport in the mammalian kidney. *Am J Physiol* **248:** F459-F471.

Gorboulev V, Ulzheimer JC, Akhoundova A, Ulzheimer-Teuber I, Karbach U, Quester S, Baumann C, Lang F, Busch AE and Koepsell H (1997) Cloning and characterization of two human polyspecific organic cation transporters. *DNA Cell Biol* **16:** 871-881.

Gornall AG, Bardwill CJ and Donid MM (1949) Determination of serum protein by means of the Biuret reaction. *J Biol Chem* **177**: 751-766.

Gross AS and Somogyi (1994) Interaction of the stereoisomers of basic drugs with the uptake of tetraethylammonium by rat renal brush-border membrane vesicles. *J Pharmacol Exp Ther* **268**: 1073-1080.

Grundemann D, Babin-Ebell J, Martel F, Ording N, Schmidt A and Schomig E (1997) Primary structure and functional expression of the apical organic cation transporter from kidney epithelial LLC-PK₁ cells. *J Biol Chem* **272**: 10408-10413.

Grundemann D, Gorboulev V, Gambaryan S, Vehyl M and Koepsell H (1994) Drug excretion mediated by a new prototype of polyspecific transporter. *Nature* **372**: 549-552.

Guia A and Bose R (1994) Simultaneous measurement of cytosolic pH and isometric tension in canine trabeculae: effect of acidosis. *Biophys J* **66**: A404.

Gwilt PR, Nahhas RR and Tracewell WG (1991) The effects of diabetes mellitus on pharmacokinetics and pharmacodynamics in humans. *Clin Pharmacokinet* **20**: 477-490.

Halperin, ML, Ethier JH and Kamel KS (1989) Amonium excretion in chronic metabolic acidosis: benefits and risks. *Am J Kidney Dis* **14**: 267-271.

Halperin, ML, Ethier JH and Kamel KS (1990) The excretion of ammonium ions in acid base balance. *Clin Biochem* **23**: 185-188.

Handler JS, Perkins FM and Johnson JP (1980) Studies of renal cell function using cell culture techniques. *Am J Physiol* **238**: F1-F9.

Hanes CS (1932) Studies on plant amylases: I. the effect of starch concentration upon the velocity of hydrolysis by the amylase of germinated barley. *Biochem J* **26**: 1406-1421.

Harvey AM and Malvin RL (1965) Comparison of creatinine and inulin clearances in male and female rats. *Am J Physiol* **209**: 849-852.

Hatch GM, Cao SG and Angel A (1995) Decrease in cardiac phosphatidylglycerol in streptozotocin-induced diabetic rats does not affect cardiolipin biosynthesis: evidence for distinct pools of phosphatidylglycerol in the heart. *Biochem J* **306**: 759-764.

Hofstee BHJ (1952) On the evaluation of the constants V_m and K_m in enzyme reactions. *Science* **116**: 329-331.

Hohage H, Morth DM, Querl IU and Greven J (1994) Regulation by protein kinase C of the contraluminal transport system for organic cations in rabbit kidney S2 proximal tubules. *J Pharmacol Exp Ther.* **268**: 294-298.

Hohage H, Stachon A, Feidt C, Hirsch JR and Schlatter E (1998) Regulation of organic cation transport in IHKE-1 and LLC-PK₁ cells. Fluorometric studies with 4-(4-dimethylaminostyryl)-N-methylpyridinium. *J Pharmacol Exp Ther* **286**: 305-310.

Holohan PD and Ross CR (1980) Mechanisms of organic cation transport in kidney plasma membrane vesicles: 1 Countertransport Studies. *J Pharmacol Exp Ther* **215**: 191-197.

Holohan PD and Ross CR (1981) Mechanisms of organic cation transport in kidney plasma membrane vesicles: 2 change in pH studies. *J Pharmacol Exp Ther* **216**: 294-298.

Holohan PD, Pessah NI and Ross CR (1975) Binding of N¹-methylnicotinamide and *p*-aminohippuric acid to a particulate fraction from dog kidney. *J Pharmacol Exp Ther* **195**: 22-33.

Horadam VW, Sharp JG, Smilack, JD, McAnalley BH, Garriott JC, Stephens MK, Prati, RC and Brater DC (1981) Pharmacokinetics of amantadine hydrochloride in subjects with normal and impaired renal function. *Annals Intern Med* **94**: 454-458.

Hosoyamada M, Sekine T, Kanai Y and Endou H (1999) Molecular cloning and functional expression of a multispecific organic anion transporter from human kidney. *Am J Physiol* **276**: F122-F128.

Ing TS, Daugirdas JT, Soung LS, Klawans HL, Mahurkar SD, Hayashi JA, Geis WP and Hano JE (1979) Toxic effects of amantadine in patients with renal failure. *Can Med Assoc J* **120**: 695-698.

Intengan HD and Smyth DD (1996) Clonidine-induced increase in osmolar clearance and free water clearance via activation of two distinct α_2-adrenoceptor sites. *Br J Pharmacol* **119**: 663-670.

Jacquemin EJ, Hagenbuch B, Steigler B, Wolkoff AW and Meier PJ (1994) Expression cloning of a rat liver Na^+ independent organic anion transporter. *Proc Natl Acad Sci USA* **91**: 133-137.

Jensen PK, Christiansen JS, Steven K, Parving H-H (1981) Renal function in streptozotocin-diabetic rats. *Diabetologia* **21**: 409-414.

Jung JS, Kim YK and LEE SH (1989) Characteristics of tetraethylammonium transport in rabbit renal plasma vesicles. *Biochem J* **259**: 377-383.

Kakyo ATM, Sakagami H, Tokui T, Nishio T, Tanemoto M, Nomura H, Hebert SC, Matsuno S, Kondo H and Yawo H (1998) Molecular characterization and tissue distribution of a new organic anion transporter subtype (oatp3) that transports thyroid hormones, taurocholate and comparison with oatp2. *J Biol Chem* **273**: 22395-22401.

Kanai N, Lu R, Bao Y, Wolkoff AW and Schuster VL (1996) Transient expression of oatp organic anion transporter in mammalian cells: identification of candidate substrates. *Am J Physiol* **270**: F319-F325.

Katsura T, Maegawa H, Tomita Y, Takano M, Inui K-I, Hori R (1991) Trans-stimulation effect on H^+-organic cation antiport system in rat renal brush-border membranes. *Am J Physiol* **261**: F774-778.

Katsura T, Takano M, Tomita Y, Yasuhara M, Inui K-I and Hori R (1993) Characteristics of organic cation transporter in rat renal basolateral membrane. *Biochem Biophys Acta* **1146**: 197-202.

Kekuda R, Prasad PD, Wu X, Wang H, Fei Y-J, Leibach FH and Ganapathy V (1998) Cloning and functional characterization of a potential-sensitive, polyspecific organic cation transporter (OCT3) most abundantly expressed in placenta. *J Biol Chem* **273**: 15971-15979.

Kim YK and Dantzler WH (1995) Intracellular pH in snake renal proximal tubules. *Am J Physiol* **269**: R822-R829.

Kim YK and Dantzler WH (1997) Effects of pH on basolateral tetraethylammonium transport in snake renal proximal tubules. *Am J Physiol* **272**: R955-R961.

Kimball SR, Vary TC and Jefferson LS (1994) Regulation of protein synthesis by insulin. *Annu Rev Physiol* **56**: 321-348.

Kinsella JL, Holohan PD, Pessah NI and Ross CR (1979a) Transport of organic ions in renal cortical luminal and antiluminal membrane vesicles. *J Pharmacol Exp Ther* **209**: 443-450.

Kinsella JL, Holohan PD, Pessah NI and Ross CR (1979b) Isolation of luminal and antiluminal membranes from dog kidney cortex. *Biochim Biophysica Acta* **552**: 468-477.

Knepper MA (1991) NH_4^+ transport in the kidney. *Kidney Int* **40, Suppl. 33:** S95-S102.

Koepsell H (1998) Organic cation transporters in the intestine, kidney, liver and brain. *Annu Rev Physiol* **60**: 243-266.

Koepsell H, Busch A, Gorboulev V and Arndt P (1998) Structure and function of renal organic cation transporters. *News Physiol Sci* **13**: 11-16.

Köppel C and Tenczer J (1985) A revision of the metabolic disposition of amantadine. *Biomed Mass Spec* **12**: 499-501.

Kriz W and Bankir L (1988) A standard nomenclature for structures of the kidney. *Am J Physiol* **254**: F1-F8.

Lineweaver H and Burk D (1934) The determination of enzyme constants. *J Am Chem Soc* **56**: 658-666.

Lockwood AH, McDonald JM, Reiman RE, Gelbald AS, Laughlin JS, Duffy TE and Plum F (1979) The dynamics of ammonia metabolism in man. *J Clin Invest* **63**: 449-460.

Lopez-Nieto C, You G, Bush KT, Barros EJG, Beier DR and Nigam SK (1997) Molecular cloning and characterization of NKT, a gene product related to the organic cation transporter family that is almost exclusively expressed in the kidney. *J Biol Chem* **272**: 6471-6478.

Lu R, Chan BS and Shuster VL (1999) Cloning of the human kidney PAH transporter: narrow substrate specificity and regulation by protein kinase C. *Am J Physiol* **276**: F295-F303.

Malvin RL, Wilde WS and Sullivan LP (1958) Localization of nephron transport by stop-flow analysis. *Am J Physiol* **194**: 135-142.

Marshal EK Jr, (1931) The secretion of phenol red by the mammalian kidney. *Am J Physiol* **99**: 77-86.

Marshall EK Jr, and Vickers JL (1923) The mechanism of the elimination of phenolsulphonphthalein by the kidney - a proof of secretion by the convoluted tubules. *Bull Johns Hopkins Hosp* **34**: 1-7.

Martel F, Vetter T, Russ H, Grundemann D, Azevedo I, Koepsell H and Schomig E (1996) Transport of small organic cations in the rat liver the role of the organic cation transporter OCT1. *Naunyn-Schmiedberg's Arch Pharmacol* **345**: 320-326.

Martinez CL, Brokl OH, Shuprisha A, Abbott DE and Dantzler WH (1997) Regulation of intracellular pH in proximal tubules of avian loopless reptilian-type nephrons. *Am J Physiol* **273**: R1845-R1854.

McKinney TD (1982) Heterogeneity of organic base secretion by proximal tubules. *Am J Physiol* **243**: F404-F407.

McKinney TD (1983) Procainamide uptake by rabbit renal proximal tubules. *J Pharmacol Exp Ther* **224**: 302-306.

McKinney TD (1984) Further studies of organic base secretion in rabbit proximal tubules. *Am J Physiol* **246**: F282-F289.

McKinney TD and Kunnemann ME (1985) Procainamide transport in rabbit renal cortical brush-border membrane vesicles. *Am J Physiol* **249**: F532-F541.

226

McKinney TD and Kunnemann ME (1987) Cimetidine transport in rabbit renal cortical brush-border membrane vesicles. *Am J Physiol* **252**: F525-F535.

McKinney TD and Speeg KV Jr (1982) Cimetidine and procainamide secretion by proximal tubules. *Am J Physiol* **242**: F672-F680.

McKinney TD, Scheller MB, Hosford M and McAteer JA (1990) Tetraethylammonium transport by OK cells. *J Am Soc Nephrol* **1**: 902-909.

Meezen E and Freychet P (1979) Rat renal glomeruli and tubules have specific insulin receptors of differing affinity. *Mol Pharmacol* **16**: 1095-1100.

Meier DKF, Mol WEM, Muller M and Kurz G (1990) Carrier-mediated transport in the hepatic distribution and elimination of drugs, with special reference to the category of organic cations. *J Pharmacokinetic Biopharm* **18**: 35-70.

Meyer-Wentrup F, Ullrich Karbach, Gorboulev V, Arndt P and Koepsell H (1998) Mebrane localization of the electrogenic cation transporter rOCT1 in rat liver. *Biochem Biophys Res Commun* **248**: 673-678.

Miller DS, Stewart DE and Pritchard JB (1993) Intracellular compartmentation of organic anions within renal cells. *Am J Physiol* **264**: R882-R890.

Moller JV and Sheikh MI (1982) Renal organic anion transport system: pharmacological, physiological and biochemical aspects. *Pharmacol Rev* **34:** 315-358.

Montrose-Rafizadeh C, Mingard F, Murer H, and Roch-Ramel F (1989) Carrier-mediated transport of tetraethylammonium across rabbit renal basolateral membrane. *Am J Physiol* **257:** F243-F251.

Morgensen CE, Christensen CK, and Vittinghus E (1983) The stages in diabetic renal disease: with emphasis on the stage of incipient diabetic nephropathy. *Diabetes* **32(Suppl 2):** 64-78.

Mori K, Ogawa Y, Ebihara K, Aoki T, Tamura N, Sugawara A, Kuwahara T, Ozaki S, Mukoyama M, Tashiro K, Tanaka I and Nakao K (1997) Kidney-specific expression of a novel mouse organic cation transporter-like protein. *FEBS Lett* **417:** 371-374.

Muhiddin KA, Johnston A and Turner P (1984) The influence of urinary pH on flecainide excretion and its serum pharmacokinetics. *Br J Clin Pharmacol* **17:** 447-451.

Nadai M, Yoshizumi H, Kuzuya T, Hasegawa T, Johno, I and Kitazawa S (1990) Effects of diabetes on disposition and renal handling of cefazolin in rats. *Drug Metab Disposit* **18:** 565-570.

Nannum P, Insogna K, Baggish D and Hayslett JP (1983) Evidence for bidirectional movement of creatinine in the rat kidney. *Am J Physiol* **244:** F719-F723.

Nelson JA (1988) A physiological function for multidrug-resistant membrane glycoproteins: a hypothesis regarding the renal organic cation-secretory system. *Cancer Chemother Pharmacol* **22:** 92-93.

Nelson JA, Dutt A and Allen LH (1995) Functional expression of the renal organic cation transporter and p-glycoprotein in *Xenopus laevis* oocytes. *Cancer Chemother Pharmacol* **37:** 187-189.

Noe B, Hagenbuch B, Steiger B, Meier PJ (1997) Isolation of a multispecific organic anion and cardiac glycoside transporter from rat brain. *Proc Natl Acad Sci* **94:** 10346-10350.

Okuda M, Saito H, Urakami Y, Takano M and Inui K (1996) cDNA cloning and functional expression of a novel rat kidney organic cation transporter, OCT2. *Biochem Biophysic Res Commun* **224:** 500-507.

Okuda M, Urakami Y, Saito, H and Inui K-I (1999) Molecular mechanisms of organic cation transport in OCT2 expressing xenopus oocytes. *Biochim Biophys Acta* **1417:** 224-231.

Ott RJ, Hui AC, Yuan G and Giacomini (1991) Organic cation transport in human renal brush-border membranes. *Am J Physiol* **261**: F443-451.

Parkes D, Amantadine (1974) *Adv Drug Res* **8**: 8-11.

Peters L (1960) Renal tubule excretion of organic bases. *Pharmacol Rev* **12**: 1-35.

Peters L, Fenton KJ, Wolf ML, and Kandel A (1955) Inhibition of the renal tubule excretion of N'-methylnicotinamide (NMN) by small doses of basic cyanine dye. *J Pharmacol Exp Ther* **113**: 148-159.

Pilkington LA and Keyl JM (1963) Stop-flow analysis of mepiperphenidol and mecamylamine in the dog. *Am J Physiol* **205**: 471-476.

Preston RA and Epstein M (1999) Effects of diabetes on cardiovascular drug metabolism. *Diabetes Care* **22**: 982-988.

Pritchard JB (1987) Luminal and peritubular steps in renal transport of *p*-aminohippurate. *Biochim Biophys Acta* **906**: 295-308.

Pritchard JB and Miller DS (1993) Mechanisms mediating renal secretion of organic anions and cations. *Physiol Rev* **73**: 765-796.

Pritchard JB, Sykes DB, Walden R and Miller DS. (1994) ATP-dependent transport of tetraethylammonium by endosomes isolated from rat renal cortex. *Am J Physiol* **266**: F966-F976.

Quebbemann AJ and Rennick BR (1969) Effects of structural modifications of catecholamines on renal tubule transport in the chicken. *J Pharmacol Exp Ther* **166**: 52-62.

Rafizadeh C, Roch-Ramel F and Schäli C (1987) Tetraethylammonium transport in renal brush border membrane vesicles of the rabbit. *J Pharmacol Exp Ther* **240**: 308-313.

Randhawa MA, Iqbal A, Nasimullah M, Akhtar M, Yousaf SM and Turner P (1995) Henderson-Hasselbalch equation is inadequate for the measurement of transmembrane diffusion of drugs and buccal absorption is a useful alternative. *Gen Pharmacol* **26**: 875-879.

Rennick BA (1981) Renal transport of organic cations. *Am J. Physiol* **240**: F83-F89.

Rennick BA and Farah (1956) Studies on the renal tubular transport of tetraethylammonium in the dog. *J Pharmacol Exp Ther* **116**: 287-295.

Rennick BA and Moe GK (1960) Stop-flow localization of renal tubular excretion of tetraethylammonium. *Am J Physiol* **198**: 1267-1270.

Rennick BA, Kandel A and Peters L (1956) Inhibition of the renal tubular excretion of tetraethylammonium and N'-methylnicotinamide by basic cyanine dyes. *J Pharmacol Exp Ther* **118**: 204-219.

Rennick BA, Moe GK, Lyons RH, Hoobler SW and Neligh R (1947) *J Pharmacol Exp Ther* **91**: 210-217.

Ries F and Klastersky J (1986) Nephrotoxicity induced by cancer chemotherapy with special emphasis on cisplatin toxicity. *Am J Kidney Dis* **8**: 368-379.

Roos A and Boron W (1981) Intracellular pH. *Physiol Rev* **61**: 296-434.

Rosenberg TH and Wilbrandt W (1955) The kinetics of membrane transports involving chemical reactions. *Exp Cell Res* **9**: 49-67.

Saito H, Yamamoto M, Inui K and Hori R (1992) Transcellular transport of organic cations across monolayers of kidney epithelial cell line LLC-PK$_1$. *Am J Physiol* **262**: C59-C66.

Schali C and Roch-Ramel F (1980) Accumulation of [^{14}C]urate and [^{3}H]PAH in isolated proximal tubular segments of the rabbit kidney. *Am J Physiol* **239**: F222-F227.

Schali C, Schild L, Overny J and Roch-Ramel F (1983) Secretion of tetraethylammonium by proximal tubules of rabbit kidneys. *Am J Physiol* **245**: F238-F246.

Scholer DW and Edelman IS (1979) Isolation of rat kidney cortical tubules enriched in proximal and distal segments. *Am J Physiol* **237**: F350-F359.

Schwab RS, England AC, Poskanzer DC and Young RR (1969) Amantadine in the treatment of Parkinson's disease. *J Am Med Assoc* **208**: 1168-1170.

Seki G, Coppola S, Yoshitomi K, Burckhardt BC, Samarzija I, Muller-Berger S and Fromter E (1996) On the mechanism of bicarbonate exit from renal proximal tubular cells. *Kidney Int* **49**: 1671-1670.

Sekine T, Cha SH, Tsuda M, Apiwattanakul N, Nakajima N, Kanai Y and Endou H (1998) Identification of multispecific organic anion transporter 2 expressed predominantly in the liver. *FEBS Lett* **429**: 179-182.

Sekine T, Nobuaki W, Hosoyamada M, Kanai Y and Endou H (1997) Expression cloning and characterization of a novel multispecific organic anion transporter. *J Biol Chem* **272**: 18526-18529.

Seyer-Hansen K (1978) Renal hypertrophy in experimental diabetes: a comparison to compensatory hypertrophy. *Diabetologia* **14**: 325-328.

Seyer-Hansen K, Hansen J and Gundersen HJG (1980) Renal hypertrophy in experimental diabetes. *Diabetologia* **18:** 501-505.

Sha'afi RI (1981) Permeability for water and other polar molecules. In Membrane Transport.. (Bonting SI and DePont JJHHM, eds) pp 29-69, Elsevier/North Holland Biomedical Press, Amsterdam.

Shafik IM and Quamme GA (1990) Micropuncture techniques in renal research. *Methods Enzymol* **191:** 72-97.

Sheikh MI and Moller JV (1970) The kinetic parameters of renal transport of p-amminohippurate in vitro. *Biochim Biophys Acta* **196:** 305-319.

Shimada H, Moewes B and Burckardt G (1987) Indirect coupling to Na of *p*-aminohippuric acid uptake into rat renal basolateral membrane vesicles. *Am J Physiol* **253:** F795-F801.

Shimomura A, Chonko AM and Grantham JJ (1981) Basis for hereogeneity of para-aminohippurate secretion in rabbit proximal tubules. *Am J Physiol* **240:** F430-F436.

Sica DA and Schoolworth AC (1996) Renal handling of organic anions and cations and renal excretion of uric acid, in *The Kidney 5th edition* (Brenner BM, ed.) pp 607-626. W.B. Saunders Co., Philadelphia.

Simonson GD, Vincent AC, Roberg KJ, Haung Y and Iwanij V (1994) Molecular cloning and characterization of a novel liver-specific transport protein. *J Cell Sci* **107**: 1065-1072.

Sitar DS, Escobar MR, Goralski KB and Stupak DG (1997) Bicarbonate and lactate infusions block renal amantadine secretion in the anaesthetized dog. *Clin Invest Med* **20(4Suppl):** #51.

Sokol PP and Mckinney TD (1990) Mechanism of organic cation transport in rabbit renal basolateral membranes. *Am J Physiol* **258:** F1599-1607.

Sokol PP, Holohan PD and Ross CR (1985) Electroneutral transport of organic cations in canine renal brush-border membranes. *J Pharmacol Exp Ther* **233:** 694-699.

Soleimani M and Bizal GL (1996) Functional identity of a purified proximal tubular anion exchanger protein: mediation of chloride/formate and chloride/bicarbonate exchange. *Kidney Int* **50:** 1914-1921.

Somani SK, Degelau J, Cooper SL, Guay DRP, Ehreshman D, Zaske D (1991) Comparison of pharmacokinetic and safety profiles of amantadine 50- and 100-mg daily doses in elderly nursing home residents. *Pharmacotherapy* **11**: 460-466.

Somogyi A and Gugler R (1985) Effect of variations in urine pH and flow rate on cimetidine renal disposition in man. *Biopharm Drug Disp* **6**: 345-349.

Speeg KV, DeLeon C and McGuire WL (1992) Uptake of the non cytotoxic transport probe procainamide in the Chinese hamster ovary model of multidrug resistance. *Cancer Res* **52**: 3539-3546.

Sperber I (1949) The excretion of piperidine, gaunidine, methylgaunine nd N^1-methylnicotinamide in the chicken. *Lantbrukshogskolans Annaler* **16**: 49-64.

Sperber I (1959) Secretion of organic anions in the formation of urine and bile. *Pharmacol Rev* **11**: 109-134.

Stone JL, Braunstein JB, Beaty TM, Sanders RA and Watkins JB (1997) Hepatobiliary excretion of bile acids and rose bengal in streptozotocin-induced and genetic diabetic rats. *J Pharmacol Exp Ther* **281**: 412-419.

Stone TW and Connick JH (1985) Quinolinic acid and other kynurenines in the central nervous system. *Neuroscience* **15**: 597-617.

Stupack DG, Escobar MR, Carlisle M, Davie T and Sitar DS (1999) Heterogeneity among β-adrenoreceptor blockers in the modulation of amantadine uptake by rat renal tubules. *Can J Physiol Pharmacol* **77 (6)**: in press.

Sweet DH, Wolff NA, Pritchard JB (1997) Expression cloning and characterization of ROAT1. *J Biol Chem* **272**: 30088-30095.

Takami K, Saito H, Okuda M, Takano M, Inui K-I (1998) Distinct characteristics of transcellular transport between nicotine and tetraethylammonium in LLC-PK₁ cells. *J Pharmacol Exp Ther* **286**: 676-680.

Takano M, Inui K-I, Okano T, Saito H and Hori R (1984) Carrier-mediated transport systems of tetraethylammonium in rat renal brush-border and basolateral membrane vesicles. *Biochim Biophys Acta* **773**: 113-124.

Tamai I, Yabuuchi H, Nezu J-I, Sai Y, Oku A, Shimane M and Tsuji A (1997) Cloning and characterization of a novel human pH-dependent organic cation transporter, OCTN1. *FEBS lett* **419**: 107-111.

Terashita S, Dresser MJ, Zhang L, Gray AT, Yost SC and Giacomini KM (1998) Molecular cloning and functional expression of a rabbit renal organic cation transporter. *Biochim Biophys Acta* **1369**: 1-6.

Thiebaut F, Tsuruo T, Hamada H, Gottesman MM, Pastan I and Willingham MC (1987) Cellular location of the multidrug-resistance gene product P-glycoprotein in normal human tissues. *Proc Natl Acad Sci USA* **84:** 7735-7738.

Tilles JG (1974) Antiviral Agents. *Annu Rev pharmacol* **14:** 469-489.

Tisher CC and Madsen KM (1996) Anatomy of the kidney, in *The Kidney 5th edition* (Brenner BM, ed) pp 3-71. W.B. Saunders Co., Philadelphia.

Tizianello A, De Ferrari G, Garibotto G, Gurreri G and Robaudo C (1980) Renal metabolism of amino acids and ammonia in subjects with normal renal function and patients with chronic renal insufficiency. *J Clin Invest* **65:** 1162-1173.

Torretti J, Weiner IM and Mudge GH (1962) Renal tubule secretion and reabsorption of organic bases in the dog. *J Clin Invest* **41:** 793-804.

Tune BM, Burg MB and Patlak CS (1969) Characteristics of p-aminohippurate transport in renal proximal tubules. *Am J Physiol* **217:** 1057-1063.

Turski WA and Schwarcz R (1988) On the disposition of intrahippocampally injected kynurenic acid in the rat. *Exp Brain Res* **71:** 563-567.

Uchiyama M and Shibuya M (1969) Distribution and excretion of ^{3}H-Amantadine HCl. *Chem Pharm Bull* **17**: 841-843.

Ueda K, Okamura N, Hirai M, Tanigawara Y, Saeki T, Kioka N, Komano T and Hori R (1992) Human P-glycoprotein transports cortisol, aldosterone, and dexamethasone, but not progesterone. *J Biol Chem* **267**: 24248-24252.

Ullrich KJ (1994) Specificity of transporters for 'organic anions' and 'organic cations' in the kidney. *Biochim Biophys Acta* **1197**: 45-62.

Ullrich KJ and Rumrich G (1990) Kidney: microperfusion-double perfused tubule in situ. *Methods Enzymol* **191**: 98-107.

Ullrich and Rumrich (1992) Renal contraluminal transport systems for organic anions (paraaminohippurate, PAH) and organic cations (N^1-methylnicotinamide, NmeN) do not see the degree of substrate ionization. *Pflugers Arch* **421**: 286-288.

Ullrich KJ, Papavassiliou F, David C, Rumrich G and Fritzsch G (1991) Contraluminal transport of organic cations in the proximal tubule of the rat kidney. I. Kinetics of N^1-methylnicotinamide and tetraethylammonium, influence of K^+, HCO_3^-, pH, inhibition by aliphatic primary, secondary and tertiary amines and mono-bisquarternary compounds. *Pflugers Arch* **419**: 84-92.

Ullrich KJ, Rumrich G, David C and Fritzsch G (1993a) Bisubstrates: substances that interact with renal contraluminal organic anion and cation transport systems. I. Amines, piperidines, piperazines, azepines, pyridines, quinolones, imidazoles, thiazoles, gaunidines and hydrazines. *Pflugers Arch* **425**: 280-299.

Ullrich KJ, Rumrich G, David C and Fritzsch G (1993b) Bisubstrates: substances that interact with both, renal contraluminal organic anion and cation transport systems. II. Zwitterionic substrates: dipeptides, cephalosporins, quinolone-carboxylate gyrase inhibitors and phosphamide thiazine carboxylates; nonionizable substrates: steroid hormones and cyclophosphamides. *Pflugers Arch* **425**: 300-312.

Ullrich KJ, Rumrich G, Neiteler K and Fritzsch G (1992) Contraluminal transport of organic cations in the proximal tubule of rat kidney. II. Specificity: anilines, phenylalkylamines, (catecholamines), heterocyclic compounds (pyridines, quinolones, acridines). *Pflugers Arch* **420**: 29-38.

Urakami Y, Okuda M, Masuda S, Saito H and Inui K-I (1998) Functional characteristics and membrane localization of rat multispecific organcic cation transporters, OCT1 and OCT2, mediating tubular secretion of cationic drugs. *J Pharmacol Exp Ther* **287**: 800-805.

Van Acker BA, Koomen GC, Koopmen MG, de Wart DR and Arisz L (1992) Creatinine clearance during cimetidine administration for measurement of glomerular filtration rate. *Lancet* **340**: 1326-1329.

Vander AJ (1995) Renal physiology, 5th ed. McGraw-Hill Inc., New York.

Verhaeghe J, Van Bree R, Van Herck E, Jans I, Zaman Z and Bouillon R (1999) Calcitrophic hormones during experimental hypocalcemia and hypercalcemia in spontaneously diabetic rats. *J Endocrinol* **162**: 251-258.

Vinay P, Gougoux A and Lemieux G (1981) Isolation of a pure suspension of rat proximal tubules. *Am J Physiol* **241**: F403-F411.

Vinay P, De Cotret PR, Schwartz H, Gougoux A and Lemieux G (1982) Cell transport and metabolism of glutamine by proximal and/or distal tubules of rat kidney. in *Biochemistry of Kidney Functions*, INSERM Symposium No. 21. (F Morel, Ed) Elsevier Biomedical Press B.V.

Vinay P, Lemieux G, Gougoux A and Lemieux C (1980) Response of the rat and dog kidney to H^+ concentration in vitro-a comparative study with slices and tubules. *Int J Biochem* **12**: 89-98.

Vinay P, Lemieux G, Gougoux A and Halperin C (1986) Regulation of glutamine metabolism in the dog kidney in vivo. *Kidney Int* **29**: 68-79.

Voet D and Voet JG (1990) Transport Through Membranes, in *Biochemistry* (Stiefel J ed) pp484-505, John Wiley & Sons Inc., New York.

Watkins JB and Dykstra TP (1987) Alteration in biliary excretory function in streptozoticin induced diabetes. *Drug Metab Disposit* **15**: 177-183.

Wedeen RP and Weiner B (1973) The distribution of p-aminohippuric acid in rat kidney slices. II. Depth of uptake. *Kidney Int* **3**: 214-221.

Weiner IM and Roth L (1981) Renal excretion of cimetidine. *J Pharmacol Exp Ther* **216**: 516-520.

Wilkinson G (1961) Statistical estimations in enzyme kinetics. *Biochem J* **80**: 324-332.

Wilson TW and Rajput AH (1983) Amantadine-dyazide interaction. *Can Med Assoc J* **129**: 974-975.

Woodhall PB, Tisher CC, Simonton CA and Roscoe RR (1978) Relationship between para-aminohippurate secretion and cellular morphology in rabbit proximal tubules. *J Clin Invest* **61**: 1320-1329.

Wong LT, Sitar DS and Aoki FY (1995) Chronic tobacco smoking and gender as variables affecting amantadine disposition in healthy subjects. *Br J Clin Pharmacol* **39**: 81-4.

Wong LTY, Smyth DD and Sitar DS (1990) Stereoselective inhibition of amantadine accumulation by quinine and quinidine in rat renal proximal tubules and cortical slices. *J Pharmacol Exp Ther* **255**: 271-275.

Wong LTY, Smyth DD and Sitar DS (1991) Differential effects of histamine H_2 receptor antagonists on amantadine uptake in the rat renal cortical slice, isolated proximal tubule and distal tubule. *J Pharmacol Exp Ther* **258**: 320-324.

Wong LTY, Smyth DD and Sitar DS (1992a) Interference with renal organic cation transport by (-) and (+) nicotine at concentrations documented in plasma of habitual tobacco smokers. *J Pharmacol Exp Ther* **261**: 21-25.

Wong LTY, Smyth DD and Sitar DS (1992b) Stereoselective inhibition of renal tubule organic cation transport in the human kidney. *Br J Clin Pharmacol* **34**: 438-440.

Wong LTY, Escobar MR, Smyth DD and Sitar DS (1993) Gender-associated differences in rat renal tubular amantadine transport and absence of stereoselective transport inhibition by quinine and quinidine in distal tubules. *J Pharmacol Exp Ther* **267**: 1440-1443.

Wright SH and Wunz TM (1987) Transport of tetraethylammonium by rabbit renal brush-border and basolateral membrane vesicles. *Am J Physiol* **253**: F1040-F1050.

Wright SH and Wunz TM (1988) Mechanism of *cis*- and *trans*-substrate interactions at the tetraethylammonium/H^+ exchanger of rabbit renal brush-border membrane vesicles. *J Biol Chem* **263**: 19494-19497.

Wu X, Prasad PD, Leibach FH and Ganapathy V (1998) cDNA sequence, transport function, and genomic organization of human OCTN2, a new member of the organic cation transporter family. *Biochem Biophys Res Commun* **246**: 589-595.

Xie H, Zhu L, Zhang YL, Legare DJ and Lautt WW (1996) Insulin sensitivity tested with a modified euglycemic technique in cats and rats. *J Pharmacol Toxicol Methods* **35**: 77-82.

Yabuuchi H, Tamai I, Nezu JI, Sakamoto K, OKU A, Shimane M, Sai Y and Tsuji A (1999) Novel membrane transporter OCTN1 mediates multispecific, bidirectional and pH-dependent transport of organic cations. *J Pharamcol Exp Ther* **289**: 768-773.

Yu J, Zheng JJ, Ong BY and Bose R (1991) Intracellular pH measurement with fluorescent dye in canine basilar arteries. *Blood Vessels* **28**: 464-474.

Zhang L, Schaner ME, Giacomini KM (1998) Functional characterization of an organic cation transporter in a transiently transfected human cell line (HeLa). *J Pharmacol Exp Ther* **286**: 354-361.

Zhang L, Dresser M D, Chun JK, Babbitt C and Giacomini M (1997a) Cloning and functional characterization of rat renal organic cation transporter (rOCT1A). *J Biol Chem* **272**: 16548-16554.

Zhang L, Dresser MJ, Gray AT, Yost SC, Terishata S and Giacomini KM (1997b) Cloning and functional expression of a human liver organic cation transporter. *Mol Pharmacol* **51**: 913-921.

Zhang L, Gorset W, Dresser MJ and Giacomini KM (1999) The interaction of n-tetraalkylammonium compounds with a human organic cation transporter, hOCT1. *J Pharmacol Exp Ther* **288**: 1192-1198.